

PHASE TRANSITIONS IN LIQUID CRYSTALS

Shri SINGH

Department of Physics, Banaras Hindu University, Varanasi - 221 005, India



ELSEVIER

AMSTERDAM – LAUSANNE – NEW YORK – OXFORD – SHANNON – TOKYO



ELSEVIER

Physics Reports 324 (2000) 107–269

PHYSICS REPORTS

www.elsevier.com/locate/physrep

Phase transitions in liquid crystals

Shri Singh

Department of Physics, Banaras Hindu University, Varanasi-221 005, India

Received March 1999; editor: D.L. Mills

Contents

1. Introduction	110	6. Re-entrant phase transitions (RPT) in liquid crystals	204
1.1. Liquid crystals: an overview	110	6.1. Examples of single re-entrance	205
1.2. Classification of liquid crystals: symmetry and structures	114	6.2. Examples of multiple re-entrance	208
2. Order parameters	120	6.3. Theories for the RPT	209
2.1. Definition of microscopic order parameters	122	7. Uniaxial nematic–biaxial nematic ($N_u N_b$) phase transition	215
2.2. Definition of a macroscopic order parameters	125	8. Phase transitions involving smectic phases	221
2.3. Relationship between macroscopic and microscopic order parameters	126	8.1. Smectic A–smectic C transition	221
3. Phase transitions in liquid crystals	126	8.2. Nematic–smectic A–smectic C ($NS_A S_C$) multicritical point	223
3.1. Thermodynamics of phase transitions	129	8.3. Transitions involving hexatic smectic phases	225
3.2. Order of phase transition	130	9. Computer simulations of phase transitions in liquid crystals	226
3.3. Experimental determination of some phase transition properties: a critical comment	131	9.1. Lebwohl–Lasher model	227
4. Nematic–isotropic phase transition	133	9.2. Hard-core models	228
4.1. Landau–de Gennes theory of the uniaxial nematic–isotropic (NI) phase transition	135	9.3. Gay–Berne model	232
4.2. The hard particle or Onsager-type theories	151	10. Phase transitions in liquid crystal polymers (LCPs)	234
4.3. The Maier–Saupe (MS) type theories	158	10.1. Nematic order in polymer solutions	235
4.4. The van der Waals (vdW) type theories	163	10.2. Nematic order in polymer melts	241
4.5. Application of density functional theory (DFT) to the NI phase transition	178	10.3. Nematic polymers with varying degree of flexibility	243
5. Nematic–smectic A (NS_A) phase transition	189	11. Phase transitions in chiral liquid crystals	244
5.1. Phenomenological description of the NS_A transition	190	11.1. Non-ferroelectric liquid crystals	244
5.2. Mean-field description of NS_A transition	193	11.2. Transitions in ferroelectric liquid crystals	251
5.3. Application of density functional theory to NS_A transition	200	12. Overview and perspectives	256
		Acknowledgements	257
		References	257

Abstract

Mesogenic materials exhibit a multitude of transitions involving new phases. Studies of these phases are of importance in a wide range of scientific fields and as such have stimulated considerable theoretical and experimental efforts over the decades. This review article presents a comprehensive overview until this date of the developments in this subject. An attempt is made to identify the essential key concepts and points of difficulty associated with the study of phase transitions. The article begins with a brief introduction about the symmetry, structure and types of liquid crystalline phases. This is followed by a discussion of the distribution functions and order parameters which are considered as the basic knowledge essential for the study of ordered phases. A brief discussion of the thermodynamic properties at and in the vicinity of phase transitions, which are required to understand the molecular structure phase stability relationship, is given. The most widely used experimental techniques for measuring these transition properties are critically examined. The remaining parts of the article are concerned with the current status of the theoretical developments and experimental studies in this field. The application of the various theories to the description of isotropic liquid-uniaxial nematic, uniaxial nematic-smectic A, uniaxial nematic-biaxial nematic, smectic A–smectic C phase transitions are reviewed comprehensively. The basic ideas of Landau–de Gennes theory and its applications to study these transitions are discussed. Since the formation of liquid crystals depends on the anisotropy in the intermolecular interactions, questions concerning its role in the mesophase transitions are addressed. The hard particle, Maier-Saupe and van der Waals types of theories are reviewed. The application of density functional theory in studying mesophase transitions is described. A critical assessment of the experimental investigations concerning reentrant phase transitions in liquid crystals is made and the factors which impede its proper understanding are identified. A survey is given of existing computer simulation studies of the isotropic to nematic transition, the nematic to smectic A transition, the smectic A to hexatic S_B transition, the smectic A to reentrant nematic transition, and transitions to the discotic phase. The current status of the study of phase transitions involving hexatic smectic, cholesteric, polymeric and ferroelectric liquid crystals is outlined. Finally, a range of unexplored problems and some of the areas which are in greatest need of future attention are identified. © 2000 Elsevier Science B.V. All rights reserved.

PACS: 64.70.Md

1. Introduction

1.1. Liquid crystals: an overview

The states of matter whose symmetric and mechanical properties are intermediate between those of a crystalline solid and an isotropic liquid are called “liquid crystals” (LC) [1–30]. The basic difference between crystals and liquids is that the molecules in a crystal are ordered whereas in a liquid they are not. The existing order in a crystal is usually both positional and orientational, i.e., the molecules are constrained both to occupy specific sites in a lattice and to point their molecular axes in specific directions. Contrary to this, the molecules in liquids diffuse randomly throughout the sample container with the molecular axes tumbling wildly. Interestingly enough, many molecular materials, in which the building blocks are anisotropic entities, exhibit more complex phase sequences. In particular, as they are heated from the solid phase at the melting point the following possibilities exist:

- (i) Both types of order (positional and orientational) disappear at the same time and the resulting phase will be an “isotropic liquid (IL)” (Fig. 1b) possessing $T(3) \times O(3)$ symmetry.
- (ii) Only orientational order disappears leaving the positional order intact and the corresponding phase is called a “plastic crystal (PC)” (Fig. 1c).

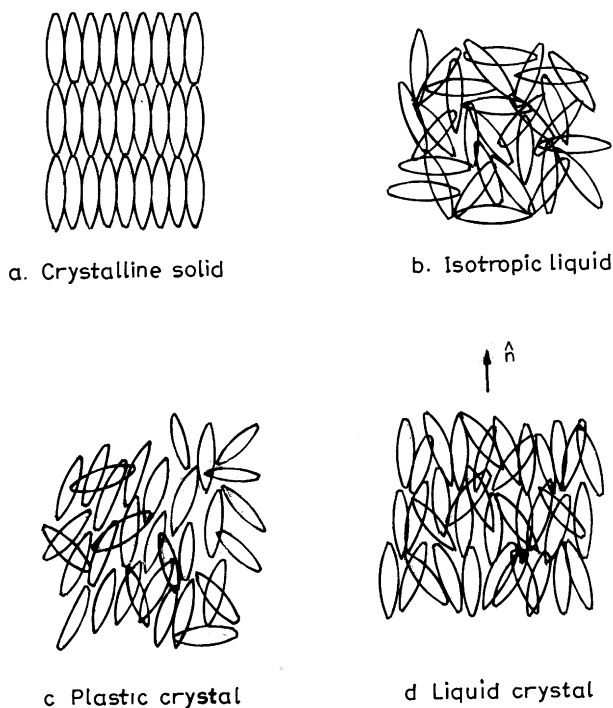


Fig. 1. The arrangement of molecules in various phases.

- (iii) The positional order either fully or partially disappears while some degree of orientational order is maintained. The phase thus derived is called “liquid crystal (LC)” phase. A more proper name would be mesomorphic phase (meaning intermediate phase) or mesophase [1–30]. In this phase (Fig. 1d) each of the molecules has a tendency to align itself along a specific direction defined by the unit vector \hat{n} which is known as the “director”.

The liquid crystal phase possesses some of the characteristics of the order, evidenced by X-ray diffraction, found in crystalline solids (Fig. 1a) and some of the disorder, evidenced by ease of flow, existing in liquids. The molecules in liquid crystal phases diffuse much like the molecules in a liquid, but they maintain some degree of orientational order and sometimes some positional order also. The amount of order in a liquid is quite small as compared to a crystal. There remains only a slight tendency for the molecules to point more in one direction than others or to spend more time in certain positions than in others. The value of latent heat (around 250 J/g) indicates that most of the order of a crystal is lost when it transforms to a mesophase. In case of a liquid crystal to isotropic liquid transition the latent heat is much smaller, typically about 5 J/g. Yet, the small amount of order in a liquid crystal reveals itself by the mechanical and electromagnetic properties typical for crystals.

Liquid crystalline materials in general may have various types of molecular structure. What they all have in common is that they are anisotropic. Either their shape is such that one axis is very different from the other two or, in some cases, different parts of the molecules have very different solubility properties. From the molecular structures liquid crystal can be divided into several types. The liquid crystals derived from the rod-like molecules are called “calamitics”. It is essential that the mesogenic molecule be fairly rigid for at least some portion of its length (Fig. 2a), since it must maintain an elongated shape in order to produce interactions that favour alignment. The liquid crystals formed from disk-shape molecules (Fig. 2b) are known as “discotics” [3,4,31–34]. Again the rigidity in the central part of the molecule is essential. Intermediate between rod-like and disk-like molecules are the lath-like species (Fig. 2c).

Transitions to the mesophases may be brought about in two different ways; one by purely thermal processes and the other by the influence of solvents. Liquid crystals obtained by the first method are called “thermotropics” whereas those obtained by the second one are “lyotropics”. Amphotropic materials are able to form thermotropic as well as lyotropic mesophases. The recipe for a lyotropic liquid crystal molecule is combining a hydrophobic group at one end with a hydrophilic group at the other end. Such amphiphilic molecules form ordered structures in both

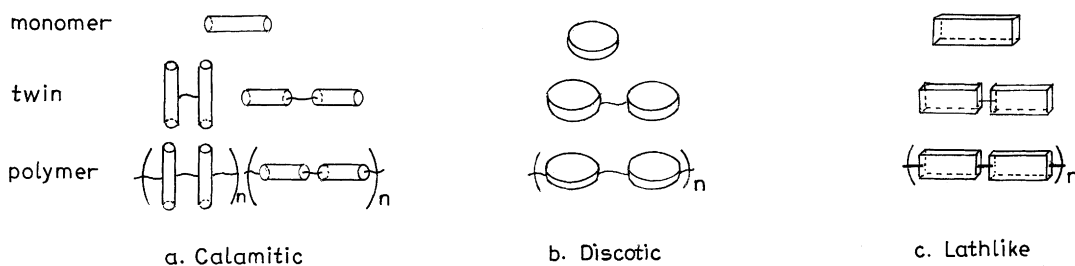


Fig. 2. Geometrical structure of liquid crystalline molecules.

polar and non-polar solvents. Good examples are soaps and various phospholipids. Both of these classes of compounds have a polar “head” group attached to a hydrocarbon “tail” group. When dissolved in a polar solvent (e.g. water), the hydrophobic tails assemble together and form the hydrophilic “heads” to the solvent. The resulting structure for soap molecules is called a “micelle” (Fig. 3a) and for phospholipids is called a “vesicle” (Fig. 3b). Both soap and phospholipids molecules also form a bilayer structure, with the hydrocarbon chains separated from the water by the “head” groups. These lamellar phases are of extreme importance, for example, in the case of phospholipids such a lipid bilayer is the structure unit for biological membranes. When these amphiphilic molecules are mixed with a non-polar solvent (e.g. hexane) similar structures result but now the polar “heads” assemble together with the non-polar “tail” groups in contact with the solvent. These are called the reversed phases (Fig. 3c).

Liquid crystals are also derived from certain macromolecules (e.g. long-chain polymers), usually in solution but sometimes even in the pure state. They are known as “liquid crystal polymers (LCPs)” [20,21,23–27]. The polymers are long-chain molecules formed by the repetition of certain basic units or segments known as monomers. Polymers having identical, repeating monomer units are called “homopolymers” whereas those formed from more than one polymer type are called

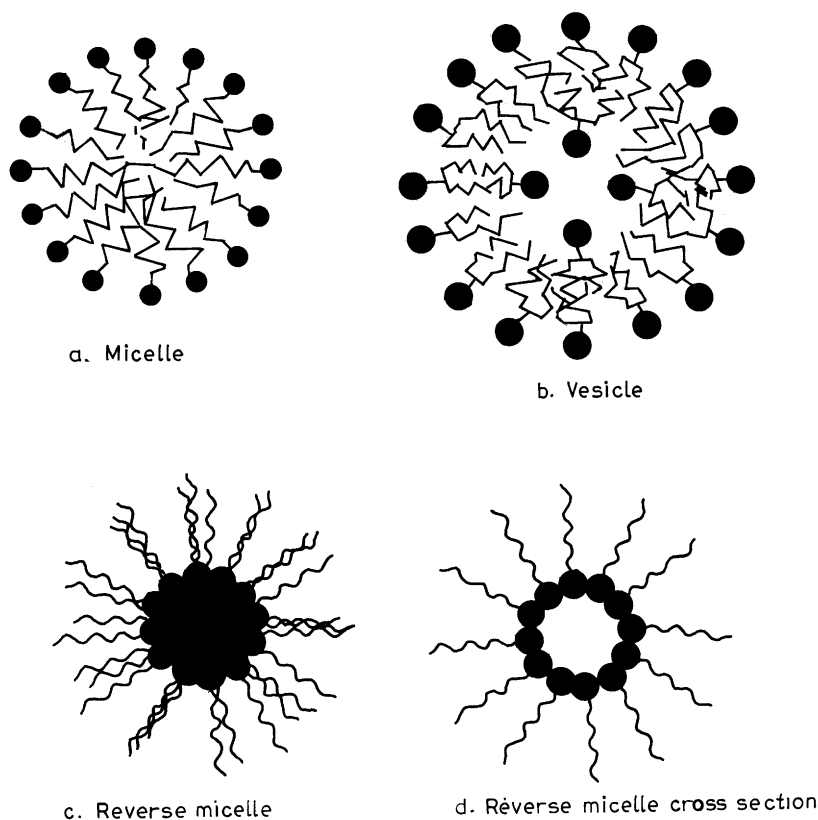


Fig. 3. Structures formed by amphiphilic molecules.

“copolymers”. In a copolymer the monomers may be arranged in a random sequence, in an alternating sequence, or may be grouped in blocks. The low molar mass mesogens can be used as monomers in the synthesis of liquid crystal polymers. On the basis of molecular anisotropy two types of structure are possible (Fig. 4) [20,21,35]. In the first type the macromolecule as a whole has a more or less rigid form, whereas in the second class only the monomer unit possesses a mesogenic structure connected to the rest of molecule via a flexible spacer. In the first kind, the mesomorphism is due to rigid macromolecule as a whole or from several monomer units made up of rigid chain segments. The dominant factor in the second class is the structure of the individual monomer units which make up the flexible macromolecule.

On the basis of the location of the mesogenic group LCPs are divided into two kinds: main-chain liquid crystal polymers (MCLCPs) and side-chain liquid crystal polymers (SCLCPs). Fig. 4 shows all types of LCP which have been chemically synthesized or whose behaviour has been studied. A rigid MCLCP can be derived if known low molar mass rod or disc-shaped mesogenic molecules can be joined rigidly to one another. A calamitic macromolecule can also be derived from the disc shaped monomer units. This type of structure also results from flexible macromolecules, which form a rigid helical superstructure, via hydrogen-bonded compounds. When the linking units are long and flexible a semiflexible polymer is derived. The degree of flexibility and the structural composition both determine the mesomorphic properties of MCLCPs. The side-chain LCPs were derived in 1978 by inserting a flexible spacer unit between the rigid mesogenic unit and the polymer backbone. In SCLCPs the flexible polymer backbone has a strong tendency to adopt a random,




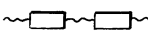

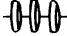
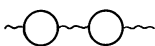
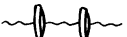
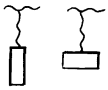

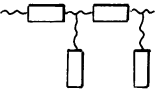
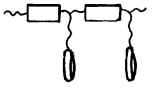
Calamitic	Discotic	
<p>Rigid Main Chain</p>   <p>Flexible Main Chain</p>  	   	LC Main Chain Polymers
		LC Side Chain Polymers
		Combined LC Polymers

Fig. 4. Schematic representation of the different types of liquid crystal polymers.

coiled conformation. When mesogenic units are attached to the flexible polymer backbone, they will have a strong tendency to adopt an anisotropic arrangement. Clearly, these two features are completely antagonistic, and where the mesogenic groups are directly attached to the backbone, the dynamics of the backbone usually dominate the tendency for the mesogenic groups to orient anisotropically; accordingly, mesomorphic behaviour is not usually exhibited. However, if a flexible spacer moiety is employed to separate the mesogenic units from the backbone, then the two different tendencies of the mesogen (anisotropic orientation) and backbone (random arrangement) can be accommodated within one polymeric system. According to this theory, the backbone should not influence the nature and thermal stabilities of the mesophases, but this is not true because the spacer unit does not totally decouple the mesogenic unit from the backbone. However, enhanced decoupling is generated as the spacer moiety is lengthened.

The nature of the mesophase depends sensitively on the backbone, the mesogenic unit and the spacers. Polymers invariably consist of a mixture of chain lengths, the size and distribution of which depend on the structural unit present and the synthesis procedure. Accordingly, there is no such thing as pure polymer and the average size of each chain is often referred to as the “degree of polymerization (DP)”. A polydispersity of one (monodisperse) denotes that all of the polymer chains are identical in size.

1.2. Classification of liquid crystals: symmetry and structures

The symmetry of liquid crystalline phases can be categorized in terms of their orientational and translational degrees of freedom. The nematic, smectic and columnar phase types (characteristic features are given below) possess, respectively, 3, 2 and 1 translational degrees of freedom, and within each type there can exist different phases depending on the orientational or point group symmetry. The point group symmetries of common liquid crystal phases are listed in Table 1. Only those phases are included which have well-established phase structures; so-called crystal smectic phases have been omitted. As discussed below, it can be seen from Table 1 that most nematics, orthogonal smectics and columnar phases are uniaxial having two equal principal refractive indices, while the tilted smectic and columnar phases are biaxial, with all three different principal refractive indices.

1.2.1. Non-chiral calamitic mesophases

Following the nomenclature as proposed originally by Friedel [36], the liquid crystals of non-chiral calamitic molecules are generally divided into two types — nematics and smectics [3–22,37].

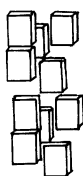
1.2.1.1. Nematic phases. The nematic phase of calamitics is the simplest liquid crystal phase. In this phase the molecules maintain a preferred orientational direction as they diffuse throughout the sample. There exists no positional order. Fig. 5a–d shows the nematic phases occurring in different types of substance. An isotropic liquid possesses full translational and orientational symmetry $T(3) \times O(3)$. In case of isotropic liquid-nematic (IN) transition the translational symmetry $T(3)$ remains as in isotropic liquid, but the rotational symmetry $O(3)$ is broken. In the simplest structure the group $O(3)$ is replaced by one of the uniaxial symmetry groups D_∞ or $D_{\infty h}$ and the resulting phase is the uniaxial nematic phase N_u (Fig. 5a) with symmetry $T(3) \times D_{\infty h}$. The molecules tend to

Table 1
Symmetries of common liquid crystal phase types

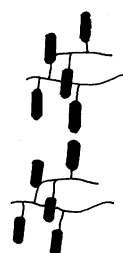
Liquid crystal phase	Point group and translational degrees of freedom	Optical symmetry uniaxial (u(+), u(–)), biaxial (b), helicoidal (h)
I. Achiral phases:		
Calamitic, micellar, nematic N or N _u	D _{∞h} × T (3)	u (+)
Nematic discotic (N _D), columnar nematic N _C	D _{∞h} × T (3)	u (–)
Biaxial nematic (N _b)	D _{2h} × T (3)	b
Calamitic orthogonal smectic or lamellar phase (S _A)	D _{∞h} × T (2)	u (+)
Tilted smectic phase (S _C)	C _{2h} × T (2)	b
Orthogonal and lamellar hexatic phase (S _B)	D _{6h} × T (1) locally D _{6h} × T (2) globally	u (+)
Tilted and lamellar hexatic phases (S _F and S _I)	C _{2h} × T (1 or 2)	b
Discotic columnar: hexagonal order of columns, ordered or disordered within columns (D _{ho} or D _{hd})	D _{6h} × T (1)	u (–)
Rectangular array of columns (D _{ro} or D _{rd})	D _{2h} × T (1)	b
Molecules tilted within columns (D _{to} or D _{td})	C _{2h} × T (1)	b
II. Chiral phases:		
Tilted nematic or cholesteric (N _t or N*)	D _∞ × T (3)	b, h, locally biaxial but globally u (–)
Tilted smectic C phase (S _C [*])	C ₂ × T(2)	b, h
Tilted and lamellar hexatic phases (S _F [*] and S _I [*])	C ₂ × T (1 or 2)	b, h



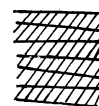
a. Nematic



b. Biaxial nematic



c. Comblike polymer



d. Lyotropic nematic

Fig. 5. The arrangement of molecules in nematic phases of nonchiral calamitic mesogens: (a) uniaxial nematic phase, (b) biaxial nematic phase, (c) nematic phase of a comblike polymer, and (d) lyotropic nematic of a stiff polymer.

align along the director \hat{n} . A biaxial nematic phase N_b may result due to the further breaking of the rotational symmetry of the system around the director \hat{n} . The existence of this phase was originally predicted on a theoretical basis [38,39]. The first N_b phase was observed in the ternary amphiphilic

system composed of potassium laurate, 1-decanol and D_2O [40] and later on it could also be derived in some relatively simple thermotropic compounds [41,42]. In the N_b case different symmetry groups, which are subgroup of $O(3)$, are in principle admissible, orthorhombic, triclinic, hexagonal or cubic. Fig. 5b illustrates the biaxial nematic phase existing in compounds with lath-like molecules ($T(3) \times D_{2h}$ symmetry). In this phase the rotation around the long axis is strongly hindered. Fig. 5c shows the structure of the nematic phase of comb-like liquid crystal polymer in which the mesophase moieties attached to the polymeric chain as the side groups have parallel orientation. The main chain may possess a liquid-like structure. Fig. 5d illustrates the lyotropic nematic phase of a rigid polymer in solution in which the rigid main chains are nearly parallel and separated by the solvent.

1.2.1.2. Smectic phases. When the crystalline order is lost in two dimensions, one obtains stacks of two-dimensional liquids: such systems are called smectics. The smectic liquid crystals have layered structures, with a well-defined interlayer spacing which can be measured by X-ray diffraction. The smectic molecules exhibit some correlations in their positions in addition to the orientational ordering. In most smectics the molecules are mobile in two directions and can rotate about one axis. The interlayer attractions are weak compared to the lateral forces between the molecules, and the layers are able to slide over one another relatively easily. This gives rise to fluid property to the system with higher viscosity than nematics.

A smectic can be defined by its periodicity in one spatial direction and by its point group symmetry. A priori no point group is forbidden. As a result an infinite number of smectic phases can be expected. The observed smectic phases differ from each other in the way of layer formation and the existing order inside the layers. The simplest is the smectic A (S_A) phase with symmetry $T(2) \times D_{\infty h}$. In this phase the average molecular axis is normal to the smectic layers (Fig. 6a).

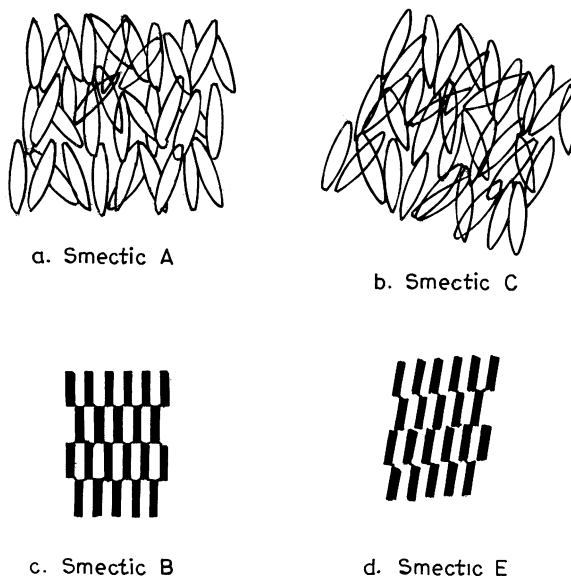


Fig. 6. The arrangement of molecules in smectic phases of nonchiral calamitic mesogens.

Within each layer the centre of gravity of molecules are ordered at random in a liquid-like fashion and they have considerable freedom of translation and of rotation around their long axis. Thus, the structure may be defined as an orientationally ordered fluid on which is superimposed a one-dimensional density wave. The flexibility of layers leads to distortions which give rise to beautiful optical patterns known as focal conic textures. When temperature is decreased, the S_A phase may transform into a phase possessing even lower symmetry. The breaking of $D_{\infty h}$ symmetry may lead to the appearance of tilting of molecules relative to the smectic layers. The phase thus derived is called smectic C (S_C) (Fig. 6b) which possesses the symmetry $T(2) \times C_{2h}$.

There exist several types of smectic phase with layer structures in which the molecules inside the layer possess effective rotational symmetry around their long axes and are arranged in a hexagonal (S_B) or pseudo-hexagonal (S_F , S_G , S_I , S_J) manner. In a S_B phase (Fig. 6c) the molecules are orthogonal with respect to the layer plane whereas in other phases they are tilted. The existence of S_B phase and other phase types of higher order has also been observed in polymeric liquid crystals. Several smectic phases in which the rotation around the long-molecular axes is strongly hindered have also been observed. The highly ordered molecules produce an orthorhombic lattice if the long axes of the molecules are orthogonal with respect to the layer planes (S_E , Fig. 6d) and a monoclinic lattice in case of a tilted arrangement of the long axes (S_H and S_K). Due to the three-dimensional order in these phases they are also considered as solids. Table 1 lists the various phases together with a few of their most important properties. The smectic D (S_D) phase is not included in this table because it is a cubic phase and thus does not form layers. The S_B (hexatic), S_I and S_F phases are 2D in character, i.e., inside the layers the molecules are oriented on a 2D lattice having no long-range correlations. The higher order smectic phases S_L (or S_B crystal), S_J , S_G , S_E , S_K , S_H possess 3D long-range order and therefore are also known as “crystal smectics”. In S_L , S_J and S_G the rotation of molecules around the molecular long axis is strongly hindered. In the S_E , S_K and S_H phases the rotational hindrance around the long axes is so strong that only 180° jumps between two favoured positions are possible.

1.2.2. Chiral calamitic phases

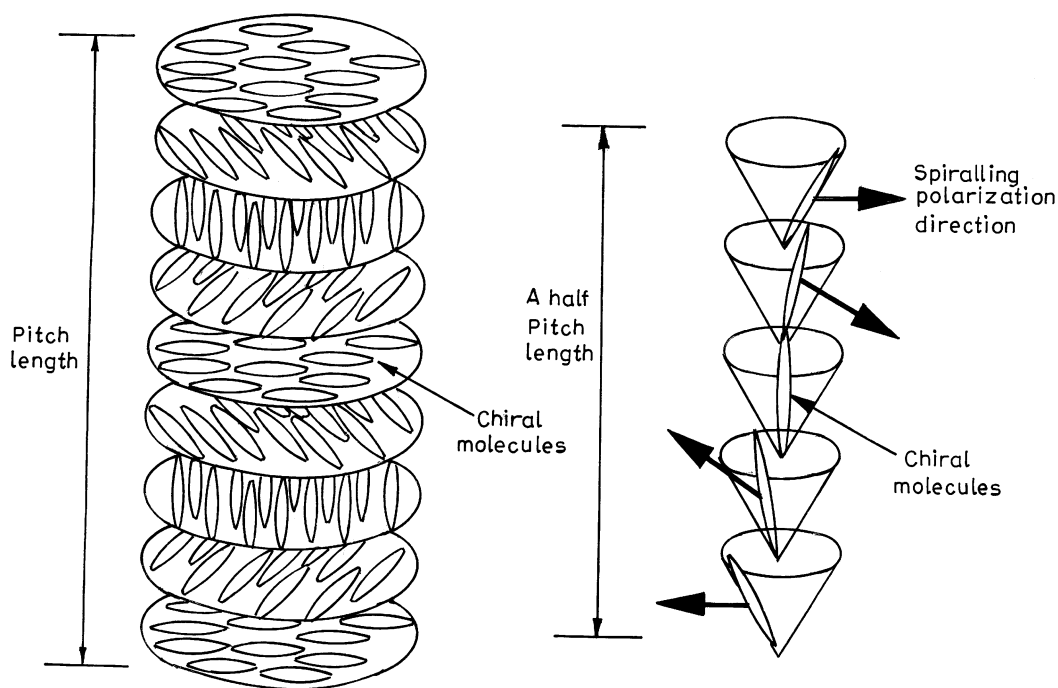
If the liquid crystal molecules are chiral (lacking inversion symmetry), then chiral phases are observed instead of certain non-chiral phases. The most important mesophases occurring in chiral materials are listed in Table 2.

1.2.2.1. Non-ferroelectric phases. In calamitics, the uniaxial nematic phase is replaced by the chiral nematic phase in which the director rotates about an axis perpendicular to the director leading to a helical structure (Fig. 7a). Hence, the name twisted nematic (N_t or N^*) or cholesteric is given to this phase. Due to the helical structure this phase possesses special optical properties which makes the material very useful in practical applications. Below their clearing point anomalous phases appear in many of them which are collectively known as “blue phases” [21,43,44]. Blue phases (BPs) occur in a narrow temperature range between the cholesteric and isotropic phases. In many chiral compounds with sufficiently high twist upto three distinct blue phases appear. The two low-temperature phases, blue phase I (BPI) and blue phase II (BP II), have cubic symmetry, while the highest temperature phase, blue phase III (BP III), appears to be amorphous.

Table 2
Mesophases in chiral materials

Phase type	Ordering	Molecular orientation	Molecular packing
<i>Nonferroelectric types</i>			
N_t (or N^*)	Helical nematic structure	Uniaxial	—
Blue phases	Cubic structure	—	—
<i>Ferroelectric smectics</i>			
S_C^*	Helical, short-range	Tilted	Random
S_I^*	No layer correlation	Tilted to side	Pseudo-hexagonal
	Short-range in-plane correlation		
S_F^*	Helical structure	Tilted to apex	Pseudo-hexagonal
S_J^*	Long-range layer correlation	Tilted to apex	Pseudo-hexagonal
	Long-range in-plane correlation		
S_C^*	No helical structure	Tilted to side	Pseudo-hexagonal
S_K^*	Long-range layer correlation	Tilted to side	Herring-bone
	Long-range in-plane correlation		
S_H^*	No helical structure	Tilted to apex	Herring-bone

1.2.2.2. Ferroelectric smectic phases. All of the smectic phases with tilted structure exhibit ferroelectric properties. Due to their low symmetry they are able to exhibit spontaneous polarization and piezoelectric properties and are known as ferroelectric liquid crystals. It is well established that any tilted smectic phase derived from chiral molecules should possess a permanent electric polarization \mathbf{P} which is oriented perpendicular to the director \hat{n} and parallel to the smectic layer plane. The presence of permanent dipoles fundamentally alters the nature of the interactions between the molecules themselves and with any cell wall or applied electric field. The ferroelectric smectic-C* (S_C^*) phase (Fig. 7b) has become very important for its fast electronic switching of the twist of the layers with respect to tilt direction. The optical activity in this phase arises as a result of molecular asymmetry. A macroscopic helical arrangement of molecules occurs as a result of precession of the molecular tilt about an axis perpendicular to the layer planes. The tilt direction is rotated through an azimuthal angle upon moving from one layer to the next. As the rotation is in a constant direction, a helix is formed which is either left- or right-handed. The helical twist sense is determined by the nature and position of the chiral centre with respect to the central core of other mesogenic material. One 360° rotation of the helix for the S_C^* phase usually extends over hundreds of layers and the azimuthal angle is generally found to be of the order of 0.1 – 0.01° .



a. Twisted nematic

b. Chiral smectic C

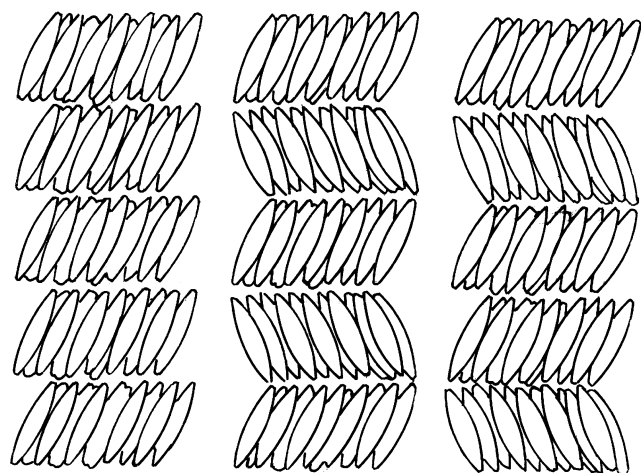
b. Ferroelectric
chiral smectic Cc. Antiferroelectric
chiral smectic Cd. Ferrielectric
chiral smectic C

Fig. 7. The arrangement of molecules in chiral calamitic mesogens: (a) twisted nematic or cholesteric (b) chiral smectic C(S_C^*), Arrow shows the direction of spontaneous polarization, (c) antiferroelectric, and (d) ferrielectric.

1.2.2.3. Antiferroelectric and ferrielectric phases. Two new associated phenomena [45–47] were observed which show fundamental differences to the situations existing in S_C^* phase. This led to two different arrangements of the molecules in their layer planes from that seen in S_C^* phase with associated variations in polarization directions. These new phases are known as antiferroelectric (Fig. 7c) and ferrielectric phases (Fig. 7d). From the suggested structure (Fig. 7c) in an antiferroelectric smectic C^* phase the molecular layers are arranged in such a way that the polarization directions in subsequent layers point in opposite directions which result in an average of the spontaneous polarization equal to zero. This structure is evidenced by the fact that when a strong electric field is applied to this phase, the layer ordering is perturbed and the phase returns to a normal ferroelectric phase. In the switching of antiferroelectric phases three states are produced: one antiferroelectric and two ferroelectric. This tristable switching occurs at a defined electric field and thus the presence of a sharp switching threshold may be useful in display applications which require multiplexing with grey scales. The structure of ferroelectric S_C^* is repeated every 360° rotation of the helix, whereas the helical structure of the antiferroelectric phase repeats every 180° rotation. The phase, therefore, appears to have a relatively short pitch and the pitch appears to change quite significantly as the temperature is changed.

In a ferrielectric smectic phase (Fig. 7d), the layers are stacked in such a way that there is a net overall spontaneous polarization. The number of layers of opposite polarization is not equal. There could be, for example, twice as many layers where the polarization direction is opposite to that of the other layer type. It also has been suggested that the stacking of the layers has two interpenetrating sublattices. There will be alternating layer structures, i.e., two layer tilted to the right and one to the left, with this arrangement repeating itself through the bulk of the phase. Thus, the ferrielectric phase will have a measurable polarization.

1.2.3. Discotic liquid crystals

In case of mesogens composed of disc-shape molecules, when the crystalline order is lost in one direction (i.e. the system is melted in one dimension), one obtains aperiodical stack of discs in columns; such systems are called discotics or columnar phases. The different columns constitute a regular 2D array and hence the structure has translational periodicity in two dimensions, but not in three. A number of variants of this columnar structure have been identified and analysed systematically in terms of 2D (planar) crystallographic space groups. The fact that the system is a 1D liquid indicates only the absence of correlations in the arrangement of the centres of mass of the molecules along a straight line. On the basis of structures clearly identified so far, the discotics fall into two distinct categories: the nematic and the columnar (Fig. 8). A smectic-like phase is also reported but the precise arrangement of the molecules in each layer is not yet fully understood. In the columnar structures the molecules are stacked upon each other, building columns which may be arranged in hexagonal, tetragonal and tilted variants. Along the axes of the columns, long-range order or disorder of the molecules can exist.

2. Order parameters

As discussed in the previous section, the most fundamental characteristic of a liquid crystal is the presence of long-range orientational order while the positional order is either limited (smectic

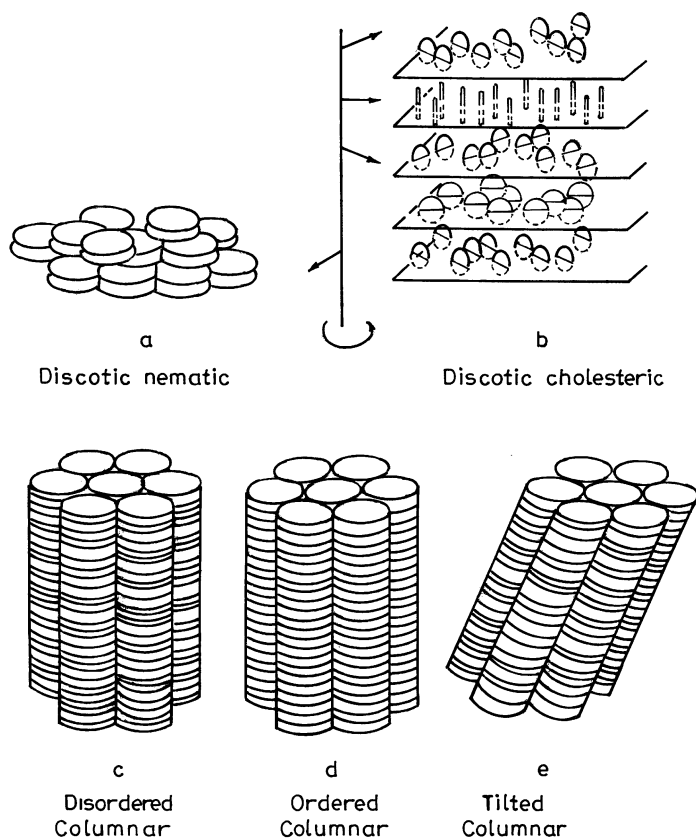


Fig. 8. The arrangement of molecules in discotic liquid crystals.

phases) or absent altogether (nematic phases). One phase differs from another with respect to its symmetry. The transition between different phases corresponds to the breaking of some symmetry and can be described in terms of the so-called order parameter (OP). It represents the extent to which the configuration of the molecules in the less symmetric (more ordered) phase differs from that in the more symmetric (less ordered) one. In general, an order parameter describing a phase transition, must satisfy the following requirements:

- (i) $Q = 0$, in the more symmetric (less ordered) phase, and
- (ii) $Q \neq 0$, in the less symmetric (more ordered) phase.

These requirements do not define the order parameter in a unique way. In spite of this arbitrariness, in many cases the choice follows in a quite natural way. In the case of liquid–vapour transition the order parameter is the difference in density between liquid and vapour phases and is a scalar. In the case of ferromagnetic transitions without anisotropic forces, the order parameter is the magnetization which is a vector with three components. In more complicated cases the choice of order parameters requires some careful considerations.

2.1. Definition of microscopic order parameters

Order parameters constructed in relation to a specific molecular model which can give a microscopic description of the system, are known as microscopic order parameters. By definition these order parameters may contain more information than just the symmetry of the phase. Various approaches have been adopted to define them. Here we introduce the order parameters of different mesophases as expansion coefficients of the singlet distribution in a suitable basis set [37,48,49]. In case the distribution depends on the positions and orientations, we define orientational, positional and mixed (orientational-positional) order parameters. The single-particle distribution function $\rho^{(1)}$ ($\equiv \rho(\Omega)$), which measures the probability of finding a molecule at a particular position and orientation, is the best candidate to be used for defining the order parameters. The singlet distribution can be defined as

$$\rho(\mathbf{r}, \Omega) = \left(\frac{N}{V} \right) \sum_{\mathbf{G}} \sum_{\ell, m, n} (2\ell + 1) e^{-i\mathbf{G} \cdot \mathbf{r}} D_{m,n}^{\ell}(\Omega) \langle e^{-i\mathbf{G} \cdot \mathbf{r}'} D_{m,n}^{\ell*}(\Omega') \rangle . \quad (2.1)$$

Here \mathbf{r} and Ω are field variables (fixed points in space) and therefore, unlike the dynamical variables \mathbf{r}' and Ω' are not affected by the ensemble average. The functions $D_{m,n}^{\ell}(\Omega)$ are the Wigner rotation matrices, $\langle \rangle$ represents the ensemble average and \mathbf{G} the set of reciprocal lattice vectors of the crystalline phase.

Eq. (2.1) can be written as

$$\rho(\mathbf{r}, \Omega) = \rho_0 \sum_{\mathbf{G}} \sum_{\ell, m, n} Q_{\ell mn}(\mathbf{G}) e^{-i\mathbf{G} \cdot \mathbf{r}} D_{m,n}^{\ell}(\Omega) , \quad (2.2)$$

where

$$\begin{aligned} Q_{\ell mn}(\mathbf{G}) &= (2\ell + 1) \langle e^{-i\mathbf{G} \cdot \mathbf{r}} D_{m,n}^{\ell*}(\Omega) \rangle \\ &= \bar{Q}_{m,n}^{\ell*} \\ &= \left(\frac{2\ell + 1}{N} \right) \int \rho(\mathbf{r}, \Omega) e^{-i\mathbf{G} \cdot \mathbf{r}} D_{m,n}^{\ell*}(\Omega) d\mathbf{r} d\Omega \end{aligned} \quad (2.3)$$

are recognized as the order parameters.

From Eq. (2.3) the following order parameters can be defined:

$$Q_{000}(0) = 1 , \quad (2.4a)$$

$$Q_{000}(\mathbf{G}) = \bar{\mu}_G = \left(\frac{1}{N} \right) \int d\mathbf{r} d\Omega \rho(\mathbf{r}, \Omega) e^{-i\mathbf{G} \cdot \mathbf{r}} , \quad (2.4b)$$

$$Q_{\ell 00}(\mathbf{G}) \equiv (2\ell + 1) \bar{\tau}_{G\ell} = \left(\frac{2\ell + 1}{N} \right) \int d\mathbf{r} d\Omega \rho(\mathbf{r}, \Omega) e^{-i\mathbf{G} \cdot \mathbf{r}} P_{\ell}(\cos \theta) , \quad (2.4c)$$

$$Q_{\ell mn}(0) \equiv (2\ell + 1) \bar{D}_{mn}^{\ell*} = \left(\frac{2\ell + 1}{N} \right) \int d\mathbf{r} d\Omega \rho(\mathbf{r}, \Omega) D_{mn}^{\ell*}(\Omega) . \quad (2.4d)$$

Here $\bar{\mu}_G$ are the positional order parameters for a monatomic lattice which is characterized by the set of reciprocal lattice vectors $\{\mathbf{G}\}$. $Q_{\ell mn}(0)$ (or $\bar{D}_{mn}^{\ell*}$) are the orientational order parameters and $Q_{\ell 00}(G)$ (or $\bar{\tau}_{G\ell}$) the mixed (orientational-positional) order parameters. It may be noted that there can be upto $(2\ell + 1)^2$ order parameters of rank ℓ . Exploiting the symmetry properties of the mesophase and of its constituent molecules and applying the effects of all the operations of the relevant space groups of the symmetry the number of order parameters can be drastically reduced [50].

In the uniaxial mesophases (e.g. N_u and S_A phases) the singlet distribution must be invariant under rotation about the director. If the director is chosen to be along the Z -axis, it follows that m must be zero in $Q_{\ell mn}$ (or $\bar{D}_{mn}^{\ell*}$). In addition, if the mesophase has a symmetry plane perpendicular to the director ($D_{\infty h}$ symmetry) only terms with even ℓ can appear in $Q_{\ell mn}$. The most important order parameters are the orientational ones defined as

$$\bar{D}_{0,n}^{\ell*} = \int d\Omega f(\Omega) D_{0,n}^{\ell}(\Omega) , \quad (2.5)$$

where the orientational singlet distribution function, defined as

$$f(\Omega) = \left(\frac{V}{Z_N} \right) \int \exp[- \beta U(\mathbf{x}_1, \mathbf{x}_2, \dots, \mathbf{x}_N)] d\mathbf{x}_2 d\mathbf{x}_3 \dots d\mathbf{x}_N \quad (2.6)$$

is normalized to unity,

$$\int f(\Omega) d\Omega = 1 . \quad (2.7)$$

$U(\mathbf{x}_1, \mathbf{x}_2, \dots, \mathbf{x}_N)$ is the potential energy of N particles and $\beta = 1/k_B T$ with k_B the Boltzmann constant. Z_N is the configurational partition function of the system,

$$Z_N = \int d\mathbf{x}_1 d\mathbf{x}_2 \dots d\mathbf{x}_N \exp [- \beta U(\mathbf{x}_1, \mathbf{x}_2, \dots, \mathbf{x}_N)] . \quad (2.8)$$

Here the \mathbf{x}_i ($= r_i, \Omega_i$) specify both the location \mathbf{r}_i of the centre of the i th molecule and its relative orientation Ω_i described by the Euler angles $(\theta_i, \phi_i, \psi_i)$. In Eqs. (2.6) and (2.8) we have used only one integration sign to indicate the possible multiple integration over all the variables whose volume elements appear.

If one assumes that the mesogenic molecules also possess cylindrical symmetry, the rotation about the molecular symmetry axis may not modify the distribution, i.e., $n = 0$ and $f(\Omega)$ has to depend only on the angle θ between the director and the molecular symmetry axis. Accordingly, we get

$$\bar{D}_{0,0}^{\ell*} (\equiv \bar{P}_{\ell}) = \int d\Omega f(\theta) P_{\ell}(\cos \theta) , \quad (2.9)$$

where the \bar{P}_{ℓ} , the ensemble average of the even Legendre polynomials, are known as the Legendre polynomial orientational order parameters. Thus, from the knowledge of $f(\Omega)$ all the orientational order parameters \bar{P}_2, \bar{P}_4 , etc., can be calculated.

For uniaxial mesophase composed of molecules of non-cylindrical symmetry some of the important orientational order parameters are given by

$$\bar{D}_{0,0}^{2*} = \bar{P}_2 = \langle P_2(\cos \theta) \rangle, \quad (2.10a)$$

$$\bar{D}_{0,2}^{2*} = \left\langle \frac{\sqrt{3}}{2} \sin^2 \theta \cos 2\phi \right\rangle, \quad (2.10b)$$

$$\bar{D}_{0,0}^{4*} = \bar{P}_4 = \langle P_4(\cos \theta) \rangle. \quad (2.10c)$$

It should be mentioned that \bar{P}_ℓ measures the alignment of the molecular \hat{e}_z axis along the space-fixed (SF) Z-axis (or the director). The order parameter $\bar{D}_{0,2}^{2*}$ is an indicator of the difference in the alignment of the molecular axes \hat{e}_x and \hat{e}_y along the director. When the mesogenic molecules possess axial symmetry, the molecular axes \hat{e}_x and \hat{e}_y are indistinguishable and the order parameters $\bar{D}_{0,2}^{2*}$, $\bar{D}_{0,2}^{4*}$, etc., vanish.

For the smectic phase with positional order in one dimension only, the singlet distribution simplifies to

$$\rho(\mathbf{r}, \Omega) = \rho_0 \sum_G \sum_{\ell, m, n} (2\ell + 1) \bar{D}_{mn}^{\ell*}(\mathbf{G}) \exp[iG_z z] D_{m,n}^{\ell}(\Omega), \quad (2.11)$$

where the Z-axis is parallel to the layer normal. Again Eq. (2.11) can be simplified by using the symmetry of the phase and the constituent molecules. For the S_A phase which has symmetry $T(2) \times D_{\infty h}$ and is composed of cylindrically symmetric molecules,

$$\rho(\mathbf{r}, \Omega) = \rho_0 \sum_{\ell}' \sum_q (2\ell + 1) \bar{D}_{0,0}^{\ell*}(q) \cos[2\pi q z / \xi_0] P_{\ell}(\cos \theta), \quad (2.12)$$

where $|G| = 2\pi q / \xi_0$, with ξ_0 being the average interlayer spacing. The prime on the summation sign indicates the condition that ℓ is even. Here $\bar{D}_{0,0}^{\ell*}(q) = \bar{\mu}_q$ and $\bar{D}_{0,0}^{\ell*}(0) = \bar{P}_{\ell}$ represent, respectively, the positional and orientational order parameters. $\bar{D}_{0,0}^{\ell*}(q) (\equiv \bar{\tau}_{q\ell})$ is the mixed (positional-orientational) order parameter.

The order parameters for the biaxial mesophases (e.g., biaxial nematic, smectic-C, etc.) can be defined by Eq. (2.3). In defining order parameters for these phases it usually is assumed that the ordered phases have the same symmetry as the constituent molecules. Thus, to characterize a biaxial nematic (N_b) phase the following orientational order parameters can be identified [51,52].

$$\bar{P}_2 = \bar{D}_{0,0}^{2*} = \langle \frac{1}{2}(3 \cos^2 \theta - 1) \rangle \equiv \langle P_2(\cos \theta) \rangle, \quad (2.13a)$$

$$\bar{\eta}_2 = \bar{D}_{0,2}^{2*} = \left\langle \frac{\sqrt{3}}{2} \sin^2 \theta \cos 2\psi \right\rangle, \quad (2.13b)$$

$$\bar{\mu}_2 = \bar{D}_{2,0}^{2*} = \left\langle \frac{\sqrt{3}}{2} \sin^2 \theta \cos 2\phi \right\rangle. \quad (2.13c)$$

and

$$\bar{\tau}_2 = \bar{D}_{2,2}^{2*} = \langle \frac{1}{2}(1 + \cos^2 \theta) \cos 2\phi \cos 2\psi - \cos \theta \sin^2 \phi \cos 2\psi \rangle. \quad (2.13d)$$

The order parameter \bar{P}_2 measures the alignment of the molecular \hat{e}_z -axis along the director, whereas $\bar{\eta}_2$ measures the departure in the alignment of the molecular \hat{e}_x and \hat{e}_y axes along the director. The other two order parameters $\bar{\mu}_2$ and $\bar{\tau}_2$ are a measure of the biaxial ordering existing in the system.

For the smectic-C phase with positional order in one dimension only, the singlet distribution is defined by Eq. (2.11) and the corresponding order parameters are identified as the positional $\bar{\mu}_q$, the orientational $\bar{D}_{0,0}^{2*}$, $\bar{D}_{0,2}^{2*}$, $\bar{D}_{2,0}^{2*}$, and $\bar{D}_{2,2}^{2*}$, and the mixed order parameter $\bar{\tau}_{q\ell}$.

2.2. Definition of a macroscopic order parameters

In most cases, the microscopic order parameters, as defined above, provide an adequate description of real mesogenic systems. However, in some cases, this microscopic description is no longer adequate and some other means must be found for specifying the degree of order. A significant difference between the high-temperature isotropic liquid and the liquid crystalline phase is observed in the measurements of all macroscopic tensor properties. Thus all macroscopic properties, e.g., the diamagnetic susceptibility, the refractive index, the dielectric permittivity, can be used to identify the macroscopic order parameter. As an example, we consider the diamagnetic susceptibility. The relationship between magnetic moment \mathbf{M} (due to the molecular diamagnetism) and the field \mathbf{H} has the form

$$M_\alpha = \chi_{\alpha\beta} H_\beta, \quad (2.14)$$

where $\alpha, \beta = x, y, z$, $\chi_{\alpha\beta}$ is an element of the susceptibility tensor χ . When the field \mathbf{H} is static, the tensor $\chi_{\alpha\beta}$ is symmetric ($\chi_{\alpha\beta} = \chi_{\beta\alpha}$). In the isotropic phase it has the simple form

$$\chi_{\alpha\beta} = \chi \delta_{\alpha\beta}. \quad (2.15)$$

For the uniaxial nematic phase, where the Z -axis is parallel to the nematic axis, χ can be written in the diagonal form

$$\chi = \begin{vmatrix} \chi_\perp & 0 & 0 \\ 0 & \chi_\perp & 0 \\ 0 & 0 & \chi_\parallel \end{vmatrix}. \quad (2.16)$$

χ_\parallel and χ_\perp are the susceptibilities parallel and perpendicular to the symmetry axis, respectively.

One finds from a comparison between Eqs. (2.15) and (2.16) that the anisotropic part of the diamagnetic susceptibility fulfills the requirement imposed on an order parameter,

$$\Delta\chi_{\alpha\beta} = \chi_{\alpha\beta} - \frac{1}{3}\chi\delta_{\alpha\beta}. \quad (2.17)$$

Thus, an order parameter tensor \mathbf{Q} can be defined as

$$Q_{\alpha\beta} = \Delta\chi_{\alpha\beta} / \Delta\chi_{\max}, \quad (2.18)$$

where $\Delta\chi_{\max}$ is the maximum anisotropy that would be observed for a perfectly ordered mesophase.

The definition (2.18) of the order parameter \mathbf{Q} covers a wider class of liquid crystals than simple uniaxial nematics. In general, \mathbf{Q} , is an arbitrary symmetric traceless second-rank tensor. Hence, it

has five independent elements. In a reference frame where \mathbf{Q} is diagonal,

$$\mathbf{Q} = \begin{vmatrix} -\frac{1}{2}(x+y) & 0 & 0 \\ 0 & -\frac{1}{2}(x-y) & 0 \\ 0 & 0 & x \end{vmatrix}. \quad (2.19)$$

Here the condition of zero trace is automatically fulfilled. In addition, it allows the possibility that all the three eigenvalues are different, $x \neq 0$, $y \neq 0$. This corresponds to a biaxial nematic phase. For the N_u phase, $x \neq 0$, $y = 0$, and $x = y = 0$ corresponds to the isotropic liquid phase.

In an arbitrary reference frame, $Q_{\alpha\beta}$ is given in terms of the parameters x and y , by

$$Q_{\alpha\beta} = \frac{3}{2}x(n_\alpha n_\beta - \frac{1}{3}\delta_{\alpha\beta}) - \frac{1}{2}y[m_\alpha m_\beta - (\hat{n} \times \hat{m})_\alpha (\hat{n} \times \hat{m})_\beta], \quad (2.20)$$

where \hat{n} , \hat{m} and $\hat{n} \times \hat{m}$ are the orthogonal eigenvectors of \mathbf{Q} corresponding to the eigenvalues x , $-\frac{1}{2}(x+y)$ and $-\frac{1}{2}(x-y)$, respectively.

2.3. Relationship between macroscopic and microscopic order parameters

When the molecules can be approximately taken as rigid, one may find a simple connection between the macroscopic tensor associated with \mathbf{Q} and the microscopic quantities defining the microscopic order parameter $\bar{Q}_{m,n}^*$ ($\equiv \mathbf{Q}^M$). In fact, the level of knowledge is not the same for all the macroscopic tensor properties. Like the macroscopic order parameter \mathbf{Q} the microscopic order parameter \mathbf{Q}^M is the symmetric traceless second-rank tensor that can be brought on a principal axis. We should mention that only in some simple cases there is a straightforward connection between the macroscopic and microscopic approaches.

A relationship between \mathbf{Q} and \mathbf{Q}^M can be written for the case of a rigid rod model by noting that the anisotropic part of the diamagnetic susceptibility is proportional to $Q_{\alpha\beta}^M$:

$$\Delta\chi_{\alpha\beta} = N\chi_a Q_{\alpha\beta}^M, \quad (2.21)$$

where N is the particle density number and χ_a is the anisotropy of the molecular magnetic susceptibility. Since by definition $\Delta\chi_{\max} = N\chi_a$, within the framework of the rigid rod model for the uniaxial nematic, one obtains

$$Q_{\alpha\beta} = Q_{\alpha\beta}^M. \quad (2.22)$$

For realistic models the relationship between \mathbf{Q} and the microscopic order parameter \mathbf{Q}^M may be quite complicated. The relationship (2.22) obviously cannot be generalized.

3. Phase transitions in liquid crystals

Among the most spectacular and remarkable macroscopic events in nature are the transformations between the various states of matter. The theoretical and experimental study of phase

transitions has a long and illustrious history spanning over a period of more than a century to the present day. It is still a very active field of study with many unsolved problems. So the field has expanded enormously; from embracing transformations between the classical states of matter, i.e., the solid, liquid and gaseous phases, to transitions to a variety of mesophases, and phases characterized by such diverse properties as superconductivity, superfluidity, magnetic ordering, surface structures, ferroelectricity, cosmological quark confinement, chaos, topological ordering, helix cooling of proteins, fluidity of biological membranes, etc.

Phase transitions are characterized by abrupt changes, discontinuities, and strong fluctuations. It has been known for a long time that such singular behaviour is a consequence of a cooperative phenomenon and thus intimately related to the interactions between the microscopic constituents of matter. It is therefore obvious that a theoretical description of phase transitions at a microscopic level will be very difficult. The main difficulty with the theoretical methods is in the attempt to include very many coupled degrees of freedom.

As discussed in Section 1, the liquid crystalline materials exhibit the richest variety of polymorphism. The transition between different phases corresponds to the breaking of some symmetry (see Table 1). As physically expected, the most common examples of phase transitions involve a transformation from an ordered (lower symmetry) phase to a relatively disordered (higher symmetry) phase (or vice versa) as the transition temperature is crossed. Usually, the system does not re-enter the original state as only one of the various field variables is changed in a continuous manner. One can predict the order of stability of the different phases on a scale of increasing temperature simply by utilizing the fact that a rise in temperature leads to a progressive destruction of molecular order. Thus, the less symmetric the mesophase, the closer in temperature it lies to the crystalline phase. This means that upon cooling the isotropic liquid, first the nematic, then smectic phases “without order”, smectic phases “with order-hexagonal structure”, smectic phases “with order-herring bone structure”, and finally solid/crystalline phases appear in a fixed sequence. If in a mesogen all of the above phases can exist, they are expected to appear according to the sequence rule, which, in a general form, may be written as

$$\begin{array}{ccccccccccccccc}
 \text{IL} & \text{---} & \text{blue} & \text{---} & \text{N} & \text{---} & \text{S}_A & \text{---} & \text{S}_C & \text{---} & \text{S}_{B(\text{hex})} & \text{---} & \text{S}_I & \text{---} & \text{S}_{B(\text{cry})} & \text{---} & \text{S}_F \\
 & & & & & & & & & & & & & & & & & | \\
 & & & & & & & & & & & & & & & & & \text{Crystal/Solid} & \text{---} & \text{S}_H & \text{---} & \text{S}_K & \text{---} & \text{S}_E & \text{---} & \text{S}_G & \text{---} & \text{S}_J
 \end{array} \tag{3.1}$$

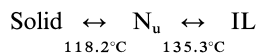
No single compound is known yet in which the complete sequence (3.1) has been observed. In most of the materials only a small part of the different phases exist which are in complete agreement with the predicted sequence. Some examples of real observed sequences are given in Table 3. In the observed sequences within a homologous series there are pronounced variations for the respective phase transition properties, e.g., for the clearing point, with increasing alkyl (or alkoxy) chain length the clearing point decreases. An even–odd effect [53] is observed in the sense that clearing points for compounds with even chain length have a higher value. In such cases, the transition properties (e.g., transition entropy, order parameter at the transition, etc.) also show a similar variation.

One of the basic reasons for the excitement and continued interest in liquid crystal phase transitions is that these transitions provide numerous examples for much of the recent theoretical

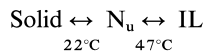
Table 3

A few typical examples of observed sequences in liquid crystals

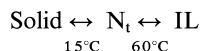
1. 4,4'-Di-methoxyazoxy benzene (p-azoxyanisole, PAA)



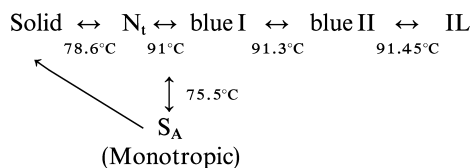
2. N-(p-methoxybenzylidene)-p'-butylaniline (MBBA)



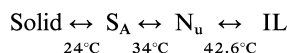
3. N-(p-ethoxybenzylidene)-p'-(β-methylbutyl) aniline



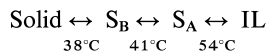
4. Cholesteryl nonanoate



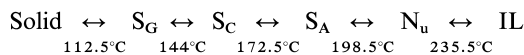
5. 4'-n-octyl-4-cyanobiphenyl



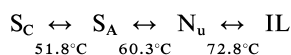
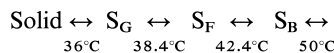
6. p,p'-dinonylazobenzene



7. Terephthal-bis-(p-butylaniline) TBBA



8. N-(4-n-Pentyloxybenzylidene)-4'-n-hexylaniline



work on critical phenomena. Since the mesophase transitions are either weakly discontinuous or continuous, they should display the behaviour associated with critical points, including strong fluctuations and diverging susceptibility. One of the most significant findings of the theoretical works is that in the vicinity of such a transition the microscopic details of the system become unimportant in describing the details of the transition. Instead, the range of the interactions, the physical dimension of the system, and symmetry of the order parameter determine the behaviour of the system very close to the transition.

Although the liquid crystals are soft systems on a macroscopic scale, they provide qualitative solutions to the complicated, often unobservable, equations on a large scale that can be observed using a polarizing microscope. Many mesophase transitions involve broken continuous symmetries in real space and their interactions on a molecular scale are short range. As a result,

fluctuations have long been known to be an important feature of LC phase transitions. Relatively little is known about fluctuation phenomena (critical phenomena) at a first-order phase transition, such as NI transitions, as compared to fluctuation-controlled second-order phase transitions. The critical phenomena [54] in LC have unique features due to a variety of symmetries of the different phases and coupling of the different order parameters. These features complicate theoretical considerations and restrict the application of methods which are successful in other cases. Another salient feature of mesogenic materials is that they have generic long-range correlation, even far from critical points or hydrodynamic instabilities [55] that they could make it difficult to access critical regimes before being finessed by a first-order phase transition. At these high temperatures, externally supplied noise can suppress the onset of macroscopic instabilities such as spatial turbulence far from any phase transition.

3.1. Thermodynamics of phase transitions

Invaluable qualitative and quantitative information about the liquid crystalline phases can be derived from the thermodynamic data at and in the vicinity of their phase transitions. The molecular structure phase stability relations can usually be understood from detailed thermodynamic data. In addition, reliable data are required for the definitive testing of the theoretical treatments. The most frequently used data for testing theories of phase transitions are (Refs. [15](a) and [6,56]);

- (i) *Transition temperatures*: These are usually determined by optical microscopy or by calorimetry and are important quantities characterizing the materials. The difference in transition temperature between the melting and clearing points gives the range of stability of the liquid crystalline phases.
- (ii) *Transition densities ρ (of more ordered phase ρ_{or} and less ordered phase ρ_{dor}) and fractional density (or volume) changes $\Delta\rho/\rho_{\text{or}}$ ($\Delta\rho = \rho_{\text{or}} - \rho_{\text{dor}}$)*: These are determined by dilatometry and play a most important role in characterizing the phase transition.
- (iii) *Transition enthalpy and transition entropy*: These may be measured by classical adiabatic calorimetry or by dynamic differential scanning calorimetry (DSC). The transition enthalpies and entropies between the solid and the liquid crystalline state, between the different liquid crystalline states and between the liquid crystalline state and the isotropic state are related to the degree of internal order present in the system. When a mesogenic material is heated from its crystalline state to above the clearing point a variety of transitions with accompanying enthalpy and entropy changes might occur.
- (iv) *Order parameters at the transition*: These can be measured by a number of methods.
- (v) *The ratio dT/dp* : Is determined by direct measurement of the effect of external pressure on the transition temperature. Since the application of pressure has a strong influence on the range of existence of mesophases, this ratio yields important information on the phase transition.
- (vi) *ΔC_p , $\Delta\alpha$, ΔK and $C_p(T)$, $\alpha(T)$ and $K(T)$ on both sides of the transition*: Here $C_p(T)$, $\alpha(T)$ and $K(T)$ are, respectively, the constant pressure heat capacity, expansion coefficient, and isothermal compressibility and Δx represents respective transition quantity.
- (vii) Another useful quantity is

$$\Gamma = -\rho(\partial\bar{P}_2/\partial\rho)_T/T(\partial\bar{P}_2/\partial T)_{\bar{P}_2} = (\partial\ln T/\partial\ln\rho)_{\bar{P}_2} . \quad (3.2)$$

This parameter was initially defined by Alben [57] as a particular sensitive probe of the relative importance of attractive and repulsive interactions. McColl and Shih [58] were first to determine Γ successfully. A plot of $\ln T$ against $\ln \rho$ at constant \bar{P}_2 is virtually linear.

3.2. Order of phase transition

In general, an n th-order phase transition is defined to be one in which the n th derivatives of the Gibbs function (or chemical potential μ) with respect to temperature and pressure change discontinuously at the point of the transition. For an a–b equilibrium phase transition,

$$G_a(T, p) = G_b(T, p), \quad (3.3)$$

i.e. the zeroth derivative is continuous. Thus, a first-order phase transition can be mathematically formulated as follows:

$$G_a - G_b = 0, \quad (3.4a)$$

$$-\left[\frac{\partial G_b}{\partial T}\right]_p + \left(\frac{\partial G_a}{\partial T}\right)_p = \Sigma_b - \Sigma_a = \Delta\Sigma = \frac{L}{T}, \quad (3.4b)$$

$$\left[\frac{\partial G_b}{\partial p}\right]_T - \left[\frac{\partial G_a}{\partial p}\right]_T = V_b - V_a = \Delta V, \quad (3.4c)$$

where $\Delta\Sigma$ and ΔV are, respectively, the changes in entropy and volume at the transition. Thus, for the first-order transition, where $\partial\mu/\partial T$ and $\partial\mu/\partial p$ are discontinuous, changes in enthalpy ΔH (or entropy $\Delta\Sigma$) and in volume ΔV are observed. The projection of the line of intersection of the μ surfaces onto the P – T plane provides a consistency relation between dT/dp and $T\Delta V/\Delta H$ through the Clausius–Clapeyron equation.

For a second-order phase transition, both ΔH and ΔV are zero, but discontinuities in the second-order derivatives of Gibbs function (or chemical potential) with respect to temperature and pressure lead to changes in the ΔC_p , $\Delta\alpha$ and ΔK , respectively. Mathematically, the second order phase transition may be characterized as

$$G_a(T, p) = G_b(T, p),$$

$$-\left[\frac{\partial G_b}{\partial T}\right]_p + \left[\frac{\partial G_a}{\partial T}\right]_p = \Sigma_b - \Sigma_a = \Delta\Sigma = 0, \quad (3.5a)$$

$$\left[\frac{\partial G_b}{\partial p}\right]_T - \left[\frac{\partial G_a}{\partial p}\right]_T = V_b - V_a = \Delta V = 0, \quad (3.5b)$$

$$\left[\frac{\partial^2 G_b}{\partial T^2}\right]_p - \left[\frac{\partial^2 G_a}{\partial T^2}\right]_p = \frac{1}{T}[C_{p_a} - C_{p_b}] = \Delta C_p/T, \quad (3.5c)$$

$$\left[\frac{\partial^2 G_b}{\partial p^2} \right]_T - \left[\frac{\partial^2 G_a}{\partial p^2} \right]_T = V[K_a - K_b] = V\Delta K, \quad (3.5d)$$

$$\left[\frac{\partial^2 G_b}{\partial p \partial T} \right] - \left[\frac{\partial^2 G_a}{\partial p \partial T} \right] = V(\alpha_b - \alpha_a) = V\Delta\alpha. \quad (3.5e)$$

In the case of liquid crystals, changes in order parameters must also be considered. The transition is said to be first-order or second-order depending on whether the order parameters change discontinuously or continuously, respectively, at the transition point. Most of the mesophase transitions are characterized as weakly first-order in nature because they are associated with a small value of ΔH and $\Delta\rho/\rho$ (or $\Delta V/V$).

3.3. Experimental determination of some transition properties: a critical comment

A knowledge of both the temperature and the heat of transition is necessary if the principles of physical analysis are to be applied to study the mesophase transitions. From this information the transition entropy may be calculated which may play a pivotal role for evaluating the type and degree of order present in the system. When a material melts, a change of state occurs from a solid to a liquid and this melting process requires energy (endothermic) from the surroundings. Similarly, the crystallization of a liquid is an exothermic process and the energy is released to the surroundings. The melting transition from a solid to a liquid is an exothermic process and the energy is released to the surroundings. The melting transition from a solid to a liquid is a relatively drastic phase transition in terms of the structural change and relatively high energy of transition is involved. The relatively small enthalpy changes show that the liquid crystal phase transitions are associated with more subtle structural changes. Although the enthalpy changes at a transition cannot identify the types of phases associated with the transitions, the magnitude of the enthalpy change is proportional to the change in structural ordering of the phases involved. Typically, a melting transition from a crystalline solid to a liquid crystal phase or the isotropic liquid phase involves an enthalpy change of around 30–50 kJ/mol. This indicates that a considerable structural change is occurring. The liquid crystal to liquid crystal and liquid crystal to isotropic liquid transitions are associated with very much smaller enthalpy changes ($\simeq 4$ –6 kJ/mol.) Other smectic and crystal smectic mesophases are also characterized by the values of similar order. The nematic-isotropic liquid transition usually gives a smaller enthalpy change (1–2 kJ/mol). The enthalpy changes of transition between different liquid crystal phases are also small. For example, the S_C to S_A transition is often difficult to detect because the enthalpy change is typically less than 300 J/mol. The enthalpy for $S_A N_u$ transition is also fairly small (1 kJ/mol) and the $S_C N_u$ transition has enthalpy less than 1 kJ/mol. These changes can be readily detected by optical methods.

The transition from one phase to another is not necessarily sharp but stretches over a certain range. The nematic-isotropic liquid transitions tend to be smaller than about 0.6–0.8K whereas crystalline smectic or smectic-isotropic liquid transitions are generally much wider. Usually, the transition of the melting point is less sharp than the clearing point leading to an absolute error of ± 1 and ± 0.1 K, respectively.

A number of techniques (e.g. optical microscopy, mottler oven, microscope hot stage, differential thermal analysis, calorimetry, Raman spectroscopy, etc.) are available for the measurement of transition quantities. Most of these quantities may be determined for both pure mesogens and mixtures. The main instruments which may be used for the measurement of transition temperatures are mottler oven, microscope hot stage and differential scanning calorimetry (DSC). The mottler oven can detect small changes in transmission as a function of temperature. For the liquid crystals, one may expect a change of optical properties for every phase transition. Under these experimental conditions, the transmission of a liquid crystal increases with decreasing order parameter. This results, for solid and smectic states, in a low transparency, while the nematic and isotropic states have a higher one. In order to perform a measurement, a melting tube is filled with the respective substance and placed into the oven. Any change in transmittance is monitored by a built-in photodiode in the oven, giving a photocurrent which is proportional to the transparency of the sample. It is the first heating process of a sample for which all phase transitions are quoted. With increasing temperature, a general increase in transmission is observed due to a general decrease of the order parameter. The determination of transition temperatures and the characterization of liquid crystal phases can be done concurrently using a hot-stage under a polarising microscope. All transition temperatures are measured upon first heating of the sample. For the melting and clearing points the first change observed in the texture is of relevance. Often transition from the crystalline to a smectic texture cannot be distinguished, because no change in optical appearance results. So in these cases both techniques, oven and hot stage, fail and the transition temperature is deduced from a DSC analysis. The existence of a temperature gradient in the hot stage may account for a possible systematic error of $\pm 1\text{--}2\text{ K}$. When a high precision is required, the mottler oven may be employed. The two methods (oven and hot-stage) are the most common techniques which are applied in the determination of phase transitions of liquid crystals.

The most widely used technique in mesophase research is the calorimetric study of the phase transitions. From the molar heat of transition, q , the entropy change of transition is calculated from the familiar relationship $\Delta S = q/T$. A large number of measurements using classical adiabatic calorimetry are available. However, the bulk of thermodynamic data presently available has been obtained by dynamic calorimetry. By the very nature of instrumentation, dynamic methods are much less accurate than adiabatic calorimetry. The expected accuracy is usually not much better than $\pm 1\%$ and in some cases only $\pm 10\%$.

The application of the methods of differential thermal analysis (DTA) and differential scanning calorimetry (DSC) has provided extremely rich data on the temperatures, heats of transition and heat capacity of various phases. In DTA the sample and reference material are heated at some linear rate. The absolute temperature and the differential temperature between sample and reference are recorded. The area beneath the differential curve is related to calories via calibration with a material of known heat of fusion. Since the area is due to temperature difference, factors such as sample and instrument heat capacity are important. When adequately calibrated, the data may be determined from the curves within an accuracy of $\pm 1\%$. The DSC involves a comparison of the sample with an inert reference during a dynamic heating or cooling programme. It employs two furnaces, one to heat the sample under investigation and the other to heat an inert reference material (usually gold). The two furnaces are separately heated but are connected by two control loops to ensure that the temperatures of both remain identical through a heating or cooling cycle. The heating or cooling rate for each is constantly identical. A balance between the sample and the

reference is maintained by adding heat via the filament. When the sample melts, for example, from a crystalline solid to a S_A phase, energy must be supplied to the sample to prevent an imbalance in temperature between the sample and the reference. This energy is measured and recorded by the instrument as a peak on a baseline. The instrument is precalibrated with a sample of known enthalpy of transition, and this enables the enthalpy of transition to be recorded for the material being examined. The sample is weighed into a small aluminium pan and then the pan is placed into a holder in a large aluminium block to ensure good temperature control. The sample can be cooled with the help of liquid nitrogen and a working temperature range of between -180°C and 600°C may be achieved.

Although the DSC reveals the presence of phase transitions in a material by detecting the enthalpy change associated with each phase transition, a precise phase identification cannot be made. However, the level of enthalpy change involved at the phase transition does provide some indication of the types of phase involved. Accordingly, DSC is used in conjunction with optical polarising microscopy to determine the mesophase types exhibited by a material. If a transition between mesophases has been missed by optical microscopy, then DSC may reveal the presence of a transition at a particular temperature or vice versa. After DSC, optical microscopy should be used to examine the material very carefully to furnish information on phase structure, and to ensure that the transitions have not been missed by DSC. This procedure hopefully may lead to the likely identity of the mesophases. Accordingly, optical polarising microscopy and DSC are important complementary tools in the identification of the types of mesophase exhibited by a material.

The DSC often has been successful in revealing the presence of chiral liquid crystal phases. In case of blue phases and TGBA phase, the range of stability of mesophases are often too small to provide a distinct enthalpy peak. The transition between the S_{Cferri}^* phase and S_{Canti}^* phase and their transition with the S_{C}^* phase involve extremely small enthalpy values. This makes detection by DSC very difficult. However, the latest DSC equipment may enable the detection of even such remarkably small enthalpy transitions.

4. Nematic–isotropic phase transition

The nematic liquid crystal is fluid and at the same time anisotropic because while preserving their parallelism the molecules slide over one another freely. The experimental observations [4,21,59] using various techniques [6,13,20] show that the order parameters decrease monotonically as the temperature is raised in the mesophase range and drop abruptly to zero at the transition temperature. In case of uniaxial nematic the order parameter \bar{P}_2 drops abruptly to zero from a value in the range of 0.25–0.5 depending on the mesogenic material at the nematic–isotropic (NI) transition temperature T_{NI} . Thus, the NI transition is first-order in nature, though it is relatively weak thermodynamically because only an orientational order is lost at T_{NI} and the heat of transition is only 1 kJ/mol. This in turn leads to large pretransitional [4,13,53,60] abrupt increases in certain other thermodynamic properties, such as the specific heat, thermal expansion and isothermal compressibility of the medium near T_{NI} . The changes of entropy and volume associated with this transition are typically only a few percent of the corresponding values for the solid–nematic transition.

The molecular theory of liquid crystals aims to understanding the physical behaviour of these materials in the mesophase range and in the vicinity of a phase transition. Moreover, the most interesting feature of a theory must be its usefulness in predicting the behaviour of the system. Accordingly, a prerequisite for a complete and satisfactory theory is a knowledge of the intermolecular interactions. However, such a knowledge is almost entirely lacking. The liquid crystal-line molecules possess a strong anisotropy in both intermolecular repulsions and attractions. As a result, in the construction of a molecular theory one faces the complications of dealing with both spatial and angular variables of the molecules [61]. Even if the essentials of the intermolecular interaction are known one might question the successful application of a theory because of the enormous calculational problems. Owing to these difficulties model potentials have been introduced, i.e., the most relevant characteristics of the molecules and their mutual interactions are represented in terms of simple models. However, this does not necessarily mean that a molecular approach is out of question.

The theory for the nematic phase at and in the vicinity of their phase transitions has been developing in several directions. In one of the most applied approaches one uses the phenomenological theory of Landau and de Gennes [62–68] in which the Helmholtz free energy is expressed in powers of the order parameters and its gradients. In the process, five or more adjustable parameters, associated with the symmetry of the system and physical processes, are required to be determined by the experiments. While this theory is physically appealing and mathematically convenient, it has many drawbacks, including the lack of quantitative predicting power about the phase diagram. In another approach, mainly developed by Faber [96], the nematic phase is treated as a continuum, in which a set of modes involving periodic distortion of an initially uniform director field is thermally excited. All orientational order is assumed to be due to mode excitations. For a system of N molecules, $2N$ modes are counted corresponding to all rotational degrees of freedom. This theory works well near the solid nematic transitions but fails close to nematic–isotropic transition. In the molecular field theories [97–145] one begins with a model in the form of interparticle potentials and proceeds to calculate the solvent-mediated anisotropic potential acting on each individual molecule. Such calculations require full knowledge of pair correlation functions. For a potential which mimics all the important features of the molecular structure this approach includes lengthy and complicated mathematical derivation and numerical computation. As a consequence, too many simplifying approximations are made in the choice of the models and in evaluation of correlation functions and transition properties.

The initial version of mean-field theory is due to Onsager [97] which ascribes the origin of nematic ordering to the anisotropic shape of molecules, i.e., to the repulsive interactions. The Maier–Saupe (MS) theory [117] and its modifications and extensions [118–130] attribute the formation of the ordered phase to the anisotropic attractive interactions. In reality, of course, both of these mechanism is operative. Thus, in the van der Waals type theories [131–139] both anisotropic hard core repulsions and angle dependent attractions are explicitly included. Another type of molecular theory has been developed by Singh [49] and others [140–145]. These works are based on the density functional approach which allows writing formally exact expressions for thermodynamic functions and one-particle distribution functions in terms of direct correlation functions. The molecular interactions do not appear explicitly in the theory. These types of theory are physically more reasonable than those of Maier–Saupe or repulsion dominant hard particle theories. However, the major difficulty with theories based on the density functional approach is

associated with the evaluation of direct correlation functions which requires a precise knowledge of intermolecular interactions. Only approximate methods are known for this purpose.

In the following subsections instead of summarizing all the research papers published so far we discuss the basic ideas involved in the aforesaid theories and its application to the uniaxial nematic–isotropic (NI) phase transitions.

4.1. Landau–de Gennes theory of the uniaxial nematic–isotropic (NI) phase transition

This section is devoted to the phenomenological model for the NI phase transition, the so-called Landau–de Gennes (LDG) theory [62–68]. It is based on Landau’s general description of phase transitions and was first developed by de Gennes [62]. The strengths of the LDG theory are its simplicity and its ability to capture the most important elements of the phase transition. In addition, it has been applied to many other transitions [10] and embellished in many ways. First all the essential ingredients of the Landau theory [65,66] will be discussed. The application of the theory to the NI transition will be summarized. Next, attention will be paid to pretransitional phenomena, for example, magnetically induced birefringence (or Cotton–Mouton effect) and light scattering.

4.1.1. The basic ideas of Landau theory

The Landau theory [65,66] is concerned with a phenomenological description of a phase transition. These transitions involve a change of symmetry. Generally the more symmetric (less ordered) phase corresponds to higher temperature and the less symmetric (more highly ordered) one to lower temperatures. The difference in symmetry between the two phases can be presented by the order parameters which are constructed in such a way that they are zero in the more symmetric phase. The mathematical description of the theory is based on the idea that the thermodynamic quantities of less symmetric phase can be obtained by expanding the thermodynamic potential in powers of order parameters and its spatial variations in the neighbourhood of the order–disorder transition point and that sufficiently close to the transition, only the leading terms of the series are important so that the said expansion becomes a single low-order polynomial. The motivation for this simple and most elegant speculations is derived from the continuity of the change of state at a phase transition of the second order, i.e., the order parameters show values near the transition point. Hence, Landau’s original procedure is, in principle, restricted to second-order phase transitions. The thermodynamic behaviour of the order parameters in the less symmetric phase is then determined from the condition that their values must minimize the postulated expansion of the thermodynamic potential.

In order to clarify Landau’s original arguments [65,66] and to discuss the main ingredients of this model, we begin by considering a macroscopic system whose equilibrium state is characterized by a spatially invariant, dimensionless, scalar order parameter Q . Though this situation is not directly related to the NI phase transition, it permits to understand the basic ingredients of the Landau approach. The general form of the thermodynamic potential $G(p, T, Q)$ is postulated, near the transition point, to be

$$G(p, T, Q) = G(p, T, 0) + h_1 Q + \frac{1}{2} A Q^2 + \frac{1}{3} B Q^3 + \frac{1}{4} C Q^4 + \dots, \quad (4.1)$$

where $G(p, T, 0)$ is the thermodynamic potential for a given temperature and pressure of the state with $Q = 0$. The numerical coefficients are introduced for convenience. The coefficients h_1, A, B, C, \dots are functions of p and T . The equilibrium state can be obtained by minimizing G with respect to Q for fixed p and T . In other words, the thermodynamic behaviour of the order parameter follows from the stability conditions,

$$\frac{dG}{dQ} = 0, \quad \frac{d^2G}{dQ^2} > 0. \quad (4.2)$$

At the transition temperature T_c these stability conditions are

$$\frac{dG}{dQ} = h_1 = 0, \quad \frac{d^2G}{dQ^2} = A = 0 \quad (4.3)$$

because of the coexistence of both the phases. This implies that (i) $h_1 = 0$, (ii) $A = a(T - T_c)$ with $a = (dA/dT)_{T_c} > 0$. The first condition is derived from the requirement that the high-temperature phase with $Q = 0$ must give rise to an extreme value of $G(p, T, Q)$. The second condition follows from the behaviour of G at $Q = 0$ for T above and below the transition temperature T_c . The function $G(p, T, 0)$ must have a minimum for $T > T_c$, i.e., $A > 0$, and a relative maximum for $T < T_c$, i.e., $A < 0$. The Landau theory postulates that the phase transition can be described by the following expression for the difference in the thermodynamic potential of the two phases:

$$\Delta G = G(p, T, Q) - G(p, T, 0) = \frac{1}{2}a(T - T_c)Q^2 - \frac{1}{3}BQ^3 + \frac{1}{4}CQ^4 + \dots \quad (4.4)$$

Here the negative sign with B has been chosen for the reason of convenience. It is further assumed that the coefficients B, C, \dots , must be weakly temperature dependent so that they can be treated as temperature independent coefficients.

The thermodynamic behaviour of the system follows directly from the stability condition,

$$\frac{dG}{dQ} = 0 = a(T - T_c)Q - BQ^2 + CQ^3 + \dots \quad (4.5)$$

Eq. (4.5) has the following solution near the transition point:

$$Q = 0, \quad \text{the high temperature phase,} \quad (4.6a)$$

$$Q = \frac{B \pm [B^2 - 4aC(T - T_c)]^{1/2}}{2C}. \quad (4.6b)$$

Now the discontinuity of Q at the transition requires $B = 0$, i.e., for the low temperature Q reads

$$Q = \pm \left[\frac{a(T_c - T)}{C} \right]^{1/2}. \quad (4.7)$$

Thus, for the reasons of stability the coefficient C must be positive. For a phase which remains invariant by replacing Q by $-Q$ such as, for example, a binary alloy, only coefficients belonging to even powers in Q survive. Thus in case of a second-order phase transition, Eq. (4.1) takes the form

$$G(p, T, Q) = G(p, T) + \frac{1}{2}A(T)Q^2 + \frac{1}{4}CQ^4 + \dots \quad (4.8)$$

It is important to mention that the Landau theory can be extended to the first-order phase transition by two possible mechanism. While the first one corresponds to the condition $B = 0$ and $C < 0$, the other considers the presence of a third-order term BQ^3 in the expansion of $G(p, T, Q)$. In the former case a stabilizing sixth-order term with coefficient $E > 0$ in Eq. (4.1) is required.

So far only spatially uniform systems have been considered above. Eqs. (4.1) and (4.8) can be generalized to include spatial variations of the order parameters by replacing Q by $Q(r)$ and including the contribution of the interaction term $\gamma[\Delta Q(r), T]$ in a power series in $\Delta Q(r)$ and retaining only the leading term

$$\gamma[\nabla Q(r)] \cong \frac{1}{2}h_2(T)[\nabla Q(r)]^2. \quad (4.9)$$

In order for the spatially uniform state to be the state of lowest free energy, $h_2(T) > 0$ and near the critical temperature, $h_2(T)$ must be approximated as a temperature-independent constant.

The above development is based on the hypotheses that the expansion (4.1) may be used and that G is an analytic function of p , T and Q . However, there exists, a priori, no reason to believe that these requirements are true because in the neighbourhood of a critical point correlations between fluctuations of the order parameter are of great importance. The problem with this theory is that the coefficients appearing in the expansion are phenomenological and their dependence on the molecular properties are not determined. It is to be expected that these coefficients have singularities as a function of p and T . These singularities present great difficulties. As a result, it is assumed that the presence of singularities does not affect the terms of the expansion. In addition, this theory does not contain any information about the molecular interactions.

Despite the above-mentioned difficulties, Landau theory has been successfully applied to a great variety of physical phenomena. It reveals the role of symmetry in physics. Mathematically, it is simpler than the mean-field (MF) theory. The inclusion of spatial variation of order parameters gives it a new dimension not found in MF theory.

The first indication about the extension of Landau theory to liquid crystals can be witnessed in the original work of Landau [65] itself where a short paragraph is devoted to the form of the probability density that defines a nematic state. Subsequently, the approach has been used extensively [3,63–68] to provide a phenomenological justification, explaining almost all observed facts in the area of liquid crystals, for example, multilayer ordering in smectic phases, various incommensurate modulations, ferroelectricity, elastostatics, interfacial phenomena. Indenbom and others [69–72] applied the group theoretical and thermodynamic concepts forming the Landau theory for studying the mesophase system.

4.1.2. The uniaxial nematic — isotropic (NI) phase transition: Landau–de Gennes theory

The nematic state is described by the symmetric tensor order parameter \mathbf{Q} with zero trace, i.e., $Q_{\alpha\alpha} = 0$. In order to describe the first-order NI phase transition, it is sufficient, according to Landau–de Gennes [64], to expand the thermodynamic potential upto fourth or sixth order in the tensor order parameter \mathbf{Q} near the transition. Since the thermodynamic potential is a scalar, the expansion can only contain terms that are invariant combinations of the elements $Q_{\alpha\beta}$ of the order parameter. In general, the expansion reads

$$g = g_0 + \frac{1}{2}A \text{Tr}(\mathbf{Q}^2) + \frac{1}{3}B \text{Tr}(\mathbf{Q}^3) + \frac{1}{4}C \text{Tr}(\mathbf{Q}^4) + \frac{1}{5}D[\text{Tr}(\mathbf{Q}^3)] \\ \times [\text{Tr}(\mathbf{Q}^2)] + \frac{1}{6}E[\text{Tr}(\mathbf{Q}^2)]^3 + E'[\text{Tr}(\mathbf{Q}^3)]^2 + \dots, \quad (4.10)$$

where g and g_0 represent the Gibbs free-energy density of the nematic and the isotropic phases, respectively. The term linear in $Q_{\alpha\beta}$ does not appear in the expansion due to the different symmetry of the two phases. In principle, the gradient terms have to be added.

From the general consideration, as discussed in Section 4.1.1, we note the following possibilities about the expansion (4.10):

- (i) The absence of a linear term in $Q_{\alpha\beta}$ allows for the existence of an isotropic phase. In case an external field is present a linear term has to be included which makes the isotropic phase impossible.
- (ii) Since the NI transition is first-order, odd terms of order three and higher are allowed.
- (iii) There are two independent sixth-order terms. The presence of the E' term indicates the possible occurrence of a biaxial nematic phase. Since for the moment we are interested only in the uniaxial phase, the E' term will be omitted.
- (iv) The NI phase transition takes place in the neighbourhood of $A = 0$. Therefore, it is assumed that the temperature dependence of the free energy is contained in the coefficient A alone and that other coefficients can be regarded as temperature independent. To describe the phase transition we write

$$A = a(T - T_{\text{NI}}^*), \quad (4.11)$$

where a is positive constant and T_{NI}^* is a temperature close to the transition temperature T_{NI} .

In order to make a comparison with molecular statistical calculations which are often performed at constant density, we consider the Helmholtz free energy density f instead of g . For the uniaxial nematic phase, we write the expansion

$$f = f_0 + \frac{1}{2}A \text{Tr}(\mathbf{Q}^2) + \frac{1}{3}B \text{Tr}(\mathbf{Q}^3) + \frac{1}{4}C \text{Tr}(\mathbf{Q}^4) + \frac{1}{5}D[\text{Tr}(\mathbf{Q}^2)\text{Tr}(\mathbf{Q}^3)] + \frac{1}{6}E[\text{Tr}(\mathbf{Q}^2)]^3. \quad (4.12)$$

For calculating the minimum of the free energy, we use the order parameter in diagonal form (Eq. (2.19)).

The invariants of \mathbf{Q} are

$$\text{Tr}(\mathbf{Q}^2) = \frac{1}{2}(3x^2 + y^2),$$

$$\text{Tr}(\mathbf{Q}^3) = \frac{3}{4}x(x^2 - y^2).$$

Choosing the uniaxial ordering along the Z -axis (the director) and $y = 0$, the free-energy density is written as

$$f = \frac{3}{4}Ax^2 + \frac{1}{4}Bx^3 + \frac{9}{16}Cx^4 + \frac{9}{40}Dx^5 + \frac{9}{16}Ex^6. \quad (4.13)$$

Here the free energy is normalized such that $f_0 = 0$.

We consider two cases. In the simplest model $D = E = 0$. For the minimum to be at finite $x = x_0$, $C > 0$, and the sign of B is opposite to the sign of x_0 . For a calamitic nematic $B < 0$ and for a discotic nematic $B > 0$. It is convenient to express the minimum value of x_0 in terms of $\bar{P}_2 (\equiv \frac{3}{2}x_0)$. With these provisos, Eq. (4.13) reads

$$f = \frac{1}{3}a(T - T_{\text{NI}}^*)\bar{P}_2^2 - \frac{2}{27}B\bar{P}_2^3 + \frac{1}{9}C\bar{P}_2^4. \quad (4.14)$$

The equilibrium value of \bar{P}_2 is obtained by minimizing the free energy (4.14) with respect to \bar{P}_2 . This means that \bar{P}_2 is determined by

$$a(T - T_{\text{NI}}^*)\bar{P}_2 - \frac{1}{3}B\bar{P}_2^2 + \frac{2}{3}C\bar{P}_2^3 = 0. \quad (4.15)$$

The solutions of Eq. (4.15) are

$$\bar{P}_2 = 0 \quad \text{the isotropic phase,} \quad (4.16a)$$

$$\bar{P}_{2\pm} = \frac{B}{4C} \left\{ 1 \pm \left[1 - \frac{24aC(T - T_{\text{NI}}^*)}{B^2} \right]^{1/2} \right\}. \quad (4.16b)$$

The correct solution which can describe the temperature dependence of the order parameter in the nematic phase is the \bar{P}_{2+} solution. The transition temperature T_{NI} can be calculated using the condition $f = f_0$, i.e.,

$$a(T_{\text{NI}} - T_{\text{NI}}^*)\bar{P}_{2\text{NI}}^2 - \frac{2}{9}B\bar{P}_{2\text{NI}}^3 + \frac{1}{3}C\bar{P}_{2\text{NI}}^4 = 0 \quad (4.17)$$

and the second relation between $\bar{P}_{2\text{NI}}$ and T_{NI} given from Eq. (4.15) as

$$a(T_{\text{NI}} - T_{\text{NI}}^*)\bar{P}_{2\text{NI}} - \frac{1}{3}B\bar{P}_{2\text{NI}}^2 + \frac{2}{3}C\bar{P}_{2\text{NI}}^3 = 0. \quad (4.18)$$

Eqs. (4.17) and (4.18) yield

$$\frac{1}{9}B\bar{P}_{2\text{NI}}^3 = \frac{1}{3}C\bar{P}_{2\text{NI}}^4. \quad (4.19)$$

Thus, the following two solutions are possible:

$$\bar{P}_{2\text{NI}} = 0, \quad T_{\text{NI}} = T_{\text{NI}}^* \quad (4.20a)$$

$$\bar{P}_{2\text{NI}} = \frac{B}{3C}, \quad T_{\text{NI}} = T_{\text{NI}}^* + \frac{B^2}{27aC}. \quad (4.20b)$$

Obviously, the result $\bar{P}_{2\text{NI}} = 0$ at $T = T_{\text{NI}}^*$ corresponds to the \bar{P}_{2-} solution whereas the \bar{P}_{2+} solution gives $\bar{P}_{2\text{NI}} = (B/3C)$ at the higher temperature $T_{\text{NI}} = T_{\text{NI}}^* + B^2/27aC$. It turns out that $\bar{P}_{2\text{NI}+}$ solution represents the thermodynamically stable solution. Eq. (4.16b) determines a third temperature T_{NI}^+ given by

$$T_{\text{NI}}^+ = T_{\text{NI}}^* + \frac{B^2}{24aC} \quad (4.21)$$

In case $T > T_{\text{NI}}^+$, the solutions \bar{P}_{2+} and \bar{P}_{2-} no longer hold because of their complex behaviour.

In conclusion, the LDG theory distinguishes four different temperature regions:

- (i) $T > T_{\text{NI}}^+$: the minimum corresponds to an isotropic phase, $\bar{P}_2 = 0$.
- (ii) $T_{\text{NI}} < T < T_{\text{NI}}^+$: the minimum of free energy is still given by $\bar{P}_2 = 0$, i.e., the isotropic phase is the thermodynamically stable state. There exist a relative minimum at $\bar{P}_2 = \bar{P}_{2+}$ and a relative maximum at $\bar{P}_2 = \bar{P}_{2-}$. As a result an energy barrier of height $f(\bar{P}_{2-}) - f(\bar{P}_{2+})$ exists between the two minima $\bar{P}_2 = 0$ and $\bar{P}_2 = \bar{P}_{2+}$. It follows that a metastable nematic phase can be

Table 4
Values of parameters in the Landau expansion for MBBA

Parameter	Value
a	$42 \times 10^3 \text{ J/m}^3/\text{K}$
B	$64 \times 10^4 \text{ J/m}^3$
C	$35 \times 10^4 \text{ J/m}^3$

obtained in this temperature region due to overheating. At T_{NI}^+ the height of barrier becomes zero. For $\bar{P}_{2+}(T_{\text{NI}}^+) = \bar{P}_{2-}(T_{\text{NI}}^+) = (B/4C)$ the associated point in the free-energy curve represents a point of inflection.

- (iii) $T_{\text{NI}}^* < T < T_{\text{NI}}$, the minimum corresponds to a nematic phase. There exists a local minimum corresponding to a possible supercooled isotropic state.

The transition entropy at T_{NI} is given by

$$\Delta\Sigma = - \left. \frac{\partial(f-f_0)}{\partial T} \right|_{T=T_{\text{NI}}} = \frac{1}{3} a \bar{P}_{2\text{NI}}^2 = \frac{aB^2}{27C^2}. \quad (4.22)$$

The latent heat per unit volume, ΔH , is given by

$$\Delta H = \frac{aB^2 T_{\text{NI}}}{27C^2}. \quad (4.23)$$

Thus, the coefficients a , B and C can be determined from the experimental values of $\bar{P}_{2\text{NI}}$, T_{NI} and ΔH . Table 4 lists the values of these parameters for MBBA.

- (iv) $T < T_{\text{NI}}^*$: the minimum corresponds to a nematic phase. The \bar{P}_{2+} solution corresponds to the lowest free-energy density, whereas the \bar{P}_{2-} solution to a relative minimum and $\bar{P}_2 = 0$ gives rise to a relative maximum.

The height h' of the energy barrier at $T = T_{\text{NI}}$ between the isotropic $\bar{P}_2 = 0$ state and the nematic state $\bar{P}_2 = \bar{P}_{2\text{NI}}$ is given by

$$h' = \frac{B^4}{11664C^3}. \quad (4.24)$$

4.1.3. The influence of external fields on the NI phase transition

In the absence of external magnetic or electric fields, nematic and isotropic liquids do not have the same symmetry. The application of fields may change the character of the NI phase transition. The effect of an applied field is that it induces orientational order in the isotropic phase that grows with increasing field intensity. For the case of positive dielectric anisotropy, the first-order phase boundary in the temperature–applied field plane terminates in a field-induced critical point. With increasing external fields, the jump at the transition vanishes at the field-induced critical point. The increase in the orientational order in the isotropic liquid results in an enhancement of the NI transition temperature, δT_{NI} . As a result, it is now possible to pass through the field-induced critical

point and observe the state beyond where nematic and paranematic states are indistinguishable. The application of a magnetic field to nematics with a negative magnetic anisotropy induces, in general, biaxial ordering and so a biaxial solution of \mathbf{Q} is required. This case will be taken up in Section 7.

In this section, the role of external fields on the physical properties of the NI phase transition will be examined within the framework of LDG theory. Suppose that a static magnetic field \mathbf{H} is applied to the system. Many applications of liquid crystals are strongly dependent on their response to such external perturbations. The application of field leads to an extra orientation dependent term in the free-energy density of Eq. (4.12):

$$f_m = -\frac{1}{2}H_\alpha H_\beta \chi_{\alpha\beta} . \quad (4.25)$$

Expressing $\chi_{\alpha\beta}$ in the order parameter elements (Eqs. (2.17) and (2.18)) this can be written as

$$f_m = -\frac{1}{2}\bar{\chi}H^2 - \frac{1}{2}\Delta\chi_{\max}H_\alpha H_\beta Q_{\alpha\beta} , \quad (4.26)$$

where $\bar{\chi} = \frac{1}{3}\chi_{\alpha\alpha}$. The first term may be omitted because it is independent of the molecular ordering. The sign of $\Delta\chi_{\max}$ must be positive. A negative sign of $\Delta\chi_{\max}$ refers to the nematic ordering in which the director is perpendicular to the field. Consequently, the field direction becomes a second axis and the phase is biaxial. Table 5 shows the field effects on all possible phases. When an electric field is applied to the system the contributing term to the free-energy density has the same form as Eq. (4.26) with $\bar{\chi}$ and $\Delta\chi_{\max}$ replaced by the average permittivity and the maximum permittivity anisotropy, respectively.

When $\Delta\chi_{\max} > 0$ the phase remains uniaxial. With the field direction \mathbf{H} and the director $\hat{\mathbf{n}}$ along the Z-axis and the order parameter defined by Eq. (2.20) with $y = 0$, the LDC free-energy density containing terms upto fourth order in order parameter, reads

$$f = -\frac{1}{2}\Delta\chi_{\max}H^2 + \frac{3}{4}Ax^2 + \frac{1}{4}Bx^3 + \frac{9}{16}Cx^4 . \quad (4.27)$$

Minimization of free energy gives

$$a(T - T_{NI}^*) = h/\bar{P}_2 - \frac{1}{3}B\bar{P}_2 - \frac{2}{3}C\bar{P}_2^2 , \quad (4.28)$$

where $h = (1/2)\Delta\chi_{\max}H^2$. Since the $\bar{P}_2(T)$ curve (Fig. 9) has a negative slope, the order of uniaxial phase with positive $\Delta\chi_{\max}N_u^+$ increases. It is clear that if $h \neq 0$, the $\bar{P}_2 = 0$ is never a solution of

Table 5
The breaking of symmetry of a phase due to a magnetic field

Phase in zero field $h = 0$	Phase in nonzero field $h \neq 0$	
	$\Delta\chi_{\max} > 0$	$\Delta\chi_{\max} < 0$
IL	N_u^+	N_u^-
N_u^+	N_u^+	N_b
N_u^-	N_b	N_u^-

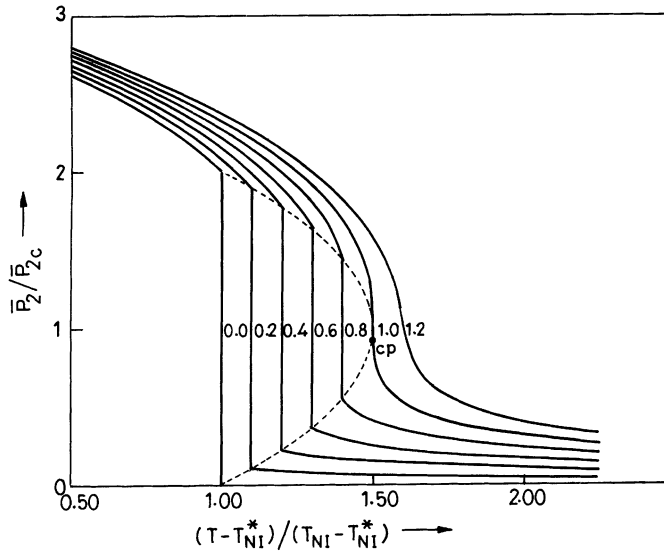


Fig. 9. The variation of order parameter with temperature for different values of the field variables. The dashed line represents the NI coexistence curve, cp is critical point and the numbers on the curves are the values of the field variables.

Eq. (4.28) and instead of an isotropic phase a small induced N_u^+ ordering is obtained. In order to differentiate between the usual N_u^+ phase and the induced N_u^+ phase, the latter one is often called the paranematic phase. The value of \bar{P}_2 in the paranematic phase is small and can be obtained from Eq. (4.28) by ignoring the coefficients B and C :

$$\bar{P}_2(h) = \frac{h}{a(T - T_{NI}^*)}. \quad (4.29)$$

Fig. 9 shows the variation of order parameter with $T - T_{NI}^*$ for different values of the field variable h . It can be seen that the jump of the order parameter at the NI phase transition is directly related to the value of the field. For smaller values of the field there exists a first-order phase transition between the paranematic and the nematic phase. The order parameter jump decreases with increasing field until the critical value h_c of the field is reached where there is no jump any more. At this point the transition becomes second order. For fields larger than h_c there is no phase transition and the nematic and paranematic phases are indistinguishable.

The location of critical point is given by

$$f'(x) = f''(x) = f'''(x) = 0 \quad (4.30a)$$

or equivalently

$$h_{cp} = -\frac{B^3}{324C^2} = \frac{1}{12}C(\bar{P}_{2NI}^0)^3, \quad (4.30b)$$

$$T_C - T_{\text{NI}}^0 = \frac{1}{54aC} = \frac{1}{2}(T_{\text{NI}}^0 - T_{\text{NI}}^*), \quad (4.30c)$$

$$\bar{P}_{2c} = -\frac{1B}{6C} = \frac{1}{2}\bar{P}_{2\text{NI}}^0. \quad (4.30d)$$

Here the superscript 0 refers to the zero field and T_C the critical point. At the phase transition there are two minima x_1, x_2 of equal energy with the conditions,

$$\begin{aligned} f(x_1) &= f(x_2), \\ f'(x_1) &= f'(x_2) = 0. \end{aligned}$$

The solution gives

$$x_{1,2} = x_c[1 \pm \sqrt{3 - 2\tau}], \quad (4.31a)$$

where

$$\tau = \left(\frac{27aC}{B^2}\right)(T - T_{\text{NI}}^*) = 1 + \frac{h}{2h_c}. \quad (4.31b)$$

The shape of the coexistence curve of the nematic and paranematic phase is parabolic. The shift in the transition temperature is proportional to h :

$$T_{\text{NI}}(h) - T_{\text{NI}}^0 = \frac{2h}{a\bar{P}_{2\text{NI}}^0}. \quad (4.31c)$$

As is obvious from the above discussion three general predictions can be made from the theory:

- (i) the existence of a paranematic phase with field-induced orientation order,
- (ii) the increase of T_{NI} with the increasing field and
- (iii) the existence of a magnetic (electric) critical point.

However, it is important to mention that the related experimental effects are very small. Taking maximum fields and typical anisotropy of the order of $|\Delta\chi_{\text{max}}| \approx 10^{-7}$ (CGS) one gets, for $T_{\text{NI}} - T_{\text{NI}}^* = 1$ K, the induced nematic order at T_{NI} of the order of 10^{-5} – 10^{-4} which is very small as compared to the typical values 0.3–0.5 at the other side of the NI phase transition. Helfrich [73] was the first to observe an increase in T_{NI} by applying an electric field. Rosenblatt [74] reported a magnetic experiment. The observed effect is so weak that the possibility of observing the magnetic critical point in thermotropic nematics is quite remote. Contrary to it, the first evidence for the existence of an electrically induced critical point was shown by Nicastrò and Keyes [75].

The possibility of the existence of critical region at the first-order transition line of the NI transition has been investigated [76] in the context of epsilon (ϵ) expansion. It has been observed that the LDG expansion with tensorial order parameter, which has a BQ^3 interaction in addition to CQ^4 (and $h = 0$), has a critical value $B = B_C$ (C, A) below which there is no transition. At the critical value the system undergoes a second-order transition with no symmetry breaking. Above the critical value of B the transition is of first-order. This is in contradiction with the prediction of Landau's theory. The results hold also for $d > 4$, since it depends only on the fact that $A_C = 0$. Thus, if at T_{NI} the behaviour is critical, assuming that in the scaling law [76] the non-analyticity

appears at the critical point (fluid-like critical point) and also on the spinodal curve, the critical indices of the absolute stability limit of the nematic phase (metastable) are $\beta_1 = \beta$ and $\alpha_1 = \gamma_1 = 1 - \beta_1$. Thus, it is obvious that there is a possibility of critical behaviour with $d = 3$ for the NI phase transition. The experimental verification of this argument has recently been given by Rzoska et al. [77].

The anomalous parts of the specific heat capacity above the transition point have been calculated [78] on the basis of the continuum theory of de Gennes. The excess specific heat capacity at constant pressure (per volume) due to fluctuations is given by

$$\Delta C_p(T) = 2.54 \times 10^{-4} T^2 [T - 318.7]^{-1/2} \text{ J/mol/K} . \quad (4.32)$$

It is found that the empirical formula (4.32) explains the observations of Anisimov [79] for MBBA. The amplitude of the order parameter fluctuation increases abnormally near T_{NI} and it brings about the anomalous increments in heat capacity.

Recently, the renormalization group (RG) technique has been used to calculate [80,81] the $T_{\text{NI}} - T_{\text{NI}}^*$ of the NI transition. The model free energy of LDG type can be written [80,81] as

$$F = \int d^d x \left[\frac{1}{4} (A Q_{ij}^2 + \nabla_k Q_{ij} \nabla_k Q_{ij}) - B Q_{ij} Q_{jk} Q_{ki} + C (Q_{ij} Q_{ij})^2 - H_{ij} Q_{ij} \right] . \quad (4.33)$$

Here $d^d x$ indicates a functional integral in d dimensions over the tensor field $\mathbf{Q} = \mathbf{Q}(\mathbf{x})$. The model (4.33) was studied extensively by the ε ($= 4 - d$) expansion technique [82]. This method relies on the fact that the MF approximation is exact for $d > 4$. It is a perturbation expansion about the solution for $d = 4$. The fixed point of the RG corresponds to a second-order phase transition with $B = 0$. The cubic coupling was found to be a relevant term, so B was treated as perturbation. The scaling form of the equation of state in the second order of ε expansion is obtained [80]:

$$\frac{H}{Q^\delta} + \frac{\beta}{Q^\omega} = f'(x') , \quad (4.34)$$

where $x' = t/Q^{1/\beta}$. The result for

$$f'(x) = 1 + x + \varepsilon f_1(x) + \varepsilon^2 f_2(x) \quad (4.35)$$

is

$$\delta = 3 + \varepsilon, \quad \omega = 1 + \frac{7}{13}\varepsilon, \quad \beta = \frac{1}{2} - \frac{3}{26}\varepsilon . \quad (4.36)$$

Here t is the reduced temperature, $t = (T - T_{\text{NI}}^*)/T_{\text{NI}}^*$. It is the temperature at which the second-order phase transition would take place if $B = 0$.

The strong point of this method over the other methods is that it needs only one kind of experimental input data, namely the jump in the order parameter at T_{NI} . The results obtained are still far away from experimental findings. The calculation has been extended near the coexistence curve [81] which is defined as the region of small external field and below the critical temperature. Mukherjee and Saha [83] have also calculated the critical exponents numerically for the $d = 3$ LDG model near the isolated critical point on the NI transition line from the recursion relations [84] in the $\eta = 0$ approximation from RG theory. It has been found that the critical exponents $\gamma = 1.277$ and $\nu = 0.638$ are in fair agreement with the best ε expansion result, $\gamma = 1.277$ and $\nu = 0.64$.

4.1.4. Density effects on the NI transition

In order to investigate the density effects at the NI transition, the free-energy density can be written [78,85–87] as

$$f[\rho, \mathbf{Q}, T] = \frac{1}{2}A^*\mathbf{Q}^2 - \frac{1}{3}B^*\mathbf{Q}^3 + \frac{1}{4}C^*\mathbf{Q}^4 + \frac{1}{2}E\rho^2 + \frac{\lambda_1}{1}\rho\mathbf{Q}^2 + \frac{\lambda_2}{2}\rho\mathbf{Q}^3. \quad (4.37)$$

The term $E\rho^2$ is the free-energy density of the isotropic phase. The coefficients λ_1 and λ_2 are the coupling constants.

Minimization of free-energy results in the following renormalization [78] of the expansion coefficients:

$$A = A^* + 2(\lambda_1/E)M, \quad (4.38a)$$

$$B = B^* - 3(\lambda_2/E)M, \quad (4.38b)$$

$$C = C^* - 2\left(\frac{\lambda_1^2}{E}\right). \quad (4.38c)$$

Here M is the quantity thermodynamically conjugate to density ρ . It is seen from Eqs. (4.38a) and (4.38b) that the interaction between \mathbf{Q} and ρ leads to the decrease of B and the increase of T^* . It is obvious that not only the director fluctuation, but also the density effects play an important role in the NI transition. The density fluctuation alters the character of the NI transition and makes it very weakly first-order. The modified form of the temperature can be expressed [85] as

$$T_{\text{NI}}^*(\rho) = T_{\text{MF}}^* + \alpha(\rho - \rho_0)^2. \quad (4.39)$$

Here α is a positive constant and ρ_0 the equilibrium density without order parameter-density coupling. T_{MF}^* is the MF absolute stability limit of the isotropic phase in the absence of any order parameter-density coupling. In this case, the free energy, given by Eq. (4.12), upto the fourth order in order parameter reads [85]

$$f[\rho, \mathbf{Q}, T] = f_0[\rho, T] + \frac{1}{2}a(T - T_{\text{MF}}^*)\mathbf{Q}^2 - \frac{1}{3}B\mathbf{Q}^3 + \frac{1}{4}C\mathbf{Q}^4 + \frac{1}{2}\lambda(\lambda - \lambda_0)^2\mathbf{Q}^2. \quad (4.40)$$

The transition temperature T_{NI} and the value of \mathbf{Q}^* (at $T = T_{\text{NI}}^*$) are obtained as

$$T_{\text{NI}} = T_{\text{NI}}^* + \frac{2B^2}{9aC} - \frac{\lambda(\rho^* - \rho_0^*)^2}{a}, \quad (4.41)$$

$$\mathbf{Q}^* = \frac{B}{2C} \left[1 + \left(1 - \frac{4\lambda C}{B^2}(\rho - \rho_0)^2 \right) \right]^{1/2}, \quad (4.42)$$

where ρ^* and ρ_0^* are the nematic and isotropic density at T_{NI} , respectively.

The variation of T_{NI} with pressure and volume can be expressed as

$$\left(\frac{dT_{\text{NI}}}{dp}\right) = \frac{-2\lambda}{3a} [(1 - 1/\lambda EQ_{\text{NI}}^2)^{2/3} P_{\text{NI}}^{-1/3} - \rho_{\text{I}}^*(1 - 1/\lambda EQ_{\text{NI}}^2)^{1/2} P_{\text{NI}}^{-2/3}] , \quad (4.43)$$

$$\frac{d(\ln T_{\text{NI}})}{d(\ln V)} = 2\lambda\rho^*(\rho^* - \rho_{\text{I}}^*)/aT_{\text{NI}} \quad (4.44)$$

with

$$E = (\rho_{\text{I}}^*/\rho^*)^2/[1 + (\rho_{\text{I}}^*/\rho^*)] . \quad (4.45)$$

Here P_{NI} is the pressure at the nematic phase.

Using the Landau expansion parameter determined from experimental data, dT_{NI}/dp and $d(\ln T_{\text{NI}})/d(\ln V)$ were calculated [85]. The calculated values of dT_{NI}/dp ($= 41.50$ K/kbar) and $d(\ln T_{\text{NI}})/d(\ln V)$ ($= 0.3964$) agree well with the experimental values of 20–40 K/kbar and 0.39, respectively and also with the low value of $T_{\text{NI}} - T_{\text{NI}}^* = 1$ K. However, the value of $Q^* - Q_{\text{NI}}$, instead of being very close ($\simeq 2\%$ experimentally), remains about 50% as obtained from the LDG expansion without incorporating any effect of density variation. This $Q^* - Q_{\text{NI}}$ discrepancy implies that the change in the value of the calculated order parameter over a small temperature interval 1 K (as $T_{\text{NI}} - T_{\text{NI}}^* \simeq 1$ K) would be much higher than that observed in the experiments: The observed value [85] of $(dQ/dT)_{T=T_{\text{NI}}} (= 0.3998)$ is in gross disagreement with the observed value 0.008. Thus it is obvious that a complete resolution of the $T_{\text{NI}} - T_{\text{NI}}^*$ puzzle remains outside the realm of a simple MF analysis where fluctuations are ignored. These results support the molecular MF results of Tao et al. [88] and also brings out the inadequacy in explaining the small value of $(Q^* - Q_{\text{NI}})/Q_{\text{NI}}$ and $(dQ/dT)_{T=T_{\text{NI}}}$ in the LDG framework.

It is seen from Eqs. (4.38a), (4.38b) and (4.38c) that as the temperature decreases and ρ increases, the quantity $\partial M/d\rho$ decreases and the coefficient C tends to zero, i.e., a tricritical point (TCP) appears. On further variation of the temperature the density coefficient changes sign. In general, two coefficients having the same symmetry in the Landau free energy vanish simultaneously, and the corresponding point is called tricritical (TCP). Since the coefficients C and A have same symmetry, $C = A = 0$ gives a TCP. In that case a positive stabilizing sixth-order term with positive coefficient has to be included in the free-energy expansion [64,86,87]. In such a situation, one way of studying the weakly first-order NI transition occurring near a TCP would be to have a B with a small non-zero value. The value of $T_{\text{NI}} - T_{\text{NI}}^*$ thus obtained, without density variation, was 7.68 K and $(Q^* - Q_{\text{NI}})/Q_{\text{NI}} \simeq 26\%$ which shows substantial improvement over the model (4.14). Taking into account the density variation, a substantial improvement in the value of $T_{\text{NI}} - T_{\text{NI}}^*$ ($\simeq 0.9999$ K) has been obtained [78] but the value of $(Q^* - Q_{\text{NI}})/Q_{\text{NI}}$ did not improve. In another approach [86], by assuming B to be so small that it can be discarded and taking small negative value of C and sixth-order stabilizing term, the first-order nature of the NI transition and the neighbourhood of the TCP both can be achieved. The value of the $T_{\text{NI}} - T_{\text{NI}}^*$ calculated from the scaling equation of state [86] is 2.55 K and that of $(Q^* - Q_{\text{NI}})/Q_{\text{NI}} \simeq 15.47\%$, which shows an improvement of 70% over the previous results. The critical exponents obtained are $\beta = 0.25$ and $\Delta = 1.25$, whereas experiments show these values to be $\beta = 0.247 \pm 0.01$ and $\Delta = 1.26 \pm 1.0$.

4.1.5. Influence of non-mesogenic impurities on the NI transition

In general, all real nematic liquid crystals contain impurities. It is well known [89] that the solute impurities which are not sufficiently rod-like and rigid in molecular structure depress the NI transition temperature. Hence, the addition of non-mesogenic impurities to the pure nematic leads to a broadening of the NI transition temperature and the appearance of a two-phase region. In the context of LDG theory this problem has been studied by Mukherjee [87]. It has been found that this two-phase region indicates the first-order character of the NI transition and the depression of the T_{NI} is related to the width of the two-phase region and the transition entropy $\Delta\Sigma$ of the pure nematic solvent

$$T_{\text{NI}} - T_{\text{NI}}^x = \frac{\Delta x}{\Delta\Sigma}, \quad (4.46)$$

where Δx is the width of the two-phase region and T_{NI}^x is the NI transition temperature in the absence of coupling between the concentration of the non-mesogenic substance and Q . Obviously, for $\Delta\Sigma \neq 0$, a two-phase region must exist at a fixed temperature. Furthermore, the lower the values of $\Delta\Sigma$, the larger the depression of the T_{NI} . The existence of two-phase region indicates the tricritical behaviour of the NI transition.

4.1.6. Landau theory of the NI transition: inclusion of fluctuations

Though the singular-like behaviour of various quantities at the NI transition is yet a puzzle, the solution could be obtained within the framework of LDG theory. Since the nature of NI transition is first order, the part of critical region, closest to the critical point is not accessible to the experiments. It was suggested by Keyes and Shane [90] that the critical exponents for quantities diverging towards T_{NI}^* before being cut off by a first-order transition at T_{NI} , should be characteristic of a TCP. The difference between critical and tricritical behaviour of the NI transition is difficult to verify. The value of the exponent β ($= 0.247 \pm 0.01$) obtained for 8 CB strongly supports the suggestion of tricritical character of the NI phase transition. On the other hand, the experimental value of specific heat near the NI phase transition of MBBA indicates that the behaviour of this transition is near tricritical and does not appear to agree with the LDG model (4.12).

In the nematic phase the “director” fluctuations are critical. Nelson and Pelcovits [91] pointed out that strongly developed director fluctuations could alter the character of the NI transition and make it very weakly first-order. The RG approach has been applied [92] to the description of fluctuation behaviour near the isolated critical point on the NI transition line. Recently, Wang and Keyes [93] have calculated the fluctuation of five components of the orientational order parameter of a nematic liquid crystal involving several types of critical and multicritical points. The critical behaviour of dielectric permittivity in the isotropic phase has been discussed by Rzoska et al. [77,94]. Thus, the study of pretransitional (fluctuation) phenomena near the first-order phase transition may provide an answer for their closeness to the second-order transition. Light scattering and magnetic birefringence measurements in the isotropic phase of nematogens present strong pretransitional effects and can be understood within the framework of LDG theory.

The two important ingredients that influence the thermodynamic functions near a phase transition are the order parameter fluctuation amplitude and the spatial correlations between the fluctuations of the order parameter. The average size of the range of correlations between

the fluctuations defines the so-called correlation length ξ . Far away from the critical point ξ is of the order of the intermolecular distance. On the other hand, near a second-order phase transition the correlations decrease very slowly with distance, indicating a divergence of ξ at the critical temperature. The Landau description of fluctuation based phenomena can be expected to be valid if the Ginzburg criterion is satisfied,

$$b\xi^2 \gg k_B T, \quad (4.47)$$

where b is the height of the barrier separating the ordered and disordered states. Close to T_{NI} the important fluctuations involve regions of volume ξ^3 . The inequality (4.47) then states that thermally activated fluctuations leading from ordered to disordered regions or vice versa do not occur with a significant probability. As a result, the LDG expansion is expected to be valid in case the fluctuations are small.

The fluctuations usually can be included in the Landau theory by calculating the free-energy density at each temperature as a function of both the order parameter and its spatial derivatives. For the low-energy (long-wavelength) fluctuations only the lower-order spatial derivatives of the order parameter are considered [13,63,64]. The free-energy density can be expanded with respect to both $\mathbf{Q}(\mathbf{r})$ and its derivatives. As there is no way of forming a scalar quantity linear in $\delta_r Q_{\alpha\beta}$, where $\delta_r = \delta/\delta x_r$, the lowest order spatial derivative invariants of $Q_{\alpha\beta}$ have the form

$$(\delta_\alpha Q_{\beta\gamma})^2, \quad (\delta_\beta Q_{\beta\gamma})^2.$$

As a result the LDG expansion that can describe the effect of the local fluctuations in the isotropic phase reads

$$\begin{aligned} f[\mathbf{Q}(\mathbf{r}), \partial_i \mathbf{Q}(\mathbf{r}), T, p] = & f_0 + \frac{1}{2}A \text{Tr} \mathbf{Q}^2 + \frac{1}{3}B \text{Tr} \mathbf{Q}^3 + \frac{1}{4}C[\text{Tr} \mathbf{Q}^2]^2 \\ & + \frac{1}{3}D[\text{Tr}(\mathbf{Q}^2)(\text{Tr} \mathbf{Q}^3)] + \frac{1}{6}E(\text{Tr} \mathbf{Q}^2)^3 + E'(\text{Tr} \mathbf{Q}^3)^2 \\ & - \frac{1}{2}\Delta\chi_{\text{max}} \mathbf{H} \mathbf{Q} \mathbf{H} - \frac{1}{12\pi} \nabla \varepsilon_{\text{max}} \mathbf{E} \mathbf{Q} \mathbf{E} + \frac{1}{2}L_1(\partial_\alpha Q_{\beta\gamma})^2 + \frac{1}{2}L_2(\partial_\beta Q_{\beta\gamma})^2 \end{aligned} \quad (4.48)$$

where f_0 represents the free-energy density of the isotropic phase without local fluctuations. Only two new expansion parameters L_1 and L_2 , which are closely related to the elastic constants, have appeared. Eq. (4.48) is the basic equation of the generalized Landau–de Gennes (GLDG) theory of the NI transition that includes long-wavelength fluctuations of the order parameter. The GLDG theory has various applications, of which the most important ones are the pretransitional effects, for example, the magnetically induced birefringence (Cotton–Mouton effect) and light scattering. The important quantities of interest are the correlation functions relevant to the pretransitional phenomena and if these correlation functions are not too large the Gaussian approximation is expected to be a good approximation. Concentrating only on pretransitional light scattering and assuming $B = C = \dots = 0$, it follows directly from Eq. (4.48) that the local fluctuations in the isotropic phase give rise to a local free-energy density of the type

$$\begin{aligned} f(\mathbf{r}) = & f_0 + \frac{1}{2}a(T - T_{\text{NI}}^*)Q_{\alpha\beta}(\mathbf{r})Q_{\beta\alpha}(\mathbf{r}) + \frac{1}{2}L_1[\partial_\alpha Q_{\beta\gamma}(\mathbf{r})] \\ & \times [\partial_\alpha Q_{\beta\gamma}(\mathbf{r})] + \frac{1}{2}L_2[\partial_\alpha Q_{\alpha\gamma}(\mathbf{r})][\partial_\beta Q_{\beta\gamma}(\mathbf{r})], \end{aligned} \quad (4.49)$$

where $Q_{\alpha\beta}(\mathbf{r})$ can be expanded in a Fourier series,

$$Q_{\alpha\beta}(\mathbf{r}) = \sum_{\mathbf{k}} Q_{\alpha\beta}(\mathbf{k}) e^{i\mathbf{k} \cdot \mathbf{r}} \quad (4.50a)$$

with

$$Q_{\alpha\beta}(\mathbf{k}) = \frac{1}{V} \int d\mathbf{r} Q_{\alpha\beta}(\mathbf{r}) e^{-i\mathbf{k} \cdot \mathbf{r}} . \quad (4.50b)$$

Substituting Eq. (4.50a) into Eq. (4.49) and integrating over the volume of the system, one obtains the following contribution of the fluctuation to the total free energy:

$$\begin{aligned} f_f = & \frac{1}{2} V a (T - T_{\text{NI}}^*) \sum_{\mathbf{k}} Q_{\alpha\beta}^*(\mathbf{k}) Q_{\alpha\beta}(\mathbf{k}) + \frac{1}{2} V L_1 \sum_{\mathbf{k}} k^2 Q_{\alpha\beta}^*(\mathbf{k}) Q_{\alpha\beta}(\mathbf{k}) \\ & + \frac{1}{2} V L_2 \sum_{\mathbf{k}} k_{\alpha} k_{\beta} Q_{\alpha\gamma}^*(\mathbf{k}) Q_{\beta\gamma}(\mathbf{k}) , \end{aligned} \quad (4.51)$$

where $k^2 = k_{\alpha} k_{\alpha}$. It is obvious that the value of f_f strongly depends on the values of the amplitude $Q_{\alpha\beta}(\mathbf{k})$. The validity of LDG theory here is based on the postulate that the appearance of a given set of amplitudes $\{Q_{\alpha\beta}(\mathbf{k})\}$ is described by a probability distribution of the form

$$P\{Q_{\alpha\beta}(\mathbf{k})\} = \frac{1}{Z} \exp(-\beta f_f) . \quad (4.52)$$

For $\mathbf{k} \neq 0$, the amplitudes are complex quantities,

$$Q_{\alpha\beta}(\mathbf{k}) = r_{\alpha\beta}(\mathbf{k}) + i s_{\alpha\beta}(\mathbf{k}) , \quad (4.53)$$

where $r_{\alpha\beta}(\mathbf{k})$ and $s_{\alpha\beta}(\mathbf{k})$ are real variables. These variables satisfy the relations

$$\begin{aligned} r_{\alpha\beta}(\mathbf{k}) &= r_{\alpha\beta}(-\mathbf{k}), & s_{\alpha\beta}(\mathbf{k}) &= -s_{\alpha\beta}(-\mathbf{k}) , \\ r_{\alpha\beta}(\mathbf{k}) &= r_{\beta\alpha}(\mathbf{k}), & s_{\alpha\beta}(\mathbf{k}) &= s_{\beta\alpha}(\mathbf{k}) . \end{aligned}$$

Since the trace of the fluctuation tensor $Q(\mathbf{k})$ is zero,

$$r_{\alpha\alpha}(\mathbf{k}) = s_{\alpha\alpha}(\mathbf{k}) = 0 .$$

For obvious reasons the relevant thermal averages based upon the tensor elements $Q_{\alpha\beta}(0)$ should be calculated. These averages are obtained [95] in the form

$$\langle Q_{xy}^2(0) \rangle = \langle Q_{xz}^2(0) \rangle = \langle Q_{yz}^2(0) \rangle = \frac{k_B T}{2V a (T - T_{\text{NI}}^*)} , \quad (4.54a)$$

$$\begin{aligned} \langle Q_{xx}^2(0) \rangle &= \langle Q_{yy}^2(0) \rangle = \langle Q_{zz}^2(0) \rangle = \frac{4}{3} \langle Q_{xy}^2(0) \rangle = \frac{4}{3} \langle Q_{xz}^2(0) \rangle \\ &= \frac{4}{3} \langle Q_{yz}^2(0) \rangle = \frac{2k_B T}{3V a (T - T_{\text{NI}}^*)} . \end{aligned} \quad (4.54b)$$

The thermal averages $\langle r_{\alpha\beta}^2(\mathbf{k}) \rangle$ and $\langle s_{\alpha\beta}^2(\mathbf{k}) \rangle$ are obtained [95] as

$$\langle r_{\alpha\beta}^2(\mathbf{k}) \rangle = \langle s_{\alpha\beta}^2(\mathbf{k}) \rangle, \quad (4.54c)$$

$$\langle r_{xx}^2(\mathbf{k}) \rangle = \langle r_{yy}^2(\mathbf{k}) \rangle = \langle r_{zz}^2(\mathbf{k}) \rangle = \frac{k_B T}{3V[a(T - T_{NI}^*) + L_1 k^2]} \quad (4.54d)$$

and

$$\langle r_{xy}^2(\mathbf{k}) \rangle = \langle r_{xz}^2(\mathbf{k}) \rangle = \langle r_{yz}^2(\mathbf{k}) \rangle = \frac{k_B T}{4V[a(T - T_{NI}^*) + L_1 k^2]}. \quad (4.54e)$$

In these equations the elastic constant L_2 has been taken to be zero. The correlation functions of the kind $\langle Q_{xx}(0)Q_{xx}(\mathbf{R}) \rangle$ and $\langle Q_{xy}(0)Q_{xy}(\mathbf{R}) \rangle$, which are of prime interest, can now be calculated in a straightforward way. The distance dependence of these functions is described in terms of the correlation length ξ , for example,

$$\langle Q_{xx}^{(0)}Q_{xx}^{(R)} \rangle = \frac{k_B T}{6\pi L_1 R} \exp(-R/\xi) \quad (4.55)$$

with ξ given by

$$\xi = \left[\frac{L_1}{a(T - T_{NI}^*)} \right]^{1/2}. \quad (4.56)$$

The correlation length ξ is a measure of the distance over which the local fluctuations are correlated. $\xi \rightarrow 0$ at infinitely high temperature and diverges as $T \rightarrow T_{NI}^*$. Near $T = T_{NI}^*$ this divergent behaviour of ξ is responsible for the so-called pretransitional phenomena, for example, the strong increase in the light scattering cross-section. With known values of the thermal averages, the depolarization ratio, i.e., the ratio between the intensities of the scattered light with polarizations parallel and perpendicular to the incident light at a scattering wave vector $\mathbf{q} = 0$, is given by

$$\frac{I_{||}^{(0)}}{I_{\perp}^{(0)}} = \frac{\langle Q_{xx}^2(0) \rangle}{\langle Q_{xy}^2(0) \rangle} = \frac{4}{3}. \quad (4.57)$$

The calculation becomes more complicated when the L_2 term is also included in evaluating thermal averages like $\langle r_{\alpha\beta}(\mathbf{k})r_{\gamma\delta}(\mathbf{k}) \rangle$. In this case three correlation lengths appear

$$\xi_1 = \left[\frac{L_1}{a(T - T_{NI}^*)} \right]^{1/2}, \quad (4.58a)$$

$$\xi_2 = \left[\frac{L_1 + \frac{1}{2}L_2}{a(T - T_{NI}^*)} \right]^{1/2}, \quad (4.58b)$$

$$\xi_3 = \left[\frac{L_1 + \frac{2}{3}L_2}{a(T - T_{NI}^*)} \right]^{1/2}, \quad (4.58c)$$

Owing to the positive sign of the correlation lengths, L_1 and L_2 must satisfy the relation

$$L_1 + \frac{2}{3}L_2 > 0. \quad (4.59)$$

Thus, only the largest distance makes sense. This means if $L_2 < 0$, ξ_1 is the correlation length whereas ξ_3 is the correlation length if $L_2 > 0$. It is important to mention that the discussion presented here is not expected to present a quantitatively correct description of pretransitional phenomena. A comparison with experiment and a detailed discussion on the results within and beyond the Gaussian approximation are presented elsewhere [64].

4.2. The hard particle or Onsager-type theories

The counterpart of phenomenological theory (Section 4.1) for liquid crystals is the molecular statistical description. A number of papers [96–145] have appeared on the statistical models of the nematic phase. These are based on the mean-field (MF) approximation in which each molecule is supposed to be subjected to an orienting field due to its interaction with all the other molecules in the medium. As mentioned earlier there are three well-known approaches to tackle the problem. The first one is due to Onsager [97] and ascribes the origin of nematic ordering to steric hindering between hard rods of anisotropic shape. The second approach, formulated by Maier and Saupe [117], states that the nematic ordering essentially originates from the anisotropic attractive interactions. In the third approach, the van der Waals type theories [131–139], both the anisotropic hard core repulsions and angle-dependent attractions are explicitly incorporated in evaluating the molecular field. In this section, we shall concentrate on the first approach and the remaining two will be discussed in Sections 4.3 and 4.4.

About 50 years ago, Onsager [97] showed that a system of long rigid rods exhibits a transition from an isotropic phase to a denser anisotropic phase. The calculation of Onsager was based on a cluster expansion for the free energy given as a functional of the distribution in orientation of the rigid particles. The model was applied later by Zwanzing [98] to a certain idealized model and the rigid rod transition was verified to the order of seventh virial. A Padé analysis of Zwanzing approach by Runnels and Colvin [100] has shown that the transition observed by Zwanzing is very stable, and in three dimensions, at least first-order. A slightly different mean-field calculation for the hard rod problem based on the well-known lattice model was made by Flory and coworkers [101,102]. The above treatments [97–102] of hard rod systems are valid only for very long rods with length to width ratio $x_0 \geq 100$ which is typical of polymeric systems. For the shorter rods ($x_0 \simeq 3$ –5 or at most $x_0 < 10$) at high densities applying the scaled particle theory (SPT) due to Cotter [103,104] has been very convenient for evaluating the excess free energy. Other treatments of hard rod systems include γ -variable expansion [105,106], application of density functional theory (DFT) [49], the functional scaling approach [110], Monte Carlo (MC) simulation [54,147–160], the role of molecular flexibility on the density change at the transition [111–113], etc. The works based on DFT and MC simulations will be discussed in Sections 4.5 and 9, respectively.

The Onsager line of approach boils down to a discussion of the thermodynamic properties of a system of hard rods. Let us consider a fluid of N rods in a volume V at temperature T . Assuming that a rod can take only v discrete orientations, the configurational partition function can be

written [104] as

$$Q_N = \frac{1}{N!} \frac{1}{v^N} \sum_{\Omega} \int d\mathbf{r} \exp[-\beta U_N] , \quad (4.60)$$

where U_N , the potential energy of interaction, is approximated as the sum of pair potentials:

$$U_N = \sum_{1 < i < j < N} u_{ij} . \quad (4.61)$$

Here $N!$ allows for the indistinguishability of the particles and v^N for the number of orientational states.

For hard particles,

$$u_{ij} = u(\mathbf{r}_{ij}, \Omega_i, \Omega_j) = \begin{cases} \infty & \text{if } i \text{ and } j \text{ overlap} , \\ 0 & \text{otherwise} . \end{cases} \quad (4.62)$$

Since the configurational space available for each molecule is v

$$\int d\mathbf{r} \exp(-\beta U_N) = V^N \exp[-\beta \phi_N(\Omega)] , \quad (4.63)$$

where the function ϕ_N depends only on the orientations. For a given configuration of the system, if there are N_1 molecules along Ω_1 , N_2 molecules along Ω_2, \dots, N_v molecules along Ω_v , ϕ_N becomes a function of occupation number and

$$Q_N = \left(\frac{V^N}{N! v^N} \right) \sum_{N_1=0}^N \sum_{N_2=0}^N \cdots \sum_{N_v=0}^N \frac{N!}{\prod_{\alpha=1}^v N_{\alpha}!} \exp[-\beta \phi_N(N_1, N_2, \dots, N_v)] \quad (4.64)$$

with $\sum_{\alpha=1}^v N_{\alpha} = N$. Introducing the mole fraction $s_i = N_i/N$ of various components and using the maximum term approximation, the configurational Helmholtz free energy of a system of hard rods can be expressed as

$$\frac{\beta A_{\text{hr}}}{N} = -\frac{1}{N} \ln Q_N = \ln \rho - 1 + \sum_{i=1}^v \tilde{s}_i \ln(\tilde{s}_i) + \frac{\beta}{N} \phi_N(\tilde{N}_1, \tilde{N}_2, \dots, \tilde{N}_v) , \quad (4.65)$$

where the tilde denotes that the distribution corresponds to the maximum term of ϕ_N and $\phi_N(\tilde{N}_1, \tilde{N}_2, \dots, \tilde{N}_v)$, as first noted by Zwanzig [98], is the excess Helmholtz free-energy relative to an ideal gas of a system of molecules having fixed orientations. Considering the continuous distribution of angles, replacing s_i by $f(\Omega_i)$ and finally converting from sums back to integrals, one obtains [104]

$$\frac{\beta A_{\text{hr}}}{N} = \ln \rho - 1 + \int f(\Omega) \ln[4\pi f(\Omega)] d\Omega + \frac{\beta}{N} \phi_N\{f(\Omega)\} . \quad (4.66)$$

Thus, the major work is to derive the excess free-energy function ϕ_N . The two most common approaches which has been used to evaluate ϕ_N are the cluster or virial expansion technique of Onsager [97] and the scaled particle theory [103,104].

Onsager [97] made a virial expansion of ϕ_N and retained terms only upto the second virial coefficient, i.e., ϕ_N was approximated as

$$\phi_N \simeq \frac{1}{2} \rho \sum_i \sum_j s_i s_j V_{\text{exc}}(\Omega_i, \Omega_j), \quad (4.67)$$

where $V_{\text{exc}}(\Omega_i, \Omega_j) (\equiv V_{\text{exc}}(\Omega_{ij}))$ is the mutual exclusion volume (or covolume) of two rods with orientations Ω_i and Ω_j , respectively. Converting from sum to integrals, Eq. (4.66) reads

$$\frac{\beta A_{\text{hr}}}{N} = \ln \rho - 1 + \int f(\Omega) \ln[4\pi f(\Omega)] d\Omega + \frac{1}{2} \rho \int f(\Omega_1) f(\Omega_2) V_{\text{exc}}(\Omega_{12}) d\Omega_1 d\Omega_2. \quad (4.68)$$

In order to calculate $V_{\text{exc}}(\Omega_{12})$ the shape of the rods must be specified. For the long rods ($L \gg d_0$), where the end effect is ignored, one obtains [3]

$$V_{\text{exc}}(\Omega_{12}) = 2L^2 d_0 |\sin \Omega_{12}|, \quad (4.69)$$

where (Ω_{12}) is the angle between the axes of two molecules with orientations Ω_1 and Ω_2 . The most convenient shape of rods, used by Onsager [97] and many others [103,104,133], is a spherocylinder, which is straight circular cylindrical capped on each end by a hemisphere of the same radius. In this case [98,133].

$$V_{\text{exc}}(\Omega_1, \Omega_2) = 8v_0 + 4al^2 |\sin \Omega_{12}|, \quad (4.70)$$

where a , l and v_0 are, respectively, the radius, cylindrical length and volume of spherocylinder.

The singlet orientational distribution function can be determined by minimizing Eq. (4.68) subject to the condition.

$$\int f(\Omega) d\Omega = 1. \quad (4.71)$$

Thus, $f(\Omega)$ can be obtained as a solution of the variational equation

$$\ln[4\pi f(\Omega_1)] = \lambda - 1 - 8v_0 \rho - 4al^2 \rho \int f(\Omega_2) d\Omega_2 |\sin \Omega_{12}|, \quad (4.72)$$

where λ is a Lagrange multiplier to be determined from the normalization condition (4.71). Eq. (4.72) is a non-linear integral equation which has to be solved numerically for $f(\Omega)$. However, it is difficult to solve Eq. (4.72) exactly. Onsager obtained an approximate variational solution which is based on a trial function of the form

$$f_1 = (\text{const}) \cosh(\alpha \cos \theta). \quad (4.73)$$

Here α is a variational parameter and θ is the angle between the molecular axis and the nematic axis. It was found [97] that in the region of interest α is large (~ 20) and the system exhibits an abrupt first-order phase transition from the isotropic ($\alpha = 20$) to the nematic ($\alpha \geq 18.6$) phase characterized by

$$\phi_{\text{nem}} = 4.5d_0/L, \quad \phi_{\text{iso}} = 3.3d_0/L, \quad \bar{P}_{2\text{NI}} \simeq 0.84, \quad (4.74)$$

where $\phi (= \frac{1}{4}\pi\rho Ld_0^2)$ represents the volume fraction of the rods. The relative density change $\Delta\rho/\rho_{\text{nem}}$, with $\Delta\rho = \rho_{\text{nem}} - \rho_{\text{iso}}$, at the transition, in the full Onsager calculation, is about 25%. This value is much too high as compared to the experimental results. The transition predicted by Onsager's approach was confirmed later by Zwanzing [98], who calculated higher virial coefficients upto the seventh restricting the molecules to take only three mutually perpendicular orientations.

Clearly, Onsager's approach only provides a qualitative insight into the effect of repulsive interactions as far as real nematics are concerned. A detailed discussion on the validity of this approach is given elsewhere [115]. It is claimed that it gives a single and qualitatively correct picture of the order–disorder transition due to the shape of the molecules. Straley [116] has argued that the truncation of the cluster expansion series after the second virial coefficient can be justified quantitatively only for very long rods ($x_0 > 100$). For shorter rods ($x_0 \leq 40$) qualitatively reliable results are expected. The numerical solutions obtained by Lasher [99] in the limit of very long rods show that the NI transition is characterized by $\Delta\rho/\rho_{\text{nem}} \simeq 0.21$ and $\bar{P}_{2\text{NI}} \simeq 0.784$.

Flory and Ronca [102] considered the application of a lattice model to treat the hard rod problem and made the calculations, in the limit of long rods, at relatively high densities. The lattice models have a few attractive features. They can be used with advantage for the evaluation of the combinatorial part of the configurational partition function, i.e., the steric factor which comprehends the spatial configurations that conform to the virtual requirement that the overlap be avoided. The partition function can be calculated exactly when all the rods are parallel ($\bar{P}_2 = 1$). The approximate form of the free energy derived for $\bar{P}_2 < 1$ becomes exact for $\bar{P}_2 = 1$. Although the approach is useful for a dense, highly ordered phase, it treats the angular function $f(\Omega)$ rather crudely. Thus, the Onsager and Flory results may supplement each other but neither of them can be taken to be entirely reliable over the whole density range.

In Flory's lattice approach each rod with parameter L/d_0 is constructed to consist of x_0 segments, one segment being accommodated by a cell of the lattice. The preferred axis of a given domain is taken along one of the principal axes of the lattice. Disorder in the orientation of the rods with respect to the preferred axis of the system is expressed by a parameter y which is determined by the projection of the rod of parameter L/d_0 in a plane perpendicular to the preferred axis. The calculations carried out for the phase equilibrium between the anisotropic (nematic) and the isotropic phases give higher values for the volume fractions at the transition as compared to Onsager's results

$$\phi_{\text{nem}} \simeq 12.5d_0/L, \quad \phi_{\text{iso}} \simeq 8d_0/L. \quad (4.75)$$

The value of $\bar{P}_{2\text{NI}}$ is not meaningful in view of the crude approximations in $f(\Omega)$. It turns out to be larger than the Onsager solution. The combined covolume of the solute species in the isotropic phase at the coexistence was found to be 7.89, whereas the critical value of the axial ratio for the coexistence of the two phases in the neat liquid is $x_{0\text{crit}} \simeq 6.417$.

Warner [108] presented a theory of nematics which derives much from the Flory approach in calculating the number of ways of placing hard rods into a limited volume. What is new is that the steric constraints of the other rods are handled in a way that is consistent for both the component of rods lying parallel and transverse to the director. The use of a lattice in calculating the configurational freedom of the rod assembly was avoided. The most striking feature of this theory is that the isotropic state is more stable than that estimated by previous theories. Consequently, the

predicted limiting athermal axial ratio, $x_{0\text{crit}}$, is greater (8.99), and the order parameter and transition entropy are smaller than in earlier approaches.

From the above discussion it follows that the Onsager [97–99] and Flory [101–107] approaches are not suitable for studying the NI phase transition in real nematics characterized by $x_0 \simeq 3\text{--}5$ (or at most $x_0 < 10$) and high density. However, these approaches are useful for describing the phase transitions in polymer liquid crystals (see Section 10) and their solutions in suitable solvents. For real nematics composed of spherocylindrical molecules the scaled particle theory (SPT) [103,104] has been used to calculate the excess free-energy function $\phi_N(\tilde{N}_1, \tilde{N}_2, \dots, \tilde{N}_v)$. The principal quantity in SPT is the work function $W_i(\alpha, \lambda, \rho)$ defined as the reversible work of adding a scaled spherocylinder of radius αa , cylindrical length λl and fixed orientation Ω_i . W_i is related to the configurational Gibbs free energy through the exact relation

$$\frac{\beta G}{N} = \sum_i s_i [\ln(s_i \rho) + \beta W_i(1, 1, \rho)] . \quad (4.76)$$

When the scaling parameters $\alpha \rightarrow 0$ and $\lambda \rightarrow 0$, that is, when the scaled particle shrinks to a point, it is shown [103] that

$$\exp[-\beta W_i] \simeq 1 - \rho \sum_j s_j V_{ij}(\alpha, \lambda) , \quad (4.77)$$

where $V_{ij}(\alpha, \lambda)$ is the volume excluded to an unscaled molecule j with orientation Ω_j by the scaled particle i with orientation Ω_i at some fixed point. At the opposite extreme when α and λ both are very large, $W_i(\alpha, \lambda)$ approaches the reversible PV work required to create a macroscopic spherocylindrical cavity in the fluid,

$$\lim_{\substack{\alpha \rightarrow \infty \\ \lambda \rightarrow \infty}} W_i = \left[\pi(\alpha a)^2 \lambda l + \frac{4\pi}{3}(\alpha a)^3 \right] P . \quad (4.78)$$

Also

$$V_{ij}(\alpha, \lambda) = \frac{4\pi}{3} a^3 (1 + \alpha)^3 + \pi a^2 l (1 + \alpha)^2 (1 + \lambda) + 2a l^2 (1 + \alpha) \lambda |\sin \Omega_{ij}| . \quad (4.79)$$

W_i was calculated by interpolating between these two limit, i.e., between very large and very small values of α and λ , and the phase transition was located by equating the Gibbs free energy and pressure of the ordered and disordered phases. The calculated transition properties are in reasonable agreement with the experimental data of p-azoxyanisole (PAA) when $x_0 \simeq 2.5$ (see Table 6). Further, it was predicted that as x_0 increases, the transition densities decrease, relative density change increases substantially and the order parameter $\bar{P}_{2\text{NI}}$ increases slightly. In case of very short spherocylinders ($x_0 < 2$) the value of relative density change is less than 1%.

A comparison of the SPT equation of state with the results of MC and MD simulations [148–151] in the isotropic phase shows that for $x_0 = 2$ and 3, SPT overestimates the pressure at the high densities. Savithramma and Madhusudana [136] obtained much better results by extending the method for hard spheres originally proposed by Andrews [146] to spherocylinders. It is based on the idea that the reciprocal of the thermodynamics “activity” is simply the probability of being

Table 6

A comparison of predicted values of mean density $\bar{\rho} = [\rho_{\text{nem}} + \rho_{\text{iso}}]/2$ and the relative density change $\Delta\rho/\bar{\rho}$ at the transition

Transition quantity	Onsager [97]	Zwanzig [98]	Flory [101]	Cotter and Martire [103]			Wulf and de Rocco [111]		
				(L/do + 1)	5	10	L	10	40
$\ddot{\rho}$	3.9 do/L	1.6 do/L	10 do/L		~ 0.35	~ 0.21		0.31	0.07
$\frac{\Delta\rho}{\bar{\rho}}$	29%	21%	$\geq 20\%$		21%	40%		2.3%	22%

able to insert a particle into a system without overlapping with other particles. Another method which improves the agreement with the simulation results is due to Barboy and Gelbart [105]. It is based on the expansion of free energy in terms of the “ y -variables” instead of the standard one in densities using virial coefficients, defined as

$$y = \rho/(1 - v_0\rho) . \quad (4.79b)$$

The expansion coefficients of y^n are related to the virial coefficients. Mulder and Frenkel [106] applied the y -expansion technique to study the NI transition in a system of ellipsoidal particles by restricting the expansion to y^2 .

Parson [107] derived an expression for the free energy of a hard rod system using “decoupling approximation”. Assuming that the system interacts through a pair potential $u(\mathbf{r}, \Omega_{12})$, the free energy was derived as

$$\frac{\beta A_{\text{hr}}}{N} = \langle \ln f(\Omega) \rangle - \frac{1}{6} \beta \int d\mathbf{r} d\Omega_1 d\Omega_2 f(\Omega_1) f(\Omega_2) \int_0^n dn' r \frac{\partial u}{\partial r} g(\mathbf{r}, \Omega_{12}; n') . \quad (4.80a)$$

For a system composed of molecules whose only anisotropy is in their shape, the pair potential can be taken of the special form $u(\mathbf{r}, \Omega_{12}) = u(r/\sigma(\hat{r}, \Omega_{12})) = u(r/\sigma)$, where σ is an angle-dependent range parameter. In the decoupling approximation $g(\mathbf{r}, \Omega_{12})$ scales as $g(r/\sigma)$. This results in a complete separation between the translational and orientational degrees of freedom. The approximation is accurate at low density, since $g \simeq e^{-\beta u}$, but deviates at higher density. Using the decoupling approximation, Eq. (4.80a) can be written as

$$\frac{\beta A_{\text{hr}}}{N} = \langle \ln f(\Omega) \rangle + \frac{1}{2} \int d\Omega_1 d\Omega_2 f(\Omega_1) f(\Omega_2) V_{\text{exc}}(\Omega_{12}) \int_0^n \alpha(n') dn' , \quad (4.80b)$$

where

$$\alpha(n) = - \int_0^\infty dy y^3 \frac{\partial u}{\partial y} g(y) \quad (4.80c)$$

and

$$V_{\text{exc}}(\Omega_{12}) = \frac{1}{3} \int d\hat{r} \sigma^3(\hat{r}, \Omega_{12}) . \quad (4.80d)$$

Here the translational degrees of freedom appear entirely in the coefficient $\alpha(n)$. When $n \rightarrow \infty$, obviously $\alpha(n) = 1$ for the hard particle fluid and one finds the Onsager result. Using the Berne and Pechukas [109] expression for $\sigma(\mathbf{r}, \Omega_{12})$

$$\sigma^2(\hat{\mathbf{r}}, \Omega_{12}) = d_0^2 \left[1 - \chi \frac{(\hat{\mathbf{r}} \cdot \hat{\mathbf{e}}_1)^2 + (\hat{\mathbf{r}} \cdot \hat{\mathbf{e}}_2)^2 - 2\chi(\hat{\mathbf{r}} \cdot \hat{\mathbf{e}}_1)(\hat{\mathbf{r}} \cdot \hat{\mathbf{e}}_2)(\hat{\mathbf{e}}_1 \cdot \hat{\mathbf{e}}_2)}{1 - \chi^2(\hat{\mathbf{e}}_1 \cdot \hat{\mathbf{e}}_2)^2} \right]^{-1}. \quad (4.81)$$

Eq. (4.80d) for fixed relative orientation $\hat{\mathbf{e}}_1 \cdot \hat{\mathbf{e}}_2 = \cos \theta_{12}$ gives [107]

$$\bar{V}_{\text{exc}} = 8(1 - \chi^2)^{-1/2}(1 - \chi^2 \cos^2 \theta_{12})^{1/2}. \quad (4.82)$$

Here $\hat{\mathbf{e}}_1$ and $\hat{\mathbf{e}}_2$ are unit vectors along the symmetry axes of the two interacting spheroids, $d_0 = 2a$ and

$$\chi = \frac{x_0^2 - 1}{x_0^2 + 1}. \quad (4.83)$$

The decoupling approximation transforms the system into a hard sphere fluid. The calculations were done for a hard rod fluid using the equation of state for the transformed hard sphere fluid. It was found that a transition to an orientationally ordered state occurs at a critical packing fraction η_c which decreases with x_0 . For $x_0 \leq 3.5$, η_c is so high that the system tends to crystallize before the ordered liquid state is reached. Using perturbation theory, the calculations were done for a soft-rod fluid, where the transformed system of spheres interacts with a potential $u(y) = \varepsilon/y^m$. When $m \rightarrow \infty$, this reduces to the hard sphere case. The transition temperature was obtained as a function of density and molecular shape and the order parameter has been found to obey the scaling law $Q = Q[\eta(\varepsilon/kT)^{m/3}]$. This scaling property suggested that $m = 12$ for a coefficient Γ (Eq. (3.2)) equal to 4.

Lee [110] introduced a functional scaling concept to study the stability of nematic ordering as a function of molecular shape anisotropy. The free-energy functional for a system of hard spherocylinder was constructed from a direct generalization of an analytic equation of state for a hard spheres under a simple functional scaling via the excluded volume of two hard non-spherical particles

$$J(\eta) \rightarrow J(\eta) \frac{1}{8} \langle V_{\text{exc}}(\hat{\mathbf{e}}_1, \hat{\mathbf{e}}_2)/v_0 \rangle. \quad (4.84)$$

This is equivalent to the decoupling approximation [107]. The generalized free energy of a system of hard spherocylinders in a closed form was obtained as

$$\frac{\beta A_{\text{hsc}}}{N} = \beta \mu_0(T) + \ln \rho - 1 + \langle \ln[4\pi f(\Omega)] \rangle + \frac{\eta(4 - 3\eta)}{(1 - \eta)^2} \left[1 + \frac{3}{2\pi} \left(\frac{(L/d_0)^2}{1 + 3L/2d_0} \right) \langle |\sin \Omega_{12}| \rangle \right]. \quad (4.85)$$

For long rods, Eq. (4.85) reduces exactly to Onsager's relation in the low-density limit. Numerical calculations were performed for a variety of length to diameter ratio x_0 of hard spherocylinders. It was found that as the ratio x_0 increases from one to infinity, $\eta_{\text{max}}(x_0)$ increases from 0.740 to 0.907. Further, the discontinuity in the packing fraction at the NI transition becomes smaller as the molecular shape anisotropy decreases. The theory was extended [110](b) to calculate the transition

Table 7

Comparison of the NI transition parameters for hard ellipsoids with the axial ratio $x_0 = 2.75$ and 3.0

x_0	Quantities	MC [156,157]	Baus, et al. [174]	Singh and Singh [142]	Mulder and Frenkel [106]	Marko [177]	Lee [110]
2.75	η_{nem}	0.570	0.512	0.347	0.462	0.518	0.552
	η_{iso}	0.561	0.501	0.329	0.449	0.517	0.544
	$\Delta\eta/\eta_{\text{nem}}$	0.016	0.021	0.052	0.028	0.002	0.014
	\bar{P}_2	—	0.548	0.532	0.552	0.010	0.517
3.0	η_{nem}	0.517	0.484	0.330	0.437	0.444	0.517
	η_{iso}	0.507	0.472	0.309	0.420	0.443	0.508
	$\Delta\eta/\eta_{\text{nem}}$	0.019	0.022	0.063	0.039	0.002	0.017
	\bar{P}_2	—	0.565	0.547	0.568	0.017	0.533

properties of hard ellipsoids of revolution. The free-energy expression of a system of N hard ellipsoids reads

$$\frac{\beta A_{\text{her}}}{N} = \beta \mu_0(T) + \ln \rho - 1 + \langle \ln[4\pi f(\Omega)] \rangle + \frac{\eta(4-3\eta)}{(1-\eta)^2} \langle (1-\chi^2)^{-1/2} (1-\chi^2 \cos^2 \theta_{12})^{1/2} \rangle . \quad (4.86)$$

Calculations were done for the thermodynamic parameters at the NI transition for hard ellipsoids with $x_0 = 2.75$ and 3.0 and the results are compared in Table 7 with those of several other approaches. It can be seen that the functional scaling results agree well with the simulation values [156,157] than other approaches.

From the above discussions, it is clear that all rigid rod calculations predict too low a value for the mean density and too large a value for the density discontinuity at the transition to be applicable to real NI transitions. The experimental value for $\Delta\rho/\rho$ for the nematic phase transitions is of the order of 1%. In fact, there is a basic difficulty with all the hard particle theories. Their properties are “athermal” and entirely density dependent. Thus, for a system of hard particles it follows that $\Gamma = \infty$, whereas experimentally $\Gamma = 4$ for PAA. Clearly, therefore, proper description of nematic phase requires inclusion of attractive interactions in theoretical treatments.

4.3. Maier–Saupe (MS) type theories

Maier and Saupe [117] assumed that nematic ordering is caused by the anisotropic part of the dispersion interaction between molecules. The shape anisotropy of the molecules was ignored entirely. In accordance with the symmetry of the structure, viz. the cylindrical distribution about the preferred axis and the absence of polarity, the orientational energy of a molecule i can be approximated as

$$u_i = -\bar{u}_2 V^{-2} \bar{P}_2 P_2(\cos \theta_i) , \quad (4.87)$$

where θ_i is the angle which the long molecular axis makes with the preferred axis and \bar{u}_2 is taken to be a constant independent of pressure, volume and temperature. The V^{-2} dependence is due to the dispersion interaction. However, it is well accepted that the exact nature of the interactions need not be specified for the development of the theory. All that is required to obtain the results of MS theory is an anisotropic potential with a particular dependence on the molecular orientations [128]. Using the V^{-2} dependence, the Helmholtz free energy can be expressed as

$$\frac{\beta A}{N} = \frac{1}{2} \beta \bar{u}_2 V^{-2} \bar{P}_2 (\bar{P}_2 + 1) - \ln \int_0^1 \exp \left[\frac{3}{2} \beta \bar{u}_2 V^{-2} \bar{P}_2 \cos^2 \theta_i \right] d(\cos \theta_i) . \quad (4.88)$$

The consistency relation is obtained by the minimization of the free energy,

$$\left(\frac{\partial A}{\partial \bar{P}_2} \right)_{V,T} = 0 , \quad (4.89a)$$

$$3 \bar{P}_2 \left(\frac{\partial \langle \cos^2 \theta_i \rangle}{\partial \bar{P}_2} \right) - 3 \langle \cos^2 \theta_i \rangle + 1 = 0 \quad (4.89b)$$

and

$$\bar{P}_2 = \langle P_2(\cos \theta_i) \rangle . \quad (4.89c)$$

The minimization of the free energy occurs at that value of \bar{P}_2 which satisfies the consistency relation. The calculations lead to a first-order NI transition at

$$\frac{\bar{u}_2}{k_B T_{\text{NI}} V_c^2} = 4.541 \quad (4.90a)$$

and

$$\bar{P}_{2\text{NI}} = 0.429 , \quad (4.90b)$$

where V_c is the molar volume of nematic phase at T_{NI} . The following expression for the volume change at T_{NI} is obtained [117,121]:

$$\Delta V = -2A \left(\frac{\partial A}{\partial V} \right)_{T=T_{\text{NI}}} \quad (4.91)$$

or

$$\begin{aligned} \frac{\Delta V}{V} = & \left(\frac{V^2}{\beta \bar{u}_2 \bar{P}_{2\text{NI}}^2} \right) \left[2 \ln \int_0^1 \exp \left\{ \frac{3}{2} \beta \bar{u}_2 V^{-2} \bar{P}_{2\text{NI}} \cos^2 \theta \right\} d(\cos \theta) \right] \\ & - \beta \bar{u}_2 V^{-2} \bar{P}_{2\text{NI}} (\bar{P}_{2\text{NI}} + 1) . \end{aligned} \quad (4.92)$$

If ΔV is known from the experiment, $\bar{P}_{2\text{NI}}$ can be determined. However, this method gives only a 1–2% change in the values of $\bar{P}_{2\text{NI}}$. Because theory contains only one unknown, \bar{u}_2 , the order parameter $\bar{P}_{2\text{NI}}$ and the entropy change $\Delta \Sigma_{\text{NI}}$ are predicted to be the universal properties of the nematogen. In addition, the calculated values $\bar{P}_{2\text{NI}} \simeq 0.44$ and $\Delta \Sigma_{\text{NI}}/R \simeq 0.417$ are found to be in

agreement with the observed value. Experimentally, $\bar{P}_{2\text{NI}}$ varies in the range of ~ 0.25 – 0.5 for different compounds [161]. The agreement between theory and experiment can be improved by extending the MS theory in a variety of ways. These include the addition of terms to the MS potential function to allow for higher rank interactions [122] and a deviation from molecular cylindrical symmetry [122] as well as using a MF approximation of higher order [126]. Marcelja [123] and Luckhurst [162] have analysed the influence of the flexible end-chain on the ordering process. In a Flory-type calculation, Marcelja [123] has included the configurational statistics of end chains and could explain the “odd–even” effect of both T_{NI} and $\bar{P}_{2\text{NI}}$ as a homologous series is ascended. Luckhurst [162] refined these calculations for compounds with two rigid cyanobiphenyl moieties linked by flexible spacers in which the odd–even alternation in T_{NI} is about 100°C .

Humphries et al. [122] employed a more general form than Eq. (4.87), for the orientational pseudo-potential, by adding the fourth Legendre polynomial, as follows:

$$u_i = -\bar{u}_2 V^{-\lambda} [\bar{P}_2 P_2(\cos \theta_i) + \lambda' \bar{P}_4 P_4(\cos \theta_i)] , \quad (4.93)$$

where λ and λ' are adjustable parameters to be determined from a comparison with the experiment. They were able to explain the variation of $\bar{P}_{2\text{NI}}$ and $\Delta\Sigma/Nk$ by a single parameter λ' and obtained agreement with the experimental temperature dependence of the order parameter when $\lambda = 4$. Further, taking account of the deviation from spherical symmetry of the pair spatial correlation function of the molecules, they modified the orientational pseudo-potential as

$$u_i = -\bar{u}_2 V^{-\gamma} [1 + \delta \bar{P}_2] \bar{P}_2 P_2(\cos \theta) . \quad (4.94)$$

Here δ denotes the deviation from the spherical symmetry of the spatial correlation function. If $\delta = 0$ and $\gamma = 2$ this form immediately reduces to Eq. (4.87). It is important to note that unless δ is equal to 0, this potential is theoretically inconsistent because the solution of the self-consistent equation does not give minima in the free energy of the system.

The volume dependence of u_i has been analysed by Cotter [119] in the light of Widom's [118] idea. It has been concluded that the MF model will be thermodynamically consistent if and only if $u_i \propto V^{-m}$, where m is a number, then Eq. (4.90a) becomes

$$\frac{\bar{u}_2}{k_B T_{\text{NI}} V_c^m} = 4.541 , \quad (4.95)$$

but $\bar{P}_{2\text{NI}}$ remains unchanged. Thus, the value of $\bar{P}_{2\text{NI}}$ does not depend critically on the volume dependence of u_i . In the entire nematic range the variation in $\bar{P}_{2\text{NI}}$ is usually only of the order of 1–2%. However, the value of the exponent m becomes very important while analysing the influence of pressure on the transition parameter. Pressure studies [58,163,164] for the case of PAA have shown that the value of Γ (Eq. (3.2)) is 4 and the thermal range of nematic phase at constant volume is about 2.5 times that at constant pressure. The $\bar{P}_{2\text{NI}}$ is almost independent of pressure. The studies of pressure-induced mesomorphism in PAA suggest that empirically $m = 4$ which has no theoretical justification. In view of Cotter's argument [119], referred to earlier, $m = 1$, irrespective of the nature of the pair potential.

There are, however, several unsatisfactory features of the MS theory. In general, MF models overestimate the strength of the transition. The predicted heat of transition from the nematic to the

isotropic phase is given by

$$H = T_{\text{NI}}[(\alpha/\beta)\Delta V - \bar{P}_2(V_c, T_{\text{NI}})] , \quad (4.96)$$

where α and β are, respectively, the coefficients of thermal expansion and isothermal compressibility of the isotropic phase at T_{NI} . The theoretical values usually are found to be about 2 or 3 times higher than the experimental values. Large discrepancies are also found in the values of C_V and β in the nematic phase. Further, the calculations based on the MF models give $(T_{\text{NI}} - T_{\text{NI}}^*)/T_{\text{NI}} \simeq 0.9$ which leads to $T_{\text{NI}} - T_{\text{NI}}^* \simeq 30\text{--}40^\circ$. The reason for these discrepancies is that the MF method neglects completely the effect of short-range order. Making use of the Bethe approximation and of cluster variation methods, the influence of short-range order on the NI transition in the MS model has been studied by several workers [120,124–127]. These approximations are identical in the isotropic phase, i.e., they give the same value of T_{NI}^* , related to the pretransitional phenomena, magnetically induced birefringence and the scattering of light by orientational fluctuations. These phenomena are qualitatively well described in these approximations. In these works, each molecule is assumed to have γ_n nearest neighbours ($\gamma_n \geq 3$), no two nearest neighbours are nearest neighbours to each other. While each such central molecule i is subjected to a potential only due to the γ_n outer molecules of the cluster, an outer molecule j is also subjected to a mean field due to the rest of the medium. In the two-site cluster (TSC) approximation the thermal averages are evaluated with the two-particle distribution function [125]

$$P_2(\hat{e}_i, \hat{e}_j) = \frac{1}{Z_{12}} \exp[\beta J P_2(\hat{e}_1 \cdot \hat{e}_2) + (\gamma_n - 1)\beta J \bar{s}(P_2(e_{1z}) + P_2(e_{2z}))] \quad (4.97a)$$

with

$$Z_{12} = \int d\hat{e}_1 \int d\hat{e}_2 \exp[\beta J P_2(\hat{e}_1 \cdot \hat{e}_2) + (\gamma_n - 1)\beta J \bar{s}(P_2(e_{1z}) + P_2(e_{2z}))] . \quad (4.97b)$$

Here \hat{e}_1 and \hat{e}_2 are unit vectors pointing in the direction of the long axis of the molecules, \bar{s} is a variational parameter and J the interaction coupling constant.

The internal energy per particle is given by

$$U = -\frac{1}{2}\gamma_n J \sigma_s \quad (4.98)$$

where σ_s , the short-range order parameter, measures the correlation between the orientations of the neighbouring molecules

$$\sigma_s = \langle P_2(\hat{e}_1, \hat{e}_2) \rangle . \quad (4.99)$$

The calculations yield $\bar{P}_{2\text{NI}} \simeq 0.40$ and the ratio $(T_{\text{NI}} - T_{\text{NI}}^*)/T_{\text{NI}} \simeq 0.05$; the exact values depend on the lattice type, the number of nearest neighbours. Haegen et al. [130] have extended the TSC approximation to a ‘4-particle cluster (FSC) approximation and obtained the result $(T_{\text{NI}} - T_{\text{NI}}^*)/T_{\text{NI}} \simeq 0.04$; again the exact value depends on the lattice type.

Another important origin of the discrepancy between the experimental and MS theoretical values is the assumption that the molecule is cylindrically symmetric so that it is sufficient to define one order parameter \bar{P}_2 . However, in real nematogens most molecules are lath-shaped and have

a biaxial character. Hence, two order parameters are required to describe the uniaxial nematic phase composed of biaxial molecules. The second-order parameter is defined as

$$D = \frac{3}{2} \langle \sin^2 \theta \cos 2\Psi \rangle . \quad (4.100)$$

The mean-field theories have been developed [122,165] by including a term in the potential function proportional to D , in addition to the usual term. It is obtained that the molecular biaxility decreases the values of $\bar{P}_{2\text{NI}}$ and gives a better agreement with the experiment.

Luckhurst and Zannoni have discussed [128] the question “why is the Maier–Saupe theory of nematic liquid crystals so successful?”. Their arguments can be summarized as follows. The MS theory is founded on a MF treatment of long-range contributions to the potential function and ignores the important short-range forces. The theory has been particularly successful in accounting, not only for the order–disorder transition, but also for the orientational properties of the nematic liquid crystal. It is founded on the MF approximation applied to a weak anisotropic pair interaction arising due to dispersion force and predicts the universal properties of the nematogens. Despite its qualitative and even semi-quantitative success MS theory has been widely criticized [119,129]. One of the major criticisms is due to its foundation on the London dispersion forces. A second attack on the theory is concerned with its complete neglect of anisotropic short-range repulsive forces. This neglect is completely unjustified as it is accepted that the scalar repulsive forces are mainly responsible for determining the organization in simple fluids [166]. However, the results of hard rod theories are in marked contrast with the MS theories. On the one hand, theories based on the short-range repulsive forces, which are expected to make the dominant contribution to the potential, give results in poor accord with experiment. On the other hand, however, the MS theory founded on long-range dispersion forces, provides an excellent description of the orientational properties of real nematogens. A formal solution to this dilemma is provided by the molecular field theories based on a complete general form of the total potential. This is separated into a scalar component and an anisotropic part which is then written in terms of the Pople expansion. The orientational part of the single-particle potential is found to be a series whose first term has the same form as the MS result with \bar{u}_2 containing contributions from all the anisotropic forces. In this respect, the MS theory is equivalent in form to one which includes both long- and short-range contributions to the anisotropic intermolecular potential. There are several unsatisfactory features of this analysis which are discussed elsewhere [128]. As a solution to these difficulties, it has been suggested [128] that both the short- and long-range forces are important in determining the molecular organization in a nematic phase but that they operate at quite different levels. The short-range forces are responsible for the formation of highly ordered groups or clusters of molecules. The possibility of cluster formation has already been mentioned in the original MS theory [117] although with different purpose. In view of Luckhurst and Zannoni [128] the net effect of the existence of clusters would be to reduce the anisotropy associated with the short-range forces while increasing the influence of long-range forces. Further, the clusters are not destroyed at the NI phase transition. The anisotropic forces between clusters are, therefore, responsible for the orientational properties of the nematic mesophase. The parameter \bar{u}_2 in the effective potential then is not determined by the interaction of two molecules, but by two clusters. From this idea the failure of theories based on the repulsive forces can also be understood. The fundamental unit in these calculations is a single particle and at the transition the orientational order is completely destroyed producing a large increase in entropy. Contrary to it for the cluster model the transition

unlocks the ordering of the clusters but not that of the molecules within the cluster; consequently, the transition entropy is small. In the language of statistical mechanics the cluster can be described in terms of the spatial and orientational pair distribution function. Then the present idea [128] is equivalent to the assumption that the distribution function exhibits short-range order, over several molecular distances, and this order is not destroyed at the NI transition. As a result, the variation in the orientational properties on passing from one phase to the other will be determined by the long-range intermolecular forces corresponding to distances over which the distribution function does change. Consequently, the MS theory, founded on long-range forces, provides a good description of nematic liquid crystals, whereas theories based on short-range forces are invariably less successful.

As is evident from the above discussion, both short- and long-range forces are important in determining the molecular organization in a nematic liquid crystal. Therefore, a realistic theoretical model of nematics should be constructed using both the repulsive and attractive interactions between molecules.

4.4. The van der Waals (vdW) type theories

As discussed earlier, the mesophase molecules possess a strong anisotropy in both intermolecular repulsions and attractions. Hence, a molecular theory should incorporate both short-range repulsive and long-range attractive forces. In addition, the real complication which one faces in the construction of a theory is dealing with both the spatial and angular variables of the molecules [61]. For the calamitic nematics several attempts have been made to develop theories [131–145,167–171] in which both parts of the interactions are explicitly included. Most of these, known as van der Waals (vdW) type theories [131–139,167–171], differ only in evaluating the properties of reference system interacting via repulsive force and are almost identical as far as treating the attractive interaction is concerned. Basic to these works is the recognition that the predominant factor in determining the liquid crystalline stability is geometric and that the role of the attractive interactions is, to a first approximation, merely to provide a negative, spatially uniform mean field in which the molecules move. While Alben [57] used an orientation-independent mean-field potential, others have used orientation-dependent mean fields. The theories [140–145] based on the density functional approach will be discussed in Section 4.5. In this section, first we present a perturbation method [61], within the mean-field approximation, to describe the equilibrium properties of nematics for a model system composed of non-spherical molecules interacting via a pair potential having both the repulsive and attractive parts. All the vdW type theories [131–139] can be derived from this scheme by considering only the first-order perturbation term. We have also discussed the salient features of all these works.

In developing a perturbation theory, one begins by writing the pair potential energy of interaction, $u(\mathbf{x}_i, \mathbf{x}_j)$, as a sum of two parts — one part is known as reference potential $u^{(0)}$ and the other perturbation potential, $u^{(p)}$, i.e.

$$u(\mathbf{x}_i, \mathbf{x}_j) = u^{(0)}(\mathbf{x}_i, \mathbf{x}_j) + \lambda u^{(p)}(\mathbf{x}_i, \mathbf{x}_j) . \quad (4.101)$$

Here $u^{(0)}$ is chosen to include the rapidly varying short-range repulsive interactions, whereas $u^{(p)}$ represents the more smoothly varying long-range attractions, λ is a perturbation parameter.

The configurational integral of the system is written as

$$Q_N = \frac{1}{N!(4\pi)^N} \int d\mathbf{r}^N \int d\Omega^N \exp[-\beta U_N(\mathbf{x}_1, \mathbf{x}_2, \dots, \mathbf{x}_N)] , \quad (4.102)$$

where U_N is approximated as the sum of pair potentials (Eq. (4.61)), $\int d\mathbf{r}^N = \int d\mathbf{r}_1 \int d\mathbf{r}_2 \dots \int d\mathbf{r}_N$ and $\int d\Omega^N = \int d\Omega_1 \dots \int d\Omega_N$. The angular integration in Eq. (4.102) can be approximated to arbitrary accuracy by dividing the unit sphere into arbitrary small sections of solid angle $\Delta\Omega$ ($n = 4\pi/\Delta\Omega$ is the number of discrete orientations) and summing over all possible orientational distributions $\{N_1, \dots, N_p, \dots, N_n\}$ where N_p is the number of molecules having orientations falling in the p th solid angle and $\sum_{p=1}^n N_p = 1$. Thus

$$Q_N = \frac{1}{N!(4\pi)^N} \sum_{N_1} \dots \sum_{N_n} \frac{N!(\Delta\Omega)^N}{N_1! \dots N_n!} \int d\mathbf{r}^N \exp[-\beta U_N(\mathbf{r}^N, N_1, \dots, N_n)] \quad (4.103a)$$

$$\simeq \left(\frac{\Delta\Omega}{4\pi} \right)^N \left[\prod_{p=1}^n \hat{N}_p! \right]^{-1} \int d\mathbf{r}^N \exp[-\beta U_N(\mathbf{r}^N, \hat{N}_1, \dots, \hat{N}_n)] . \quad (4.103b)$$

Here the tilde denotes the maximum term values.

Assuming the pairwise additivity of interaction potential (Eq. (4.61)) and dividing the total potential into two parts, one obtains

$$Q_N = \left(\frac{\Delta\Omega}{4\pi} \right)^N \left[\prod_{p=1}^n N_p! \right]^{-1} \int d\mathbf{r}^N \exp[-\beta u_N^{(0)}(\mathbf{r}^N, \bar{N}_1, \dots, \bar{N}_n)] \\ \times \exp[-\beta u_N^{(p)}(\mathbf{r}^N; \hat{N}_1, \dots, \hat{N}_n)] \quad (4.104)$$

and

$$\frac{\partial \ln Q_N}{\partial \lambda} = -\frac{1}{2V} \beta \sum_{p=1}^n \sum_{p'=1}^n \tilde{N}_p \tilde{N}_{p'} \int d\mathbf{r} u^{(p)}(\mathbf{r}, \Omega_p, \Omega_{p'}) g(\mathbf{r}, \Omega_p, \Omega_{p'}) , \quad (4.105)$$

where

$$g(\mathbf{r}, \Omega_p, \Omega_{p'}) = \frac{V^2}{Q_N} \left(\frac{\Delta\Omega}{4\pi} \right)^N \left[\prod_{p'=1}^n N_{p'}! \right]^{-1} \int d\mathbf{r}^N \exp[-\beta U_N(\mathbf{r}^N, \hat{N}_1, \dots, \hat{N}_n, \lambda)] . \quad (4.106)$$

Integration of Eq. (4.105) leads to

$$\ln Q_N = \ln Q_N^0 - \frac{\beta}{2V} \int_0^\lambda d\lambda \sum_{p=1}^n \tilde{N}_p \sum_{p'=1}^n \hat{N}_{p'} \int d\mathbf{r} u^{(p)}(\mathbf{r}, \Omega_p, \Omega_{p'}) g(\mathbf{r}, \Omega_p, \Omega_{p'}) . \quad (4.107)$$

Choosing a continuous function $f(\Omega)$ to describe the orientational distribution such that

$$\tilde{N}_p = N f(\Omega_p) d\Omega_p \quad (4.108)$$

the Helmholtz free energy can be expressed as

$$\frac{\beta A}{N} = \frac{\beta A^{(0)}}{N} + \frac{1}{2} \rho \beta \int_0^1 d\lambda \int f(\Omega_p) d\Omega_p \int f(\Omega_{p'}) d\Omega_{p'} \\ \int d\mathbf{r} u^{(p)}(\mathbf{r}, \Omega_p, \Omega_{p'}) g(\mathbf{r}, \Omega_p, \Omega_{p'}) . \quad (4.109)$$

Writing the expansions

$$g(\mathbf{r}, \Omega_p, \Omega_{p'}) = g^{(0)}(\mathbf{r}, \Omega_p, \Omega_{p'}) + \lambda g^{(1)}(\mathbf{r}, \Omega_p, \Omega_{p'}) + \dots, \quad (4.110a)$$

$$A = A^{(0)} + \lambda A^{(1)} + \lambda^2 A^{(2)} + \dots \quad (4.110b)$$

and inserting these expressions into Eq. (4.109), one obtains on equating the coefficients of λ^r from both sides

$$\frac{\beta A^{(r)}}{N} = \frac{1}{2r} \beta \rho \int f(\Omega_p) d\Omega_p \int f(\Omega_{p'}) d\Omega_{p'} \int d\mathbf{r} u^{(p)}(\mathbf{r}, \Omega_p, \Omega_{p'}) g^{(r-1)}(\mathbf{r}, \Omega_p, \Omega_{p'}), \quad (4.111)$$

where r denotes the order of perturbation. All the zeroth-order terms refer to quantities corresponding to the reference system. Now, if we define the effective one-body potential as

$$\Psi^{(r)}(\Omega) = \frac{1}{2r} \rho \int f(\Omega_{p'}) d\Omega_{p'} \int d\mathbf{r} u^{(p)}(\mathbf{r}, \Omega_p, \Omega_{p'}) g^{(r-1)}(\mathbf{r}, \Omega_p, \Omega_{p'}). \quad (4.112)$$

Eq. (4.109) reads

$$\frac{\beta A}{N} = \frac{\beta A^{(0)}}{N} + \frac{1}{2} \beta \int f(\Omega_p) d\Omega_p \left[\sum_{r=1}^{\infty} \Psi^{(r)}(\Omega) \right]. \quad (4.113)$$

All the vdW-type mean-field theories [131–139] can be derived from Eq. (4.113) by considering only the first-order perturbation term which is written as

$$\Psi^{(1)}(\Omega_1) = \rho \int f(\Omega_2) d\Omega_2 \int d\mathbf{r} u^{(p)}(\mathbf{r}, \Omega_1, \Omega_2), g^{(0)}(\mathbf{r}, \Omega_1, \Omega_2), \quad (4.114)$$

where $g^{(0)}(\mathbf{r}, \Omega_1, \Omega_2)$ is the pair correlation function (PCF) for the reference system. The contribution of the reference system $A^{(0)}$ is evaluated in different ways in these works [131–139].

In the derivation of free energy as a function of $f(\Omega)$ by Gelbart and Baron [133] the molecular shape repulsions are treated within the approximation of scaled particle theory and the long-range attractions enter directly through a mean-field average. Basic to the Gelbart and Baron approach is the formulation of the effective one-body potential as an average over the pair attraction which excludes all relative positions denied to a pair of molecules because of their anisotropic hard cores. The Helmholtz free-energy equation reads

$$\frac{\beta A}{N} = \frac{\beta A_{\text{hr}}}{N} + \frac{1}{2} \beta \int d\Omega_1 f(\Omega_1) \bar{\Psi}_{\text{GB}}^{(1)}(\Omega_1). \quad (4.115)$$

with

$$\bar{\Psi}_{\text{GB}}^{(1)}(\Omega_1) = \rho \int f(\Omega_2) d\Omega_2 \int d\mathbf{r} \exp[-\beta u_{\text{hr}}(\mathbf{r}, \Omega_1, \Omega_2)] u_{\text{att}}(\mathbf{r}, \Omega_1, \Omega_2). \quad (4.116)$$

For A_{hr} the relation derived, for a system of hard spherocylindrical molecules of length L and diameter $2a$ by Cotter [103] using scaled particle theory was used by Gelbart and Baron [133]:

$$\frac{\beta A_{\text{hr}}}{N} \simeq \frac{\beta A_{\text{hsc}}}{N} = \int f(\Omega) \ln[4\pi f(\Omega)] d\Omega + \frac{2rv_0\rho}{(1-v_0\rho)^2} \left(1 + \frac{1}{2}qv_0\rho\right) \int d\Omega_1 \int d\Omega_2 f(\Omega_1)f(\Omega_2) \sin \theta_{12} + \{\text{term independent of } f(\Omega)\}, \quad (4.117)$$

where $v_0 = \pi a^2 L + \frac{4}{3}\pi a^3$ is the rod volume, $r = aL^2/v_0$, $q = \frac{4}{3}\pi a^3/v_0$, and θ_{12} is the angle between two rods. It is important to note that the relation (4.117) was revised by Cotter [132](b).

Using both the isotropic- and orientation-dependent parts of the attractive potential, i.e.,

$$u_{\text{att}}(\mathbf{r}, \Omega_1, \Omega_2) = U_{\text{att}}^{\text{iso}}(\mathbf{r}) + U_{\text{att}}^{\text{aniso}}(\mathbf{r}, \Omega_1, \Omega_2), \quad (4.118)$$

it has been shown [133](b) that the main contribution to the angular dependence of the attractive energy arises from the coupling between $u_{\text{att}}^{\text{iso}}$ and the hard-rod exculsion. Since $\exp(-\beta U_{\text{hr}})$ can assume only two values 0 and 1, Eq. (4.116) can be written as

$$\bar{\Psi}_{\text{GB}}^{(1)}(\Omega_1) = \rho \int f(\Omega_2) d\Omega_2 \int_{\xi(\Omega_1, \Omega_2)} d\mathbf{r} [u_{\text{att}}^{\text{iso}}(\mathbf{r}) + u_{\text{att}}^{\text{aniso}}(\mathbf{r}, \Omega_1, \Omega_2)]. \quad (4.119)$$

It is obvious, from Eq. (4.119), that both parts, isotropic as well as anisotropic of the attractive pair potential contribute to the orientation dependence of the mean-potential $\bar{\Psi}^{(1)}$. Thus, even in case of a spherically symmetric attractive interactions, the effective potential felt by a single molecule would be orientation-dependent. Contrary to it, this would not be true in case the hard cores are replaced by the hard spheres because then the domain of integration ξ becomes independent of Ω_1 and Ω_2 and only $u_{\text{att}}^{\text{aniso}}$ contributes to the orientation dependence of $\bar{\Psi}^{(1)}$.

Taking the form of attractive pair potential

$$u_{\text{att}}(\mathbf{r}, \Omega_1, \Omega_2) = -\frac{1}{r^6} [C_{\text{iso}} + C_{\text{aniso}} \cos^2 \Omega_{12}], \quad (4.120)$$

where C_{iso} and C_{aniso} are the interaction constants and expanding $\bar{\Psi}^{(1)}$ as

$$\bar{\Psi}_{\text{GB}}^{(1)}(\rho, \Omega) = A_0\rho + A_2\rho\bar{P}_2P_2(\cos \theta) + A_4\rho\bar{P}_4P_4(\cos \theta), \quad (4.121)$$

Gelbart and Gelbart [133] characterized $\xi(r, a, l)$ analytically, then evaluated the integrals of Eq. (4.119) numerically and obtained the coefficient A_L 's in terms of C_{iso} for x_0 (length–breadth ratio) = 1, 2, 3 and 4.2 and taking for each case $C_{\text{iso}}/C_{\text{aniso}} = 8, 50$ and 250. They also checked the convergence of the series (4.121). Using Onsager's [97] one-parameter representation of $f(\Omega)$,

$$f(\Omega) = \xi \cosh(\xi \cos \theta) / 4\pi \sinh \xi,$$

the order parameters were calculated; ξ was chosen to give $\bar{P}_2 = 0.52$, $\bar{P}_4 = 0.13$, $\bar{P}_6 = 0.017$ for $x_0 = 3$ and $C_{\text{iso}}/C_{\text{aniso}} = 8$.

Cotter [132] considered the application of the van der Waals approach to a model system of hard spherocylinders (with cylindrical length ℓ and radius a) subjected to a spatially uniform mean field potential.

$$\bar{\Psi}_{\text{cot}}^{(1)} = -\varepsilon_0\rho - \varepsilon_2\rho\bar{P}_2P_2(\cos\theta), \quad (4.122)$$

where ε_0 and ε_2 are the positive energy parameters. Using the rederived [132] scaled particle expression for A_{hr} ,

$$\begin{aligned} \frac{\beta A_{\text{hr}}}{N} \equiv \frac{\beta A_{\text{hsc}}}{N} &= \langle \ln[4\pi f(\Omega)] \rangle + \ln\left(\frac{\rho}{1-v_0\rho}\right) + \frac{3v_0\rho}{(1-v_0\rho)} \\ &+ \frac{[(4+q-\frac{1}{2}q^2)v_0^2\rho^2 + 2rv_0\rho[3-(1-q)v_0\rho]\langle\langle|\sin\Omega_{12}|\rangle\rangle]}{3(1-v_0\rho)^2} \end{aligned} \quad (4.123)$$

with the additional approximation

$$\langle\langle|\sin\Omega_{12}|\rangle\rangle \equiv \int d\Omega_1 d\Omega_2 f(\Omega_1)f(\Omega_2)|\sin\Omega_{12}| = \frac{\pi}{4} - \frac{5\pi}{32}\bar{P}_2^2 \quad (4.124)$$

extensive numerical calculations were carried out [132](b) for the NI transition for the parameter values $x_0 = 3$, $v_0 = 230\text{\AA}^3$, $\varepsilon_0/v_0k = 25000k$ and $\varepsilon_2/v_0k = 2000k$. The results were compared with the experimental data of PAA (see Table 8). A satisfactory qualitative agreement between theory [132] and experiment was found; for example, the model system exhibits (i) a first-order NI phase transition, (ii) the temperature dependence of the order parameter (at constant P or constant ρ) of roughly the correct shape, (iii) nearly linear plots of $\ln T$ versus $\ln \rho$ at constant \bar{P}_2 with slope 3.9, (iv) increases in T_{NI} with increasing pressure of the correct order of magnitude, and (v) large pretransitional increases in the compressibility, expansivity, and specific heat as T_{NI} is approached from below. The model could not explain the premonitory phenomena observed experimentally in the isotropic phase above T_{NI} . As obvious from the Table 8, no satisfactory quantitative agreement with experiment was found; the predicted values of the relative density discontinuity, entropy of transition, slope of the P – T coexistence curve are too large and the order parameter at the transition $\bar{P}_{2\text{NI}}$ are too large whereas the mean reduced density at the transition is too small.

Baron and Gelbart [133] applied their GvdW theory to systems with spherocylindrical hard cores and attractive forces described by Eq. (4.120) and made the calculations using Eq. (4.123) for A_{hr} and approximating $f(\Omega)$ by the Onsager representation. The use of Onsager's relation for $f(\Omega)$ introduces substantial errors and so the quantitative agreement between theory and experiment cannot be expected. However, it is important to note that the Gvdw approach [133] in which $\bar{\Psi}^{(1)}$ is determined from the model pair potential, is clearly superior in comparison to the use of an essentially phenomenological pseudo-potential (Eq. (4.122)) by Cotter [132]. Further, despite its quantitative inadequacies, the van der Waals approach indicates that the anisotropy of the short-range intermolecular repulsions plays a major role in determining nematic order and stability and cannot be neglected, even to a first approximation. For model system with hard cores plus attractions, anisotropic hard cores are clearly necessary for explaining the behaviour of nematogens in even a qualitative manner.

A number of computer simulation studies [148–153] on systems of hard spherocylinders with $x_0 = 2$ and 3 have been reported. A comparison of these results in the isotropic phase with the results of SPT shows that while SPT gives reasonably good values at the low densities, it overestimates the pressure as the density is increased. Savithramma and Madhusudana [136] extended the Andrews method [146] to derive the thermodynamic properties of an ensemble of spherocylinders. They used this extended model to study the NI transition properties and made calculations in the MF approximation for a system of hard spherocylinders, by using the virial coefficients of the isotropic phase as well as for hard spherocylinder superimposed by the attractive potential of the form (4.122). In the calculation they adjusted the potential parameters so as to get $T_{\text{NI}} = 409$ K and $\eta_{\text{nem}} \simeq 0.62$, where $\eta = \rho v_0$ is the packing fraction. From these calculations it was found that (i) the calculation based on the extended Andrews model can be carried out upto $x_0 = 2.9$ while those based on SPT could only be made upto $x_0 = 2.45$, (ii) the trend of different transition quantities as a function of x_0 are similar to those as given by SPT, (iii) in case of Andrews model, $\Gamma = 4$ for $x_0 = 2.075$, which is substantial improvement over $x_0 = 1.75$ of SPT, and (iv) the present calculation leads to reasonably good agreement with the experimental data.

Ypma and Vertogen [134] suggested that a nematic can be looked upon as a normal liquid and derived an equation of state based on the following point of view. The spatial ordering in the liquid was considered to be determined by the hard-core repulsion which was, to a first approximation, replaced by a hard-core repulsion. The orientational ordering, resulting due to the effect of the eccentricity of the hard core and the superimposed anisotropic attraction interaction, were treated in two ways. First a molecular-field approximation was applied. Second using a two-particle orientational distribution function the short range orientational order was investigated. The molecules were assumed to interact through the van der Waals dispersion forces. Following Bellemans [170] the free-energy of the system was expressed in terms of the properties of an assembly of hard spheres. The distance of closest approach between two molecules was expressed as

$$D(\Omega_1, \Omega_2) = D_0[1 - \alpha(\Omega_1, \Omega_2)] , \quad (4.125)$$

where D_0 is the diameter of an equivalent hard sphere of the reference system and α is defined such that the average over all orientations

$$\langle \alpha(\Omega_1, \Omega_2) \rangle = \int d\Omega_1 d\Omega_2 f(\Omega_1) f(\Omega_2) \alpha(\Omega_1, \Omega_2) \quad (4.126)$$

vanishes in the isotropic phase. Expanding $\alpha(\Omega_1, \Omega_2)$ in terms of Legendre polynomial, and truncating the series after the first term,

$$\alpha(\Omega_1, \Omega_2) = \alpha_2 P_2(\cos \theta_{12}) \quad (4.127)$$

the configurational free energy of the reference hard-core system was expressed as

$$\frac{\beta A_{\text{hc}}}{N} = \frac{\beta A_{\text{hs}}}{N} - \frac{12\eta(1 + \frac{1}{2}\eta)}{(1 - \eta)^2} \alpha_2 \langle P_2(\cos \theta_{12}) \rangle + \langle \ln[4\pi f(\Omega)] \rangle , \quad (4.128)$$

where

$$\frac{\beta A_{\text{hs}}}{N} = \ln\left(\frac{\rho}{1 - \eta}\right) + \frac{3}{2(1 - \eta)^2} - \frac{5}{2} . \quad (4.129)$$

In the model calculations [134] two particular choices of the attractive potential were considered:

$$u_{\text{att}}(\mathbf{r}, \Omega_1, \Omega_2) = -r^{-6}[\varepsilon_0 + \varepsilon_2 P_2(\cos \theta_{12})] \quad (4.130a)$$

and

$$u_{\text{att}}(\mathbf{r}, \Omega_1, \Omega_2) = -[\varepsilon_0 + \varepsilon_2 P_2(\cos \theta_{12})]/V. \quad (4.130b)$$

In Eq. (4.130b) the interaction constants ε_0 and ε_2 have been divided by the volume V in order to get an extensive expression for the total attractive interaction energy.

Now the total Helmholtz free energy can be written as [134]

$$\frac{\beta A}{N} = \frac{\beta A_{\text{hs}}}{N} + \langle \ln[4\pi f(\Omega)] \rangle - \frac{12\eta(1 + \frac{1}{2}\eta)}{(1 - \eta)^2} \alpha_2 \bar{P}_2^2 + \frac{1}{2} \beta \rho \int d\mathbf{r} g_{\text{hs}}(\mathbf{r}) [\varepsilon_0(r) + \varepsilon_2(r) \bar{P}_2^2]. \quad (4.131)$$

Thus in the approach of Ypma and Vertogen the mean potential was expressed in terms of hard-sphere radial distribution function $g_{\text{hs}}^{(r)}$

$$\bar{\Psi}_{\text{YV}}^{(1)} = \rho \int f(\Omega_1) d\Omega_1 \int d\mathbf{r} g_{\text{hs}}(\mathbf{r}) [\varepsilon_0(r) + \varepsilon_2(r) \bar{P}_2 P_2(\cos \theta_1)]. \quad (4.132)$$

As discussed in Section 4.3, in order to account for the nearest-neighbour correlations between molecular orientations, at least a two-particle orientational distribution function is required. Using a cluster variation method, such a function was derived [125] and then Eq. (4.131) is modified as [134]

$$\frac{\beta A}{N} = \frac{\beta A_{\text{hs}}}{N} + \frac{1}{2} \beta \rho \int d\mathbf{r} g_{\text{hs}}(\mathbf{r}) \varepsilon_0(r) + \frac{\beta A_{\text{orient}}}{N}, \quad (4.133)$$

where

$$\frac{\beta A_{\text{orient}}}{N} = -\frac{1}{2} \gamma_n \ln Z_{12} + (\gamma_n - 1) \ln Z_1 \quad (4.134)$$

with

$$Z_1 = \int d\Omega \exp[B_2(\eta, T) \bar{s} P_2(\cos \theta)] , \quad (4.135a)$$

$$Z_{12} = \int d\Omega_1 d\Omega_2 \exp \left[\frac{B_2(\eta, T)}{\gamma_n} P_2(\cos \theta_{12}) + \frac{\gamma_n - 1}{\gamma_n} B_2(\eta, T) \bar{s} [P_2(\cos \theta_1) + P_2(\cos \theta_2)] \right]. \quad (4.135b)$$

Here

$$B_2(\eta, T) = \frac{24\eta(1 + \frac{1}{2}\eta)}{(1 - \eta)^2} \alpha_2 - \beta \rho \int d\mathbf{r} \varepsilon_2(r) g_{\text{hs}}(r). \quad (4.135c)$$

Extensive numerical calculations were done for the model potential (4.130) for $\alpha_2 = 0$ (spherical molecules) as well as $\alpha_2 \neq 0$ non-spherical molecules. The use of Eq. (4.130b) allows an interesting comparison with the results of Cotter [132](b). Similar trends of the variation of NI transition properties were observed as those of Cotter's work. As can be seen from Table 8, except for Γ the overall agreement of the hard sphere model ($\alpha_2 = 0$) is better than that of Cotter's model. Although Cotter's basic assumption of a spherocylindrical molecular shape seems more realistic than a spherical shape, it is expected that her model may predict much worse results if the excluded volume of two spherocylinders is accounted more accurately. Similar results were obtained by the hard sphere model with a distance-dependent interaction potential (4.130a) which corresponds to the van der Waals dispersion forces.

The influence of a slightly non-spherical molecular shape ($\alpha_2 \neq 0$) on the NI transition properties was studied by taking the model potential (4.130b) and treating the orientational coordinates in MF approximation. For a given set of interaction strengths the variation of packing fraction, order parameter, relative density change, etc., were studied as a function of the eccentricity parameter α_2 . It was found that even small values of α_2 have a strong influence on the thermodynamic properties at the transition. With increasing α_2 the steric hindering becomes more effective, shifting the phase transition to lower densities with increasing density change and jump of the order parameter. Further, except for Γ and (dT_{NI}/dp) , results for the transition properties have worsened somewhat as compared to hard-sphere model, but still are in better agreement with experiment than Cotter's results for spherocylinders (see Table 8). The extensive calculations were also performed to analyse the effects of short-range orientational correlations on the NI transition. It was found that (i) the transition temperature, the discontinuity in the order parameter, the density and the entropy decrease if short-range orientational order is included, (ii) the short-range orientational correlations have strong influence on the transition properties, (iii) as the number of nearest neighbour increases the results become worse in comparison with the MF approximation, and (iv) the overall agreement with experiment is quite satisfactory with smaller number of nearest neighbours $\gamma_n = 3$ or 4.

The first-order perturbation theory (Eqs. (4.113) and (4.114)) was applied by Singh and co-workers [61,137] to study in detail the NI transition in a model system of hard ellipsoidal molecules with a superposed attractive potential described by the dispersion and quadrupolar interactions. The following form for the attractive potential was adopted:

$$u_{\text{att}}(\mathbf{r}, \Omega_1, \Omega_2) = -C_{\text{id}}r^{-6} - (C_{\text{ad}}r^{-6} + C_{\text{aq}}r^{-5})P_2(\cos\theta_{12}). \quad (4.136)$$

The first term represents the isotropic component of the dispersion interaction and the second and third terms describe, respectively, the anisotropic dispersion and quadrupolar interactions. C_{id} , C_{ad} and C_{aq} are their respective constants. The potential (4.136) assumes that $r > D(\mathbf{r}, \Omega_1, \Omega_2)$, where $D(\mathbf{r}, \Omega_1, \Omega_2)$ is the distance of closest approach between two ellipsoids, and depends on the intermolecular separation but not on the orientation of the intermolecular vector. It also depends on the angle between the two molecules only and not on their orientations Ω_1 and Ω_2 . This is certainly a drastic oversimplification of the intermolecular potential of the real liquid crystals. However, there are two reasons of our choice of such a simple trial potential. First, such a pair potential is in accord with the MS theory and, secondly, it provides a convenient means to study the effects of attractive interactions.

Taking Eq. (4.136) and the Berne and Pechukas expression [109] for $D(\mathbf{r}, \Omega_1, \Omega_2)$ (see Eq. (4.81)), the following expression for the effective one-body potential was obtained [61,137] as

$$\bar{\Psi}^{(1)} = -\varepsilon_0 - \varepsilon_2 \bar{P}_2 P_2(\cos \theta_1) - \varepsilon_4 \bar{P}_4 P_4(\cos \theta_1), \quad (4.137)$$

where

$$\varepsilon_0 = (\frac{1}{12}\pi x_0) C_{\text{id}}^* [A_0^{(6)} + \frac{1}{5}(C_{\text{ad}}^*/C_{\text{id}}^*) A_2^{(6)}] \eta I_6(\eta) + \frac{1}{10}(\frac{1}{6}\pi x_0)^{2/3} C_{\text{aq}}^* A_2^{(5)} \eta I_5(5), \quad (4.138a)$$

$$\begin{aligned} \varepsilon_2 = & (\frac{1}{12}\pi x_0) C_{\text{id}}^* [A_2^{(6)} + \{A_0^{(6)} + \frac{2}{7}(A_2^{(6)} + A_4^{(6)})\} (C_{\text{ad}}^*/C_{\text{id}}^*) \eta I_6(\eta)] \\ & + \frac{1}{2}(\frac{1}{6}\pi x_0)^{2/3} C_{\text{aq}}^* [A_0^{(5)} + \frac{2}{7}(A_2^{(5)} + A_4^{(5)})] \eta I_5(\eta), \end{aligned} \quad (4.138b)$$

$$\begin{aligned} \varepsilon_4 = & (\frac{1}{12}\pi x_0) C_{\text{id}}^* [A_4^{(6)} + \{\frac{18}{35}A_2^{(6)} + \frac{20}{77}A_4^{(6)}\} (C_{\text{ad}}^*/C_{\text{id}}^*)] \eta I_6(\eta) \\ & + \frac{1}{2}(\frac{1}{6}\pi x_0)^{2/3} C_{\text{aq}}^* [\frac{18}{35}A_2^{(5)} + \frac{20}{77}A_4^{(5)}] \eta I_5(\eta) \end{aligned} \quad (4.138c)$$

with

$$C_{\text{id}}^* = C_{\text{id}}/v_0^2, \quad C_{\text{ad}}^* = C_{\text{ad}}/v_0^2, \quad C_{\text{aq}}^* = C_{\text{aq}}/v_0^2, \quad r^* = r/D(\Omega_{12}), \quad (4.138d)$$

and A_L 's are the constants appearing in the integral

$$I_n(\theta_{12}) = \int \frac{d\hat{r}}{D^{n-3}(\hat{r}, \Omega_{12})} \quad (4.138e)$$

$$= \frac{1}{D_0^{n-3}} [A_0^{(n)} + A_2^{(n)} P_2(\cos \theta_{12}) + A_4^{(n)} P_4(\cos \theta_{12}) + \dots] . \quad (4.138f)$$

The integrals $I_n(\eta)$ are defined as

$$I_n(\rho, T) = \int_0^\infty dr^* r^{*2-n} g_{\text{hs}}^{(0)}(r^*) . \quad (4.138g)$$

Starting from the pressure equation for a system of hard ellipsoids of revolution interacting via a pair potential u_0 satisfying the relation

$$\begin{aligned} u_0(\mathbf{r}, \Omega_{12}) & \equiv u_{\text{her}}(\mathbf{r}, \Omega_{12}) = u_{\text{her}}(r/D(\Omega_{12})) \\ & = \begin{cases} \infty, & r^* < 1, \\ 0, & r^* > 1, \end{cases} \end{aligned} \quad (4.139)$$

the following expression for the Helmholtz free energy of reference system was derived [61]:

$$\begin{aligned} \frac{\beta A^0}{N} & \equiv \frac{\beta A_{\text{her}}}{N} \\ & = (\ln \rho - 1) + \langle \ln[4\pi f(\Omega)] \rangle + \frac{\eta(4-3\eta)}{(1-\eta)^2} [F_0(\chi) - F_2(\chi) \bar{P}_2^2 - F_4(\chi) \bar{P}_4^2], \end{aligned} \quad (4.140)$$

where

$$F_0(\chi) = (1 - \chi^2)^{-1/2}(1 - \frac{1}{6}\chi^2 - \frac{1}{40}\chi^4 - \dots), \quad (4.141a)$$

$$F_2(\chi) = \frac{1}{3}\chi^2(1 - \chi^2)^{-1/2}(1 + \frac{3}{14}\chi^2 + \frac{5}{56}\chi^4 + \dots) \quad (4.141b)$$

and

$$F_4(\chi) = \frac{1}{35}\chi^4(1 - \chi^2)^{-1/2}(1 + \frac{15}{22}\chi^2 + \frac{525}{1184}\chi^4 + \dots). \quad (4.141c)$$

Extensive numerical calculations were done for two model potentials; the first one assumes $C_{aq} = 0$, and the second $C_{ad} = 0$. These choices enable us to investigate separately the effects of anisotropic dispersion and quadrupole interactions on the transition properties. From these calculations it was found that (i) with increasing x_0 the phase transition is shifted to higher temperature, lower density with increasing density change and jump of the order parameter, (ii) the interaction parameters have a strong influence on the thermodynamic properties [137] and the effects are more pronounced in case of quadrupolar interaction [137], (iii) for a given x_0 and ratio of the interaction strength the quadrupole interaction predicts a jump in transition temperature, the smaller values for η and Γ but higher values of $C_{id}^*/\kappa, \Delta\rho/\rho_{nem}, \bar{P}_2, \Delta\Sigma/N\kappa$ and (dT_{NI}/dp) in comparison with the anisotropic dispersion interaction, (iv) when the \bar{P}_4 term is included in the calculation, $\bar{P}_2, \Delta\rho/\rho_{nem}$ and $\Delta\Sigma/N\kappa$ increase whereas η decreases slightly, and (v) the pressure dependence of the transition properties is in accordance with the experiments; the application of pressure increases the temperature range of the existence of nematic order.

For the potential model (4.136) with $C_{aq} = 0$, Singh and Singh [61] carried out the calculations based on the experimental data of PAA. Setting $\varepsilon_4 = 0$ the criterion adopted in this calculation for selecting the values of ε_0 and ε_2 was to adjust T_{NI} and η_{nem} to 409 K and 0.62, respectively, which are the experimental values for PAA. The results are given in Table 8. It may be seen from the table that the values reported by Savithramma and Madhusudana [136] and ours [61] are almost identical and are in quite good agreement with the experimental data of PAA. Singh, Lahiri and Singh [137] also investigated the influence of short-range orientational correlation on the transition properties by using a two-site cluster (TSC) variation method. Though the results demonstrate (Table 8) that the short-range orientational order has a strong influence on the NI transition properties, the theoretical values are overall in poor agreement with the experiment as compared to our earlier work.

Tjipto-Margo and Evans [167] have incorporated the convex peg potential [172] into a vdW theory of NI phase transition. In the convex peg model, the molecules are envisioned to have a hard (biaxial) core embedded in a spherically symmetric square well,

$$u(\mathbf{r}, \Omega_1, \Omega_2) = \begin{cases} \infty & \text{for } r \in V_{exc}(\Omega_1, \Omega_2) \\ -\varepsilon & \text{for } r \leq \sigma \end{cases} \quad (4.142)$$

Eq. (4.142) represents repulsion if the cores overlap (reside within the excluded volume V_{exc}) and attraction if the centre-to-centre distance is less than or equal to the sum of the largest semi-major axes (σ). Thus, the anisotropies in the convex peg potential are derived from both its repulsive and attractive regions. For formal calculations the hard core was represented as a general convex body whereas, in the numerical work, by a biaxial ellipsoid [173]. In accordance with the GvdW theories

the repulsive interactions were treated to all orders using a resummation technique and the attractive interactions were incorporated to the lowest order. The thermodynamic system was considered to be a fluid of hard biaxial ellipsoids with semi-axis lengths a, b and c . The hard ellipsoid fluid can sustain three stable fluid phases, the uniaxial and biaxial nematic phases and the isotropic fluid. For the formation of biaxial phase, the a, b and c axes lengths of the biaxial ellipsoid must closely approximate the geometric mean condition $a^2 = bc$ and the fluid density must reside in a small density domain. Tjpto-Margo and Evans [167] did not put these restrictions and consequently, set the two macroscopic biaxial order parameters to zero in the calculations. Global phase diagrams were determined and the NI transition properties were calculated (see Table 8). It was found that (i) the model predicts one uniaxial nematic and two isotropic phases (vapour and liquid), (ii) the nematic–vapour, the nematic–isotropic liquid, the vapour–isotropic liquid phases as well as a nematic–vapour–isotropic liquid triple point coexist, (iii) due to the differing strengths of the attractive forces for the prolate and oblate bodies, the prolate–oblate symmetry is broken in this model. However, in the limit of very high temperature and very high densities this symmetry is exhibited, (iv) the “first-orderness” of the NI transition increases as temperature decreases and (v) the NI phase transition properties agree satisfactorily with the experimental data of PAA.

It is important to mention here that while Ypma and Vertogen [134] have used deformed hard sphere model and the Bellmann [170] type expansion to calculate the properties of reference system, Cotter [132] and Savithramma and Madhusudana [136] have used SPT. The latter authors have also extended a method given by Andrews [146] for hard spheres to calculate the properties of hard spherocylinders. Singh and Singh [61,137] have described the repulsive interaction by the repulsion between hard ellipsoids of revolution. These authors performed the calculations by assuming that the pair correlation function $g(\mathbf{r}, \Omega_{12})$ for a fluid of hard ellipsoids of revolution scales as $g(r/D(\Omega_{12}))$ [107]. Though this approximation introduces anisotropy in the pair correlation function and is exact at very low density, it cannot be expected to be correct at liquid density. In fact, the g of nematic phase must depend on $f(\Omega)$ as well as on $r/D(\Omega_{12})$. It is difficult to assess the error introduced by this decoupling approximation but it gives compressibility factor for the isotropic phase which is in very good agreement with the simulation values. On the other hand, by construction the “convex peg in a round hole” potential underestimates the effects of attractive anisotropy because all the anisotropy is obtained as a result of the hard core interaction. This model has to be selected in such a way as to fit and to understand the temperature dependences of second virial coefficient of simple non-spherical molecules [172]. Further, since convex peg model has attractive forces in its Hamiltonian, this model system supports a thermodynamically stable vapour phase. Owing to the effective anisotropic attractive forces, the first-order character of the NI transition is significantly enhanced as compared to that of a hard uniaxial body. However, this enhancement is compensated by the biaxiality and the resulting NI transition becomes weakly first-order.

Flory and Ronca [138] extended the lattice model treatment [102] to a system of hard rod molecules subjected to orientation-dependent mutual attractions. They derived the energy relations, for a system at constant volume, by considering interactions between pair of segments in contact, rather than in terms of interactions between entire molecules. A characteristic temperature T^* was defined to measure the intensity of these interactions. The orientational energy of the system as a whole was basically of the MS type. Numerical calculations were reported with

the following findings: (i) steric effects of molecular shape asymmetry, embodied in the axial ratio x_0 , are of foremost importance, (ii) the reduced temperature $\tilde{T}_{\text{NI}} = T_{\text{NI}}/x_0 T^*$ at which the NI transition takes place in the neat liquid decreases with decrease in x_0 below its athermal limit $x_{\text{ocrit}} = 6.417$ for $\tilde{T}_{\text{NI}}^{-1} = 0$, and (iii) both the transition entropy and the orientational heat capacity C_p are monotonic through the transition; C_p diverges at a temperature appreciably above T_{NI} , where the metastable anisotropic state becomes unstable. The application of lattice model has also been considered by Dowell [138](c) to examine the question-what happens to the relative stabilities of isotropic liquid, nematic, smectic A_1 and smectic S_A phases formed by rigid cores and partially flexible tails? She assumed site-site hard repulsions, then added soft repulsions and London dispersion attractions using segmental Lennard–Jones (12-6) potentials, and finally added dipolar interactions which include dipole–dipole forces and segmental dipole-induced dipole forces. The results obtained show that it is not necessary to invoke dipolar forces to have stable liquid crystal phases and that the dipolar forces increase the stability of these phases in systems with Lennard–Jones interactions. The dipolar forces also shift the temperature ranges of these phases closer to ambient. In an other work [138](b) the NI transition properties were calculated for molecules composed of rigid cores having semiflexible tails and interacting through Lennard–Jones potential. The calculated values of transition properties are in agreement with the experimental data of PAA. These works [138] elucidate the importance of realistic intermolecular potentials, particularly the role of soft repulsions in describing an order–disorder transition between two phases.

An orientation-averaged pair correlation theory was proposed by Woo and coworkers [171] which is based on the Bogoliubov–Born–Green–Kirkwood–Yvon (BBGKY) theory and takes account of the pair spatial correlations arising from the intermolecular attractions and repulsions. In this theory a Lennard–Jones (12-6) potential was employed but the anisotropy of the pair correlation function was not considered. Secondly, it is somewhat difficult to solve the second BBGKY equation. Nakagawa and Akahane [168] introduced the pair spatial correlation function approximately into the MF theory in terms of an orientation-averaged pair potential and studied its effects on the NI phase transition in the decoupling approximation [107] which decouples the orientations and positions. The approximated pair spatial correlation function [172] is much simpler than Woo's and co-workers [171] but involves the deviation from the spherical symmetry. The numerical calculations were done for a model potential of Lennard–Jones (12-6) type and retaining the leading coefficients of the orientation-averaged pair potential. It was found that the anisotropy of a pairwise intermolecular potential increases both the long-range orientational order and the NI transition temperature. The order parameter change near the transition point is in good agreement with the data for PAA but the transition entropy and C_v do not agree satisfactorily.

The molecular-field theories have been reformulated by Vertogen and de Jeu [175] in such a way that they can be used analytically. Based on the so-called spherical version of the models the equation of state for nematics was derived as a generalization of the theory of simple liquids [176] and the calculations were performed in the MF approximation. Starting from this equation of state for nematics the two well-known approaches, Onsager [97] and Maier-Saupe [117], can be recovered by a vector of variable length, such that its thermally averaged length is always equal to one. In view of the mathematical difficulties it is extremely hard to arrive at a reliable equation of state for a simple model of nematics from the first principle. Therefore, only a qualitatively correct equation of state has been discussed by Vertogen and de Jeu [175]. In complete analogy with the

theory of simple liquids [176], the partition function of the model system is given by

$$Z = Z_{\text{hr}} \left\langle \exp \left[\frac{1}{2} \beta \sum_{\kappa \neq \ell} u_{\text{att}}(r_{\kappa\ell}, \Omega_{\kappa}, \Omega_{\ell}) \right] \right\rangle_0, \quad (4.143)$$

where Z_{hr} denotes the partition function of the hard-rod model and the thermal average is taken with respect to the hard-rod system. Thus, the calculation of the equation of state contains two parts: the calculation of the partition function of the hard-rod model and the calculation of the thermal average for an assumed attractive interaction. The problem thus boils down to the calculation of

$$Z_{\text{hr}} = \frac{1}{N! (\lambda \tau)^{3N}} \int \prod_{i=1}^N d\mathbf{r}_i d\Omega_i \exp \left[-\frac{1}{2} \beta \sum_{\kappa, \ell=1}^N u_{\text{hr}} \right], \quad (4.144)$$

where the constant τ is given by

$$\tau = \frac{h}{[(2\pi)^{5/3} k_B T I_1^{2/3} I_3^{1/3}]^{1/2}}. \quad (4.145)$$

Here I_1 and I_3 are the principal moments of inertia of the cylinder with I_3 about the cylinder axis. The calculation of the partition function is still an unsolved problem. According to the van der Waals approximation the integral over the position coordinate (Eq. (4.144)) can be approximated in a qualitative sense as

$$Z(\Omega_1, \Omega_2, \dots, \Omega_N) = \frac{1}{N!} \prod_{i=1}^N \left[V - \frac{1}{2} \sum_{j \neq i}^N V_{\text{exc}}(\Omega_{12}) \right]. \quad (4.146)$$

Thus

$$Z_{\text{hr}} = \frac{1}{(\lambda \tau)^{3N}} \int Z(\Omega_1, \Omega_2, \dots, \Omega_N) d\Omega_1 d\Omega_2 \dots d\Omega_N \quad (4.147)$$

with

$$Z(\Omega_1, \Omega_2, \dots, \Omega_N) = \frac{V^N}{N!} \exp \left\{ \sum_{i=1}^N \ln \left[1 - \frac{1}{2V} \sum_{j \neq i}^N V_{\text{exc}}(\Omega_{12}) \right] \right\}. \quad (4.148)$$

In a straightforward manner the van der Waals expression for the Helmholtz free energy per cylinder is given by

$$\beta A_{\text{hr}}/N = 3 \ln \lambda + 3 \ln \tau + \ln \rho - 1 - \ln [1 - \frac{1}{2} \rho \langle V_{\text{exc}}(\Omega_{12}) \rangle] + \langle \ln f(\Omega) \rangle. \quad (4.149)$$

It is extremely difficult to evaluate the thermal average over the hard-rod system and so has to be approximated

$$\left\langle \exp \left[\frac{1}{2} \beta \sum_{\kappa \neq \ell} u_{\text{att}}(r_{\kappa\ell}, \Omega_{\kappa}, \Omega_{\ell}) \right] \right\rangle_0 = \exp \left[\frac{1}{2} \beta \sum_{\kappa \neq \ell} \langle u_{\text{att}}(r_{\kappa\ell}, \Omega_{\kappa}, \Omega_{\ell}) \rangle_0 \right], \quad (4.150)$$

where

$$\langle u_{\text{att}}(\mathbf{r}_{\kappa'}, \Omega_{\kappa}, \Omega_{\ell}) \rangle_0 = \frac{1}{V^2} \int d\mathbf{r}_{\kappa} d\mathbf{r}_{\ell} d\Omega_{\kappa} d\Omega_{\ell} g_{\text{hr}}(\mathbf{r}_{\kappa'}, \Omega_{\kappa}, \Omega_{\ell}) u_{\text{att}}(\mathbf{r}_{\kappa'}, \Omega_{\kappa}, \Omega_{\ell}). \quad (4.151)$$

In the spirit of vdW theory, Eq. (4.150) can be approximated as

$$\left\langle \exp \left[\frac{1}{2} \beta \sum_{\kappa \neq \ell} u_{\text{att}}(\mathbf{r}_{\kappa'}, \Omega_{\kappa}, \Omega_{\ell}) \right] \right\rangle_0 = \exp \left[\frac{1}{2} N \beta \rho \bar{u}_0 + \frac{1}{2} N \beta \rho \bar{u}_2 \langle P_2(\cos \theta_{12}) \rangle \right]. \quad (4.152)$$

Starting from the approximate expression

$$V_{\text{exc}}(\Omega_{12}) = A_0 - A_1 P_2(\cos \theta_{12}) \quad (4.153)$$

for the excluded volume of two rods, the Helmholtz free energy in the spherical version of the model is obtained [175] as

$$\begin{aligned} \frac{\beta A}{N} = & 3 \ln \lambda + 3 \ln \tau + \ln \rho - \frac{7}{4} - \ln \left[1 - \frac{1}{2} \rho (A_0 - A_1 \bar{P}_2^2) \right] \\ & - \frac{1}{2} \beta \rho \bar{u}_0 - \frac{1}{2} \beta \rho \bar{u}_2 \bar{P}_2^2 - \frac{1}{4} \beta \bar{P}_2 - \frac{3}{4} \left(B^2 \bar{P}_2^2 - \frac{2}{3} B \bar{P}_2 + 1 \right)^{1/2} \\ & + B \bar{P}_2^2 - \frac{2}{3} \ln \frac{2\pi}{3} - \ln(1 - \bar{P}_2) - \frac{1}{2} \ln(1 + 2\bar{P}_2), \end{aligned} \quad (4.154)$$

where the coefficients A_0 and A_1 are determined by calculating the two simplest excluded volume corresponding to two parallel and perpendicular rods [175]. For two parallel rods

$$A_0 - A_1 = \frac{4}{3} \pi d_0^3 + 2\pi L d_0^2,$$

whereas for the two mutually perpendicular rods

$$A_0 + \frac{1}{2} A_1 = \frac{4}{3} \pi d_0^3 + 2\pi L d_0^2 + 2L^2 d_0.$$

The parameter B is given by

$$B = \frac{\rho A_1}{1 - \frac{1}{2} \rho [A_0 - A_1 \langle P_2(\cos \theta_{12}) \rangle]} + \rho \beta \bar{u}_2. \quad (4.155)$$

Using the thermodynamic relation the equation of state is given by

$$\beta p = \frac{\rho}{1 - \frac{1}{2} \rho (A_0 - A_1 \bar{P}_2^2)} - \frac{1}{2} \beta \rho^2 \bar{u}_0 - \frac{1}{2} \beta \rho^2 \bar{u}_2 \bar{P}_2^2. \quad (4.156)$$

As expected the equation of state (4.156) is found to describe the NI transition rather well from the qualitative point of view. The experimental curve of order parameter and the values of transition density can be reproduced fairly well by an appropriate choice of the parameters. However, the required parameter values do not correlate with the molecular structure. Thus, the derived equation of state is unable to describe the structure–property relationship in a physically satisfactory way. The discrepancies are not at all surprising in view of the simplicity of the model. Some of

these can be attributed to rather poor approximation methods, which overestimate a number of quantities, e.g., the influence of the excluded volume. Another most important source of the difficulties in interpretation is the poor representation of the intermolecular interactions and the neglect of molecular flexibility.

4.5. Application of density functional theory (DFT) to the NI phase transition

The density functional theory [37,49,140–145,177–195] is developing as a cost-effective procedure for studying the physical properties of non-uniform systems. The theory was pioneered by Kohn and others [179,180] and Mermin [181] for a quantum mechanical many-body system. Its initial classical version and development are by Lebowitz and Percus [182] and the present form by Saam and Ebner [183] and Yang et al. [184]. The general formalism of the classical version of DFT has played useful role in the development of approximate integral equations for the pair distribution functions of a uniform fluid [184]. The theory has subsequently been used profitably in the study of freezing of a variety of fluids, solid–melt interfaces, nucleation, liquid crystals, two-dimensional systems, molten salts, binary mixtures, aperiodic crystals or glasses, quasi-crystals, the elastic properties of solids and liquid crystals, spectroscopic properties, dislocations and other topological defects, flexoelectricity in liquid crystals, interfacial phenomena and wetting transitions, etc. In a review, Singh [49] has given an excellent account of DFT, its application to some of above development and prospects. The application of the theory to study the elastostatics in liquid crystals has been given in a self-contained manner by me [37]. Few other articles and monographs [186–194] are also available. Thus the theory has been clearly discussed several times in literature and the essentials of the approach are well documented. Therefore, we present [49,142] here a brief account of the theory relevant to the phase transition studies in liquid crystals.

In the absence of external field, the singlet distribution function is written as

$$\rho(\mathbf{x}) = \frac{1}{\Lambda} \exp[\beta\mu + C(\mathbf{x})], \quad (4.157)$$

where Λ is the cube of the thermal wavelength associated with a molecule, $-k_B T C(\mathbf{x})$ is the solvent-mediated potential field acting at \mathbf{x} . The single-particle direct correlation function $C(\mathbf{x})$ is a functional of $\rho(\mathbf{x})$ and is related to the Ornstein–Zernike (OZ) direct correlation function by the relation

$$\frac{\delta C(\mathbf{x}_1)}{\delta \rho(\mathbf{x}_2)} = C(\mathbf{x}_1, \mathbf{x}_2). \quad (4.158)$$

The excess Helmholtz free energy, defined as

$$\beta\Delta A = \beta(A - A_{\text{id}}) \quad (4.159)$$

is also related to $C(\mathbf{x})$ through the relation

$$\frac{\delta(\beta\Delta A)}{\delta \rho(\mathbf{x})} = -C(\mathbf{x}). \quad (4.160)$$

Here βA_{id} is the ideal gas part of the reduced Helmholtz free-energy

$$\beta A_{\text{id}} = \int d\mathbf{x} \rho(\mathbf{x}) \{ \ln[\rho(\mathbf{x})A] - 1 \}. \quad (4.161)$$

These are the starting equations of the density functional theory and have been used to develop a variety of approximate forms for the free-energy functionals. The functional integration of Eq. (4.158) from some initial density ρ_f (of isotropic liquid) to final density $\rho(\mathbf{x})$ (of the ordered phase) gives

$$C(\mathbf{x}_1; \{\rho(\mathbf{x})\}) - C(\mathbf{x}_1; \rho_f) = \int \tilde{C}(\mathbf{x}_1, \mathbf{x}_2; \rho(\mathbf{x})) \Delta\rho(\mathbf{x}_2) d\mathbf{x}_2, \quad (4.162)$$

where

$$\tilde{C}(\mathbf{x}_1, \mathbf{x}_2; \rho(\mathbf{x})) = \int_0^1 d\alpha C(\mathbf{x}_1, \mathbf{x}_2; [\rho_f + \alpha\{\Delta\rho(\mathbf{x})\}]) \quad (4.163)$$

and

$$\Delta\rho(\mathbf{x}_i) = \rho(\mathbf{x}_i) - \rho_f. \quad (4.164)$$

In the above equations, the braces $\{\}$ indicate the functional dependence of the quantities on the single-particle distribution function. Parameter α characterizes a path in density space along which the chemical potential remains constant. From a functional Taylor expansion, it follows that

$$\begin{aligned} C(\mathbf{x}_1, \mathbf{x}_2; [\rho_f + \alpha\{\Delta\rho(\mathbf{x})\}]) \\ = C(\mathbf{x}_1, \mathbf{x}_2; \rho_f) + \alpha \int d\mathbf{x}_3 C(\mathbf{x}_1, \mathbf{x}_2, \mathbf{x}_3; \rho_f) \Delta\rho(\mathbf{x}_2) \Delta\rho(\mathbf{x}_3) + \dots \end{aligned} \quad (4.165)$$

Combining Eqs. (4.162) and (4.165) we obtain

$$\ln[\rho(\mathbf{x}_1)/\rho_f] = \int d\mathbf{x}_2 C(\mathbf{x}_1, \mathbf{x}_2; \rho_f) \Delta\rho(\mathbf{x}_2) + \frac{1}{2} \int d\mathbf{x}_2 d\mathbf{x}_3 \Delta\rho(\mathbf{x}_2) C(\mathbf{x}_1, \mathbf{x}_2, \mathbf{x}_3; \rho_f) \Delta\rho(\mathbf{x}_3). \quad (4.166)$$

This is a non-linear equation and relates the single-particle density distribution of the ordered phase to the direct correlation function of the coexisting liquid.

From the functional Taylor expansion of (4.160) from ρ_f to $\rho(\mathbf{x})$ and using Eqs. (4.162)–(4.165), one obtains

$$\begin{aligned} \beta(\Delta A - \Delta A_f) = & - \int d\mathbf{x} C(\mathbf{x}; \rho_f) \Delta\rho(\mathbf{x}) - \frac{1}{2} \int d\mathbf{x}_1 d\mathbf{x}_2 \Delta\rho(\mathbf{x}_1) C(\mathbf{x}_1, \mathbf{x}_2; \rho_f) \Delta\rho(\mathbf{x}_2) \\ & - \frac{1}{6} \int d\mathbf{x}_1 d\mathbf{x}_2 d\mathbf{x}_3 \Delta\rho(\mathbf{x}_1) \Delta\rho(\mathbf{x}_2) C(\mathbf{x}_1, \mathbf{x}_2, \mathbf{x}_3; \rho_f) \Delta\rho(\mathbf{x}_3). \end{aligned} \quad (4.167)$$

The grand thermodynamic potential which is generally used to locate the transition is defined as

$$-W = \beta A - \beta\mu \int d\mathbf{x} \rho(\mathbf{x}). \quad (4.168)$$

Substituting the value of βA , we obtain correct to second order in $\Delta\rho(\mathbf{x})$:

$$\begin{aligned}\Delta W = W - W_f &= \int d\mathbf{x} [\rho(\mathbf{x}) \ln\{\rho(\mathbf{x})/\rho_f\} - \Delta\rho(\mathbf{x})] \\ &- \frac{1}{2} \int d\mathbf{x}_1 d\mathbf{x}_2 \Delta\rho(\mathbf{x}_1) C(\mathbf{x}_1, \mathbf{x}_2; \rho_f) \Delta\rho(\mathbf{x}_2) \\ &- \frac{1}{6} \int d\mathbf{x}_1 d\mathbf{x}_2 d\mathbf{x}_3 \Delta\rho(\mathbf{x}_1) \Delta\rho(\mathbf{x}_2) C(\mathbf{x}_1, \mathbf{x}_2, \mathbf{x}_3; \rho_f) \Delta\rho(\mathbf{x}_3) ,\end{aligned}\quad (4.169a)$$

where W_f is the grand canonical thermodynamic potential of the isotropic liquid. Combining Eqs. (4.166) and (4.169a) we get for ΔW an expression which is found to be convenient in many applications,

$$\begin{aligned}\Delta W = &- \int d\mathbf{x} \Delta\rho(\mathbf{x}) + \frac{1}{2} \int d\mathbf{x}_1 d\mathbf{x}_2 [\rho(\mathbf{x}_1) + \rho_f] C(\mathbf{x}_1, \mathbf{x}_2; \rho_f) \Delta\rho(\mathbf{x}_2) \\ &+ \frac{1}{6} \int d\mathbf{x}_1 d\mathbf{x}_2 d\mathbf{x}_3 [2\rho(\mathbf{x}_1) + \rho_f] \Delta\rho(\mathbf{x}_2) C(\mathbf{x}_1, \mathbf{x}_2, \mathbf{x}_3; \rho_f) \Delta\rho(\mathbf{x}_3) .\end{aligned}\quad (4.169b)$$

Eqs. (4.166), (4.169a) and (4.169b) are the basic equations of the theory of freezing and of interfaces of ordered phase and its melt. Of interest is the solutions of $\rho(\mathbf{x})$ of Eq. (4.166) having symmetry of ordered phase. These solutions, inserted into Eqs. (4.169a) and (4.169b), give the grand potential difference between the ordered and liquid phases. The phase with the lowest grand potential is taken as the stable phase. Phase coexistence occurs at the value of ρ_f which makes $\Delta W = 0$ for the ordered and liquid phases.

The grand thermodynamic potential is considered to be a functional of the singlet distribution $\rho(\mathbf{r}, \Omega)$. Eqs. (4.169a) and (4.169b) can be written as

$$\Delta W = W - W_f = \Delta W_1 + \Delta W_2 \quad (4.170)$$

with

$$\frac{\Delta W_1}{N} = \frac{1}{\rho_f V} \int d\mathbf{r} d\Omega [\rho(\mathbf{r}, \Omega) \ln(\rho(\mathbf{r}, \Omega)/\rho_f) - \Delta\rho(\mathbf{r}, \Omega)] \quad (4.171a)$$

and

$$\frac{\Delta W_2}{N} = - \frac{1}{2\rho_f V} \int d\mathbf{r} d\Omega_1 d\Omega_2 \Delta\rho(\mathbf{r}_1, \Omega_1) C(\mathbf{r}, \Omega_1, \Omega_2) \Delta\rho(\mathbf{r}_2, \Omega_2) . \quad (4.171b)$$

The density of the ordered phase can be obtained by minimizing ΔW with respect to arbitrary variation in the ordered phase density subject to the constraint that there is one molecule per lattice site (for perfect crystal) and/or orientational distribution is normalized to unity. Thus

$$\ln[\rho(\mathbf{r}_1, \Omega_1)/\rho_f] = \frac{\lambda}{L} + \int d\mathbf{r}_2 d\Omega_2 C(\mathbf{r}_1, \Omega_1, \Omega_2; \rho_f) \Delta\rho(\mathbf{r}_2, \Omega_2) , \quad (4.172)$$

where λ_L is a Lagrange multiplier which appears in the equation because of constraint imposed on the minimization. For locating transition one attempts to find the solution of $\rho(\mathbf{r}, \Omega)$ of Eq. (4.172) which has symmetry of the ordered phase. Below a certain liquid density, say ρ' , the only solution is $\rho(\mathbf{r}, \Omega) = \rho_f$. Above ρ' a new solution of $\rho(\mathbf{r}, \Omega)$ can be obtained which corresponds to the ordered phase. The phase with lowest grand potential is taken as the stable phase. The transition point is determined by the condition $\Delta W = 0$. Implicit in this approach is an assumption according to which system is either entirely liquid or entirely ordered phase, no phase coexistence is permitted. This signifies the mean-field character of the theory.

For axially symmetric molecules, the singlet density of the nematic phase can be expressed as

$$\rho(\mathbf{r}, \Omega) = \rho_n f(\Omega) \quad (4.173)$$

with

$$\rho_n = \rho_f(1 + \Delta\rho^*) \quad (4.174)$$

and

$$f(\Omega) = 1 + \sum'_{\ell \geq 2} (2\ell + 1) \bar{P}_\ell P_\ell(\cos \theta), \quad (4.175)$$

where $\Delta\rho^* = (\rho_n - \rho_f)/\rho_f$ is the relative change in the density at the transition and ρ_n be the number density of the nematic phase. For a uniaxial phase of cylindrically symmetric molecules, $f(\Omega)$ depends only on the angle θ between the director and the molecular symmetry axis. The orientational singlet distribution is normalized to unity (Eq. (2.7)).

In case of the nematic phase, it is convenient to use the following ansatz for $f(\Omega)$:

$$f(\Omega) = A_0 \exp \left[\sum_{\ell} \lambda_{\ell} P_{\ell}(\cos \theta) \right]. \quad (4.176)$$

A_0 is determined from the normalization condition (2.7). When $\lambda_{\ell} \rightarrow 0$, $f(\Omega) \rightarrow 1$ corresponding to the isotropic phase.

The entropy term in Eq. (4.171a) can be reduced to the form

$$\frac{\Delta W_1}{N} = -\Delta\rho^* + (\rho_n/\rho_f) \left\{ \ln \left[\frac{\rho_n A_0}{\rho_f} \right] + \sum'_{\ell \geq 2} \lambda_{\ell} P_{\ell}(\cos \theta) \right\}. \quad (4.177)$$

The interaction term $\Delta W_2/N$ is evaluated using Eq. (4.176) for $f(\Omega)$,

$$\frac{\Delta W_2}{N} = -\frac{1}{2} \Delta\rho^* \hat{C}_{00}^{(0)} - \frac{(1 + \Delta\rho^*)^2}{2} \sum_{\ell_1, \ell_2 \geq 2}^2 \bar{P}_{\ell_1} \bar{P}_{\ell_2} \hat{C}_{\ell_1 \ell_2}^{(0)} \quad (4.178)$$

where $\hat{C}_{\ell_1, \ell_2}^{(0)}$ is the structural parameter. Expanding $C(\mathbf{r}, \Omega_1, \Omega_2)$ in spherical harmonics in space-fixed frame

$$C(\mathbf{r}, \Omega_1, \Omega_2) = \sum_{\ell_1 \ell_2} \sum_{m_1 m_2 m} C_{\ell_1 \ell_2 \ell}(r) C_g(\ell_1 \ell_2 \ell; m_1 m_2 m) Y_{\ell_1 m_1}(\Omega_1) Y_{\ell_2 m_2}(\Omega_2) Y_{\ell m}^*(\hat{r}), \quad (4.179)$$

from Eq. (4.172) one finds the expression for the order parameter as [142]

$$(1 + \Delta\rho^*)\delta_{\ell_0} + \bar{P}_\ell = \int d\Omega_1 P_\ell(\cos\theta_1) \exp\left[\lambda + \rho_f \sum_{\ell_1\ell_2} [(2\ell_1 + 1)(2\ell_2 + 1)]^{1/2} \times C_{\mathbf{g}(\ell_1\ell_20; 000)} P_\ell(\cos\theta_1) \bar{P}_\ell \int dr r^2 C_{\ell_1\ell_20}(r)\right]. \quad (4.180)$$

In order to find the solutions of above equations, the values of $C_{\ell_1\ell_2}e(r)$ are required. $C_{\ell_1\ell_2}e(r)$ can be obtained by solving the integral equations [142](c–e).

4.5.1. Modified weighted-density approximation (MWDA)

The theory of weighted density approximation (WDA) was originally proposed by Nordholm [196] and Tarazona [197], later refined by Curtin and Ashcroft [198], and finally modified (MWDA) by Denton and Ashcroft [199].

The Helmholtz free energy of an inhomogeneous system can be expressed as the sum of two contributions: (i) an ideal gas part A_{id} (known exactly), and (ii) an excess contribution A_{ex} due to interaction between the particles,

$$A[\rho(\mathbf{r}, \Omega)] = A_{\text{id}}[\rho(\mathbf{r}, \Omega)] + A_{\text{ex}}[\rho(\mathbf{r}, \Omega)], \quad (4.181)$$

where both terms in Eq. (4.181) are unique functional [186] of the one-particle density $\rho(\mathbf{r}, \Omega)$. The first term is given by

$$A_{\text{id}}[\rho(\mathbf{r}, \Omega)] = \beta^{-1} \int_V d\mathbf{r} d\Omega \rho(\mathbf{r}, \Omega) \{\ln[\rho(\mathbf{r}, \Omega)A] - 1\}. \quad (4.182)$$

The second term of Eq. (4.181) is the excess Helmholtz free energy of the non-uniform system. Unlike the ideal gas contribution, this term is not known exactly, and is the focus of attention in the approximations presented by density functional theories. In the MWDA the excess free energy of the non-uniform system is approximated by the excess free energy of a uniform system, but evaluated at a weighted density $\hat{\rho}$:

$$A_{\text{ex}}[\rho(\mathbf{r}, \Omega)] = A_{\text{ex}}^{\text{MWDA}}[\rho(\mathbf{r}, \Omega)] = Nf_0(\hat{\rho}), \quad (4.183)$$

where $f_0(\hat{\rho})$ is the excess free energy per particle of a uniform system at density $\hat{\rho}$. The weighted density is defined by [199]

$$\hat{\rho} = \frac{1}{N} \int d\mathbf{r}_1 d\Omega_1 \rho(\mathbf{r}_1, \Omega_1) \int d\mathbf{r}_2 d\Omega_2 \rho(\mathbf{r}_2, \Omega_2) w(\mathbf{r}_1, \mathbf{r}_2, \Omega_1, \Omega_2, \hat{\rho}) \quad (4.184)$$

with the constraint that the weight function $w(\mathbf{r}_1, \mathbf{r}_2, \Omega_1, \Omega_2, \hat{\rho})$ must satisfy the normalization condition

$$\int d\mathbf{r}_1 d\mathbf{r}_2 d\Omega_1 d\Omega_2 w(\mathbf{r}_1, \mathbf{r}_2, \Omega_1, \Omega_2; \hat{\rho}) = 1. \quad (4.185)$$

For the molecular fluid, the explicit form for w can be written as

$$w(\mathbf{r}_1, \mathbf{r}_2, \Omega_1, \Omega_2; \hat{\rho}) = -\frac{1}{2f'_0(\hat{\rho})} \left[\beta^{-1} C(\mathbf{r}_1, \mathbf{r}_2, \Omega_1, \Omega_2; \hat{\rho}) + \frac{1}{V} \hat{\rho} f''_0(\hat{\rho}) \right]. \quad (4.186)$$

The primes on $f_0(\hat{\rho})$ indicate derivative with respect to density. For the nematic phase, one obtains [142]

$$\hat{\rho} = \rho_n \left[1 - \frac{\pi x_0 d_0^3}{12 \hat{\eta} \beta f'_0(\hat{\rho})} (\bar{P}_2^2 \hat{C}_{22}^{(0)} + \bar{P}_4^2 \hat{C}_{44}^{(0)}) \right]. \quad (4.187)$$

Having computed $\hat{\rho}$, the next step is to substitute $\hat{\rho}$ into Eq. (4.183) to calculate $A_{\text{ex}}^{\text{MWDA}}$. Using Eqs. (4.173) and (4.176), the non-uniform ideal gas contribution $A_{\text{id}}[\rho(\mathbf{r}, \Omega)]$ becomes

$$\beta A_{\text{id}}[\rho(\mathbf{r}, \Omega)] = V \rho_n \left[\ln(A_0 \rho_n A) - 1 + \sum_{\ell} \lambda_e \bar{P}_{\ell} \right]. \quad (4.188)$$

The total free energy of the nematic phase is now written as

$$\beta A = \beta N f_0(\hat{\rho}) + V \rho_n \left[\ln(A_0 \rho_n A) - 1 + \sum_{\ell} \lambda_e \bar{P}_{\ell} \right]. \quad (4.189)$$

4.5.2. Calculations and results

The usual approach to the above theory is to first obtain some approximation to evaluate the DPCF, $C(\mathbf{r}, \Omega_1, \Omega_2)$, appearing in Eq. (4.170). Next to choose a parametrization of the one-body density that is appropriate for the kind of expected phase transitions. With these two requirements specified, the functional (4.170) is completely defined and the calculation proceeds by the minimization of ΔW with respect to the parameters in $\rho(\mathbf{r}, \Omega)$. When a configuration other than the isotropic liquid satisfies $\Delta W = 0$, the ordered and isotropic phases coexist and all the transition properties can be identified.

The ordered phase (translationally and/or orientationally) coexists with the isotropic liquid when

$$\left(\frac{\partial}{\partial \xi_i} \right) (\Delta W/N) = 0 \quad (4.190a)$$

and

$$\Delta W/N = 0, \quad (4.190b)$$

where ξ_i are variational parameters appropriate for the phase under investigation. Eqs. (4.190a) and (4.190b) show a stability condition and a phase coexistence condition. The DFT calculations are done by minimizing Eq. (4.170) with respect to the variational parameters ρ_n, λ_2 and λ_4 . (Eq. (4.172)). The coexistence point is then located by varying ρ_f with $\Delta W/N = 0$. In MWDA the effective density $\hat{\rho}$ is computed [142](f, g) first and then the free energy (Eq. (4.189)) is minimized with respect to ρ_n, λ_2 and λ_4 . The transition densities of the coexisting phases are determined by equating the pressure and chemical potential of the two phases.

The structural parameters for the nematic phase are defined as [142]

$$\hat{C}_{\ell_1 \ell_2}^{(0)} = (2\ell_1 + 1)(2\ell_2 + 1) \rho_f \int d\mathbf{r} d\Omega_1 d\Omega_2 C(\mathbf{r}, \Omega_1, \Omega_2) P_{\ell_1}(\cos \theta_1) P_{\ell_2}(\cos \theta_2) . \quad (4.191)$$

Using Eq. (4.179) and after simplification, Eq. (4.191) can be written as

$$\hat{C}_{\ell_1 \ell_2}^{(0)} = \left[\frac{(2\ell_1 + 1)(2\ell_2 + 1)}{4\pi} \right]^{1/2} \rho_f C_g(\ell_1 \ell_2, 0, 0, 0) \int d\mathbf{r} r^2 C_{\ell_1 \ell_2 0}(\mathbf{r}) . \quad (4.192)$$

The theory was successfully applied to the study of crystallization of particles interacting via spherical pair potentials including the case of hard spheres [200–203]. Singh and Singh [142] have pioneered the study of transitions to the plastic and nematic states, within decoupling approximation [107], in the hard ellipsoidal system using this theory. The calculation for isotropic–plastic transition was performed by assuming the crystalline lattice of the plastic phase to be fcc with lattice parameter a determined self-consistently by the relation

$$a = (4/\rho_0)^{1/3}, \quad \rho_0 = \rho_f(1 + \Delta\rho^*) .$$

It was predicted [142] that the equilibrium positional freezing (plastic) on fcc lattice takes place for the value of $\hat{C}_{0,0}^1 = 1 - 1/S(|G_m|)$, where $S(|G_m|)$ is the first peak in the structure factor of the centre of mass] $\simeq 0.67$ or $S(G_m) \simeq 3.07$. The equilibrium orientational freezing (nematic) takes place when the orientational correlation $\hat{C}_{2,2}^0 \simeq 4.45$. Further, it was found [142] that the plastic phase stabilizes first for $0.57 \leq x_0 \leq 1.75$ and the nematic phase for $x_0 < 0.57$ and $x_0 > 1.75$. Though these values are in reasonable agreement with simulation results [156], this work [142](b) suffers with some uncertainties, the most important of which is the lack of information about $C(\mathbf{r}, \Omega_1, \Omega_2)$, which even in the case of the isotropic state is a function of four independent variables. This forces the use of what is essentially a guess for $C(\mathbf{r}, \Omega_1, \Omega_2)$. Other problems with the initial application of the density functional approach are that the oriented crystal phase was not considered and that the parametrization of the plastic phase was done so that the rather narrow real-space lattice peaks associated with hard-core crystallization could not be generated. In an attempt to remedy some of these problems, Marko [177] applied DFT to study the properties of plastic phase at the isotropic–plastic transition, of oriented solid phase at the isotropic–solid transition, and of nematic phase at the isotropic–nematic transition in a fluid of prolate hard ellipsoids. In this study [177] the direct correlations were computed with a variational technique based on the Percus–Yevick (PY) equation for the correlation functions. Trial correlation functions are chosen and then the optimal solution is obtained using the PY equation. The calculation procedure involves the direct calculation of the excess grand potential for the ordered phase, followed by the resulting non-linear functional. The first step is to specify the one-body distribution in terms of as few parameters as possible which can describe the ordered phase reasonably. For the plastic phase, the trial one-body density is taken as a sum of Gaussian distributions centred on real-space lattice sites and is described by three parameters

$$\rho(\mathbf{x}) = \rho \sum_{t \in T_t} A(\pi\sigma_t^2)^{-3/2} \exp[-\sigma_t^{-2}(r - ct)^2] , \quad (4.193)$$

where ρ_ℓ is the ordered phase density, σ_ℓ is the lattice site distribution width, c is the lattice constant and Δ is the volume per lattice site. In case of fcc lattice $\Delta = c^3/\sqrt{2}$. T_f is the set of fcc lattice vectors with unit nearest-neighbour spacing.

The trial density for the nematic was taken as

$$\rho(\mathbf{x}) = \rho_\ell \exp[a_1(\hat{e} \cdot \hat{z})^2 + a_2(\hat{e} \cdot \hat{z})^4] \left[\int_0^1 dx' \exp(a_1 x'^2 + a_2 x'^4) \right]^{-1}, \quad (4.194)$$

where a_1 and a_2 parametrize the orientational distribution function. The trial DCF and pair distribution were assumed to be of the form

$$C(\mathbf{r}, \Omega_1, \Omega_2) = C_0(r^*((1 + \alpha P_2(\cos \theta_{12}))) \quad (4.195a)$$

and

$$g(\mathbf{r}, \Omega_1, \Omega_2) = g_0(r^*)(1 + \alpha P_2(\cos \theta_{12})), \quad (4.195b)$$

where C_0 and g_0 are, respectively, the hard-sphere DCF and PY correlation function [204], and $r^* = r_{12}/D(\Omega_{12})$. The integration of the PY equation squared over the hard-core region yields a functional that quantifies the accuracy of the trial solution, and thus should be minimized with respect to α to obtain the best solution. The integration over only the core region emphasizes the DCF rather than the pair distribution, and limits the integration to a finite region, which is important numerically. The error functional was defined as

$$I(\alpha) = \int d\mathbf{x}_1 \left\{ 1 + C(\mathbf{x}_1, 0; \alpha) + \rho \int d\mathbf{x}_2 C(\mathbf{x}_2, 0; \alpha) [g(\mathbf{x}_1, \mathbf{x}_2; \alpha) - 1] \right\}^2. \quad (4.196)$$

$I(\alpha)$ was computed numerically for prolate ellipsoids with anisotropies $x_0 = 1.0, 1.22, 1.53, 2.0$ and 3.0 and for the packing fractions $\eta = 0.1, 0.2, \dots, 0.7$ over appropriate ranges of α ($\eta = 0.7405$ is the close-packing density). This correction makes the DCF more negative, corresponding to a larger free-energy cost, for parallel ellipsoidal configurations. For perpendicular configurations, the correction makes the DCF less negative, corresponding to a smaller free-energy cost of these configurations.

The DCF thus evaluated were used in free-energy functional (4.170) with the plastic and nematic distributions (Eqs. (4.193) and (4.194)) and global minima were determined over ranges of liquid density. The isotropic–plastic, isotropic–solid and isotropic–nematic transition properties were calculated. It was found that (i) for small anisotropies ($x_0 < 1.5$) the isotropic–fluid to isotropic–crystal densities are unaffected by the small correction. However, the results show an increase in transition density as the anisotropy increases which is in accordance with MC simulations but indicates the opposite trend as observed by Singh and Singh [142] (b), (ii) for $2 \leq x_0 \leq 3$, although the isotropic–nematic transition density agrees well with the simulation results [156], the density discontinuity is too small, and (iii) the results of density functional calculations depend crucially on the approximations made for the pair DCF. Thus it is feasible to obtain information about the DCF by the numerical means, even in case of orientation-dependent interactions.

A general method was developed by Perera et al. [205] to solve numerically the hypernetted chain (HNC) and Percus–Yevick (PY) integral equation theories for fluids of hard non-spherical

Table 9
Comparison of the NI phase transition properties for hard ellipsoids of length-to-breadth ratio $x_0 = 3$.
 $P^* = P v_0 / k_B T$, $\mu^* = \mu / k_B T$

Quantity	MC simulation [156](a)	Singh and coworkers [142](e, f)	Singh and Singh [142](b)	Colet et al. [174](b)	Marko [177](b)	Perera et al. [143]	Holyst and Poniewiers ki [210]	Singh et al. [145]
		DFT/WDA	DFT/MWDA					
η_{iso}	0.507	0.466	0.471	0.309	0.72	0.493	0.418	0.454
η_{nem}	0.517	0.479	0.490	0.322	0.484	0.494	0.436	0.494
$\Delta\rho/\rho_{\text{nem}}$	0.019	0.027	0.041	0.040	0.024	0.002	0.041	0.038
$\bar{P}_{2\text{NI}}$	0.50	0.745	0.552	0.547	0.560	0.017	0.657	0.546
$\bar{P}_{4\text{NI}}$	—	0.474	0.266	0.197	—	—	0.358	—
P^*	9.786	6.429	6.662	—	—	—	—	—
μ^*	25.150	17.982	18.480	—	—	—	—	—

particles forming nematic phase. The explicit numerical results were given for fluids of hard ellipsoids of revolution with length-to-width ratio varying from 1.25 to 5.0 as well as for fluids of hard spherocylinders with length-to-width ratio varying from 2 to 6 [205](a). Theoretical results were compared with the available MC data [156,148–153] for the equation of state and the pair correlation function. The DCF for the isotropic phase were obtained. It was shown that the DFT results are strongly dependent upon the approximation used for the isotropic direct pair correlation function. Using these results the isotropic–nematic transition properties were calculated [143] for the hard ellipsoids and spherocylinders. For the hard ellipsoids all results were obtained using HNC DCF because no phase changes were found with PY values. It was found that for $x_0 = 3$ the MC transition density is about 20% higher, whereas the MC fractional density change is smaller than the density functional results [143]. These values are compared in Table 9 with other values. For spherocylinders with $x_0 = 6$ it was observed that the second-order DFT theory combined with the HNC DCF yields a transition density which is about 14% lower than the MC values. In addition to hard particles fluid the calculations were also carried out [143] for fluids characterized by pair potentials of a generalized MS type,

$$u(1,2) = u_0(r) + u_2(r)P_2(\cos \theta_{12}), \quad (4.197)$$

with

$$u_2(r) = -4\bar{s}\epsilon(\sigma/r)^6 \quad (\text{model I}) \quad (4.198a)$$

and

$$u_2(r) = -4\bar{s}\epsilon \left[\left(\frac{\sigma}{r} \right)^{12} + \left(\frac{\sigma}{r} \right)^6 \right] \quad (\text{model II}). \quad (4.198b)$$

Here $u_0(r)$ was taken to be the usual Lennard–Jones interaction and \bar{s} is a variable determining the strength of the anisotropic interaction. The transition properties for both the models were

calculated and it was found that in both cases the transition temperatures are considerably higher than the absolute stability limits given by the HNC theory. Further, the fractional changes in density found for both models (Eqs. (4.198a) and (4.198b)) are about an order of magnitude larger than those obtained for hard ellipsoids and spherocylinders.

A second-order density functional theory was used by Ram and Singh [142] to study within decoupling approximation the isotropic–nematic transition in a HER system. The direct pair correlation function of coexisting isotropic liquid was obtained by solving the OZ equation using the PY closure relation. In this work, the PY integral equation was solved numerically at densities which span beyond the range studies by Perera and co-workers [143,205] and it was shown that the IN transition takes place for ellipsoids with $x_0 \geq 3.0$. The IN transition properties were calculated for several values of x_0 and it is found that a system spontaneously transforms to a nematic phase when the structural parameters $\hat{C}_{22}^{(0)}$ and $\hat{C}_{44}^{(0)}$ attain, respectively, values close to 4.40 and 1.12. These numbers vary, though very weakly, with x_0 , as x_0 is increased the value of $\hat{C}_{22}^{(0)}$ is decreased while $\hat{C}_{44}^{(0)}$ increases. The transition parameters are compared in Table 9 with other results. Singh and co-workers [142](d) solved the PY integral equation for two model fluids: HER fluid represented by a Gaussian overlap model and a fluid the molecules of which interact via a Gay–Berne model potential. These model systems are expected to capture some of the basic features of real ordered phases. For example, a system of HER has been found [156,206] to exhibit four distinct phases, isotropic fluid, nematic fluid, plastic solid and ordered solid. The simulation results [207,208] show that the Gay–Berne (GB) pair potential is capable of forming nematic, smectic A, smectic B and an ordered solid in addition to the isotropic liquid.

The GB pair potential model is written as

$$u(\mathbf{r}, \Omega_1, \Omega_2) = 4\varepsilon(\hat{\mathbf{r}}, \Omega_1, \Omega_2) \left[\left(\frac{\sigma_0}{r - \sigma(\hat{\mathbf{r}}, \Omega_1, \Omega_2) + \sigma_0} \right)^{12} - \left(\frac{\sigma_0}{r - \sigma(\hat{\mathbf{r}}, \Omega_1, \Omega_2) + \sigma_0} \right)^6 \right], \quad (4.199)$$

where $\varepsilon(\hat{\mathbf{r}}, \Omega_1, \Omega_2)$ and $\sigma(\hat{\mathbf{r}}, \Omega_1, \Omega_2)$ are angle-dependent strength and range parameters and are defined as

$$\varepsilon(\hat{\mathbf{r}}, \Omega_1, \Omega_2) = \varepsilon_0(1 - \chi^2[\hat{\mathbf{e}}_1 \cdot \hat{\mathbf{e}}_2]^2)^{-1/2} \\ \times \left\{ 1 - \chi' \frac{(\hat{\mathbf{r}} \cdot \hat{\mathbf{e}}_1)^2 + (\hat{\mathbf{r}} \cdot \hat{\mathbf{e}}_2)^2 - 2\chi'(\hat{\mathbf{r}} \cdot \hat{\mathbf{e}}_1)(\hat{\mathbf{r}} \cdot \hat{\mathbf{e}}_2)(\hat{\mathbf{e}}_1 \cdot \hat{\mathbf{e}}_2)}{1 - \chi'^2(\hat{\mathbf{e}}_1 \cdot \hat{\mathbf{e}}_2)^2} \right\}^2 \quad (4.199a)$$

and

$$\sigma(\hat{\mathbf{r}}, \Omega_1, \Omega_2) = \sigma_0 \left[1 - \chi' \frac{(\hat{\mathbf{r}} \cdot \hat{\mathbf{e}}_1)^2 + (\hat{\mathbf{r}} \cdot \hat{\mathbf{e}}_2)^2 - 2\chi'(\hat{\mathbf{r}} \cdot \hat{\mathbf{e}}_1)(\hat{\mathbf{r}} \cdot \hat{\mathbf{e}}_2)(\hat{\mathbf{e}}_1 \cdot \hat{\mathbf{e}}_2)}{1 - \chi'^2(\hat{\mathbf{e}}_1 \cdot \hat{\mathbf{e}}_2)^2} \right]^{-1/2} \quad (4.199b)$$

with $\chi' = (\sqrt{k'} - 1)/(\sqrt{k'} + 1)$; k' is the ratio of the potential well depths for the side-by-side and end-to-end configurations. It is important to note that in this calculation [142](d) the OZ equation using PY closure was solved numerically considering 30 harmonic coefficients, whereas only 14

Table 10

The NI transition parameters for GB fluid [142](f, g) ($x_0 = 3.0$, $k' = 5.0$) at $T^* = 0.95$ and 1.25. Here $P^* = p\sigma_0^3/\varepsilon_0$, $\mu^* = \mu/\varepsilon_0$ and $\rho^* = \rho\sigma_0^3$

T^*	Theory	ρ_{iso}^*	ρ_{nem}^*	$\Delta\rho^*/\rho_{\text{nem}}^*$	$\bar{P}_{2\text{NI}}$	$\bar{P}_{4\text{NI}}$	P^*	μ^*
0.95	MD[207](a)	0.308	0.314	0.019	0.50		3.50	12.70
	DFT	0.322	0.328	0.018	0.675	0.372	3.398	11.28
1.25	MD[207](a)	0.323	0.331	0.024	0.50		5.70	20.90
	DFT	0.378	0.382	0.010	0.676	0.377	10.903	34.27
	MWDA	0.377	0.380	0.008	0.443	0.182	10.675	33.66

coefficients were included by Ram and Singh [142] in their calculation. Though the results found for these models, HER and GB, are in qualitative agreement with the simulation results [205,207], the quantitative agreement is not satisfactory. Secondly, the HNC and PY approximations do not give thermodynamic consistency for the virial and compressibility routes to calculate pressures. So in an other work Singh and co-workers [142](e) developed a thermodynamically consistent (TC) integral equation for the pair correlation functions of molecular fluids which interpolates continuously between the HNC and PY approximations. The TC integral equation is a generalization of Rogers and Young [209] method devised for atomic fluids to an angle-dependent pair potential. More importantly, the thermodynamic consistency between the virial and compressibility equation of state has been achieved through a suitably chosen adjustable parameter. The solutions obtained by using TC equation have been found to be in accurate agreement with the simulation results [205–207].

Taking the values of the spherical harmonic coefficients of the DPCF as obtained from the TC closure relation, Singh and co-workers [142](f, g) calculated NI phase transition properties for the HER fluid represented by a Gaussian overlap model and GB fluids using the DFT and MWDA methods. The results [142] for hard ellipsoids of length-to-width ratio $x_0 = 3.0$ are compared in Table 9 with MC simulation and various other calculations. It can be seen from Table 9 that the work of Singh and Singh [142], using the functional Taylor expansion and the decoupling approximation, yields too small densities at the transition. Marko's [177] version gives almost correct density but predicts an extremely small density jump and order parameter. Further, the transition densities obtained by Singh et al. [142] using DFT and MWDA approximation agree very well with the MC simulation [156](a) results. The fractional density change is overestimated as compared to simulation values. The transition points at two temperatures $T^* = 0.95$ and 1.25 were determined [142] for the GB fluid. The results obtained using the harmonics of DPCF from the PY integral equation are compared in Table 10 with the MD results [207]. It can be seen that the NI transition is predicted at higher density whereas the fractional density changes are small as compared to MD results [207]. Further, the coexistence densities increase with increasing temperature. At lower temperature the fractional density change is in better agreement with MD value as compared to its value at higher temperature. The DFT and MWDA overestimate the pressure and chemical potential as the temperature is increased.

5. Nematic–smectic A (NS_A) phase transition

In spite of considerable research activity over the last three decades the nematic-to-smectic phase transitions remain one of the principal unsolved problems in statistical physics of condensed matter. The uniaxial nematic-to-smectic A (NS_A) transition involves a rearrangement of the centres of the molecules; the centres are disordered in the nematic state and ordered in the smectic state. The ordering in the S_A phase is such that the molecular centres are, on average, arranged in equidistant planes with interplanar spacing ξ_0 . Within these layers the molecules move at random, with the restriction that the director remains perpendicular to the smectic layers. Consequently, the density changes its behaviour at the S_AN transition from periodic to homogeneous. The one-dimensional density wave characterizing the S_A phase is associated with the Landau–Peierls instability. In the thermodynamic limit there exist no long-range translational order in the S_A phase. Thus, the theory of S_AN transition is a theory of one-dimensional melting. Since covering all aspects of the transition is not possible here, we shall summarize some molecular models developed to describe the origin and details of S_A ordering and S_AN transition.

During the past 25 years, many high-resolution heat capacity and X-ray studies have been devoted to the S_AN transition [211–225]. Most of the focus has been on the critical exponents in the hope of determining the universality class of this transition. The most extensively measured critical exponents are $\delta, \gamma, \nu_{\parallel}$ and ν_{\perp} , where the last two correspond to the divergence of the correlation lengths parallel and perpendicular to the director, respectively. In summarizing the data, it is convenient to specify the McMillan ratio $T_{\text{NA}}/T_{\text{NI}}$. At first, DSC seemed to indicate that most of the observed NS_A transitions were discontinuous, with only those below the tricritical value of 0.87 being continuous. Later work using adiabatic scanning calorimetry and AC calorimetry showed that pretransitional effect has been interpreted as latent heats in the DSC experiment, and that continuous behaviour occurred up to much higher values of the McMillan ratio. The critical exponents for the susceptibility and correlation lengths are measured from diffuse X-ray scattering experiments in the nematic phase [3,21]. At first, the X-ray structure factor is fit to the following form:

$$\frac{\chi}{1 + \xi_{\parallel}^2 q_z^2 + \xi_{\perp}^2 q_{\perp}^2 (1 + c \xi_{\perp}^2 q_{\perp}^2)},$$

where c is a constant. Next, the temperature dependence of χ , ξ_{\parallel} and ξ_{\perp} are fit to power laws to find the critical exponents γ , ν_{\parallel} and ν_{\perp} , respectively. For the McMillan ratio below about 0.93, these exponents are close to the 3D XY universality class, $\alpha = -0.007$, $\gamma = 1.316$, $\nu_{\parallel} = \nu_{\perp} = 0.669$. Above a ratio of roughly 0.93, they are no longer fairly constant but tend to approach their tricritical values, $\alpha = 0.5$, $\gamma = 1.0$, $\nu_{\parallel} = \nu_{\perp} = 0.5$, as the McMillan ratio approaches unity. It is important to mention that the value of the McMillan ratio at the tricritical point is not universal and that the crossover from 3D XY values to tricritical values is not the same for different homologous series, but the trend in the critical exponents is very similar.

The theory of S_AN transition has received considerable attention [226–260] than any other smectic transition, partially due to the analogy with the superconducting normal transition. In spite of all these efforts, the situation remains very complicated with numerous questions unresolved. Frenkel and co-workers [156,159] have performed the computer simulation studies on a system of

hard spherocylinders to observe the $S_A N$ transition. A list of the references to much of the theoretical and experimental work is given in an article by Garland and Nounesis [264]. Longa [264] has discussed the application of the Landau and molecular-field theories to the $S_A N$ transition very well.

At the NS_A phase transition the continuous translational symmetry of the nematic phase is spontaneously broken by the appearance of one-dimensional density wave in the S_A phase. Close to the transition the onset of quasismectic features in the nematic phase may lead to a drastic change in certain important properties (elastic coefficients, transport properties, cholesteric pitch, etc.) [3,261]. Original theories due to McMillan [234] and de Gennes [62] suggested that the NS_A transition could be first or second order. The order of transition changes at a tricritical point (TCP). Alben [262] predicted a ^3He – ^4He like TCP in binary liquid crystal mixtures. However, Halperine et al. [263] argued that the NS_A transition can never be truly second order, which of course rules out the possibility of a TCP. This controversy has spurred experimental studies [211–225] which have shown that NS_A transition can indeed be continuous when measured to the dimensionless temperature $((T - T_{NA})/T_{NI}) \simeq 10^{-5}$. In a recent paper, Lelidis and Durand [265] predicted the field-induced TCP in NS_A transition. Thus, in spite of early controversies, it is witnessed now that the NS_A transition is continuous in the absence of special circumstances [215,266] in accordance with the suggestion of McMillan [234] and de Gennes [62] for a specific models. The salient features of the NS_A transition have been documented well by several authors [13,267,268].

5.1. Phenomenological description of the NS_A transition

The Landau–de Gennes theory for the NI transition (Section 4.1) can be extended to the NS_A transition. We start by defining an order parameter for the smectic A phase. The order parameter for this transition is $|\psi|$, the amplitude of the density wave describing the formation of layers in the smectic A phase. Since the difference between a value of $-|\psi|$ and $|\psi|$ only amounts to a shift of one-half layer spacing in the location of all the layers, no change in the free energy per unit volume results. Therefore, the expansion in terms of the powers of $|\psi|$ can only contain even-power terms.

Let us begin with a simple case. The S_A phase is characterized by a density modulation in a \hat{z} direction orthogonal to the layers [3]

$$\rho(\mathbf{r}) = \rho_0 + \rho_1 \cos(qz - \Phi), \quad (5.1)$$

where ρ_1 represents the first harmonic of the density modulation and Φ an arbitrary phase. In the nematics $\rho_1 = 0$, whereas in S_A phase ρ_1 becomes the natural candidate for the order parameter. In the vicinity of the NS_A transition the free energy per unit volume may be expanded in powers of ρ_1 :

$$f_{S_A} = \frac{1}{2}\alpha_2\rho_1^2 + \frac{1}{4}\alpha_4\rho_1^4 + \cdots. \quad (5.2)$$

At certain temperature T_0 , the coefficient $\alpha_2 \simeq \alpha_0(T - T_0)$ vanishes. Above this temperature it is positive. The coefficient α_4 is always positive. Only on these considerations, a second-order transition could be obtained $T_{AN} = T_0$. However, a number of complications are to be taken into consideration. First, the influence of coupling between ρ_1 and S , the nematic order parameter, is to

be accounted for because of this coupling the optimal value of S does not coincide with $S_0(T) (\equiv \bar{P}_2)$ obtained in the absence of smectic order.

Let

$$\delta S = S - S_0(T). \quad (5.3)$$

The coupling term, to the lowest order, must have the form

$$f_{AN} = -C\rho_1^2\delta S, \quad (5.4)$$

where C is a positive constant. Further, to the free-energy density must be added the nematic free-energy density f_N which is minimum for $\delta S = 0$:

$$f_N = f_N(s_0) + \frac{1}{2\chi}\delta S^2, \quad (5.5)$$

where $\chi(T)$, the response function, is large in the vicinity of NI transition but is small for $T < T_{NI}$.

The total free-energy density

$$f = f_N + f_{S_A} + f_{AN} \quad (5.6)$$

must be minimized with respect to δS . This leads to

$$\delta S = \chi C\rho_1^2 \quad (5.7)$$

and

$$f = f_N(s_0) + \frac{1}{2}\alpha_2\rho_1^2 + \frac{1}{4}\alpha'_4\rho_1^4, \quad (5.8)$$

$$\alpha'_4 = \alpha_4 - 2\chi C^2. \quad (5.9)$$

The sign of α'_4 critically determines the order of transition. Clearly, the sign of α'_4 can change depending on whether χ is large or small, i.e., whether the nematic range is narrow or wide.

- (i) If $T_0 \sim T_{NI}$, $\chi(T_0)$ is large and α_4 becomes negative. The stability requires that ρ_1^6 term with positive coefficient must be added to Eq. (5.8). In this case the transition takes place at a higher temperature $T_{AN} > T_0$, and is first order.
- (ii) If $T_0 \ll T_{NI}$, $\chi(T_0)$ is small and $\alpha_4 \sim \alpha_2 > 0$. The resulting transition is of second order and $T_{AN} \sim T_0$.
- (iii) The point at which $\alpha_4 = 0$ is a tricritical point. Thus, the change from a second order to first order is induced by the coupling between ρ_1 and S .

It is well known that the layer fluctuations play an important role in smectics. The layer displacement $u(\mathbf{r})$ appears through

$$\Phi(\mathbf{r}) = -qu(\mathbf{r}). \quad (5.10)$$

Consequently, the smectic order can be described by introducing the complex order parameter [62,134]

$$\psi(\mathbf{r}) = \rho_1(\mathbf{r})e^{-iqu(\mathbf{r})}, \quad (5.11)$$

where $q = 2\pi/\xi_0$. Now near the transition, the free-energy density may be expanded in powers of ψ . Since the spatially dependent order parameter has been defined, we must add to the free energy the gradient terms that express the tendency for the smectic to be homogeneous. Keeping all these features in view, the general expansion for the free energy density can be written as

$$f = f_N(T, Q, \nabla Q) + f_{S_A}(T, \psi, \nabla\psi) + f_{AN}(Q, \psi, \nabla Q, \nabla\psi) + f_{\text{ext}}(Q, \psi, \nabla Q, \nabla\psi, P), \quad (5.12)$$

where $f_N(T, Q, \nabla Q)$ is the free-energy density of the nematic phase (see Section 4.1), $f_{S_A}(T, \psi, \nabla\psi)$ corresponds to the smectic A phase, f_{AN} is the contribution from the coupling between Q (nematic order parameter) and ψ and f_{ext} is the free-energy density associated with the coupling of the order parameters and the external perturbation:

$$f_{S_A} = \frac{1}{2}\alpha_2|\psi|^2 + \frac{1}{4}\alpha'_4|\psi|^4 + \frac{1}{2}C_{\parallel}\left|\frac{\partial\psi}{\partial z}\right|^2 + \frac{1}{2}C_{\perp}\left(\left|\frac{\partial\psi}{\partial x}\right|^2 + \left|\frac{\partial\psi}{\partial y}\right|^2\right), \quad (5.13)$$

where $C_{\parallel} \neq C_{\perp}$ because of the nematic anisotropy. At the lowest order coupling term we can write

$$f_{AN} = \frac{1}{2}DQ|\psi|^2 + \frac{1}{2}EQ^2|\psi|^2, \quad (5.14)$$

where D and E are coupling constants. D is chosen negative to favour S_A phase when the nematic phase exists and $E > 0$. Generally, this term allows for reentrant effects (see Section 6). Because of (Q, ψ) coupling the NS_A phase transition can be of second or first order.

In writing the expansion (5.13) the implicit assumption has been made that the director \hat{n} is fixed in the Z -direction. In reality, \hat{n} fluctuates. So the gradient terms have to be taken in direction parallel and perpendicular to \hat{n} . Owing to this the C_{\perp} term is modified. Using the notation

$$\nabla_{\perp} = \left(\frac{\partial}{\partial x}, \frac{\partial}{\partial y}\right),$$

it becomes

$$C_{\perp}|\nabla_{\perp} - iq\delta\hat{n}_{\perp})\psi|^2, \quad (5.15)$$

where $\delta\hat{n}_{\perp} = \hat{n} - \hat{z}$. When the director fluctuation is taken into account the Frank–Oseen elastic contribution [37] has to be added to the total free energy.

A number of conclusions have been reached on this problem. The transition seems always to be first order in four dimensions due to the coupling between the smectic order parameter and the director fluctuation [263]. In three dimensions, the behaviour on the low and high sides of the transition can be reversed from the 3D XY behaviour, i.e., an inverted 3D XY model [269,270]. A dislocation-loop melting theory, in which a divergence in the density of dislocation loops destroys the smectic order, yields anisotropic critical behaviour in the correlation lengths [271,272]. A non-inverted behaviour has been observed in MC simulations [54]. A self-consistent one-loop theory employing intrinsically anisotropic coupling between the director fluctuations and the smectic order parameter predicts a gradual crossover from isotropic behaviour to strongly anisotropic behaviour [273,274]. Thus, the NS_A transition is very complicated with many factors influencing the behaviour near the transition. Coupling between the smectic order parameter and the nematic order drives the transition towards tricritical behaviour, while coupling between the smectic order and nematic director fluctuations drives it into an anisotropic regime. While the

McMillan ratio is a convenient indicator of the strength of both of these couplings, it is quite imprecise. Yet the general trends with McMillan ratio are clearly evident [264].

5.2. Mean-field description of NS_A transition

McMillan [234] presented an elegant description of smectic A phase by extending the Maier Saupe (MS) theory of the nematic phase to include the one-dimensional translational order of the S_A phase. A similar but somewhat more general treatment, based on the theory of melting [275], was proposed independently by Kobayashi [233]. Kobayashi developed a formalism of the translational and orientational ordering but due to the two particle distribution for the ordered phase the detailed numerical results for realistic potential were hard to obtain. A number of other refinements and extensions [236–242,250,260] were proposed but McMillan's model remains the simplest one for its computational convenience and comparison with experiments and explains all the qualitative features of the S_{AN} and S_{AI} transitions. A more simpler treatment of the S_{AN} transition as compared to Kobayashi–McMillan approach has been given by Meyer and Lubensky (ML) [235]. The ML model limits the discussion of the S_{AN} transition to the case of the ideal orientational order, i.e. the temperature dependence of the orientation of the molecules is neglected.

We shall first describe the essential features of most widely used McMillan model. The physical idea behind the model is based on the structure of molecules exhibiting S_A phase. The mesogenic materials forming S_A phase typically have a central aromatic core and flexible alkyl chains at the two ends. The aromatic moieties have large polarizabilities and thus the dispersion interaction energy is very strong between the cores. Consequently, this can lead to the formation of a layered arrangement as in S_A phase if the alkyl chains are sufficiently long and serve to efficiently separate the aromatic cores in layers. McMillan assumed that the anisotropic interaction is short-ranged and can be expressed as

$$U_{12}(r_{12}, \cos \theta_{12}) = - \left(\frac{V_0}{Nr_0^3 \pi^{3/2}} \right) e^{-(r_{12}/r_0)^2} P_2(\cos \theta_{12}), \quad (5.16)$$

where r_0 is of the order of the length of the rigid section of the molecule, and the exponential term reflects the short range character of the interaction.

If the layer thickness is ξ_0 the self-consistent one-particle potential that a test molecule would experience, retaining only the leading term in the Fourier expansion, can be written as

$$u_1(z, \cos \theta) = - V_0 [\bar{P}_2 + \bar{\sigma} \alpha \cos(2\pi z/\xi_0)] P_2(\cos \theta), \quad (5.17)$$

where the McMillan parameter α is given by

$$\alpha = 2 \exp[-(\pi r_0/\xi_0)^2]. \quad (5.18)$$

\bar{P}_2 is the usual orientational order parameter and $\bar{\sigma}$ is an order parameter which couples translational and orientational orders. Eq. (5.17) ensures that the energy is a minimum when the molecule is in the smectic layer with its axis along Z .

The single-particle distribution function is given by

$$f_1(z, \cos \theta) = \exp[-\beta u_1(z, \cos \theta)]. \quad (5.19)$$

Using this distribution function and the interaction potential (5.16) the one-body potential is recalculated

$$u_1(z_1, \cos \theta_1) \equiv \frac{N \int d^3x_2 d\Omega_2 u_{12} f(z_2, \cos \theta_2)}{\int d^3x_2 d\Omega_2 f(z_2, \cos \theta_2)} = -V_0 [P_2(\cos \theta_1) \langle P_2(\cos \theta_2) \rangle + \alpha \cos(2\pi z_1/\xi_0) P_2(\cos \theta_1) \langle \cos(2\pi z_2/\xi_0) P_2(\cos \theta_2) \rangle] . \quad (5.20)$$

Self-consistency of Eqs. (5.17) and (5.20) demands that

$$\bar{P}_2 = \langle P_2(\cos \theta) \rangle , \quad (5.21a)$$

$$\bar{\sigma} = \langle \cos(2\pi z/\xi_0) P_2(\cos \theta) \rangle . \quad (5.21b)$$

Eq. (5.21) must be solved self-consistently for both the order parameters, the order parameter \bar{P}_2 defines the orientational order, exactly as in MS theory, and $\bar{\sigma}$ is a measure of the amplitude of the density wave describing the layered structure. These equations exhibit three types of solutions: (i) $\bar{P}_2 = \bar{\sigma} = 0$, no order, characteristic of the isotropic liquid phase, (ii) $\bar{P}_2 \neq 0$, $\bar{\sigma} = 0$, orientational order only, the theory reduces to the MS theory of the nematic phase; and (iii) $\bar{P}_2 \neq 0$, $\bar{\sigma} \neq 0$, orientational and translational order characteristic of the S_A phase.

The free energy of the system is given by

$$A = U - T\Sigma , \quad (5.22)$$

where the internal energy

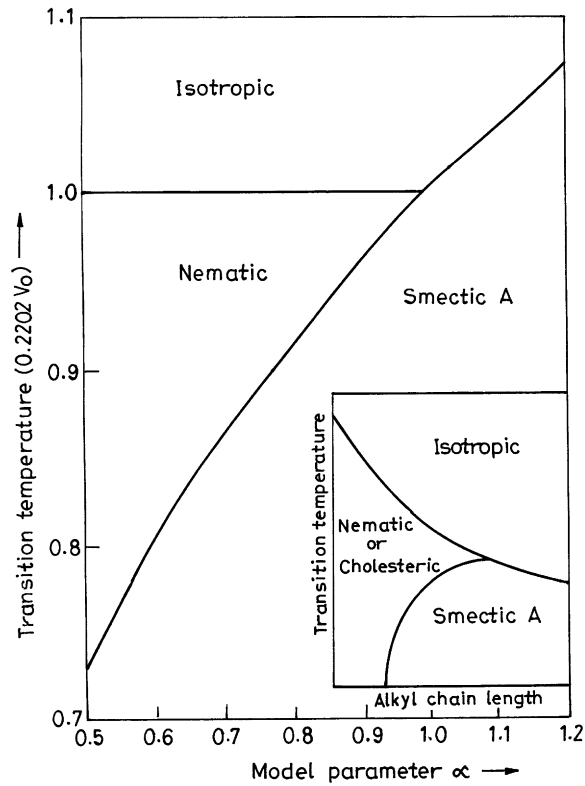
$$U = -\frac{1}{2}NV_0(\bar{P}_2^2 + \alpha\bar{\sigma}^2) \quad (5.22a)$$

and the entropy is evaluated through

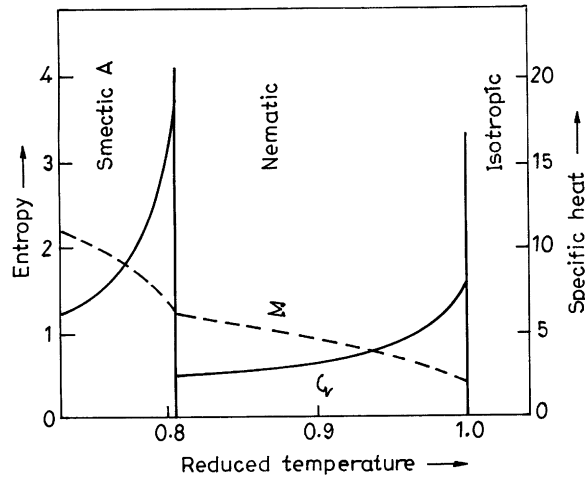
$$-T\Sigma = NV_0(\bar{P}_2^2 + \alpha\bar{\sigma}^2) - N\kappa_B T \ln \left[\frac{1}{\xi_0} \int_0^{\xi_0} d\xi_0 \int_0^1 d(\cos \theta) f_1(z, \cos \theta) \right] . \quad (5.22b)$$

At any temperature the phase with the lowest free energy is thermodynamically stable.

As obvious two physical parameters V_0 and α enter the theory. V_0 determines the T_{NI} and fixes the temperature scale of the model. α , a dimensionless parameter, is a measure of the strength of layering interactions and can vary between 0 and 2. The interplanar distance is determined by the competition between the anisotropic forces which produce the smectic order and excluded volume effects. The smectic condensation energy is greater for larger values of α , that is for larger ξ_0 . Experimentally, the layer thickness is of the order of the molecular length. The parameter α increases with increasing chain length of the alkyl tails. Eq. (5.21) were solved self-consistently and the order parameters, entropy, specific heat as a function of temperature for several values of α were evaluated and the transition parameters were calculated. The main results of calculations are shown in Fig. 10. For $\alpha < 0.70$ and $T_{AN}/T_{NI} < 0.87$ the model predicts the second-order $S_A N$ transition. For $\alpha > 0.98$, the S_A phase transforms directly into the isotropic phase, while for $\alpha < 0.98$ there is a $S_A N$ transition followed by a NI transition at higher temperature. Hence $\alpha = 0.7$



a.



b.

Fig. 10. (a) Phase diagram for theoretical model parameter α . Inset: typical phase diagram for homologous series of compounds showing transition temperatures versus length of the alkyl end-chains [234]; (b) The variation of entropy Σ and specific heat C_V with reduced temperature for $\alpha = 0.6$. A second order S_A -N transition and a first order NI transition are exhibited by the model [234].

and $T_{AN}/T_{NI} = 0.87$ correspond to a tricritical point at which the first-order transition terminates to a second-order transition. Fig. 10(a) shows that the theoretical phase diagram broadly reflects the experimental trends in homologous series. However, it was found that the theoretical S_{AN} transition entropy is somewhat higher than the experimental values. McMillan made an attempt, in a later paper [226], to improve the agreement by using a modified pair potential

$$U_{12}(r_{12}, \cos \theta_{12}) = -(V_0/Nr_0^3\pi^{3/2})\exp(-(r_{12}/r_0)^2)(P_2(\cos \theta_{12}) + \delta). \quad (5.23)$$

The three parameters were fixed by the criterion that the theory gives transition temperatures and entropies. The results were essentially the same as those obtained by the two-parameter model (Eq. (5.16)) but some quantitative improvements were obtained. McMillan [234] himself suggested that if the excluded volume effect is included in Eq. (5.16) it would favour \hat{n} to be parallel to \hat{z} . Further, it was suggested by Priest [260] that a generalized rank-2 tensor model would give rise to additional terms which favour \hat{n} to be parallel to \hat{q} . In most homologous series, the S_{AN} transition point T_{AN} reaches a maximum value for some chain length and tends to decrease for higher homologues.

Woo and co-workers [250] have used a pairwise potential of the type

$$U(1, 2) = V_0 \exp \left[- \left(\frac{r_{12}}{r_0} \right)^2 \right] [- \delta - P_2(\mathbf{\Omega}_1 \cdot \mathbf{\Omega}_2) + \varepsilon \{ P_2(\mathbf{\Omega}_1 \cdot \hat{r}_{12}) + P_2(\mathbf{\Omega}_2 \cdot \hat{r}_{12}) \}]. \quad (5.24)$$

Four physical parameters V_0 , δ , r_0 and ε appear in the theory; δ is a measure of the interaction which gives rise to the translational order even in the absence of orientational order and ε roughly accounts for the steric effects, which help to keep \hat{n} parallel to \hat{q} . The four parameters of the model are adjusted to fit the measured transition temperature curves and approximate triple point. For each homologous series, V_0 determines one point on the T_{NI} curve, while r_0 (or α) measures the length of the central section of the molecule. Both these parameters are chosen at the outset and thereafter held fixed. The remaining two parameters δ and ε are adjusted to fit rest of the experimental phase diagram. The model predicted the phase diagrams similar to that of experimental one. Further the parameter ε is sufficient to generate a reasonably good fit to the experimental phase diagram. The role of the end chains is merely to cause a larger interplanar spacing in the S_A phase and thus does not affect the model interaction. The characteristic feature of the S_A phase that the director prefers to be perpendicular to the smectic layers is incorporated into the model (5.24). The connection between ε and the structure of molecules can explain the differences in phase transition properties between homologous series whose molecules are of similar structure but differ in the length of rigid section. Sokalski [251] has used a corner potential with Lennard–Jones type of interaction

$$U(1,2) = 4\varepsilon[(\sigma/r)^m - (\sigma/r)^n], \quad (5.25)$$

where σ depends on the orientations of the molecules. It was shown that the model (5.25) exhibits the smectic A, nematic and isotropic phases.

Kloczkowski and Stecki [237] considered a model system of hard spherocylinders superimposed with the attractive $1/r^6$ potential for the S_A phase. By using stability analysis these authors have

shown that this type of potential allows for the S_A phase formation. The influence of attractive tail on the S_A phase formation was studied and it was found that the additional centre to centre r^{-6} potential produces an instability of the isotropic or nematic phases, towards the S_A phase formation. The calculations were performed for spherocylinders with length to diameter ratio 5 and 10 for different values of additional attractive potential parameters. This type of potential was also used by Nakagawa and Akahane [276] in their treatment of the S_A phase formation. These authors [241] also developed a McMillan-type theory for binary mixtures including both intermolecular repulsions and attractions.

As discussed above, the original version [234] of McMillan's theory contains just two order parameters, the orientational order parameter \bar{P}_2 and a mixed orientational–translational order parameter $\bar{\sigma}$ defined as $\langle \cos(2\pi z/\xi_0) P_2(\cos \theta) \rangle$. In this theory occurrence of the mixed order parameter results in a strong correlation between the orientational and translational coordinates. It has been argued that this strong correlation may be responsible for the quantitative failure of the McMillan theory. In a later paper [226], McMillan introduced a purely translational order parameter $\bar{\tau}$ ($= \langle \cos 2\pi z/\xi_0 \rangle$) to improve the quantitative agreement. This third term has the effect of stabilizing the S_A phase and so allows a second-order $S_A N$ transition to occur at a higher temperature by reducing the relative correlation between orientational and translational coordinates. In fact, the basic structure of the theory remains unchanged. Despite success the introduction of third-order parameter leads to the complication of the theoretical treatments in obtaining both analytic and numerical solutions. Katriel and Kventzel [236] have shown that this complication could be removed by writing the mixed order parameter as a product of the pure orientational and translational order parameters:

$$\bar{\sigma} = \langle P_2(\cos \theta) \rangle \langle \cos(2\pi z/\xi_0) \rangle = \bar{P}_2 \bar{\tau} . \quad (5.26)$$

This decoupling approximation has the additional advantage that the strength of correlation between the translational and orientational coordinates is readily controlled. The results obtained using this simplification (Eq. (5.26)) exhibit the main features of the isotropic–nematic–smectic A transitions in a satisfactory manner. Kventzel et al. [242] made a quantitative comparison of the two theories, McMillan's three order parameter theory [276] and Katriel and Kventzel [236] theory. These authors [242] have demonstrated the validity of the decoupling approximation for the mixed order parameter in both the models. For the decoupled model the phase diagram involving isotropic, nematic, smectic A and plastic phases was constructed and the $S_A N$ transition properties, which include the second-order transition temperature and tricritical point, the transition entropy and the change in the order parameters, etc., were evaluated in detail. These properties have been found to agree well with the predictions of McMillan's theory for a wide range of strength parameters.

A lattice model for the S_A phase was proposed by Dowell and Ronis and Rosenblatt [249]. Dowell investigated the effects of temperature, pressure, tail chain flexibility and tail chain length on the relative stabilities of the isotropic, nematic, smectic A and reentrant nematic phases (see Section 6) using a lattice model [112] having only hard repulsions. The method provides a way to determine on an individual basis which of the molecular features are sufficient and/or necessary for the existence and relative stabilities of various phases. The thermodynamic and molecular ordering properties, such as S_A order parameter, core and tail intermolecular orientational order parameters, tail intramolecular orientational order parameter, density and entropy, were evaluated, in

these phases and at the phase transitions. It has been found that for the formation of S_A phase in real system the presence of semiflexible tail chains of significant length is essential and that as the length of tail chain is shortened the S_A phase disappears. Further, the dipolar phase is not necessary in this steric packing model to form S_A phase but do effect the stability ranges of temperature and pressure of the phases. As seen in Section 4.2, systems of hard particles, interacting through the excluded-volume effect, have played a fundamental role in the understanding of structural phase transitions in liquid crystals. Onsager made a major contribution to our understanding of nematic phase in a system of hard spherocylinders. Stroobants et al. [159](a) provided evidence for the appearance of S_A order in the system of perfectly parallel hard spherocylinders from simulation studies (see Section 9). Stimulated by the simulation results, Mulder [255] developed a density functional calculation and Wen and Meyer [244] analysed the origin of the S_A phase in a parallel hard-rod system. In their later work [244], these authors described how the appearance of S_A order reduces the excluded volume of the nematic phase and calculated the entropy for a system of parallel right circular cylinders. The argument can be expressed quantitatively; there are three contributions to the entropy changes in going from the S_A order to the nematic order; a term describing directly the changes in long-range order, a term due to the change of packing density within each layer, and a term due to the change in axial freedom of motion of each rod. The first term has been expressed in terms of the distribution function of the centres of mass of the rods, and the second term in terms of 2D packing density. The third term is significant as compared to the other two terms. The calculation demonstrated that a second-order NS_A phase transition takes place as the packing fraction was raised to 0.202 times the value for the close packing. One of the limitations of this model is that the results have no dependence on the length to diameter ratio of the rods. Holyst and Poniewierski [246] studied a system of hard parallel cylinders in the framework of smooth density approximation. Using a bifurcation analysis, it was shown that apart from the nematic phase, smectic A, solid (or crystalline B) and columnar phases should also occur in this system. This approach fails to distinguish between a solid phase and a crystalline smectic B phase. Hosino et al. [243] had earlier found the persistence of the $S_A N$ transition when hard cylinders were allowed to have three orthogonal orientations. Taylor et al. [248] constructed an excluded volume theory for the S_A and columnar phases of a system of hard spherocylinders using the scaled particle theory to treat dimensions possessing full translational freedom, combined with a simple cell model to describe the positionally ordered dimensions. These authors obtained a phase diagram remarkably similar to that obtained from the Monte Carlo calculation (see Fig. 24 below) [159]. The predicted smectic layer spacing at the nematic–smectic cross-over is also almost identical to the MC results. The model suffers with the serious limitation that all transitions are required to be discontinuous. Consequently, the second-order nematic–smectic transitions as demonstrated also by the MC results was found to be first order.

A number of experimental works [277–283] show that the molecular biaxility has to be incorporated in the theoretical treatment in order to describe the structural and thermodynamic properties of smectics. The first attempt of such consideration was made by the Everyanov and Primak [253] within the framework of McMillan model generalized to the biaxial molecules. These authors [253](a) investigated the influence of smectic layering on the order parameters of solute molecules as well as on their positional orientational correlations. In the later paper [253](b) the thermodynamics of $S_A N$ phase transition in a system of biaxial molecules was studied. The orientational translational ordering of the molecule can be characterized by a set of five order

parameters, \bar{P}_2 , $\bar{\tau}$, $\bar{\sigma}$ and the other two defined as

$$\bar{G} = \frac{3}{2} \langle \sin^2 \theta \cos 2\phi \rangle \equiv S_{x_1 x_1} - S_{y_1 y_1}, \quad (5.27a)$$

$$\bar{K} = \frac{3}{2} \langle \sin^2 \theta \cos 2\phi \cos(2\pi z/\xi_0) \rangle. \quad (5.27b)$$

Taking into account these order parameters within the framework of the McMillan model generalized to biaxial molecules the molecular pseudopotential was written as [253](a)

$$\begin{aligned} u_1(\theta, \phi, z) = & -V_0 \left[\bar{P}_2 + \lambda_1 \bar{G} \right] P_2(\cos \theta) + \alpha \left(\bar{\sigma} + \lambda_1 \bar{K} \right) \\ & \times P_2(\cos \theta) \cos(2\pi z/\xi_0) + \left(\lambda_1 \bar{P}_2 + \lambda_2 \bar{G} \right) \frac{3}{2} (\sin^2 \theta \cos 2\phi) \\ & + \alpha \left(\lambda_1 \bar{\sigma} + \lambda_2 \bar{K} \right) \frac{3}{2} \sin^2 \theta \cos 2\phi \cos(2\pi z/\xi_0) + \alpha \delta \bar{\tau} \cos(2\pi z/\xi_0), \end{aligned} \quad (5.28)$$

where λ_1 and λ_2 are the biaxial parameters

$$\lambda_1 = \frac{2u_{220}}{\sqrt{6}u_{200}} \quad \text{and} \quad \lambda_2 = \frac{2u_{222}}{3u_{200}}. \quad (5.29)$$

Here $u_{2pq} = u_{2qp}$ are the expansion coefficients of the pairwise potential for the effective anisotropic intermolecular interactions. Thus, in addition to three adjustable parameters in McMillan's theory there is a supplementary parameter, in the model using the relation $\lambda_2 = \lambda_1^2$. For the first-order S_{AN} transition these four parameters can be evaluated from independent measurements of T_{NI} , T_{AN} , $\Delta\Sigma_{AN}$ and the correlation $\bar{G}(\bar{P}_2)$ in the nematic phase near T_{AN} or from the other set of experimental data. The sign of the parameters \bar{G} and \bar{K} coincide with the sign of λ_1 , so that changing the sign of λ_1 does not influence the values of T_{NI} , T_{AN} and $\Delta\Sigma_{AN}$. The extensive numerical calculations were performed and it was found that the biaxiality modifies the phase diagram of the McMillan model. With increasing biaxiality parameter $\lambda (= (3/2)^{1/2} \lambda_1)$, T_{NI} increases but the dependence $T_{AN}(\lambda)$ is weaker and more complex. For each value of δ and λ there is a critical value $\alpha_c(\delta, \lambda)$ such that the inequality $T_{AN}(\delta, \lambda) \geq T_{AN}(\delta, 0)$ are valid for $\alpha \geq \alpha_c$. For each value of λ there is a limited range of changes $0 < \delta \leq \delta_1(\lambda)$, where $\alpha_{icp}(\delta, \lambda) \leq \alpha_c(\delta, \lambda)$. With δ and α being constant the entropy change $\Delta\Sigma_{AN}$ decreases with increasing λ . For sufficiently high values of δ and for α corresponding to a narrow nematic range increasing λ can result in changing the S_{AN} transition from first to second order. The parameter δ strengthens the layering tendency independent of orientational ordering and has to increase as the alkyl chain is lengthened at fixed length r_0 of the molecular aromatic core. It is expected that the anisotropic steric interactions do make a significant contribution to the effective value of λ . The change $\Delta\bar{G}(T_{AN})$ and the dependence $\bar{G}(T)$ in the smectic phase are determined by the change of the order parameter \bar{P}_2 at T_{AN} and its dependence on the temperature. The character of the dependence of the derivative $d\bar{G}/dT$ on temperature changes qualitatively both for the first- and second-order S_{AN} transitions. It is important to mention here that the qualitative considerations, which are in agreement with known experiments,

show that the maximum manifestation of the pseudopotential biaxiality should be expected for mesogens having sufficiently long end chains and narrow nematic ranges.

5.3. Application of density functional theory to NS_A transition

Lipkin and Oxtoby [140] were first to consider the application of the density functional approach to the mean-field theory of the isotropic–nematic–smectic A transition. This theory incorporates the steric effect through the pair correlation function and gives the result that \mathbf{q} is parallel to \hat{n} . These authors constructed a set of self-consistent equation for the order parameters,

$$\delta_{\ell 0} \delta_{p0} + \mu_{p\ell} = \frac{2\ell + 1}{4\pi V} \int d\Omega P_\ell(\cos \theta) \int d\mathbf{r} \exp(-i\mathbf{G}_q \cdot \mathbf{r}) \times \exp \left[\sum_q \exp(i\mathbf{G}_q \cdot \mathbf{r}) \sum_{\ell_1 \ell_2} (2\ell_1 + 1) J(q, \ell_1 \ell_2) \mu_{q\ell_2} P_{\ell_1}(\cos \theta) \right], \quad (5.30)$$

where $\mu_{q\ell}$ are the order parameters of the theory and

$$J(q, \ell_1 \ell_2) = J((q, \ell_2 \ell_1)) = \frac{\rho_0}{(4\pi)^{3/2}} \sum_{\ell} G(\ell_1 \ell_2 \ell; 00) i^\ell \left\{ \frac{2\ell + 1}{(2\ell_1 + 1)(2\ell_2 + 1)} \right\}^{1/2} C_{\ell_1 \ell_2 \ell}(\kappa_q) \quad (5.31)$$

with

$$C_{\ell_1 \ell_2 \ell}(\kappa_q) = 4\pi \int_0^\infty dr r^2 j_\ell(\kappa_q r) C_{\ell_1 \ell_2 \ell}(r), \quad (5.32)$$

j_ℓ is a spherical Bessel function.

The free-energy difference between isotropic fluid and the ordered state was written as [140]

$$\beta \Delta A = \rho_0 V \left[-\mu_{00} + J(0, 00) \mu_{00} + \frac{1}{2} \sum'_{q\ell_1 \ell_2} J(q, \ell_1 \ell_2) \right] \mu_{q\ell_1} \mu_{q\ell_2}, \quad (5.33)$$

where the summation excludes the term with $q = l_1 = l_2 = 0$. Eq. (5.33) is a direct generalization of the work of Sluckin and Shukla [141] to the molecular system. A self-consistent solutions of Eqs. (5.32) and (5.33) relate the phase diagram of the isotropic, nematic and S_A phases to the direct correlation function of the isotropic liquid. Truncating the order parameter expansion at the lowest term ($q = 0, \pm 1, \ell = 0, 2$) and relating the term μ_{00} to the density change between the isotropic liquid and liquid crystal a connection with the McMillan theory was established. With these approximations the excess free energy was reformulated as

$$\frac{\beta \Delta A}{N} = \frac{1}{2} J(0, 22) \mu_{02}^2 + J(1, 00) \mu_{10}^2 + J(1, 22) \mu_{12}^2 + 2J(1, 02) \mu_{10} \mu_{12} - \ln \left(\frac{1}{\xi_0} \right) \int_0^{\xi_0} dz \int_0^1 d(\cos \theta) \times \exp[5J(0, 22) \mu_{02} P_2(\cos \theta) + \cos(2\pi z / \xi_0) \{2J(1, 00) \mu_{10} + 2J(1, 20) \mu_{12} + [10J(1, 20) \mu_{10} + 10J(1, 22) \mu_{12}] P_2(\cos \theta)\}] . \quad (5.34)$$

Eq. (5.34) has the same form as obtained in the McMillan theory if the following identifications are made.

$$J(0,22) \rightarrow \frac{1}{25}\beta V_0 ,$$

$$J(1,22) \rightarrow \frac{1}{50}\beta V_0 \alpha ,$$

$$J(1,00) \rightarrow \frac{1}{2}\beta \alpha \delta V_0 ,$$

$$J(1,20) \rightarrow 0 .$$

Thus, here an extra cross-term between μ_{10} and μ_{12} appears which is absent in the McMillan theory of smectic A.

The density functional theory has been used to study the S_A N transition in a system of parallel hard spherocylinders [144,255–257] as well as system with orientational degrees of freedom [258]. Mahato et al. [259] developed a density wave theory which involves the direct correlation function of ellipsoids of revolution and showed that the S_A phase is metastable with respect to the bcc crystal in such a system. Mulder [255] made an attempt to locate the NS_A transition in a system of perfectly aligned hard spherocylinders (PAHSC) by using a bifurcation analysis of the free-energy functional in the second virial coefficient approximation and obtained a second-order transition of mean-field type towards a smectic phase. He also studied the effect of higher-order terms in the density expansion on the location of the bifurcation point by considering the influence of the third- and fourth-order terms. The values of critical packing fraction and wavelength are in good agreement with the simulation values [159] as compared to the results obtained by Hosino et al. [243] using the method of symmetry breaking potential in the second virial coefficient approximation,

$$\eta_M^* \simeq 0.37, \quad \eta_{MC}^* \simeq 0.36, \quad \eta_H^* \simeq 0.729 ,$$

$$\lambda_M^* \simeq 1.34, \quad \lambda_{MC}^* \simeq 1.27, \quad \lambda_H^* \simeq 1.414 .$$

A more systematic calculation was reported by Somoza and Tarazona [144,257]. These authors constructed a free-energy functional for a system of parallel hard spherocylinders [257] as well as for a system of hard bodies with arbitrary shape and orientational distribution [144]. Somoza and Tarazona [257] constructed a free-energy functional by generalizing the Lee's functional scaling method [110] of hard-sphere reference system to the parallel hard ellipsoid (PHE) and then to use the latter as the reference system for the real hard bodies (HB). The interaction part of the free-energy functional expressed as

$$\Delta A[\rho(r, \Omega)] = \int dr \int d\Omega \rho(r, \Omega) \Delta \Psi_{PHE}[\bar{\rho}(r)] \frac{\int dr' \int d\Omega' \rho(r', \Omega') M_{HB}(r - r', \Omega, \Omega')}{\int dr' \rho(r') M_{PHE}(r - r')} \quad (5.35)$$

was evaluated at the effective density $\bar{\rho}(r)$. Here M_{PHE} and M_{HB} are the respective Mayer functions, which give the second virial coefficients by integration over all the variables. A criterion has to be defined for choosing the reference PHE. It should reflect both the molecular shape and the orientational distribution function. An empirical rule was proposed [257,144] the

basis of the tensor of inertia of the HB, $\langle I^{\text{HB}}(\Omega) \rangle$, averaged over the orientations with the function $\rho(\mathbf{r}, \Omega)$,

$$\langle I^{\text{HB}} \rangle = \int d\Omega \rho(\mathbf{r}, \Omega) I^{\text{HB}}(\Omega) / \rho(\mathbf{r}) . \quad (5.36)$$

The length of the PHE along the principal axes are taken so that the eigenvalues of its inertial tensor are proportional to the corresponding eigenvalues of the hard-body tensor of inertia:

$$\frac{I_1^{\text{PHE}}}{\langle I_1^{\text{HB}} \rangle} = \frac{I_2^{\text{PHE}}}{\langle I_2^{\text{HB}} \rangle} = \frac{I_3^{\text{PHE}}}{\langle I_3^{\text{HB}} \rangle} . \quad (5.37)$$

These equations together with the equal volume condition $V_{\text{PHE}} = V_{\text{HB}}$, fully specify the PHE. Eq. (5.35) may be regarded as a way to study the general HB system as a perturbation from the PHE system, for which the direct mapping onto HS can be used. The density profiles and the free-energy of S_A phase were evaluated numerically and a second-order NS_A phase transition was observed. The treatment was extended [144] to a system of HB with arbitrary shape and orientational distribution. The phase diagram was evaluated for a system of parallel hard spherocylinder, and its dependence only on the ratio L/d_0 was observed. The use of different volumes for the PHSC and PHE as to give the same close packing density, together with Eq. (5.37) gave the best results for the molecules of intermediate elongation ($2 \leq L/d_0 \leq 5$). The use of equal volume for the reference and real molecules and Eq. (5.37) underestimates the critical density by about 10%. The continuous character of the NS_A phase transition for the PHSC provided an easy way to calculate the phase diagram based on the analysis of the stability of the nematic against a density modulation. In order to achieve this, Somoza and Tarazona [144] calculated the direct correlation function for the homogeneous phase from the second functional derivative of Eq. (5.35). From the Fourier transform of the direct correlation function $C(\mathbf{q})$, the structure factor $S(q)$ was obtained which, contrary to the case of a simple fluid, depends not only on the modulus of the wave vector \mathbf{q} but also on its direction (relative to the nematic director). The numerical results show that the inclusion of the contribution to the direct correlation function coming from the real HB Mayer function changes this qualitatively because it induces a non-trivial dependence of $C_{\text{HB}}(\mathbf{q})$ with the direction of the wave vector. A stable S_A phase is observed (see Fig. 11) in an interval of densities between the nematic and the crystal phases. This provides an insight into how the slight difference in the shape between the PHE and the PHSC may lead to such dramatic changes in the phase diagram.

Poniewierski and Holyst [258] used density function theory to study the NI and NS_A phase transitions in systems of hard spherocylinders with full translational and orientational degrees of freedom. The free-energy functional was constructed in the spirit of the smooth density approximation (SDA) as developed by Tarazona [197] and also by Curtin and Ashcroft [198] for the inhomogeneous hard-sphere fluids. Both phase transitions, NI and NS_A were observed in a wide range of length-to-width ratio L/d_0 and the results tend to Onsager's limit of $L/d_0 \rightarrow \infty$. In an other paper these authors [256] applied the SDA theory to study the NS_A transition for the system of perfectly aligned hard spherocylinders. The free-energy functional was constructed as

$$\frac{\beta A}{N} = \ln(\rho \Lambda^3) - 1 + \frac{1}{2\pi} \int_0^{2\pi} \varphi(\xi) \ln \varphi(\xi) d\xi + \frac{1}{2\pi} \int_0^{2\pi} \varphi(\xi) \Delta \psi(\rho \bar{\varphi}(\xi)) d\xi , \quad (5.38)$$

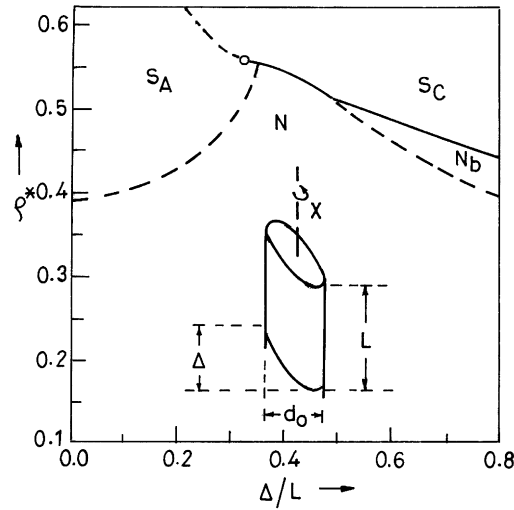


Fig. 11. Phase diagram for a system of parallel hard oblique cylinders. N, S_A , S_C and N_R phases may appear. The dashed lines are continuous transitions and the full lines first order transitions. The circle separates first and second order phase transitions between the S_A and S_C phases.

where

$$\bar{\varphi}(\xi) = 1 + \sum_{n=1}^{\infty} \bar{\mu}_n \omega(n\kappa) \cos(n\xi) \quad (5.39)$$

and

$$\omega(n\kappa) = \left[\frac{4\pi}{(n\kappa)^3} \{ \sin[n\kappa(d_0 + L)] - \sin(n\kappa L) \} - \frac{4\pi d_0}{(n\kappa)^2} \cos[n\kappa(d_0 + L)] \right] / v_0. \quad (5.40)$$

For two parallel spherocylinders $v_0 = 2\pi L d_0^2 + \frac{4}{3}\pi d_0^3$. $\bar{\mu}_n$ is the n th-order parameter and k the smectic wave vector. The minimization of $\beta A/N$ with respect to μ_n and k provides the equilibrium solution for the density wave of the S_A phase. The bifurcation analysis was used to locate the transition and numerical calculations were performed by taking

$$\Delta\psi(\rho) = \kappa_B T \frac{\eta(4 - 3\eta)}{(1 - \eta)^2}. \quad (5.41)$$

Using bifurcation analysis, the density ρ^* at which the nematic solution becomes unstable with respect to the perturbations of the symmetry of the S_A phase was obtained and the following asymptotic relation for the difference between the free energies of the smectic and nematic phases was arrived at

$$\Delta A_{S_{AN}} \sim -(\rho - \rho^*)^2.$$

The variation of the transition density ρ^*/ρ_{cp} (ρ_{cp} is the close packing density) with L/d_0 was studied. It was found that ρ^*/ρ_{cp} ranges from 0.31 for $L/d_0 \rightarrow \infty$ to 0.41 for $L/d_0 = 0.5$ which agrees with the simulation results [159] within 25%. Further, the NS_A transition occurs for all the values of L/d_0 whereas in simulations NS_A transition is not observed for $L/d_0 \leq 0.25$.

6. Re-entrant phase transitions (RPT) in liquid crystals

An exception to the sequence rule (3.1) and observed sequences (Table 3) of phase transitions in liquid crystals was discovered, at atmospheric pressure, in the year 1975 by Cladis [284] in certain strongly polar materials. In a binary mixture of two cyano compounds, HBAB [*p*-[*p*-hexyloxybenzylidene)-amino]benzonitrile} and CBOOA [*N*-*p*-cyanobenzylidene-*p*-*n*-octyloxyaniline], over a range of compositions, the following sequence was observed on cooling the mixture from the isotropic phase,

$$IL \rightarrow N_u \rightarrow S_{A_d} \rightarrow N_R \rightarrow \text{solid} , \quad (6.1)$$

where N_R stands for a second nematic, known as re-entrant nematic, which appears at lower temperature. The smectic-A phase existing between two nematics was identified to be the partially bilayer phase S_{A_d} . A similar result was reported by Cladis et al. [285] in many other binary mixtures and in a pure compound COOB (4-cyano-4'-octyloxy biphenyl) at high pressures (see Fig. 12). They also observed that the pure compounds CBNA (*N*-*p*-cyanobenzylidene-*p*-nonylaniline), CBOA (*N*-*p*-cyanobenzylidene-*p*-octylaniline) and COB (4-cyano-4'-octylbiphenyl), although possessing bilayer smectic-A phase, did not show re-entrant behaviour for pressure under 10 kbar.

X-ray and microscopic studies [286] show that the re-entrant nematic phase is quite different from the classical (higher-temperature) nematic phase. The transition from smectic-A to re-entrant nematic phase is reversible from the point of view of X-ray and optical results. The possibility that the re-entrant nematic is actually a smectic-C phase was excluded [289] on the experimental grounds; N_R phase is uniaxial whereas S_C is biaxial. The defect structure of re-entrant nematic observed in cylindrical geometry was identical to that observed for the classical nematic. For mixtures forming a N_R phase the birefringence [287] has been found to be continuous at both the transitions NS_A and $S_A N_R$. The magnitude of the increase at the NS_A transition point and the decrease on going from the S_A phase to the N_R phase has been found to depend on the length of smectic A range and tend to zero as this vanishes.

The above example of the phase transition (6.1) shows that the high-symmetry phase may re-enter at lower temperature than low-symmetry phase in a rather unexpected way. This kind of phenomenon is termed as “re-entrant phenomenon”. A system is said to be exhibiting re-entrant phase transitions (RPT) if a monotonic variation of any thermodynamic field results in two (or more) phase transitions and attains a state which is macroscopically similar to the initial state or the system re-enters the original state. The phenomenon of RPT is intrinsically novel and the continued interest in this problem [288] is underlined by its discovery in amazingly diverse systems in addition to liquid crystals, e.g., binary gases [289–291], liquid mixtures [292–296], ferroelectrics [297], organometallic compounds [298], granular superconductors [299], gels [300], aqueous electrolytes [301], antiferromagnets [302], etc. The subject is reviewed well by Cladis [303] for liquid crystals and by Narayan and Kumar [288] by multicomponent liquid mixtures.

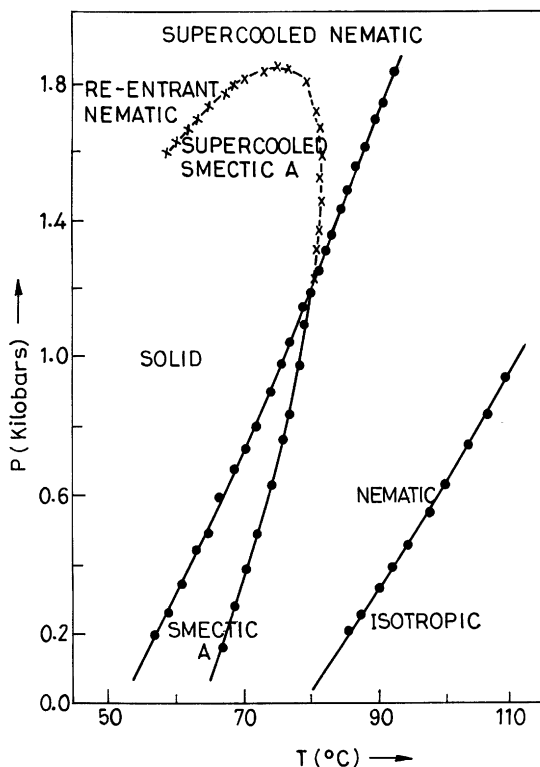


Fig. 12. P - T phase diagram for COOB [285]. Data taken on the $N_R S_A$ transition in the supercooled liquid are shown as crosses (X).

The discovery of re-entrant behaviour [284] in liquid crystals has resulted in extensive studies [288,303,304], both experimental and theoretical, of this intricate kinds of phenomenon. Much of the experimental work has been concerned with the synthesis of the other re-entrant systems, the establishment of their phase diagrams as a function of temperature, pressure and composition and the determination of orientational order and its change at the phase transitions. The main concern of theoretical work has been to understand the microscopic origin and the true nature of RPT. A few representative examples of RPT in liquid crystals are illustrated below.

6.1. Examples of single re-entrance

There are quite a few studies [286,287,305–312] on the binary mixture of hexyloxy-cyanobiphenyl (6 OCB) and 4'-*n*-octyloxy-4-cyanobiphenyl (8 OCB) which exhibit nematic re-entrance as a function of temperature, pressure and composition. Kortan et al. [310] reported a high-resolution X-ray study of the smectic A fluctuation in the nematic phases of this mixture with emphasis on the region of concentration when the smectic phase barely forms or becomes unstable before the correlation length has truly diverged. A number of unusual phenomena were observed in this region, e.g., dramatically increased bare lengths for the smectic correlation, critical

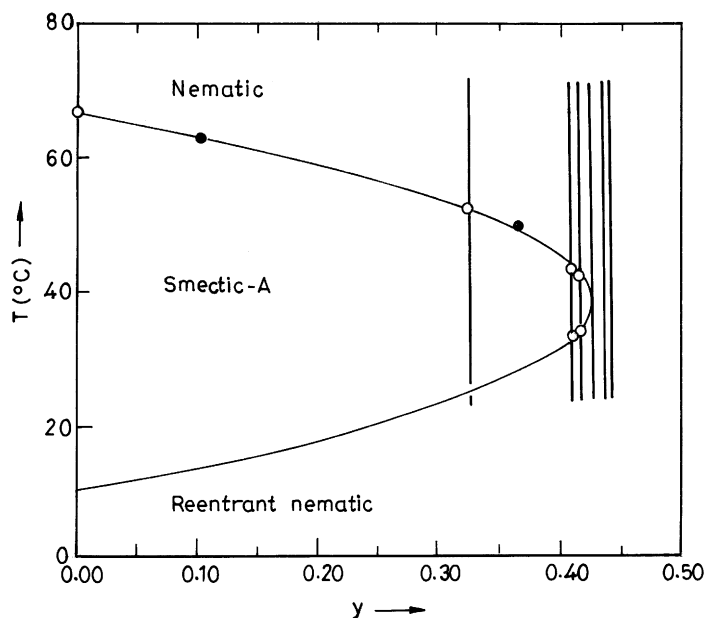


Fig. 13. The phase diagram for 6OCB/8OCB mixture [310]. The concentration y is the molecular ratio 6OCB:8OCB. The open and solid circles represent, respectively, the data obtained by X-ray scattering and light scattering experiments. The vertical lines indicate the experimental path.

exponents which may be as large as twice those found in pure 80CB crossover effects, etc. The phase transition temperature was measured by observing the temperature at which the minimum in the width of q_1 scans occurred rather than being treated as adjustable parameter. Fig. 13 shows the phase diagram so obtained. The influence of pressure on the S_A/N and NI phase boundaries were studied [308] as a function of mole fraction of 60CB by DTA and optical microscopy. It was found that the maximum pressure of occurrence of the smectic A phase decreases with increasing mole fraction (y) of 6 OCB until $y \simeq 0.3$ where no smectic phase exists. Further, the pressure behaviour of the NI transition gets drastically affected by structural changes occurring at lower temperatures. Although they could not ascertain whether this effect is due to the influence of the smectic ordering or due to the presence of re-entrant nematic at farther temperatures or due to a combination of both, it was tentatively concluded that the classical or high-temperature nematic, in the concentration range of the existence of the re-entrant nematic, possesses a molecular ordering which is somewhat different from the ordering of the nematic phase occurring at higher concentrations.

The orientational order and its change at the phase transitions for the 6 OCB/8 OCB has been studied [287] by measuring its optical birefringence, a quantity which can be determined with considerable precision. For the mixture exhibiting re-entrant nematic phase the birefringence is found to be continuous at both the transitions; nematic-smectic A and smectic A-reentrant nematic. It is important to note that the birefringence in the smectic A phase is found to be greater than that obtained by an appropriate extrapolation from the results in the nematic phase. Contrary to it birefringence of the N_R phase is observed to be less than that determined by extrapolation from

the smectic A phase. The magnitude of the increase in case of nematic–smectic A transition and the decrease on going from smectic A to reentrant nematic phase are found to depend on the range of stability of smectic A phase. Emsley et al. [312] investigated in detail the orientational behaviour of this mixture using deuterium NMR spectroscopy, a technique which is able to provide information about the orientational order of the individual components of a mixture. More importantly, this technique can determine the order parameters for the rigid subunits in a mesogenic molecules. This variation in the order parameter has been determined in the mixture 6 OCB/8 OCB as well as in the pure components as a function of temperature. The order parameters were found to undergo subtle changes at the transition from the smectic A to the reentrant nematic phase.

One of the important features of the RPT in liquid mixtures is the existence of a closed-loop phase diagram with upper and lower critical solution temperatures (T_u and T_L , respectively). A double critical point (DCP) results when the T_u and T_L are made to coincide. Such systems provide richer informations as they permit a multitude of paths by which a critical point can be approached. A wide variety of phases can be obtained in these systems by mere variation of temperature, pressure, composition, additional components, etc. Perhaps the first closed-loop existence curve was obtained by Hudson [313] for nicotine/water mixture while trying to crystallize nicotine from its aqueous solution. Since then the closed-loop phase diagrams have been reported in many systems [288]. Fig. 14 shows a closed-loop nematic–smectic A phase boundary observed [314] in mixtures of $\bar{7}$ -CBP (4-*n*-heptyloxy-4'-cyanobiphenyl) and a binary mixture of CBOOA and $\bar{8}$.0.5 (4-*n*-pentylphenyl-4-*n*-octyloxy-benzoate) as a function of temperature, pressure and composition. It can be seen that the pressure reduces the area of smectic A phase and the re-entrance vanishes (i.e. a DCP is attained) at 145 bar.

In principle, the re-entrant phases can occur [249,138,304,315] in non-polar system also. The experimental evidence in support of this prediction has been unveiled by the Halle group [316,317].

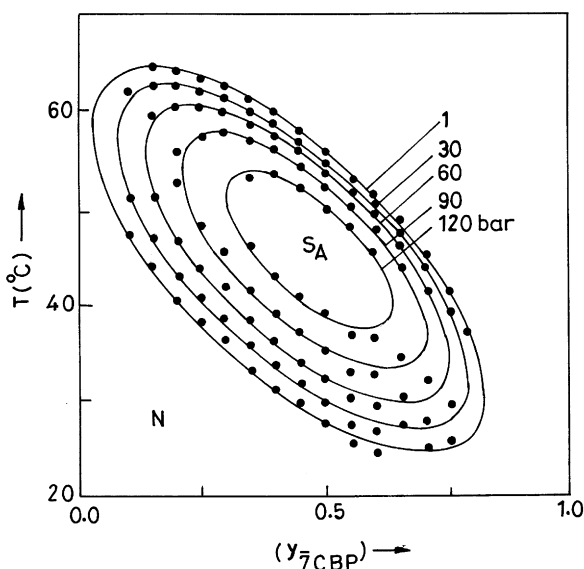
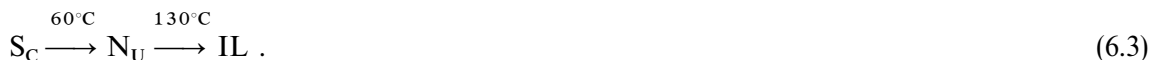


Fig. 14. T - y phase diagram of the system [$\bar{8}$.0.5/CBOOA ($y_{\text{CBOOA}} = 0.88$)]/ $\bar{7}$ CBP for different pressures [314].

A nematic reentrant system of non-polar compounds, with one component a side-chain LC polymer, has been reported [318] which exhibits this kind of inversion of symmetry. The polymer is an atactic polymethylsiloxane substituted with 4-undecyloxyphenyl ester of 4-methoxybenzoic acid ($P_{11,1}$) which follows the phase sequence



The second component is a symmetrically substituted compound, the 4'-heptyloxybenzoate of 6-heptyloxynaphthyl-2, exhibiting the order of phase stability



Hence $S_c \rightarrow N_u$ transition is monotropic.

The re-entrant sequence ($N_R-S_A-N_u-\text{IL}$) has been observed in a homologous mixture composed of 60% (weight) of the low molecular weight compound and 40% (weight) of polymer by using optical polarizing microscopy and X-ray analysis. On cooling the mixture the focal conic S_A texture transforms at 70°C into a Schlieren twinkling nematic, which is similar to the high-temperature nematic texture above 129°C . This is connected on the X-ray pattern with a change from a resolution limited Bragg spot to a diffuse scattering at small angles indicative of the loss of the layered structure at long range. It has been found [318] that the layer thickness in the S_A phase of the mixture is noticeably larger than both the molecular length of the mesogenic groups side-chain of the polymer (33.5 Å) and the length of the low molecular weight compound. Similar anomalies of the periodicity has been observed in the pure $P_{11,1}$ for which the layer thickness increases continuously with decreasing temperature as for some re-entrant polar compounds [319].

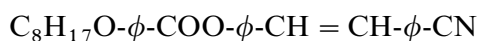
The re-entrant behaviour has also been observed in discotic liquid crystals. In a hexa-*n*-alkanoates of truxene for the higher homologues the following sequence is observed [320,321], on cooling:



It has been conjectured that the truxene molecules are probably associated in pairs and that these pairs break up at higher temperatures and might be responsible for this extra ordinary behaviour.

6.2. Examples of multiple re-entrance

High-resolution X-ray scattering and heat capacity studies of the nematic–smectic A transitions in 4'-(4''-*n*-alkoxybenzyloxy)-4-cyanostilbene with the alkyl chain of length 7 (T7) and 8 (T8) were reported by Evans-Lutterodt et al. [322]. It was observed that the material T7 exhibits only a single nematic–smectic A_1 (S_{A_1} , monolayer) transition in which the S_{A_1} period is commensurate with the molecular length L whereas T8,

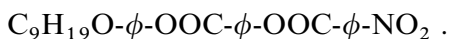


exhibits [322,323] with decreasing temperature, the double-re-entrance sequence

$$IL \rightarrow N_u \rightarrow S_{A_d} \rightarrow N_R \rightarrow S_{A_1} \rightarrow \text{solid} . \quad (6.5)$$

Here ϕ represents a benzene ring and S_{A_d} period is incommensurate with $d \simeq 1.2L$. It has been observed that in the re-entrant nematic phase of T8, S_{A_d} and S_{A_1} fluctuations are essentially independent; the S_{A_d} fluctuations change over from being S_A -like to S_C -like with decreasing temperature in the N_R phase.

Probably, the most spectacular case of multiple reentrance has been observed [319,324,325] in the material 4-nonyloxyphenyl-4'-nitrobenzoyloxybenzoate (DB90NO₂) with molecular structure [326],



This compound exhibits three nematic, four smectic A and two smectic C phases in the following sequence, on cooling:

$$IL \rightarrow N_u \rightarrow S_{A_d} \rightarrow N_R \rightarrow S_{A_d} \rightarrow N_R \rightarrow S_{A_1} \rightarrow S_{\bar{C}} \rightarrow S_{A_2} \rightarrow S_{C_2} \rightarrow \text{solid} . \quad (6.6)$$

Here S_{A_2} is bilayer and $S_{\bar{C}}$ and S_{C_2} are two different forms of smectic C phase [326]. This unusual behaviour was rationalized in terms of the gradual cross-over from dominant S_{A_d} to dominant S_{A_1} fluctuations with decreasing temperature.

6.3. Theories for the RPT

From the molecular point of view, only approximate qualitative explanations of the re-entrant behaviour have been possible. As discussed above, the liquid crystal systems exhibiting re-entrance consist of organic molecules usually with three or four aromatic rings with ester linkages and having polar cyano or nitro-end groups. Apart from pure compounds, re-entrant polymorphism, on cooling, has also been shown by binary mixtures of polar–polar, polar–non-polar and non-polar–non-polar compounds. Further, as a homologous series is ascended, the re-entrant phase sequence is exhibited by the higher homologs which are neither very short nor very long. These experimental observations indicate that the dipolar force plays a crucial role in the re-entrant polymorphism. However, the observation of single re-entrance [316,317] in a binary mixture of non-polar compounds probably cannot be caused because of dipolar forces. Reviews of theories and experiments for the re-entrant polymorphism are available [303,327,328] which present an account of the subject. The first tentative model for the nematic re-entrance was proposed by Cladis et al. [285]. A number of other elaborate models [304,329–336] have been proposed which emphasize the role of attractive forces and/or hard core repulsions to exhibit the phase sequence and assume some sort of bimolecular organisation (dimers) or even trimers or n -mers [333] with antiparallel association that compensates (not always fully) the dipole moments. These theories essentially show that the high-temperature smectic phase is an induced phase and the re-entrant nematic phase is brought about by a competition between two incommensurate lengths. This two length concept is one of the main ingredient of the Landau theory of the re-entrant phase sequence [230,337,338]. The frustrated spin gas model [333] is able to show the multiple re-entrance and the sensitive dependence of re-entrance on the molecular chain length and pressure. In case of

single re-entrance observed in a binary mixture of non-polar compound, the experimental results [317] on the layering thickness give no indication in favour of the kind of molecular organization as found in re-entrant systems with polar compounds. A lattice model was proposed by Dowell [138,249,315] for the re-entrant phase sequence of non-polar system. The Dowell model holds the change in chain configuration responsible for the re-entrance. It was shown by Bose et al. [331] that the re-entrant phenomenon is built in the McMillan model if one explicitly incorporates the effect of tail chain conformations in the molecular potential instead of treating the chains as an extension or rigid part. This model is based on a molecular-field approach and predicts the single-re-entrant phase sequence with lowering of temperature in an idealized non-polar system.

The Cladis model [284,285] utilizes the fact that the re-entrance appears only in compounds, exhibiting layered phases, of amphiphilic molecules having both a polar (aromatic rings with polar heads) and a non-polar (alkyl or alkoxy chains) part. The two parts of the molecule are assumed to be immiscible. The molecules move freely within each layer and with difficulty between the layers. There exist no correlation between molecules in different layers. Usually, in most of the liquid crystals, the polar segments of the molecules occupy a middle position with hydrocarbon chains extending outward (Fig. 15). These kinds of configurations prefer to form a monolayer smectic A phase. In case of re-entrance, owing to antiparallel correlations, the molecules form dimers which are assumed to be somewhat bulgy in the middle (Fig. 15). As a result, bilayer, but incommensurate, smectic A phases are probable. Once the smectic S_{Ad} phase is formed the bulgy parts are lined up in a plane, whereas the alkyl chains cannot fill the rest of the space. With decreasing temperature (i.e. promoting the dimer formation) and also possibly with the stiffening of the end chains, the packing becomes so unfavourable that the smectic A phase becomes unstable and nematic re-entrance appears. In order to explain the re-entrance at elevated pressure the Cladis model assumes that the stability of bilayer smectic A phase is because of polar–polar (long-range electrostatic) and non-polar non-polar (short-range) interactions and that the layer spacing extends with increasing pressure. The increase in layer spacing may be due to slight compacting of the flexible non-polar part. This weakens the efficiency of the non-polar segments to hold the layer together and with

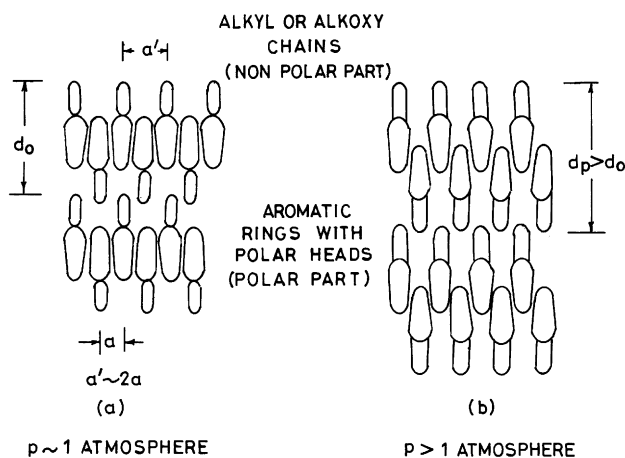


Fig. 15. Schematic representation of a bilayer smectic-A phase (a) 1 atm. and (b) under pressure.

pressure the repulsive interaction of the aromatic rings increases and pushes the layers apart, if the pressure is increased further (and temperature decreased) a transition takes place between less dense smectic and more dense nematic which is the characteristic of the high-pressure side of the re-entrant phase diagrams (Fig. 12). The forces stabilizing the layers are the short-range attractive hydrocarbon (non-polar–non-polar) interactions. These forces are proportional to the length of the hydrocarbon chains. The increasing repulsive interaction of the aromatic rings with increasing pressure drives the layers apart.

The Luckhurst–Timimi model [329] of re-entrant polymorphism is a simple extension of the McMillan theory [234] of the smectic-A liquid crystals in which the scaled strength parameters related with the stability of smectic-A phase are allowed to vary with temperature. This theory has been successful in explaining the experimental results, as described in Section 6.1 for the 6 OCB/80CB mixture. However, in order to show re-entrance they had to assume that the strength parameter associated with mixed order parameter is linearly temperature dependent over the region of interest. Dong [307] presented a detailed comparison of this approach with the phenomenological Landau-type theory.

As discussed above within both the Landau and microscopic mean-field theories, re-entrance appears only if either the order parameter of interest is coupled to an additional degrees of freedom or the Hamiltonian is explicitly temperature-dependent. It was shown by Katriel and Kventzel [236,339] that the re-entrant nematic and smectic phases are exhibited by a fully self-consistent treatment of a simplified McMillan's type model involving coupled nematic and smectic order parameters without any explicit temperature-dependent factors. A re-entrant isotropic phase was shown to be exhibited by explicit temperature-dependent Hamiltonian as well as by a two-state model. The molecular theory of Luckhurst and Timimi [329] involves three coupled equations in the orientational, positional and mixed-order parameters. The simplification proposed by Katriel and Kventzel [236] involves the decoupling of mixed order parameter (Eq (5.26)) as a product of the pure orientational and positional order parameters. It was shown that the Hamiltonian so obtained by the decoupled model exhibits reentrance for appropriate choices of model parameters.

The most successful microscopic theory is probably the “frustrated spin gas model” [333–335] which invokes the possible dipolar frustration of the molecules in re-entrant systems. The dipolar interactions, under the molecular close packing conditions, may or may not be frustrated, depending on the positional fluctuations. Thus, the theory incorporates the coupled degrees of freedom of dipolar orientations and molecular positions. The idea is that when in the plane normal to the average molecular axis, frustration is (is not) lifted by the positional fluctuations normal to the plane, the smectic (nematic) phase is realized. These molecular positional fluctuations normal to the plane are called permeation fluctuations. The calculations with this “frustrated spin gas model” have been able to reproduce remarkably the single- as well as double- re-entrance sequences and also the sensitive dependence of re-entrant polymorphism on the molecular chain length and pressure. The basic idea of microscopic mechanism involved here is shown in Fig. 16. On a two-dimensional triangular lattice triplets of molecules are considered. The molecules are taken to have an aliphatic tail on a polar head along the molecular axis. We begin by considering the limit of complete positional order [Fig. 16a]. The close packing arrangement in two dimensions is triangular. The interaction between the dipoles is antiferroelectric. Since each elementary triangle of the array is frustrated an antiferroelectric long-range order cannot be supported. In case the local distribution is like Fig. 16b, with one weak and two strong bonds, frustration will be lifted,

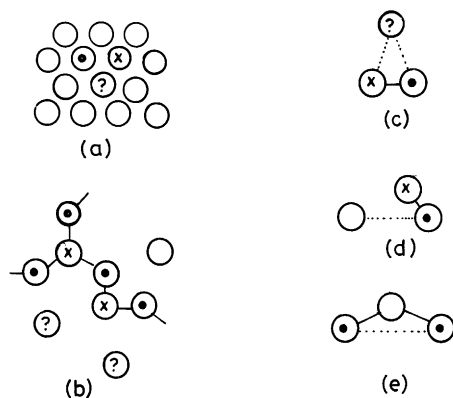


Fig. 16. Positional configuration of a layer normal to the molecular axes. Molecular dipoles which are frustrated are, respectively, indicated by crosses, closed circles or question marks. Strong and weak bonds are shown with full and dotted lines, respectively.

and two dimensional antiferroelectric order can propagate across the unit. If the arrangements is like in Fig. 16c, with one strong and two weak bonds, frustration will still, persist, which will destroy the possibility of the existence of antiferroelectric order. However, in any actual local distribution, each elementary triangle is between these two cases, one strong, one intermediate, and one weak bond [Fig. 16d]. The ordering character of the unit can be determined depending on the distance between the intermediate bond and the strong bond or the weak bond. If there are enough of the former type of units, they will percolate across the system and form an infinite network (“polymer”) of positionally disordered, but antiferroelectrically ordered molecules [Fig. 16e]. Each layer, consecutively along the Z -direction, will have its own network. These networks will not pass through each other because this would involve disrupting infinitely many strong bonds. This leads to the density modulation along the Z -axis, i.e., the smectic phase. Two points are worth mentioning here. First, even in the presence of the network, many antiferroelectrically ordered but finite clusters slide up and down the Z -axis and provide the constant background to the smectic modulation. Second, although the percolating network must be sustained for the smectic modulation, individual molecules join it and leave it as time progresses. Finally, as the system is further cooled, it may be possible that local positional order will set in turning on frustration, eventually destroying the network, and re-entering the nematic phase.

The microscopic pair potential through which the molecules interact is assumed to be of dipolar type

$$U(\mathbf{r}_1, \hat{\mathbf{s}}_1, \mathbf{r}_2, \hat{\mathbf{s}}_2) = \frac{A\hat{\mathbf{s}}_1 \cdot \hat{\mathbf{s}}_2}{r_{12}^3} - \frac{3B(\hat{\mathbf{s}}_1 \cdot \hat{\mathbf{r}}_{12})(\hat{\mathbf{s}}_2 \cdot \hat{\mathbf{r}}_{12})}{r_{12}^5}. \quad (6.7)$$

For the purely dipolar interaction $A = B$; $\hat{\mathbf{s}}_1$ and $\hat{\mathbf{s}}_2$ are unit vectors along the Z -direction perpendicular to the two-dimensional lattice and r_i is the position of the dipolar head of the molecule i . When $A > B$ steric hindrance wins and if $A < B$ the van der Waals or amphiphilic

attraction wins. The important positional fluctuations for the re-entrant systems were found to be permeation fluctuations, occurring along the Z -direction, which is parallel to the average molecular axis and normal to the smectic layers. Since for a given molecule the molecular architecture may not be smooth, a nearest-neighbour molecule has n positions of preferred relative permeation. These “notches” are taken to be separated by ℓ/n , where ℓ is the effective molecular length.

The nematic–smectic A phase boundaries can be approximated in the following way. A special prefacing transformation is used to evaluate the effect of the positional fluctuations on the dipole–dipole interactions. In a finite-cluster approximation, a triplet of nearest-neighbour dipoles is considered. With one dipole fixed, the partition function is summed over the n^2 permeational configurations of the two other dipoles. The result is a triplet spin Hamiltonian, into which have been projected the average strongest, intermediate, and weakest antiferroelectric couplings,

$$\begin{aligned} \exp(H_{123} + G) &\equiv \exp(K_S s_1 s_2 + K_I s_2 s_3 + K_W s_3 s_1 + G) \\ &\equiv \sum_{r_{2,3}} \exp[-\beta U(\mathbf{r}_1, \hat{s}_1, \mathbf{r}_2, \hat{s}_2) - \beta U(\mathbf{r}_2, \hat{s}_2, \mathbf{r}_3, \hat{s}_3) - \beta U(\mathbf{r}_3, \hat{s}_3, \mathbf{r}_1, \hat{s}_1)] , \quad (6.8) \end{aligned}$$

where the three molecules are labeled 1, 2 and 3 such that (12), (23) and (31) always span the strongest, intermediate, and weakest antiferroelectric couplings, respectively. K_S , K_I and K_W correspond to the strongest, intermediate, and weakest couplings, specific to each positional configuration. G is the free energy contribution of the degrees of freedom summed over in the prefacing transformation. The result is a distorted triangle of Ising spins. The nematic–smectic phase boundaries are located with Houtappel’s condition [340]

$$\sinh(2K_S)\sinh(2K_S) + \sinh(2K_I)\sinh(2K_W) + \sinh(2K_W)\sinh(2K_S) > 1 . \quad (6.9)$$

This condition corresponds to a two-dimensional distorted triangular Ising model. If both K_S and K_I are positive, in-plane ferromagnetic order sets in. This corresponds to $\langle \hat{s}_1, \hat{s}_2 \rangle \cong 1$. This phase was identified [3](b), as S_A . If $K_S \cdot K_I < 0$; $\langle \hat{s}_1 - \hat{s}_2 \rangle < 0$, local antiferroelectric order sets in, which describes the S_{A_d} phase. Since condition (6.9) corresponds to a two-dimensional system, the transitions are, of course, strongly displaced towards low temperatures as compared to what they should be in a three-dimensional system. This approach reproduces satisfactorily the double re-entrance as well as the multiple re-entrance. In its present form, although, the spin gas model cannot describe the $S_A S_C$ transition and the more ordered phases, but it is able to predict smectics with different thicknesses. Madhusudana and Rajan [336] have made an interesting remark that whereas dipolar interactions favour antiparallel short-range order, induction (dipole-induced dipole) interactions favour parallel short-range order. The interplay between these two tendencies may also explain the existence of two natural lengths and re-entrances.

The above procedure can be extended [335] to the calculation of specific heat. After the prefacing transformation, the free-energy per molecule can be expressed as

$$f = G + \ln \lambda(K_S, K_I, K_W) \quad (6.10)$$

with

$$\ln \lambda(K_S + K_I + K_W) = \lim_{N \rightarrow \infty} \left[\frac{1}{N} \ln \sum_{|S|} \exp \left(\sum_{\langle ijk \rangle} H_{ijk} \right) \right] . \quad (6.11)$$

Here the last sum is over the N up-triangle formed in a plane of N -spins. The specific heat per molecule at constant pressure is given by

$$C = \frac{\partial}{\partial T} \kappa_B T^2 \frac{\partial}{\partial T} f. \quad (6.12)$$

This is evaluated with the chain rule, requiring the first and second temperature derivatives of G and K_α . λ can be evaluated by using Houtappel's exact expression

$$\begin{aligned} 8\pi^2 \ln(\lambda/2) = & \int_0^{2\pi} d\omega_1 \int_0^{2\pi} d\omega_2 \ln[\cosh(2K_s)\cosh(2K_l)\cosh(2K_w) \\ & + \sinh(2K_s)\sinh(2K_l)\sinh(2K_w) - \sinh(2K_s)\cos\omega_1 - \sinh(2K_l)\cos\omega_2 \\ & - \sinh(2K_w)\cos(\omega_1 + \omega_2)] . \end{aligned} \quad (6.13)$$

The interest here is in the relative magnitude of the specific-heat signals at the different phase transitions, which are strongly influenced by the functions $G(T)$ and $K_\alpha(T)$ of the prefacing transformation. In the calculation it has been found [335] that the “transition enthalpy” is much larger for the S_{A_1} -to- N_R transition than for the N_R -to- S_{A_1} transition.

Dowell [138,249,315] proposed a general lattice model for condensed phases with orientational and/or partial or total positional ordering of the molecules in the system. The positional ordering can be in one, two, or three dimensions. Each molecule is composed of a rigid core and one or two semiflexible tails and has site–site hard repulsive intermolecular interactions. Let each molecule have r rigid core segments, sf semiflexible tail segments, $(r - 1)$ rigid bonds, and sf semiflexible tail bonds. The configurational partition function Q_C for a whole system of molecules in this model is given by

$$Q_C = \Omega \exp\left[-\frac{E_C}{K_B T}\right],$$

where Ω is the total number of distinguishable ways to arrange the molecules in the system and E_C is the average intermolecular energetic contribution to the Q_C . Infinitely hard repulsions are implicitly included in Ω as the two molecular segments are not allowed to occupy the same lattice site. E_C includes attractions and soft repulsions between intermolecular segments. In case the molecules have hard repulsions only, $E_C = 0$ and Q_C is equal to zero. In order to calculate the general partition function Ω , the molecules are placed on the lattice, molecule by molecule, segment by segment. The general relation for the partition function was derived by Dowell [249] and applied [138](c) to the special cases of smectic-A and nematic liquid crystals and isotropic liquids in bulk phases. The relative stabilities of the isotropic, nematic, smectic-A and re-entrant nematic phases were studied as a function of temperature, pressure, tail flexibility, and tail length. The role of the semiflexible tails in stabilizing the smectic-A and re-entrant nematic phases was explicitly excluded.

In this model [138,249] the molecules are assumed to interact via site–site (segmental) hard repulsions. The lengths of the core and the tails can be varied as well as the flexibility of the intramolecular bonds in the tails. The model holds the change in chain configuration responsible

for the re-entrance in a single-component non-polar system. It is seen that a segregated packing of cores besides cores and chains beside chains occurs with a lowering of temperature leading to a usual smectic phase. With further lowering of temperature, the chain becomes less flexible, and the packing differences between the rigid cores and tail chains decrease. Thus, the need for the segregated packing of rigid cores with cores (and tail chains with tail chains) is overcome by the entropy of unsegregated packing, leading to a disappearance of the re-entrant nematic.

7. Uniaxial nematic–biaxial nematic ($N_u N_b$) phase transition

As indicated in Section 1.2.1, in the N_u phase the molecules tend to align along the director \hat{n} . A further breaking of rotational symmetry around the director \hat{n} may lead to the formation of a biaxial nematic (N_b) phase. The existence of this phase was predicted on a theoretical basis by Freiser [38]. He showed that the simplest generation of interaction employed in the Maier–Saupe (MS) theory leads to a first-order IN transition followed, at lower temperature, by a second-order transition to a biaxial state. Considering a hard-plate lattice model, Shih and Alben [349] showed that the system composed of rectangular plates which are neither very square nor very rod-like in shape may exhibit N_b phase at high pressure. At some lower pressure the N_b phase undergoes a second-order phase transition to a N_u phase which at a still lower pressure exhibits a first-order NI transition. The hard-plate lattice model was solved by Alben [39] within the framework of mean-field approximation and a number of interesting results were obtained. For example, the introduction of plate-like molecules increases the NI transition temperature of rod-like molecules. At a lower temperature, the N_u phase can undergo a second-order transition to a more highly ordered N_b phase. Between the two regions N_u^+ (positive optical anisotropy) and N_u^- (negative optical anisotropy), Alben's calculation showed that the two second-order lines between the N_u and N_b phases form a sharp cusp separating the rod-like nematic phase N_u^+ and plate-like nematic phase N_u^- and that the cusp touches the first-order isotropic–uniaxial nematic transition line. The intersection of the two second-order lines and the first-order transition line forms a special critical point. From the Alben's phase diagram it is difficult to analyse the details of the thermodynamic and critical behaviour in the region between N_u^+ and N_u^- transitions.

The experimental discovery of the long-predicted N_b phase has been by Saupe and co-workers [40,343,344] and others [345,346]. These authors studied the phase diagram and critical properties of the ternary system potassium laurate-1-decanol- D_2O over concentration ranges where nematic phases are likely to occur (Fig. 17). It was shown that in the limited concentration range the observed phase sequences on heating/cooling may be: isotropic, uniaxial nematic (N_u^+), biaxial nematic (N_b) and uniaxial nematic (N_u^-). Thus, an intermediate N_b phase is formed for a certain concentration range while in other ranges a direct first-order $N_u^+ - N_u^-$ transition occurs. The $N_u^+ - N_b$ or $N_u^- - N_b$ transition appears to be second order. Experimentally, transitions have been observed that seem to lead directly from $N_u^+ - N_u^-$ via a first-order transition. In certain micellar nematics the phase diagrams suggest the existence of a Landau point on the nematic–isotropic transition line. The nematic phase formed can be positive or negative uniaxial and even biaxial, depending on the shape of the micelles. The phase diagram of the mixture of rod-like and plate-like molecules of comparable size and in comparable amounts also indicates the existence of a Landau point. Evidence has been found that the mixture undergoes a transition to two coaxial uniaxial

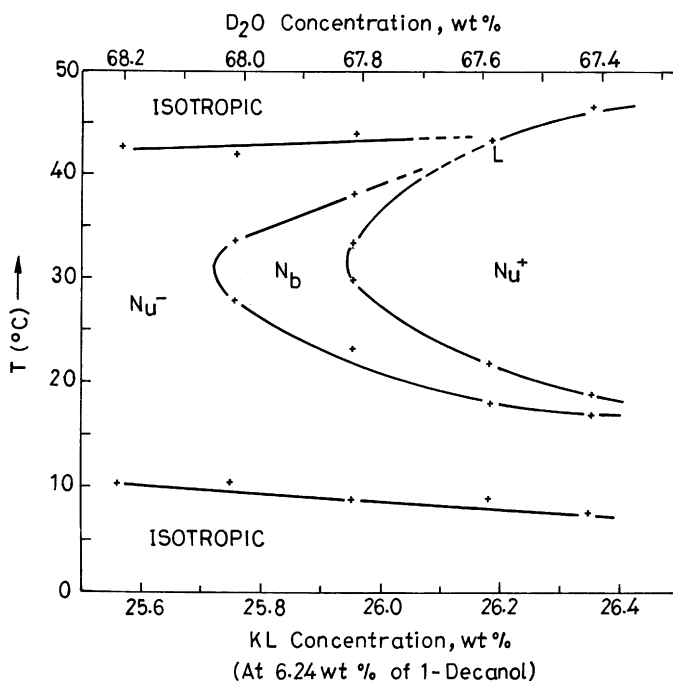


Fig. 17. Phase diagram of the potassium laurate/1-decanol/D₂O system [40]. L is the approximate location of the Landau point.

phases, rather than to a single biaxial phase. The suggestion was made by Chandrasekhar [347] that a thermotropic N_b phase can be prepared by bridging the gap between rod- and disc-like mesogens, i.e., by synthesizing a mesogen that combines the features of the rod and the disc. This has proved to be useful and the N_b phase has been observed in some relatively simple compounds [41,42].

A number of important ideas concerning the N_b phase have been discussed theoretically [341,342,92,347–360]. These theoretical investigations show that an isolated critical point is obtained in the phase diagram, where the N_b – N_u^+ and N_b – N_u^- phase boundaries meet a first-order N_u^+ – N_u^- line. At this isolated critical point the cubic coefficient of the order parameter in the effective Hamiltonian becomes zero.

In order to construct within the framework of the LDG theory the simplest model for the both uniaxial and biaxial phases, one must retain the following terms in the free-energy expansion (4.10):

$$f = \frac{1}{2}A \text{Tr}(\mathbf{Q}^2) + \frac{1}{3}B \text{Tr}(\mathbf{Q}^3) + \frac{1}{4}C[\text{Tr} \mathbf{Q}^2]^2 + E'[\text{Tr} \mathbf{Q}^3]^2. \quad (7.1)$$

For stability it is required that $C > 0$ and $E' > 0$. Instead of considering only A as the controllable variable, a phase diagram has to be constructed as a function of A and B . Using Eq. (2.19) the free-energy expansion becomes [64]

$$f(x, y) = \alpha_0(x) + \alpha_2(x)y^2 + \alpha_4(x)y^4, \quad (7.2)$$

where

$$\alpha_0(x) = \frac{3}{4}Ax^2 + \frac{1}{4}Bx^3 + \frac{9}{16}Cx^4 + \frac{9}{16}E'x^6, \quad (7.3a)$$

$$\alpha_2(x) = \frac{1}{4}A - \frac{1}{4}Bx + \frac{3}{8}Cx^2 - \frac{9}{8}E'x^4, \quad (7.3b)$$

$$\alpha_4(x) = \frac{1}{8}C + \frac{9}{8}E'x^2. \quad (7.3c)$$

Minimization with respect to y gives

$$y = 0, \quad \text{uniaxial} \quad (7.4a)$$

$$y = -\alpha_2(x)/\alpha_4(x), \quad \text{biaxial} \quad (7.4b)$$

$$f_u(x) = \alpha_0(x), \quad \text{uniaxial} \quad (7.4c)$$

and

$$f_b(x) = \alpha_0(x) - \alpha_2^2(x)/2\alpha_4(x). \quad (7.4d)$$

Since always $\alpha_2(x) > 0$, the biaxial solution (7.4b) is only allowed when $\alpha_4(x) < 0$. Further, whenever the biaxial solution is allowed, $f_b(x) < f_u(x)$. The resulting phase diagram is shown in Fig. 18. It can be seen that apart from the usual first-order NI transition (solid line) two second-order $N_u^+ - N_b$ and $N_b - N_u^-$ transition (broken lines) occur. The biaxial phase is sandwiched between N_u^+ and N_u^- phases. All four phases meet in a bicritical point, called the Landau point and located

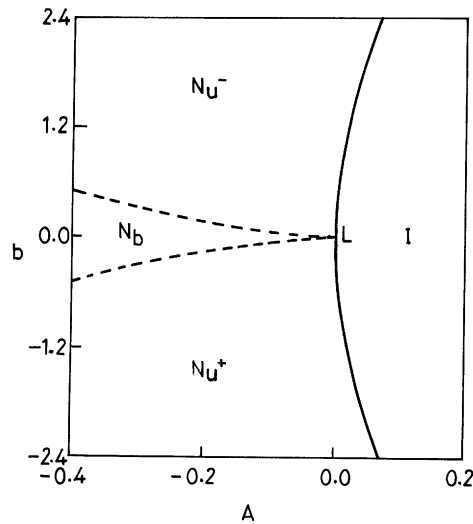


Fig. 18. Phase diagram with a biaxial nematic phase obtained from the free-energy (7.1), with $C = 2.67$, $E' = 3.56$ [64]. Solid lines represent phase transition of first-order and dashed lines second-order. A is a measure for the temperature, b is the degree of flatness of the molecules. L is the Landau point.

at $A = B = 0$. The NI transition is second-order here. The isotropic–nematic line of phase transition is given by

$$A = \frac{3}{4}Cx^2 + \frac{9}{4}E'x^4 \quad (7.5a)$$

and

$$B = \frac{9}{2}Cx + 18E'x^3. \quad (7.5b)$$

The uniaxial nematic–biaxial nematic transition defined by

$$A = -\frac{3}{2}Cx^2, \quad (7.6a)$$

$$B = -\frac{9}{2}E'x^3 \quad (7.6b)$$

indicates that the width of the biaxial region is proportional to $(T^* - T)^{3/2}$.

The phase diagram without E' term (Fig. 19) shows that the width of the biaxial region shrinks to zero leaving a first-order $N_u^+ - N_u^-$ transition. The topology of the phase diagram in the vicinity of the Landau point does not change even if the free-energy expansion is carried out to higher orders. The critical exponents for the Landau point using renormalization group method have been calculated by several authors [82,350].

In principle, following possibilities may lead to the spontaneous formation of a one-component biaxial nematic phase:

- (i) A molecular symmetry that is not (effectively) uniaxial.
- (ii) Strong correlation of molecules leading to aggregates of molecules having no uniaxial symmetry.
- (iii) Application of an external field.

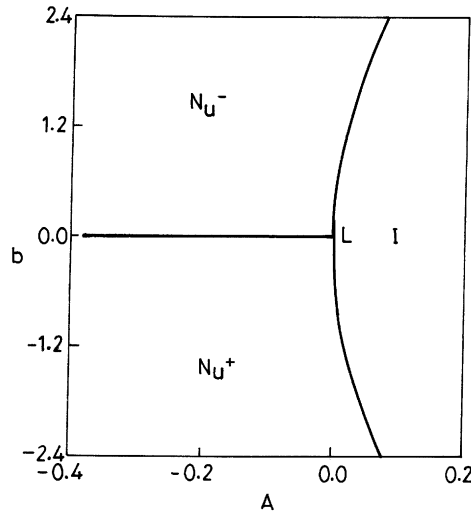


Fig. 19. Phase diagram without biaxial nematic phase, obtained from the free-energy (7.1), with $C = 2.67$, $E' = 0$ [64]. Symbols are the same as in Fig. 18.

Associated with the second possibility a N_b phase has been observed in lyotropic systems of amphiphilic (soap-like) solutions in water. In these solutions, the molecules tend to cluster into aggregates so that the hydrophilic groups occupy the surface to optimize contact with water, while the lipophilic tails occupy the inert part of the aggregates [361]. These so-called micelles behave somewhat like large-scale molecules such that under a suitable choice of temperature, concentration and sometimes additional solvents they tend to exhibit smectic or nematic structure. Depending on the shape of the micelles the nematic phase can be positive or negative uniaxial and even biaxial, since the shape changes with concentration. The complete phase diagram of the potassium laurate/1-decanol/ D_2O system is shown in Fig. 17. In case of one-component thermotropic systems, theoretical studies [38,358] indicate that for systems with molecules without axial symmetry, a N_b phase at lower temperature is necessary rather than just possible. However, in an experiment the system may form smectic and crystalline phases before this temperature is reached. Hence, to form the N_b phase the uniaxial nematic temperature range should be reduced, possibly by lowering the value of $|B|$. One possible way to circumvent these problems is to consider another system exhibiting N_b phase: a mixture of rod-like and plate-like molecules of comparable size and in comparable amount [39,351].

In order to analyse the influence of external fields on the N_b phase, a magnetic field term is included in the free-energy expansion (7.1). With the field along the Z -axis, a term $-hx$ is added to $\alpha_0(x)$ in Eq. (7.3a). The resulting phase diagram is shown in Fig. 20. Here the biaxiality is partly spontaneous (large) and partially induced. In the dashed area the spontaneous biaxiality is predominant. Although the two biaxial regions are clearly distinguishable, no sharp boundary

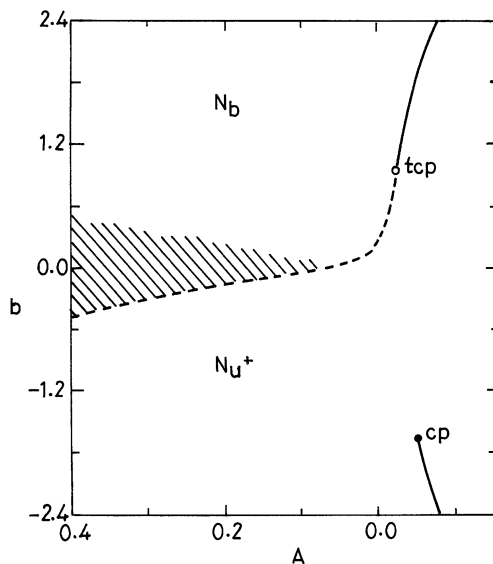


Fig. 20. Phase diagram of Fig. 18 modified by a magnetic field $h = 0.0018$ [64]. In the cross-hatched area spontaneous biaxiality is predominant.

exists between them. The second-order $N_u^+ - N_b$ transition is given by [64]

$$A = \frac{4h}{9x} - \frac{3}{2}Cx^2, \quad (7.7a)$$

$$B = \frac{4h}{9x^2} - \frac{9}{2}E'x^3, \quad (7.7b)$$

$$x \leq x_{\text{tcp}}. \quad (7.7c)$$

At the tricritical point $x = x_{\text{tcp}}$ with

$$\frac{729}{4}CE'x_{\text{tcp}}^8 + 12hE'x_{\text{tcp}}^5 + \frac{16}{3}hCx_{\text{tcp}}^3 - \frac{16}{81}h^2 = 0 \quad (7.8)$$

when $x > x_{\text{tcp}}$, Eqs. (7.7a), (7.7b) and (7.7c) gives the superheating limit of the N_b phase. The isolated critical point corresponds to the equation

$$A = \frac{4}{3}h/x + \frac{3}{2}Cx^2 + \frac{27}{4}E'x^4, \quad (7.9a)$$

$$B = -\frac{4h}{3x^2} - 6Cx - 18E'x^3, \quad (7.9b)$$

$$x = x_{\text{cp}} \quad (7.9c)$$

with x_{cp} given by

$$-h + 9Cx_{\text{cp}}^3 + 81E'x_{\text{cp}}^5 = 0. \quad (7.10)$$

Here $x < x_{\text{cp}}$ corresponds to the supercooling limit of the paranematic phase, whereas $x > x_{\text{cp}}$ to the superheating limit of the nematic phase.

Very recently, Mukherjee [342] has constructed a free-energy expansion to reestablish the above predictions and to calculate the temperature dependence of order parameter and thermodynamic quantities. The accurate measurements of all the order parameters and of the specific heat in the neighbourhood of the biaxial transition temperature are still lacking. Mukherjee's work provides theoretical calculations for these quantities and the phase diagram obtained [342] is slightly different from the phase diagram of earlier works [38,39,51]. In Mukherjee's phase diagram the actual stability limit of all the phases is indicated and the temperature dependence of the order parameters are calculated in all the phases; this is absent in Alben's work.

It is important to mention here that the experimental observations should resolve whether transitions such as $N_u^+ - N_b$, $N_u^- - N_b$, $I - N_b$, etc., actually occur. At the present time it seems that all known uniaxial phases are of type N_u^+ , while only in few materials the N_b has been observed. Thus, for answering the questions related to the uniaxial nematic–biaxial nematic phase transition the available data are yet insufficient and there is a need to generate experimental data on the biaxial nematic phase.

8. Phase transitions involving smectic phases

This section covers the smectic A to smectic C transition and other transitions involving smectics and the N-S_A-S_C multicritical point. Only a brief summary is presented. Transitions involving bilayer smectic phases are given elsewhere [3,390].

8.1. Smectic A–smectic C transition

The S_A–S_C transition is characterized by the onset of a tilt in a one-dimensional layered matrix. A number of experiments [3] have been carried out using a variety of techniques (calorimetric, optical, X-ray scattering, ESR, NMR, neutron scattering, etc.) which confirmed the earlier prediction by Taylor et al. [362] that the S_A–S_C transition is continuous. Many of these experiments, however, probably do not reliably obtain the asymptotic behaviour near the transition. The critical fluctuations for the S_A–S_C transition are those in the molecular tilt. Most of these transitions show mean-field behaviour for the same reason as superconductors do; the intrinsic coherence lengths are long and reduce the fluctuations until very close to T_{AC} . The mean-field value of the critical exponent β characterizing the temperature dependence of the tilt angle in the S_C phase was clearly shown. A second-order S_A–S_C transition in a 3D space has been discussed by Kats and Lebedev [363] using renormalization group technique.

For a given set of layers, to describe the smectic C order, one must specify the magnitude ω of the tilt angle, and also the azimuthal direction of tilt, specified by an angle ϕ (see Fig. 21). The tilt angle ω of the molecules can point in any azimuthal direction; there are thus two independent components: $\omega_x = \omega \cos \phi$ and $\omega_y = \omega \sin \phi$. Thus, due to the azimuthal degeneracy of the tilt angle one can use a complex order parameter $\psi_1 (= \omega \exp(i\phi))$ to describe the transition. If one neglects the coupling to the layers' undulation mode, a remarkable analogy is seen with superfluid helium. An overall change of the phase ϕ does not modify the free energy. This leads to the following possibilities:

The S_C–S_A transition may be continuous. The specific heat should show a singularity [3,382]. Below T_{CA} the tilt angle should obey the law

$$\omega = \text{const } |t|^\beta \quad (8.1)$$

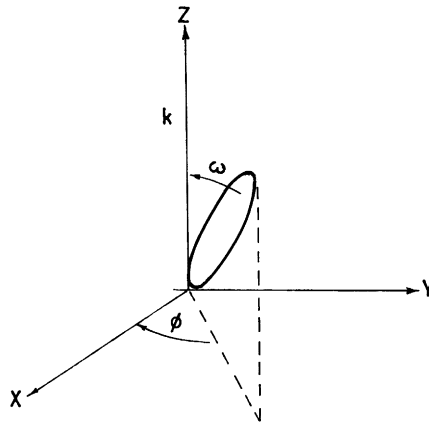


Fig. 21. Smectic C tilt angle: κ is the layer normal, ω the tilt amplitude, ϕ the azimuthal angle.

with $\beta \simeq 0.35$ and $t = (T - T_{CA})/T_{CA}$. Above T_{CA} the application of a magnetic field that is oblique with respect to the optic axis of the smectic phase induces the tilt angle

$$\omega = C_1 \frac{\chi_a H_x H_z}{k_B T_{CA}} t^{-\gamma}, \quad (8.2)$$

where $\gamma \simeq 1.33$ is the susceptibility critical exponent. The predicted tilt is small (about 10^{-2} rad for $t \simeq 10^{-4}$ near room temperature) because the diamagnetic energy $\chi_a H^2$ is very weak as compared to $k_B T_{CA}$. Starting from S_A phase and decreasing T towards T_{CA} , one expects to observe the onset of a strong (depolarized) light scattering due to fluctuations in the tilt angle.

The application of Landau theory to the S_A – S_C transition was first considered by de Gennes [364], who treated the tilt angle as the relevant order parameter. It has two components: the magnitude $|\omega|$ and the azimuthal angle ϕ . This shows an analogy with the superfluid–normal fluid transition. So as usual the free-energy density of S_C phase can be expressed as

$$f_C = A|\omega|^2 + \frac{1}{2}D|\omega|^4 + \frac{1}{3}E|\omega|^6. \quad (8.3)$$

The total free energy involves the order parameter due to the density wave, $|\psi_1|$, and its coupling with the orientational order parameter \mathbf{Q} . It has been shown [365], from an analysis of the specific heat anomaly near the second-order S_A – S_C transition, that the sixth-order term in Eq. (8.3) is unusually important.

Several theories for the S_C phase were developed taking into account the specific features of the molecules. Wulf [366] proposed a steric model which considers, a zig-zag shape for the molecules and assumes that the tilted structure results due to freezing of free rotation around the long axis. It was shown [366] that the steric effects, in particular, the zig-zag gross shape of the smectogenic molecules, may be able to account for the second-order S_A – S_C phase transition. In S_C phase the biaxial order parameters play a primary role and may grow to values of $O(10^{-1})$. McMillan [367] took note of the molecular transverse dipoles which are present in all the smectogenic compounds and developed a model for the S_A – S_C transition in which the molecules rotate freely about their long axes in the S_A phase, leading to the dipolar ordering. Incorporating the dipole–dipole interaction of the permanent molecular dipole moments the theory [367] predicts three orientationally ordered phases; (1) with the physical properties of the S_C phase (tilted director, optically biaxial, second-order S_A – S_C phase transition), (2) a two-dimensional ferroelectric, and (3) a low-temperature ordered phase which is both tilted and ferroelectric. If there are two oppositely oriented net dipoles directed away from the geometric centre of the molecules, the medium will not exhibit ferroelectric properties. The presence of the two dipoles with longitudinal components also favours the tilting of molecules in the layers to minimize the energy of the oriented dipoles. However, NMR and other experiments clearly show that the molecules are practically freely rotating about their long axes in the S_C phase in disagreement with the assumptions of both Wulf and McMillan. Cabib and Benguigui [368] made an attempt to overcome this problem by postulating a special type of molecular structure in which only the longitudinal components of two symmetrically placed outboard dipoles are effective. However, most of the mesogenic compounds do not have such a structure. Based on the argument that many compounds have only one overall dipole moment, Van der Meer and Vertogen [369] proposed that in such cases the tilting optimizes the attractive energy due to dipole-induced dipole interaction. This interaction remains effective even if the molecules rotate freely. Priest [370] developed a model for the nematic, smectic A and

smectic C phases in which the intermolecular interactions are characterized by second-rank tensor quantities and are supposed to produce orientational order of the molecules. The model predicts that free rotation is possible for uniaxial molecules and that the extent of this rotation being hindered depends on the degree of biaxiality in certain intrinsic molecular second-rank tensors. According to the model, the uniaxial molecules can exhibit S_C state. The model predicts a second-order S_A – S_C transition with two independent degrees of freedom having divergent fluctuations. With the decreasing temperature the tilt angle of S_C phase is predicted to grow continuously from zero and to asymptotically saturate at 49.1° . However, the model fails to identify the physical origin of the proposed interactions. The model considered by Matsushita [371] incorporates the excluded volume effects due to the hard-rod features of the molecules which actually favour the S_A phase. If the mesogenic molecules are uniaxial these models do not give rise to a biaxial order parameter in the S_C phase. They describe only a tilted S_A phase rather than the S_C phase with its intrinsically biaxial symmetry. Goossens [372] has shown that none of the above models using attractive interactions are satisfactory. In these molecular models the tilt angle does not appear as a natural order parameter. Only in the Wulf and McMillan models the S_C phase is characterized by new order parameters. But they are unsatisfactory because of the stringent requirement that rotations about the long axes of the molecules should be frozen out. A detailed calculation of the intermolecular interactions between molecules of ellipsoidal shape has been carried out by Goossens [372]. The attractive potential arising from the anisotropic dispersion energy and permanent quadrupole moments has been considered. The mean-field potential depends strongly on the anisotropy of the excluded volume. It has been shown that the relative weights of the three terms proportional to $\langle \cos qz \rangle^2$, $\langle \cos(qz)p_2(\cos \theta) \rangle$ and $\langle \cos qz \rangle \langle \cos qz p_2(\cos \theta) \rangle$ depend on the L/d_0 ratio of the ellipsoidal molecules. Further, from the calculations for a tilted director, about which the orientational order is still considered to be uniaxial, it was shown that the extra mean-field energy contains a term proportional to $\sin^2 \omega$. The angle of tilt is proportional to a new order parameter which goes to zero at a temperature which can be identified with T_{AC} . Very recently, Gießelmann and Zugenmaier [521] have developed a model for the S_A – S_C phase transition which is, in principle, analogous to a ferromagnetic phase transition with spin number $s \rightarrow \infty$. Assuming a bilinear mean-field potential, the macroscopic tilt angle has been calculated by Boltzmann statistics as a thermal average of the molecular tilt. The calculation gives an equation of state for the S_C phase which is self-consistent field equation involving the Langevin function of a reduced tilt and a reduced temperature. An excellent agreement with the experimental results has been obtained.

8.2. The nematic–smectic A–smectic C ($NS_A S_C$) multicritical point

The existence of $NS_A S_C$ multicritical point was shown independently by Sigaud et al. [373] and Johnson et al. [374]. It is the point of intersection of the N – S_A , S_A – S_C and N – S_C phase boundaries in a thermodynamic plane, e.g., in the T – P or T – y (concentration) diagram. All three phase transitions are continuous in the vicinity of it and at the point itself the three phases are indistinguishable [375]. It has been observed in the T – y diagram of binary liquid crystal mixtures [373,374]; for the P – T diagram of a single-component mesogenic material [376]. High-resolution studies have been carried out [3,4] in both T – y and P – T planes and it is now accepted that the topology of the phase diagram in the vicinity of $NS_A S_C$ multicritical point exhibits

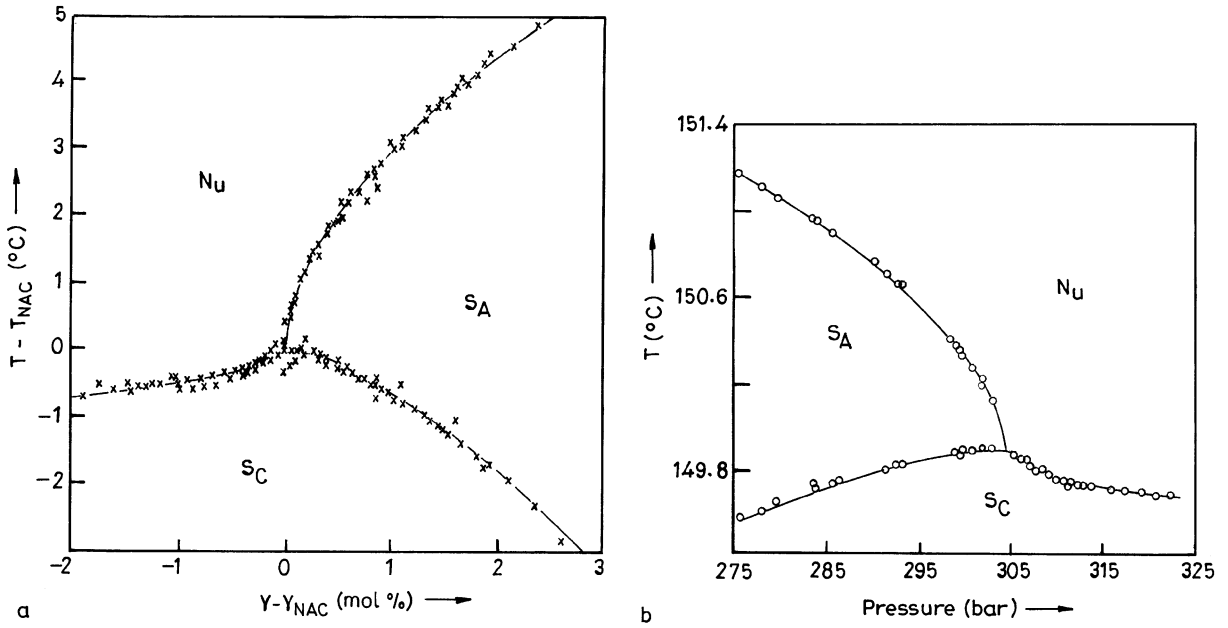


Fig. 22. Topology of phase diagrams in the vicinity of the $NS_A S_C$ multicritical point. (a) The temperature–concentration ($T-y$) data for four binary liquid crystal systems [377]; (b) The pressure–temperature ($P-T$) data for a single component system [376].

universal behaviour (Fig. 22). It has been found that [376] the analysis of the phase boundaries gives identical exponents for both the $T-y$ and $P-T$ diagrams showing the universal behaviour of $NS_A S_C$ point. Further, in the $N-S_A$ case only two components of the mass density wave exhibit large fluctuations near T_C , whereas at the $N-S_C$ transition “skewed” cybotactic groups (i.e. S_C type fluctuations) are concentrated on two rings in the reciprocal space. Thus, the natural order parameter has an infinite number of components. In the description of the $NS_A S_C$ point one should be free to move from one type of fluctuations to the other.

The phase boundaries obey simple power laws

$$T_{NA} - T_{NAC} = A_{NA}|X - X_{NAC}|^{\phi_1} + B(X - X_{NAC}), \quad (8.4a)$$

$$T_{NC} - T_{NAC} = A_{NC}|X - X_{NAC}|^{\phi_2} + B(X - X_{NAC}), \quad (8.4b)$$

$$T_{AC} - T_{NAC} = A_{NC}|X - X_{NAC}|^{\phi_3} + B(X - X_{NAC}). \quad (8.4c)$$

Here X is either the pressure or the concentration. All experimental data are consistent with $\phi_1 = \phi_2 \simeq 0.57 \pm 0.03$ and $\phi_3 \simeq 1.4-1.7$. The $N-S_A$ and $N-S_C$ lines have the same slope parallel to the temperature axis at the $NS_A S_C$ point, whereas that of S_A-S_C line is orthogonal. An alternative fit has been proposed by Anisimov [377] in which $\phi_1 = \phi_3 \simeq 0.67 \pm 0.03$ and $\phi_2 \simeq 0.87 \pm 0.04$. With this fit, all phase boundaries are tangent and parallel to the temperature axis at the $NS_A S_C$ point which can only be fortuitous and approximate.

There have been several theoretical descriptions [365,378–381,230] on the $\text{NS}_\text{A}\text{S}_\text{C}$ point. The framework of the Chen–Lubensky model [379] seems to correspond more closely to the experiment. It is in some way a generalization of de Gennes model [364] of the $\text{N}-\text{S}_\text{A}$ and $\text{N}-\text{S}_\text{C}$ transition. However, the Landau theory is not able to shed any light on the physical origin of the tilt. A simple model based on the quadrupolar nature of the molecules was proposed [131] which made use of the idea that a gradient in the scalar orientational order parameter \bar{P}_2 implies that of the quadrupole density, and hence leads to an order electric polarization of the medium [380]. The resulting dielectric self-energy due to associated order electric polarization is given by

$$f_{\text{oe}} = \frac{1}{2}\alpha^2 \bar{P}_2^2 |\psi_1|^2 (\cos^2 \omega' - \frac{1}{3})^2, \quad (8.5)$$

where α is related to the quadrupole moment of each molecule and the dielectric constant along the Z -axis, ω' the orientation of the principal axis of the quadrupole tensor of the medium with respect to the direction of the gradient in the scalar order parameter \bar{P}_2 . Eq. (8.5) will be minimized when $\cos^2 \omega' = \frac{1}{3}$. This mechanism operates only in case of a layered structure, i.e., in the smectic phase. The total free-energy density can be expressed as

$$f = \frac{1}{2}a(T - T_{\text{AN}})|\psi_1|^2 + \frac{1}{4}D|\psi_1|^4 - \frac{1}{4}C_1|\psi_1|^2 \left(\cos^2 \omega' - \frac{1}{3} \right) + \frac{1}{3}\alpha^2 |\psi_1|^2 \bar{P}_2^2 \left(\cos^2 \omega' - \frac{1}{3} \right)^2. \quad (8.6)$$

The relative stability of the S_C and S_A phases is determined by the ratio $\bar{P}_2(T)\alpha^2/C_1$. As temperature decreases, $\bar{P}_2(T)$ increases. It has been found that the calculated α^2/C versus $(1 - T/T_{\text{NI}})^{1/2}$ phase diagram looks similar to the experimental one close to the $\text{NS}_\text{A}\text{S}_\text{C}$ point.

Grinstein and Toner [383] applied the renormalization group technique and considered the application of a dislocation loop model to the $\text{NS}_\text{A}\text{S}_\text{C}$ multicritical point and made a striking prediction: four, rather than three phases meet at the point where $\text{S}_\text{A}-\text{N}$ and $\text{S}_\text{A}-\text{S}_\text{C}$ phase boundaries cross. A new, biaxial nematic phase was found to intervene between the nematic and smectic C phases. It exhibits the orientational long-range order of the S_C phase, whereas the translational properties are those of the nematic. However, the layer has only short-range positional order. These four phases meet at a decoupled tetracritical point. This prediction is supported by the fluctuation-corrected mean-field theory of Lubensky [357]. The high-resolution specific heat measurements of Wen et al. [384] have shown anomalous variations near the $\text{S}_\text{C}-\text{N}$ transition very close to the $\text{NS}_\text{A}\text{S}_\text{C}$ point. They suggested that these anomalous variations may be due to biaxial fluctuation.

8.3. Transitions involving hexatic smectic phases

With the discovery of hexatic phases a whole class of many transitions related to the hexatic order became possible, for example,

$$\text{S}_{\text{BCry}} \leftrightarrow \text{S}_{\text{Bhex}}; \text{S}_\text{A} \leftrightarrow \text{S}_{\text{Bhex}}; \text{S}_{\text{GCry}} \leftrightarrow \text{S}_\text{F}; \text{Cry} \leftrightarrow \text{S}_\text{I}; \text{S}_\text{F} \leftrightarrow \text{S}_\text{I}; \text{S}_\text{F} \leftrightarrow \text{S}_\text{C}; \text{S}_\text{I} \leftrightarrow \text{S}_\text{C}, \text{ etc.}$$

Since there exists no symmetry difference between S_C , S_F and S_I phases, one can infer that either a first-order phase transition or no transition at all between these phases may occur. It might be

interesting to look for critical points in these systems. Further, it has been observed [3] that the S_{Bhex} phase differs from the S_{A} phase by the existence of a sixfold modulation of the X-ray diffuse scattering ring corresponding to in-plane molecular correlations. If the X-ray beam is incident orthogonal to the smectic planes, the angular dependence of the maximum of the X-ray scattering intensity may be expressed as

$$I(\chi) = I_0 + I_6 \cos 6(\chi - \phi) + \text{higher harmonic} , \quad (8.7)$$

where χ is the angle between the in-plane component of the wave vector transfer q and an arbitrary reference axis X (see figure on p. 547, Ref. [3](b)). For S_{A} phase $I_6 = 0$ but for S_{Bhex} phase $I_6 \neq 0$. Thus, a complex order parameter can be chosen to describe S_{Bhex} phase

$$\psi_6 = I_6 e^{6i\phi} . \quad (8.8)$$

The Landau free-energy expansion exactly similar to that of Eq. (5.13) can be written and it is expected that the $S_{\text{A}}-S_{\text{Bhex}}$ transition may belong to the superfluid helium universality class [385]. Calorimetric measurements on the $S_{\text{A}}-S_{\text{Bhex}}$ transition show a critical exponent of the specific heat $\alpha \simeq 0.6$, which are inconsistent with any available theory but not too far from the tricritical value 0.5 [386]. In two dimensions, the $S_{\text{Bhex}}-S_{\text{Bcry}}$ transition can be second order in a dislocation unbinding picture, whereas in three dimensions, the transitions towards a crystalline phase are of first order. The difference between two- and three-dimensional behaviour can be clearly seen in an a.c. calorimetric study [387]. The existence of a continuous $S_{\text{A}}-S_{\text{Bhex}}$ transition is confirmed by these experiments [387,388]. Pleiner and Brand [389] observed anisotropic anomalies in the damping and velocity of ultrasound near the $S_{\text{A}}-S_{\text{Bhex}}$ transition. Based on generalized hydrodynamics these authors explained this anisotropy by an anisotropic, reversible dynamical coupling between the bond orientational order parameter and elongational flow. It was found that only in-plane elongational flow induces bond orientational order at the transition.

9. Computer simulations of phase transitions in liquid crystals

Computer simulations have played a key role in developing the understanding of phase transitions and critical phenomena in liquid crystals [21,54,147–160,205–208,391–413]. A survey of the existing numerical studies of N–I, N– S_{A} , $S_{\text{A}}-S_{\text{B}}$, $S_{\text{A}}-N_{\text{R}}$ transitions and transitions to the discotic phase is given in this section. The primary issues addressed in these simulation studies and the main results obtained from them are summarized.

The models studied in numerical simulations of mesophase transitions may be classified into two categories called as molecular models and field models. Three broad classes of molecular models used in liquid crystal simulations are Lebwohl–Lasher lattice models, hard particle models and Gay–Berne models. In the molecular models, the description is in terms of the molecules constituting the system and their interactions. The interactions included in these models must describe both translational and orientational orders. In reality, the mesogenic molecules consist of rigid cores and flexible side chains. As a result, it is quite difficult to construct a model that provides a realistic description of the interaction between two such molecules. Even if one could construct a realistic model for the intermolecular interactions, it would be extremely difficult and time-consuming to simulate the properties of liquid crystalline system. Owing to these reasons, the simulations are

usually carried out for much simpler models in which the molecules are assumed to be simple non-spherical rigid objects such as rotational ellipsoids, spherocylinders, parallel plate cylinders, cut spheres, etc. The interaction between two such molecules is also assumed to have a simple form. Most of the simulations carried out for such models assume only a hard-core repulsion between two molecules [391], arising from the excluded volume interactions. A posteriori justification for the study of such models comes from the observation that these models do exhibit some of the phases found in real liquid crystals. The principle of universality provides another justification for such studies which states that the parameters characterizing the critical behaviour near a continuous phase transition do not depend on the microscopic details of the system and are determined by a few factors such as the dimensionality of space and the symmetry of the order parameter. Few attempts [392] have also been made to include in the simulation model the van der Waals interaction and dipolar interactions in an approximate way. The field models provide a coarse-grained description of the system in terms of an order parameter field appropriate for the ordered state under consideration. A model of this kind is defined by a Ginzburg–Landau free-energy expressed as a functional of the order parameter field. In some cases, due to symmetry or other considerations, terms coupling the order parameter to other non-ordering fields may have to be included in the free-energy functional. A typical example is that of de Gennes model [62] for the N–S_A transition. It is important to note that unlike molecular models, a field model is specific only to the transition in which long-range order described by the particular order parameter field sets in and it cannot be used to describe other phase transitions which may be exhibited by the same physical system. The order parameter field appearing in models of this kind are continuous functions of the spatial coordinates. The results obtained from the numerical studies of such models can be compared directly with those obtained from the analytic calculations.

9.1. Lebwohl–Lasher model

The questions which have to be addressed in simulations of N–I transition are concerned with the (i) determination of the minimal characteristics of molecules and their interactions exhibiting nematic order and (ii) estimation of the magnitudes of the discontinuities shown by various thermodynamic functions (e.g. order parameter, density, internal energy and entropy) at the first-order transition in a 3D system. The first model used in the N–I simulation is the Lebwohl–Lasher model [147] which is the lattice version of the MS model of a nematic. It assumes that each site of a simple cubic lattice is occupied by a classical unit vector. The Hamiltonian for the model is defined as

$$H = -J \sum P_2(\hat{e}_i \cdot \hat{e}_j), \quad (9.1)$$

where the sum is over nearest-neighbour pairs of lattice sites and $J > 0$ measures the strength of the nematic coupling. Because the molecules are fixed on the sites of a lattice, translational motion is absent. The Monte Carlo (MC) simulation carried out by Lebwohl and Lasher [147] showed that this model exhibits a strongly first-order N–I transition near $J/k_B T = 0.89$. The order parameter at the transition exhibits a jump from zero to about 0.33 while the transition entropy is very close to $1.09J$. This model has been intensively investigated using MC technique [152,155,393–395]. Further numerical work on similar models of the I–N transition has been pursued by others [154,155]. The accuracy of Lebwohl and Lasher's results were improved by Jensen et al. [154] by

simulating the behaviour of same model on larger lattices. Luckhurst and Romano [155] have carried out simulations of a system in which the molecules are not confined to a lattice. These authors assumed that the molecules interact via a MS type anisotropic potential with Lennard–Jones-type distance dependence. The influence of an external field on the thermodynamic behaviour of the Lebwohl–Lasher model was studied by Luckhurst et al. [155]. The results obtained for the dependence of the order parameter and the internal energy on the value of the external field were in qualitative agreement with the predictions of mean-field theory. Zhang and co-workers [396,397] have simulated a simple cubic lattice with upto 28^3 sites. The free-energy function allows the determination of the limits of stability of the nematic and isotropic phases. Zhang et al. [396] estimated that these temperatures are within 5×10^{-4} reduced temperatures of T_{NI} which is in reasonable agreement with the experimental data.

The Lebwohl and Lasher model has also been extended to model nematics in porous media such as aerogels [403,404]. The Hamiltonian for the extended model is given by

$$H = -J \sum_{\langle ij \rangle} P_2(\hat{e}_i \cdot \hat{e}_j) - D \sum_i P_2(\hat{e}_i \cdot \hat{n}_i), \quad (9.2)$$

where D is the strength of coupling to the random axis which mimics the local pore environment selecting a preferred direction for the nematic order within the pore. Cleaver and co-workers [403] studied this model for $D/J = 1$ using MC techniques on lattices upto 64^3 in size. These authors did not find any evidence for a first-order phase transition and their data are consistent with the absence of nematic long-range order at low temperatures.

9.2. Hard-core models

The first computer simulations of anisotropic hard-core models were carried out by Vieillard-Baron [148] in two dimensions. Frenkel and Mulder [156] carried out a systematic study of the properties of a three-dimensional system of hard ellipsoids of revolution by using MC simulation. These authors studied the behaviour of this system for values of x_0 lying in the range between 3 and $1/3$. The results show a first-order N–I transition with a density change of about 2% at the transition only in the range $x_0 > 2.5$ or $x_0 < 0.4$. The phase diagram obtained is shown in Fig. 23. In addition to the isotropic and nematic phases, they also found orientationally ordered and disordered (plastic) crystalline phases in the high-density region of the phase diagram. An interesting feature of the phase diagram is its approximate symmetry between oblate and prolate ellipsoids. However, the values found by Frenkel and Mulder [156] appear to change for the larger systems studied [405]. Allen and Frenkel [158] have observed for $x_0 = 3$ pretransitional nematic fluctuations in the isotropic phase. A number of authors [157,406,407] have performed numerical simulations of molecular models of two-dimensional nematics. Frenkel and Eppenga [157](b) have carried out simulations to study the thermodynamics of a system of infinitely thin hard needles in two dimensions. They observed at high densities a stable nematic with algebraic decay of orientational correlations. The behaviour of a system of two-dimensional ellipses with aspect ratios 2, 4 and 6 have been simulated by Cuesta and Frenkel [406]. For the aspect ratios 4 and 6, a stable nematic phase with a power-law decay of orientational correlations was found. While the N–I transition in the system with the aspect ratio 6 was found to be continuous, the system with aspect

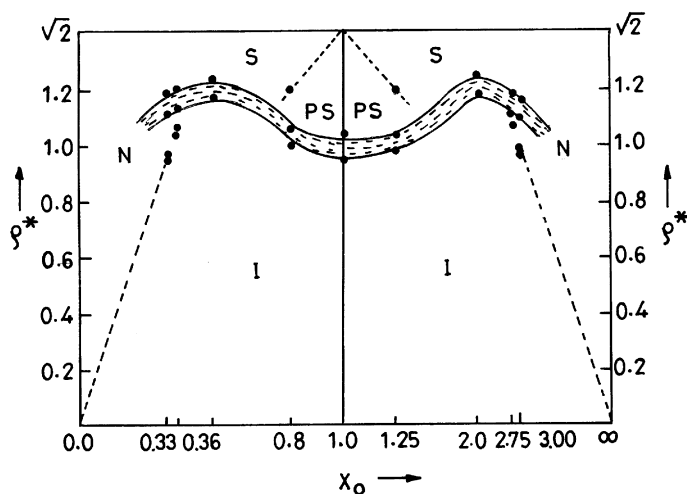


Fig. 23. Phase diagram of a HER system obtained by MC simulation [156](a). The reduced density ρ^* is defined such that the density of regular close packing is equal to $\sqrt{2}$ for all x_0 . The shaded areas indicate two phase coexistence. The phases shown are: I-isotropic, S-orientationally ordered crystal, PS-orientationally disordered (plastic crystal) and N-nematic phase.

ratio 4 was found to undergo a first-order transition. Denham et al. [407] have studied by MC simulation a two-dimensional version of the Lebwohl–Lasher model. The results obtained show a continuous I–N transition with a power-law decay of orientational correlations.

Allen [391] has carried out a rough survey of the phase diagram of a biaxial phase which can be produced if the molecules are no longer modelled as ellipsoids of revolution, but rather spheroids with unequal semi-axes a, b and c . It has been found that the biaxial phase is stable only for a narrow range of values of the semi-axes near the critical value $b/a \simeq \sqrt{10}$. Further, an approximate symmetry is observed under the transformation $(a, b, c) \leftrightarrow (c, ca/b, a)$. The role of topological defects in the three-dimensional I–N transition has been studied by Lammert et al. [408]. These authors considered a system whose Hamiltonian contains, in addition to the microscopic interactions producing nematic ordering, a new term which is related to the extra core energy for the line defects. A phase diagram was obtained in which the I–N transition continues to be second order for large but finite values of the core energy of the defect line. The first-order I–N transition is retained when the core energy is lower than a critical value.

Simple arguments [160,393] suggest that hard-core systems composed of ellipsoids cannot exhibit smectic phases. Therefore, molecules of other shapes have to be considered in the studies of transitions involving smectic phases. Frenkel and co-workers [159,160,156,398] have performed extensive MC and MD simulations to study the properties of a system of hard spherocylinder characterized by the different values of the ratio of L/d_0 . The first simulations were carried out for perfectly aligned systems. The phase diagram is shown in Fig. 24. It was found that a stable smectic phase appears for $L/d_0 > 0.5$. The later work [156,160,398] showed that a system of freely rotating spherocylinders exhibits a smectic phase if length-to-width ratio is higher than 3. The phase diagram obtained by Veerman and Frenkel [398] is shown in Fig. 25. The N–S_A transition for

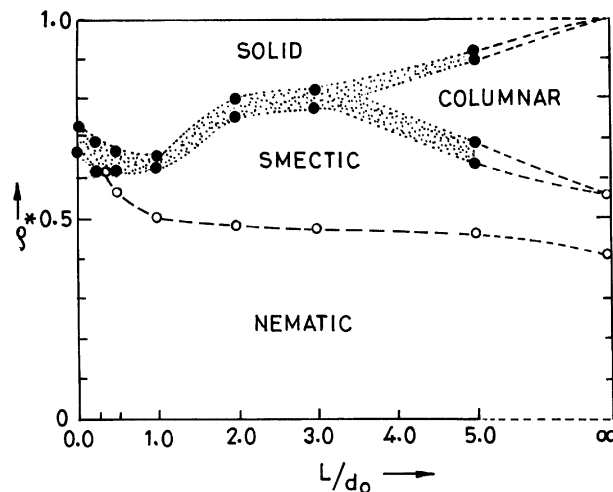


Fig. 24. Phase diagram of a system of hard parallel spherocylinder obtained from MC simulation studies [159].

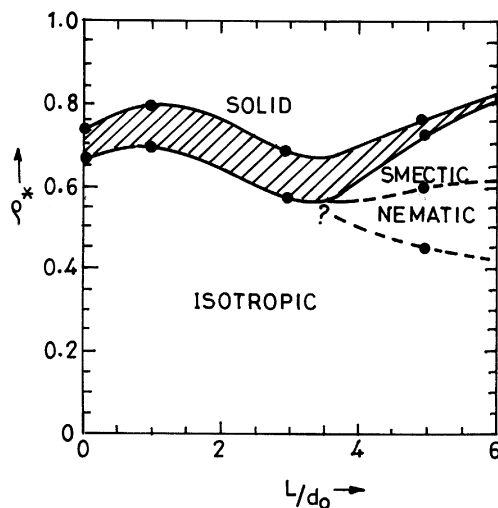


Fig. 25. Phase diagram of a system of freely rotating hard spherocylinders [398](b). The shaded area is the two-phase region separating the densities of the coexisting solid and fluid phases.

$L/d_0 = 5$ appears to be continuous in the simulation. However, due to the accuracy of the results a weakly first-order transition cannot be ruled out. The simulation data could not fully resolve the phase diagram near the point indicated by the question mark (?). In this region, the existence of two triple points is suggested, an isotropic–smectic–solid triple point at L/d_0 slightly higher than 3 and an isotropic–nematic–smectic triple point at a higher values of L/d_0 but less than 5. Dasgupta [409]

carried out a MC simulation of a discretized version of the de Gennes model, for understanding the nature of the N–S_A transition. This model neglects the fluctuation of the magnitude of the smectic order parameter. No sign of a first-order transition was found in these simulations. The observed behaviour is qualitatively consistent with the predictions of finite-size scaling theory for a continuous phase transition. This simulation produces strong evidence for the de Gennes model.

Using an improved version of the frustrated spin gas model [334], Netz and Berker [392] carried out MC simulations and obtained phase diagrams which show the expected nematic re-entrance. With an appropriate choice of the model parameters, the simulations also show the existence of a S_C phase which arises due to a lock-in of molecular permeation and rotation. The onset of the S_C phase is detected by monitoring the tilt angle of the layer relative to the Z-axis. This work suggests a microscopic origin of the S_C phase. Further, the model exhibits some of the modulated smectic A phases (such as A₁, \tilde{A}_1 and A_d phases) and indicates the reason for their occurrence in terms of microscopic properties of the molecules and their interactions.

Frenkel [160] has addressed the question whether hard-core models can exhibit columnar phases by using MC simulations to study the thermodynamic behaviour of a system of cut spheres with excluded volume interactions. A cut or truncated sphere is a sphere cut-off at the top and bottom by two parallel cuts. It is characterized by the ratio L/d_0 where L is the distance between the cuts. Veerman and Frenkel [398] have studied the cases $L/d_0 = 0.1, 0.2$ and 0.3 . For $L/d_0 = 0.1$, the system forms a nematic phase at the reduced density $\rho^* \simeq 0.33$ ($\rho^* = \rho/\rho_{cp}$, where ρ_{cp} is the density for close packing). At $\rho^* \simeq 0.5$ the nematic undergoes a strong first-order transition to a columnar phase with $\rho^* \simeq 0.53$. At the higher densities $\rho^* = 0.8$, a columnar–crystalline transition occurs. At $\rho^* = 0.5$ a transition to a cubatic phase having cubic symmetry but no translational order occurs. The nematic order parameter in this phase is zero. For $L/d_0 = 0.3$ both the nematic and cubatic phases are absent and a direct isotropic fluid–solid transition takes place. Frenkel [160] simulated the thermodynamic behaviour for $L/d_0 = 0.1$ and 0.2 . The system with $L/d_0 = 0.1$ was found to exhibit an I–N transition at the reduced density $\rho^* = 0.335$ and a strongly first-order transition to a columnar phase at $\rho^* = 0.49$. The transition to crystalline phase occurs for $\rho^* > 0.8$. The system with $L/d_0 = 0.2$ did not exhibit any nematic ordering even at higher density of fluid branch. For $\rho^* > 0.58$ strong evidence of cubatic phase was found.

Birgeneau and Litster [410] suggested that the S_B phase found in many liquid crystals may be a realization of a stacked hexatic phases which are characterized by short-positional order and quasi-long-range bond-orientational order. Evidence for the existence of local herring-bone packing of the molecules near the S_A–S_B transition has been seen in the X-ray scattering studies [411]. Jiang et al. [412] have studied the thermodynamic behaviour of a model system defined by the reduced Hamiltonian

$$H/\kappa_B T = \frac{-J_1}{T} \sum_{\langle ij \rangle} \cos(\Psi_i - \Psi_j) - \frac{J_2}{T} \sum_{\langle ij \rangle} \cos(\phi_i - \phi_j) - \frac{J_3}{T} \sum_i \cos(\Psi_i - 3\phi_i) \quad (9.3)$$

in two dimensions by MC simulation. In Eq. (9.3) $\langle ij \rangle$ represents nearest-neighbour pairs of sites on a d -dimensional hyper-cubic lattice, the two angular variables, Ψ_i and ϕ_i , are located at each lattice site i ($-\pi \leq \Psi_i, \phi_i \leq \pi$) and the dimensionless coupling constants J_1 , J_2 and J_3 are all positive. The values of J_1 and J_3 were kept fixed at 1.0 and 2.1, respectively, and the behaviour of

the system as a function of temperature was simulated for different values of J_2 . For $J_2 = 0.3$ results of simulations show two transitions. The transition at the higher temperature exhibits a rounded heat capacity peak in accordance with the expectation for a two-dimensional XY transition. At lower temperature the transition exhibits a sharp heat-capacity peak. For $J_2 = 1.4$ a single transition with a broad heat capacity peak is obtained. For intermediate values of J_2 (e.g. $J_2 = 0.85$ and 0.95) a single continuous transition with a sharp heat capacity anomaly is observed.

9.3. Gay–Berne model

DeMiguel and coworkers [207,399] have performed the most complete simulation of the Gay–Berne (GB) potential (Eq. (4.199)) with its original parametrization. These authors simulated 256 molecules using MD simulation in the canonical (NVT) ensemble. The phase diagram obtained is shown in Fig. 26. The N–I transition is found to be first order. It has not been possible to ascertain whether the S_B phase is crystalline or hexatic because of the small system size considered in the simulation. The biaxial $S_B(t)$ phase is a tilted version of the S_B phase. These authors [207] also studied a purely repulsive GB potential, defined by subtracting the attractive part of the potential at a given relative molecular orientation, and observed the NI transition for fixed T at a slightly higher values of ρ^* . Further, the S_B and $S_B(t)$ phases do not appear and the system remains nematic even at high density. This signifies the role of the attractive part of the potential in stabilizing smectic phases. DeMiguel and co-workers [399] have also studied the rotational

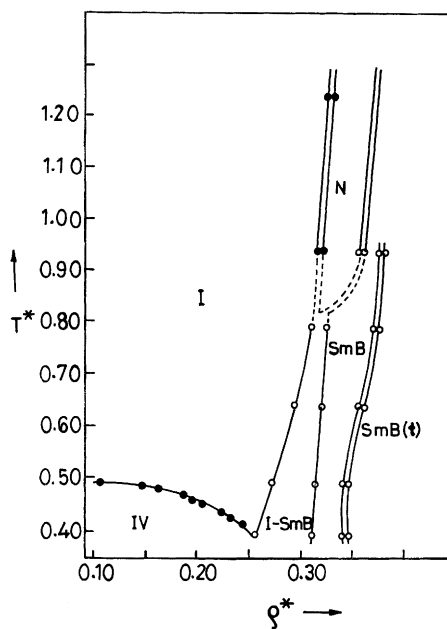


Fig. 26. Phase diagram for the Gay–Berne fluid obtained from the MD simulation [207](b). The dashed lines are extrapolations of the data. $T^* = \kappa_B T / \varepsilon_0$ and $\rho^* = \rho \sigma_0^3$.

and translational dynamics of the GB fluid in the isotropic and nematic phases. Various autocorrelation functions were studied. The behaviour of translational velocity autocorrelation function indicates that in the nematic the molecules diffuse along cylindrical cages whose long axes are parallel to the director.

Luckhurst et al. [208] performed an extensive MD simulation of a reparametrized GB potential in which the side by side configuration is supposed to be more stable relative to the cross and tee configurations: 256 particles were simulated using molecular dynamics. In addition to the isotropic, nematic, smectic B phases, a smectic A phase also appeared. A more systematic parametrization was carried out by Luckhurst and Simmonds [400], who constructed a site–site potential for *p*-terphenyl. This potential is not uniaxial, but the biaxiality was projected out and then the result was mapped onto the GB potential by examining various configurations of molecular pairs. Luckhurst and Simmonds [400] then simulated 256 particles interacting with this new potential and isotropic, nematic and smectic A phases were found. The nematic phase disappears when the reduced density is too low. These authors also compared the results of a number of GB simulations with those of a hard ellipsoid system (see Fig. 27). The good agreement shows that the N–I transition is dominated by the excluded volume effects. On the other hand, the attractive potential dominates the formation of smectic phases as observed in GB system. Thus, it is concluded that hard ellipsoids do not exhibit smectic phases and hard spherocylinder do so only if length to width ratios exceed 4. The reparametrized GB potential has also been used to simulate a system of 256 discotic molecules by Emerson and coworkers [413]. A phase diagram was obtained consisting of isotropic, discotic–nematic and columnar phases.

Tsykalo [402] was the first to modify the Berne Pechukas potential to include chirality, and later Memmer and co-workers [401] modified the GB potential. The total potential consists of the GB

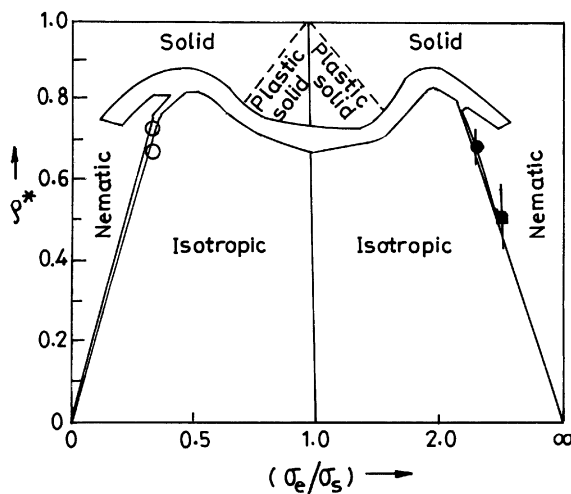


Fig. 27. Phase diagram of hard ellipsoids (Fig. 23) along with the data points resulting from simulations of the GB potential due to Luckhurst and simmonds [400]. Vertical lines indicate the approximate density range where a NI transition was observed at constant density. The symbols ■, ○ and ● correspond to the different values of length to breadth ratios in the GB potential.

term plus an additional chiral interaction:

$$u_{\text{chiral}} = 4g\varepsilon(\hat{r}, \hat{e}_i, \hat{e}_j) \left(\frac{\sigma_0}{r - \sigma(\hat{r}, \hat{e}_i, \hat{e}_j) + \sigma_0} \right)^7 (\hat{e}_i \cdot \hat{e}_j)(\hat{e}_i \times \hat{e}_j \cdot \hat{r}) \quad (9.4)$$

The parameter g measures the strength of the chiral coupling. Memmer and co-workers [401] simulated a system of 256 particles interacting with this new potential. The phase diagram was determined by adjusting the chiral coupling. A cholesteric phase was observed for $0.6 < g < 0.7$, while for $1.0 < g < 1.1$ a phase with geometric structure of blue phase appeared.

10. Phase transitions in liquid crystal polymers (LCPs)

As discussed in Section 1, it is precisely the combination of the polymer-specific properties together with the properties specific to the liquid crystal phase that gives rise to the specifics of liquid crystal polymers (LCPs) and sustains the basic and applied interests in studying them. This unique combination of properties has led to a multitude of new perspectives which are not possible for the conventional materials in the crystalline or amorphous state and opens wide perspectives toward their scientific understanding and technological applications.

The properties of LCPs are far more involved than a simple combination of two areas of science. As a result, the understanding, at the molecular level, about their behaviour is much more worse as compared to the liquid crystal systems. Our main interest in the present section is to pinpoint some of the outstanding problems in LCPs and then to describe, in brief, the salient features of some of the work done. The key issue centres around the questions — to what extent the ordered liquid crystal state influences the kinetics, polymerization, stereochemistry and rheological behaviour of the polymers. What is the effect of the spacer unit, mesogenic unit, polymer backbone, distribution of chain sizes, flexibility of different units, etc., on the mesomorphic behaviour. Some of these questions will be examined with specific reference to the phase transition properties.

In liquid crystal polymers ordering of all three known types can occur: nematic, cholesteric and smectic. However, the identification of the mesophases generated by polymers is usually far more difficult than for low molar mass materials [429,436]. Usually, the nematic phase is readily characterized but smectic phases, especially the highly ordered analogues, are often uncharacterized and simply denoted by S or S_x. Many LCPs, like conventional polymers, exhibit a glass transition temperature (T_g) which is defined as the temperature at which the material becomes less rigid and more rubbery. The main-chain liquid crystal polymers (MCLCPs) consist of chain units that vary in size. The distribution of chain sizes leads to wide ranges of melting to a LC phase and wide ranges over which the polymers clears, to the isotropic liquid. Accordingly, biphasic regions are observed over wide temperatures ranges. In MCLCPs, both nematic and smectic phases have been found. Rigid polymers of different chain size usually exhibit the nematic phase because the packing in a layer like manner becomes inconvenient. However, the polymers with flexible units between the mesogenic moieties can easily arrange in a layer like manner. The flexible spacer tends to play the same role as the terminal chains in low molar mass mesogens, and so the longer the spacer units the greater the smectic tendency. For the generation of a side chain liquid crystal polymers (SCLCPs) the flexible spacer unit, that links the mesogenic unit to the polymer backbone,

normally is essential. In SCLCPs, the increased ordering generated on polymerization means that smectic phases predominate and the nematic phase is only exhibited by polymers with a short spacer and a short terminal chain. The variation in spacer length affects both the freedom of the mesogenic unit from the polymer backbone and overall length of the side-chain unit. When the spacer length is reasonably short, even–odd effects are seen in the clearing points of polymers. The additional ordering on polymerization causes liquid crystal phases to be more ordered than for the monomeric analogue and transition temperatures and clearing points are higher. As a consequence, a monomer unit exhibiting a nematic phase on polymerization may exhibit to a smectic phase of higher clearing point. Similarly, relatively small monomeric units may not form liquid crystal phases but on polymerization nematic phase may result. The most important aspect of a polymer backbone, with reference to liquid crystallinity, is the flexibility. As the flexibility of polymer backbone increases, the T_g is reduced, leading to the formation of a wider mesophase range. However, the clearing points often fall with increased flexibility, but not too significant and not in all cases. Another important aspect regarding the backbone relates to the average size of the backbone overall, i.e., the degree of polymerization (DP) and the polydispersity. Mesophase transitions and T_g tend to rise with increasing degree of polymerization but achieve a constant value when a certain DP is reached. The degree of polymerization may also decide about the kind of mesophase to be observed.

All of the rigid rod polymers are thermally intractable, i.e., they chemically degrade at temperatures below their melting points. As a result these polymers must be solubilized in order to exhibit mesophase formation. At present much of the academic activities focuses on thermotropic semiflexible polymers. In this section, we shall restrict our attention to the nematic state of solutions and melts of polymers of varying architecture, interacting semiflexible polymers and main chain nematic polymers with spacer of varying degree of flexibility [23–27,414,416,417,447].

10.1. Nematic order in polymer solutions

10.1.1. An athermal solution of long rigid rods

Assuming that the liquid crystalline order arises from purely steric causes, Onsager [97] proposed the first molecular theory of nematic ordering for an athermal solution of cylindrical, long, rigid rods of length L and diameter d_0 ($L \gg d_0$). This system can be taken as a model for a system of rigid chain macromolecules with so insignificant flexibility that it cannot be manifested in the length L . The basic steps of Onsager method consists of the following. Consider a system of N rods distributed in volume V such that their concentration is $c = N/V$ and the volume fraction of rods in the solution is $\varphi = \pi c L d_0^2/4$. The free energy of solution of rods is written as

$$A = NT \left[\ln c + \int f(\hat{e}) \ln [4\pi f(\Omega)] d\Omega + \frac{1}{2} c \int f(\hat{e}_1) f(\hat{e}_2) B_2(\Omega_{12}) d\Omega_1 d\Omega_2 \right]. \quad (10.1)$$

The first term is due to the translational motion of rods, the second describes the losses of orientational entropy owing to liquid crystalline order and the third term is the free energy of interaction of the rods in the second virial approximation. When only steric interactions of the rods are present,

$$B_2(\Omega_{12}) = 2L^2 d_0 \sin \Omega_{12}, \quad (10.2)$$

where Ω_{12} is the angle between unit vectors, \hat{e}_1 and \hat{e}_2 . A simple estimate of virial coefficients, giving $B_2 \sim L^2 d_0$ and the third virial coefficient $B_3 \sim L^3 d_0^3 \ln(L/d_0)^8$, shows that the second virial approximation ($cB_2 \gg c^2 B_3$) is valid under the condition $c \ll 1/Ld_0^2$ or $\varphi \ll 1$. In the limit $L \gg d_0$ a liquid crystalline transition in the solution of rods occurs precisely at $\varphi \ll 1$.

For each concentration the free energy of the system must be a minimum; the resulting minima correspond to possible phases. Above a certain concentration such a minimum is obtained by a state in which part of the system is isotropic and the other part nematic (with different concentrations c_i^* and c_a^* , respectively; $c^* = (L/d_0)\varphi$ is a dimensionless concentration). It turns out that for low concentrations of the rods in solution ($c^* \ll 1$), the anisotropic (nematic)–isotropic (liquid) transition is first order. When $c^* < c_i^*$ the solution is isotropic, when $c^* > c_a^*$ it is anisotropic, and when $c_i^* < c < c_a^*$ the solution separates into isotropic and anisotropic phases. The Onsager trial function gives the following results:

$$c_i^* = 3.340, \quad c_a^* = 4.486, \quad \alpha = 18.58, \quad \bar{P}_{2NI} = 0.848. \quad (10.3)$$

Here α is the variational parameter. Using a Gaussian distribution function leads to the following results [414]:

$$c_i^* = 3.45, \quad c_a^* = 5.12, \quad \alpha = 33.4, \quad \bar{P}_{2NI} = 0.91. \quad (10.4)$$

These results show that the coexisting concentrations and nematic order parameter depend critically on the exact form of the distribution function employed in the calculation.

Of course, the integral equation arising upon the exact minimization of the free energy can be solved numerically to a high degree of accuracy. Using this procedure, the following values were obtained [415]:

$$c_i^* = 3.290, \quad c_a^* = 4.191, \quad \bar{P}_{2NI} = 0.7922. \quad (10.5)$$

The results (10.3) and (10.5) show that the use of the variational method leads to a very small error ($\sim 5\%$) in determining the characteristics of the mesophase transitions. The application of the Onsager method has been considered to the case of high concentrations also. The details are given elsewhere [416,417]. Here at this stage we would like to mention that the Onsager method can be generalized for describing solutions of any arbitrary concentration.

Another approach for the above problem was developed by Flory [101]. Using the lattice model of polymer solutions, Flory [101] replaced flexible chains with rigid rods and demonstrated the formation of an ordered phase above a critical volume fraction of rods that depend on the rod aspect ratio ($x_0 = L/d_0$). The liquid crystal phase transition was studied [102,138] using a modified variant of Flory theory and for an athermal solution ($x_0 \gg 1$) the results are

$$c_i^* = 7.89, \quad c_a^* = 11.57, \quad \bar{P}_{2NI} = 0.92. \quad (10.6)$$

Upon comparing the results (10.3) and (10.6) we can conclude that the results of lattice model although qualitatively correct differ quantitatively rather strongly from the exact results (in the limit $x_0 \gg 1$) of Onsager.

10.1.1.1. Polydispersity. In an experimental situation, most often the polymer solutions prove to be polydisperse. That is, they are composed of macromolecules of differing masses. This may have

strong influence on the isotropic–nematic phase transition. The influence of polydispersity on a nematic transition has been studied by using both the Onsager method [415,418–421] and the Flory theory [422–425]. The qualitative results of these studies coincide.

Let us consider a simple bidisperse system composed of particles of equal diameter d_0 but different lengths L_1 and L_2 . Let φ_1 and φ_2 be the volume fractions in the solution of rods of the first and second type, respectively, and let

$$\varphi = \varphi_1 + \varphi_2 \quad \text{and} \quad q = L_2/L_1 > 1.$$

z is the weight fraction of the long rods

$$z = \varphi_2/\varphi$$

and \bar{L}^w is the weight-average length of the rods

$$\bar{L}^w = L_1(1 - z) + zL_2. \quad (10.7)$$

Just like a monodisperse system, the nematic transition occurs at $\varphi \sim d_0/\bar{L}^w$. Using the Onsager method, a computer calculation [415] was performed for $q = 2$ to obtain the phase diagram. Numerical calculations [415,426] have also been performed for two systems with length ratios $q = 2$ and 5. From these results the following features can be noted (see Fig. 28).

- (i) The polydispersity leads to a small decrease in the lower (isotropic) boundary of the separation region and simultaneously to a strong increase in its upper (anisotropic) boundary. The longer rods preferentially go into the anisotropic phase.

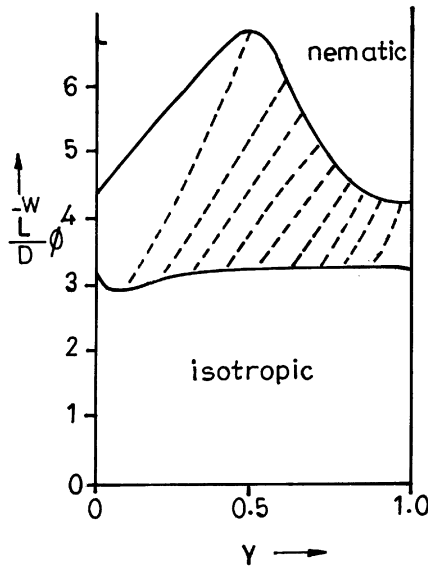


Fig. 28. Volume fraction scaled by the weight-averaged length against mole fraction of the longer rods for a bidisperse mixture of rods ($L_2/L_1 = 2$) [415,426]. The broken lines indicate in which two phases compositions falling in the two-phase region will divide.

- (ii) The relative width of the separation region, i.e., the concentration difference between isotropic and nematic phase may be much larger as compared to the monodisperse case.
- (iii) A weak variation in $\bar{L}^w \phi_i / d$ with mole fraction of the longer rods is found. This implies that the molecular weight dependence of the bifurcation density is a good indication for the onset of phase separation.
- (iv) The mean-order parameter $\bar{P}_{2N}^M = (1 - z)\bar{P}_{2,1} + z\bar{P}_{2,2}$ is found to be appreciably higher ($\simeq 0.92$) than in the monodisperse case ($\simeq 0.79$).
For the length ratio $q = 5$ similar, but more pronounced, results were obtained with two additional features.
- (v) For certain compositions a phase sequence of isotropic–nematic–re-entrant isotropic–re-entrant nematic has been observed as a function of concentration.
- (vi) For some compositions the system shows a biphasic region where the system separates into two different nematic phases, or even a three-phase region in which an isotropic phase coexists with two nematic phases.

10.1.2. Athermal solutions of partially flexible polymers

The real rigid-chain macromolecules always have a certain finite flexibility. The macromolecules may differ with respect to the mechanism of the flexibility of the polymer chain. The simplest kind belongs to the freely linked chain, which amounts to a sequence of hinged rigid rods of length L and diameter d , with $L \gg d$ (Fig. 29a). The orientation of each successive rod, in the equilibrium state, is random and is independent of the orientation of previous ones. Consequently, the mean-square distance between the ends of the chain $\langle R^2 \rangle$ is given by

$$\langle R^2 \rangle_0 = L\ell, \quad \ell \gg L, \quad (10.8)$$

where ℓ is the total contour length of the chain.

In case the polymer chain has any other mechanism of flexibility, for example, if the orientations of adjacent links are correlated, Eq. (10.8) is still satisfied but with a renormalized length L . This renormalized length is known as the effective (Kuhn) segment of the polymer chain.

In a persistent mechanism of flexibility, the flexibility arises from the accumulated effect of small oscillations in the valence angles. A persistent macromolecule can be represented in the form of a homogeneous cylindrical elastic filament of diameter d (Fig. 29b). The elasticity of the filament is such that it can be substantially bent only on scales of the order of L . Most of the macromolecules belong to this class of polymeric objects. On the basis of the relationship between ℓ and L , rigid chain macromolecules can belong to one of the three following fundamental classes: (a) if $L \gg \ell \gg d$ the flexibility of polymer chain can be neglected; this refers to the case of limiting rigid-chain

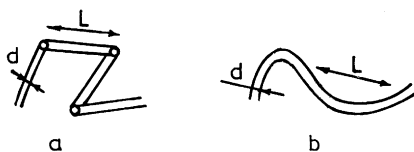


Fig. 29. The simplest mechanism of flexibility (a) Freely linked chain, (b) persistent chain.

macromolecules (or rigid rods); (b) if $\ell \gg L \gg d$, the rigid-chain macromolecule includes many Kuhn segments; this refers to the case of semiflexible macromolecule which stays in the state of a random coil, (c) $\ell \sim L$: in real experiments this kind of macromolecule is found rather often.

Using the continuum approach (the Onsager approach) the transition of an athermal solution of partially flexible polymer chains to an anisotropic phase has been studied [427,430] extensively. In full analogy with the Onsager method, these studies [427,428] led to the following conclusions: For the model shown in Fig. 29, the orientational ordering of the athermal solution has the features of a first-order phase transition and occurs at low concentrations of the polymer in solution. When $\varphi < \varphi_i$, the solution is homogeneous and isotropic; when $\varphi > \varphi_a$ it is homogeneous and anisotropic; and when $\varphi_i < \varphi < \varphi_a$ it separates into isotropic and nematic phases, with $\varphi_i \sim \varphi_a \sim d/L \ll 1$. For an athermal solution of freely linked semiflexible chains [427],

$$c_i^* = 3.25, \quad c_a^* = 4.86, \quad \omega = \frac{c_a^*}{c_i^*} - 1 = 0.5, \quad \bar{P}_{2\text{NI}} = 0.87, \quad \dots \quad (10.9)$$

On comparing the results of (10.9) with the results of (10.3) and (10.5) it is found that hinge linking of the rods in long chains leads only to quite insignificant changes in the characteristics of isotropic–nematic transition. The region of phase separation is somewhat expanded, while the order parameter of the orientationally ordered phase is slightly increased.

For an athermal solution of persistent semiflexible chains the following result was obtained [428]:

$$c_i^* = 10.48, \quad c_a^* = 11.39, \quad \omega = 0.09, \quad \bar{P}_{2\text{NI}} = 0.49. \quad (10.10)$$

It is obvious that for the same d/L the orientational ordering in a solution of persistent chains occurs at sufficiently larger concentrations than in a solution of freely linked macromolecule. The relative concentration jump of the polymer as well as the order parameter at the transition are considerably smaller.

The phase transition in case of a persistent chain was calculated in the Gaussian approximation and the following result was obtained:

$$c_i^* = 7.77, \quad c_a^* = 9.71, \quad \alpha = 12.34, \quad \bar{P}_{2\text{NI}} = 0.759. \quad (10.11)$$

A somewhat better result was obtained [414] by the use of the Onsager trial function

$$c_i^* = 5.41, \quad c_a^* = 6.197, \quad \alpha = 6.502, \quad \bar{P}_{2\text{NI}} = 0.61. \quad (10.12)$$

Solving the non-linear integro-differential equation, Vroege and Odijk [431] obtained the result

$$c_i^* = 5.124, \quad c_a^* = 5.509, \quad \bar{P}_{2\text{NI}} = 0.4617. \quad (10.13)$$

The conformations of the semiflexible macromolecules in the liquid crystalline phase also depend on the mechanism of the flexibility. A very important conformational characteristic is the mean square of the projection \mathbf{R}_z of the segment joining the ends of the chain on the director direction (Z -axis), $\langle \mathbf{R}_z^2 \rangle$,

$$\langle \mathbf{R}_z^2 \rangle = \chi_0 \langle \mathbf{R}^2 \rangle_0. \quad (10.14)$$

Here $\langle \mathbf{R}^2 \rangle_0 = \ell L$ is the mean square of the distance between the ends of the chain in the isotropic phase and χ_0 is the susceptibility of the system to an external orienting field. It has been found that in the nematic solution the freely linked chains are somewhat extended in the direction of the axis of orientational order. However, the magnitude of $\langle \mathbf{R}_z^2 \rangle$ increases by a factor of not more than three as compared to its value in the isotropic phase. In case of persistent flexibility, the behaviour of susceptibility is completely different. For this case the susceptibility χ_0 , and hence $\langle \mathbf{R}_z^2 \rangle$, sharply increases according to an exponential law upon increasing the concentration of the nematic solution. In other words, the macromolecules are strongly stretched out along the director. This effect may be referred to as stiffening of persistent macromolecules in the liquid crystalline state.

The problem of orientational ordering in solutions of polymer chains has been addressed [432,433] assuming other flexibility mechanism also.

10.1.3. Non-athermal polymer solutions

Efforts were made [434,435] to analyse the role of attractive forces of the links in nematic ordering of a solution of rigid-chain polymers. Since the treatment in these studies was based to some degree on the Flory lattice approach, exhaustive solution of the problem could not be obtained. One of the problems which arise in a system of non-athermal polymer solutions involves the fact that the separated anisotropic phase can be very concentrated and the second-virial approximation of Onsager is not applicable.

This problem was first studied consistently by Khokhlov and Semenov [436] by using the continuum approach. The attractive force was approximated as

$$u_{\text{att}} = -\frac{\ell N \varphi}{2d} (u_0 + u_a \bar{P}_2^2). \quad (10.15)$$

Here u_0 and u_a are constants describing, respectively, the isotropic and anisotropic components of the attractive forces. Eq. (10.15) was rewritten as

$$u_{\text{att}} = -\frac{\ell N \varphi \Theta}{d} \left(1 + \frac{u_a}{u_0} \bar{P}_2^2 \right). \quad (10.16)$$

Here $\Theta (= u_0/2)$ is the theta temperature of the polymer solution which is defined as the temperature at which the osmotic second virial coefficient vanishes. In the actual calculation it was assumed that $u_a/u_0 = 0$.

For a solution of persistent macromolecules the phase diagrams were calculated for the liquid crystalline transition in terms of φ and Θ/T for several values of ℓ/d . It was found that in the region of relatively high temperatures, a narrow corridor of phase separation into isotropic and anisotropic phases lying in the dilute solution region exists. Contrary to it, at low temperatures the region of phase separation is very broad such that an isotropic, practically fully dilute phase, and a concentrated, strongly anisotropic phase coexist. These two regimes are separated by the interval between the triple-point temperature T_t and the critical temperature T_c ($T_c > T > T_t$), in which there are two regions of phase separation between isotropic and anisotropic phases, and between two anisotropic phases having differing degrees of anisotropy. The temperatures T_t and T_c substantially exceed the Θ -temperature. The interval between T_c and T_t becomes narrower as the ratio L/d decreases and drops out when $(L/d)_{C_1} = 125$. When $L/d < 125$ there are no critical or

triple points on the diagram, and one can refer only to the crossover temperature T_{cr} between the narrow high-temperature corridor of phase separation and the very broad low-temperature region of separation. With decreasing L/d , the temperature T_{cr} decreases. For $(L/d)_{\text{C}_2} \simeq 50$, one obtains triple and critical points corresponding to an additional phase transition between two isotropic phases. The concentration of one of these phases is extremely low. The influence of attractive interaction on the order parameter of a nematic solution of persistent macromolecules at the transition point was also analysed. It was found that the attractive forces affect the value of \bar{P}_2 very substantially when $T/\Theta \leq 2$.

10.2. Nematic order in polymer melts

The liquid crystalline polymer melts are dense system and often called “thermotropic liquid crystals”. The applications of methods discussed above cannot be applied in a straightforward manner because the large parameter ℓ/d cannot be used. We discuss below the application of mainly three approaches: Onsager, Maier and Saupe and Flory.

10.2.1. Melts of linear homopolymers

In the thermotropic solutions neither the concentration c nor the volume fraction φ can be used as the external parameter. The role of pressure was studied [437] in detail with the results that the influence of normal atmospheric pressure on the mesophase ordering is negligibly small. A substantial increase in the region of stability of the nematic phase can be expected only at high pressure of the order of 10^3 atm. When pressure becomes infinitely large in melt of any particles that are anisodiametric to any degree and have a rigid steric core of interaction, a liquid crystalline phase can be observed.

The phase diagram for a melt of long persistent chain was calculated [437] as a function of T/Θ and L/d for $u_a/u_0 = 0.1$ at atmospheric pressure. From the results the following features are evident: existence of three phases-isotropic and anisotropic melts, and also a gas-like phase (at high temperatures) was observed. The nematic order can occur only if the asymmetry parameter L/d is smaller than the critical value $(L/d)_c \approx 50$. When $(L/d) > (L/d)_c$ the melt in the equilibrium state is always a nematic (at any temperatures). However, the critical value $(L/d)_c$ depends on the mechanism of flexibility of the chain. For example, for freely linked flexibility it was found [437] that $(L/d)_c \approx 7$, while for a melt of rigid rods $(L/d)_c \approx 3.5$. In the formal limit, $L/d \rightarrow 0$ it is seen that the steric interactions are inessential and the mesophase ordering occurs only due to the anisotropy of the attractive forces. The results obtained for $L/d = 0$ are close to those obtained by Rusakov and Shliomis [438] in the limit $L/d \rightarrow 0$. It is worth mentioning that these results are exact to any extent only at small values of L/d , while in the most interesting region $L/d \gg 1$ the steric interactions always dominate and the anisotropy of attractive forces is always a secondary one.

Some additional features were observed [438,439] which do not depend qualitatively on whether steric forces are taken into account or not. These works show that the order parameter at the transition point depends on the length of the persistent macromolecule ℓ . When $\ell \ll L$ the order parameter $\bar{P}_{2\text{NI}} = 0.43$. As ℓ increases the value of $\bar{P}_{2\text{NI}}$ decreases and reaches a minimum value 0.34. When $\ell \leq L$, $\bar{P}_{2\text{NI}}$ slightly increases to the value $\bar{P}_{2\text{NI}} = 0.36$. Regarding the conformations of the macromolecules it was found that in the nematic phase the macromolecules are stretched

along the axis of ordering (the Z -axis). The degree of extension can be characterized by the parameter

$$y = \langle R_z^2 \rangle / \langle R_x^2 \rangle .$$

Here R_x and R_y are the projections of the vector joining the ends of the polymer chain. The magnitude of this parameter at the transition point depends on the length of the macromolecules. When $\ell \ll L$, $y_0 = 3.25$. As ℓ increases, y_0 decreases reaching the minimum value $y_0 = 2.77$, and then increases substantially to the value $y_0 = 14.4$ in the limit of very long persistent chains ($\ell \gg L$). With decreasing temperature of the nematic melt (for $\ell \gg L$) the polymer chains unfold further; the value of y increases exponentially.

10.2.2. Melts of linear copolymers

The nematic ordering in melts of linear copolymers was studied [440–443] by using a generalization of the lattice method [441] for an athermal melt as a function of L/d and α (α is the volume fraction of the flexible component) for the case $\ell_0/d = 1.5$ (ℓ_0 is the length of the effective segment of the flexible region). Two set of transitions, isotropic–nematic and weakly anisotropic–strongly anisotropic, were observed. The second transition between two nematic ends at a critical point with coordinates $(L/d)_c = 10$, $\alpha_c = 0.2$. Upon decreasing the flexibility of the flexible fragments of the chain (i.e., decreasing ratio ℓ_0/d), the region of stability of the weakly anisotropic phase narrows and is shifted towards larger α .

10.2.3. Melts of comb-like polymers

In a mean-field approximation of Meier–Saupe type, the nematic ordering in melts of comb-like polymers with rigid fragments in the side chains was studied [443] by incorporating only the interaction of the mesogenic fragments. It was found that the orientational properties of the system substantially depend on the length L' of the fragment of the main chain between adjacent branches. The length of the spacer linking the mesogenic group with the main chain is assumed to be very small. When $L' > \ell$, the mesophase ordering occurs in a similar manner as the low-molecular-weight system. The order parameter at the transition is $\bar{P}_{2NI} = 0.43$. When the density of the side branches increases (i.e. ℓ/L' increases), the order parameter at the transition decreases monotonically. As the length of flexible fragments L' decreases \bar{P}_{2NI} either increases or decreases very slightly. Thus, the order parameter for the comb-like polymer, always stays smaller than for their linear analogs. This conclusion is in agreement with experimental data [444–446].

When the density of side branches is sufficiently large ($\ell/L' > (\ell/L')_c$) the \bar{P}_{2NI} becomes negative. In this case the main chains are oriented along the director, while conversely the mesogenic groups lie preferentially in the easy plane. The critical value of density for a persistent chain is found to be [443]

$$\left(\frac{\ell}{L'} \right)_c = 18 .$$

Fig. 30 shows the phase diagram [443] of a melt of comb-like macromolecules as a function of ℓ/L' and T . N_+ and N_- correspond to the different conformations of the macromolecule and N_b is a biaxial nematic phase.

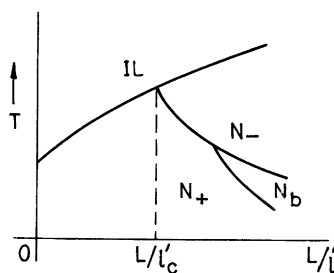


Fig. 30. Phase diagram of a melt of comlike macromolecules in the variables L/l' (effective density of side branches)-temperature [443]. IL -isotropic phase, N_+ -phase of “easy-axis” type, N_- -phase of “easy plane” type, N_b -biaxial phase.

10.3. Nematic polymers with varying degree of flexibility

Within the lattice model, Flory [101,449] initiated the study of transitions in semiflexible polymers and presented a simple heuristic treatment of the properties of concentrated, self-avoiding polymers as a function of their stiffness. He found a first-order transition from a disordered state to an entirely ordered state. Kim and Pincus [449] gave the mean-field treatments of such transitions. Assuming polymers to be non-chiral, a simple model for the interacting semiflexible polymer was developed by Petschek [448]. He used Ursell–Mayer perturbation expansion technique to systemize the calculation of the properties of the system. Using group theoretical arguments, the details of this expansion were analysed and a relationship with field theory could be established. It was found that the isotropic–nematic transition in systems of long, semiflexible polymers can be controlled either by the usual tensor order parameter or by a hidden, vector-like order parameter. This vector like order parameter is expected to control the behaviour only if the fluctuations are important in determining the behaviour of the material near the transition. Which of the two order parameters is the controlling order parameter depends on the details of the configuration and interaction energies of the polymer system. However, the results of the calculations on simple models have no immediate consequences for the behaviour of the realistic polymer system and it is not evident what physical systems, if any, would be expected to have transitions which are controlled by vector-like order parameters.

Wang and Warner [450] modelled main chain liquid crystal polymers as either worms or jointed rods. These authors presented a model, which accounts for molecular parameters such as the lengths of the mesogenic group and the spacer units and the interactions between them, to describe the non-homogenous nematic polymers. The mesogenic groups have been modelled as rods in a quadrupolar potential whereas the spacers were treated exploiting the spheroidal approach. The spacers have been found to have an order differing from the mesogenic units. If the spacer is not very long and thus in effect is inflexible, one end of the spacer can retain to some extent the orientation of the other end, allowing orientational correlation between spacers mediated by the intermediate mesogenic unit. This provides the chain a global rod-like behaviour as the nematic field becomes strong or the temperature low. The influence of the physical linkage and the van der Waals interaction between the rods and the worms was examined. The nematic–isotropic transition and some other properties, such as the orientational order of the two components, i.e. the

mesogenic units and the spacer, and the latent entropy were calculated as functions of the molecular parameters. In accordance with the experimental observations it was found that the reduced transition temperature (the temperature reduced by T_{NI} of MS model for pure rods) decreases significantly when the length of the flexible spacer b increases while the latent entropy increases. The effect of interactions, between mesogenic units u_{aa} , spacer units u_{bb} and mesogenic–spacer units u_{ab} , on the nematic–isotropic transition temperature was studied. The ratio u_{bb}/u_{aa} does not visibly affect the properties of the polymer. The order parameter of the mesogenic unit at the transition does not vary, remaining at about 0.434, while there is a significant variation in that of the flexible spacer.

11. Phase transitions in chiral liquid crystals

11.1. Non-ferroelectric liquid crystals

11.1.1. Transitions in cholesteric (or chiral nematic) liquid crystals

The cholesteric phase is a twisted variant of the nematic phase. Obviously, the interaction energy between the chiral molecules should contain extra terms giving rise to the helical structure of the director in addition to the potential energy of the nematic phase. Goossens [451](a) made the first attempt to develop a statistical model of the cholesteric phase by extending the Maier–Saupe theory to incorporate the chiral nature of the intermolecular coupling. It was shown that the second-order perturbation energy due to the dipole–quadrupole interaction must be included to explain the helicity. This type of interaction can be considerably simplified because of the rapid rotations of the molecules around their long molecular axes. Consequently, in a first approximation, the molecules may be assumed to rotate uncorrelated. Based on the general idea of Goossens, a model was proposed by van der Meer et al. [452–455] which allows the molecules to rotate freely about their long principal axes of inertia. The relevant interaction between two molecules 1 and 2 boils down essentially to

$$u_{ij} = -J_{ij}[(\hat{e}_i \cdot \hat{e}_j) - 3(\hat{e}_i \cdot \hat{r}_{ij})(\hat{e}_j \cdot \hat{r}_{ij})]^2 - K_{ij}[(\hat{e}_i \cdot \hat{e}_j) - 2(\hat{e}_i \cdot \hat{r}_{ij})(\hat{e}_j \cdot \hat{r}_{ij})](\hat{e}_i \times \hat{e}_j \cdot \hat{r}_{ij}). \quad (11.1)$$

The first term in Eq. (11.1) is the Maier–Saupe-induced dipole–dipole interaction and arises due to the anisotropy of the molecules giving rise to the nematic state. The second term is the chiral interaction arising due to the dipole–quadrupole part of the dispersion interaction. The coupling constants J_{ij} and K_{ij} denote the respective interaction strengths and depend on the separation r_{12} .

The model (11.1) was solved by van der Meer et al. [452] in the molecular-field approximation under the further assumption that the system is locally nematic. One of the serious problems with these models [451,452,456] is that in their present form they fail to provide a satisfactory explanation for the fact that in most cholesterics the pitch decreases with rise of temperature. Experimentally, it is observed that the helical wave number q of a cholesteric system varies with temperature. For mesogens exhibiting a cholesteric–smectic phase transition at some temperature T_{cs} , presmectic fluctuations are responsible for the strong temperature dependence of q near T_{cs} . van der Meer et al. [452] made an attempt to consider only the approximately linear temperature dependence of the intrinsic pitch and not the one resulting due to the smectic short-range ordering.

In order to obtain a temperature-dependent q these authors included extra terms

$$-L_{ij}(\hat{e}_i \cdot \hat{e}_j)^4 + M_{ij}(\hat{e}_i \cdot \hat{e}_j)^3 \{(\hat{e}_i \times \hat{e}_j) \cdot \hat{r}_{ij}\}$$

in the interaction potential (11.1). The model was solved and it was found that the temperature dependence of the helical wave number q can be determined by the ratio of the order parameters $\bar{P}_4/\bar{P}_2 (=x)$,

$$q = \frac{1}{r} \left[\frac{(7K - 3M) - 4Mx^2}{(14J + 12L) + 16Lx^2} \right]. \quad (11.2)$$

In fact, \bar{P}_2 and \bar{P}_4 depend on q , i.e., Eq. (11.2) is an implicit equation for $q(T)$. Thus, it was found that the magnitude of the reciprocal pitch varies nearly linearly with temperature in agreement with the experiment.

Scholte and Vertogen [458] proposed a simplified version of the model (11.1) and solved it analytically in the mean-field approximation. These authors considered the model (11.1) with one modification. The vector \bar{e} is no longer a unit vector but requires only to satisfy the so-called spherical constraints

$$\sum_{i=1}^N e_i^2 = N. \quad (11.3)$$

As pointed out by Vertogen and van der Meer [456] this modification boils down, with regards to the thermodynamics, to a weakening of the constraint $e_i^2 = 1$ to the constraints $\langle e_i^2 \rangle = 1$, the thermodynamic expectation value of its length squared must be one. The solution gives two independent order parameters, R and S defined by

$$\langle a_x^2 \rangle = \frac{1}{3}(1 - 2S), \quad (11.4)$$

$$\langle a_y^2 \rangle = \frac{1}{3}(1 + S - R), \quad (11.5)$$

$$\langle a_z^2 \rangle = \frac{1}{3}(1 + S + R). \quad (11.6)$$

The excess free energy per particle reads

$$\beta\Delta A = \frac{1}{9}\beta J(3S^2 + A(q)R^2) - \frac{3S}{1-2S} + \frac{2}{3}\beta JS - \frac{1}{2}\ln(1-2S) - \frac{1}{2}\ln[(1+S)^2 - R^2]. \quad (11.7)$$

Here the helix wave number q is determined by the relation $\partial A(q)/\partial q = 0$. It is clear that the description of the cholesteric state must be based upon more than one order parameter. In Scholte and Vertogen's (SV) model two order parameters appear. In case of large values of the pitch only one order parameter suffices, because the deviation of local uniaxiality is of the order of $(qr)^2$. In the present case this deviation is given by

$$\langle a_x^2 \rangle - \langle a_y^2 \rangle = 0.222(qr)^2. \quad (11.8)$$

Thus, the assumption of van der Meer et al. [452] regarding local uniaxiality is fully justified if the deviation of uniaxial symmetry is of the order of 10^{-5} and consequently negligible. Further, it is important to mention that the SV model gives rise to a pitch, which does not influence the jump on the nematic order parameter upto the order $(qr)^2$ and does not depend on temperature.

Evans [459] addressed the question whether the short-range repulsive interactions associated with a chiral molecular backbone can also achieve macroscopically chiral fluids and what are the typical pitches resulting from the hard-body models. The chiral body was represented by a hard convex twisted ellipsoidal core, with and without an encircling isotropic square well. A stability analysis, within the framework of a density functional theory, was employed to calculate the wavelength of the pitch at the isotropic–chiral nematic transition. The transition densities were taken from the work of Tjijto-Margo and Evans [173] and the chiral pitch was derived by the minimization of the bifurcation density with respect to the chiral wave vector. A general expression for the chiral pitch was derived for hard and soft bodies,

$$p = \frac{2\pi}{3} \frac{\langle C(1,2)r^2 P_2(\hat{e}_1 \cdot \hat{e}_2) \rangle}{\langle C(1,2)\hat{r} \cdot \hat{e}_y \hat{e}_2 \cdot \hat{e}_z \hat{e}_2 \cdot \hat{e}_x \rangle}. \quad (11.9)$$

The sign of p determines the sense of the rotation (left- or right-hand polarization). The chiral pitch was expressed in terms of a ratio of moments of the direct correlation function and this ratio was evaluated within the Person–Lee [102–110] framework for the direct correlation function to give

$$p = \frac{8\pi}{15} \frac{\int d\Omega_1 d\Omega_2 J(1,2) R^2 P_2(\hat{e}_1 \cdot \hat{e}_2)}{\int d\Omega_1 d\Omega_2 J(1,2) \hat{R} \cdot \hat{e}_y \hat{e}_2 \cdot \hat{e}_z \hat{e}_2 \cdot \hat{e}_x}, \quad (11.10)$$

where $J(1,2)$ is the Jacobian and R is the center-to-center vector on the excluded volume surface of the full size bodies. In the present model, the chiral pitch was found to be density and temperature independent with values in the visible region of the spectrum. This finding is an artefact of the Parson–Lee model. It is expected that the long range potential softness may account for the increase of the pitch with decreasing temperature. The role of the critical fluctuations in the vicinity of a structural transition point has also been investigated [457].

11.1.2. Blue phases

Blue phases (BPs) are mesophases which occur in a narrow temperature range just below the clearing point, usually between the isotropic liquid phase and cholesterics of sufficiently short pitches [43,44,460]. They occur in a system of chiral molecules, though not all chiral compounds exhibit blue phases. In several chiral compounds up to three blue phases are thermodynamically stable. The two lower temperature phases, blue phase I (BPI) and blue phase II (BP II), possess cubic symmetry, while the highest temperature phase, blue phase III (BP III), appears to be amorphous. As early as 1906, Lehmann [461] detected the blue phase as a stable, optically isotropic modification not identical to the cholesteric phase. The very first observation of this phase was described by Reinitzer [1] in his famous letter to Lehmann [2]. He reported a blue violet light reflection just below the clearing point of cholesteryl benzoate which was actually caused by the BPI (see Ref. [462, p. 172]).

Blue phases are prominent in cholesteric systems of sufficiently small pitches. The BP no longer exists when the cholesteric pitch exceeds a critical value, P_c . For comparison of different systems the pitch is measured at the cholesteric blue phase transition temperature. These results show [43,44] the important influence of the pitch on the stability of blue phases. It can be seen from Table 11 that the critical pitches, P_c , do not adopt a universal value but depend on both the molecular structure and the composition of the system. Furthermore, even the ratio P_m/P_c depends on the structure of the mixed systems.

Table 11

Critical pitches for monomorphic (P_c) and dimorphic blue phases (P_m) in cholesteric mixed systems at $T_{C1/BP}$

System	P_c/nm	P_m/nm	P_m/P_c
Cholesteric/nematic mixtures			
CN/PCPB	383	333	0.87
CN/CCH7	439	410	0.93
CN/PCH7	410	356	0.87
CN/CB7	398	336	0.84
CC/CCH7	407	330	0.81
CC/PCH7	395	345	0.87
CC/CB7	350	271	0.77
CV/80BE	415	340	0.82
CM/80BE	390	265	0.68
CB/80BE	355	270	0.76
Compensated mixtures			
CN/CBAC	647	443	0.53
	573	556	0.97
CN/CC	540	472	0.87
	490	370	0.76
Induced BPs			
CA/PCPB	310	305	0.98
	373	309	0.83
CEEC/EBBA	610	462	0.76
	490	413	0.84

Abbreviations: CA cholesteryl acetate; CV cholesteryl valerate; CC cholesteryl chloride; CN cholesteryl nonanoate; CM cholesteryl myristate; CB cholesteryl benzoate; CEEC cholesteryl ethoxyethoxyethycarbonate; EBBA 4-ethoxy benzylidene-4'-n-butylaniline; CBAC 4- cyanobenzylidene-4'-aminocinnamic acid opt.act. amylester; PCPB p- pentyl-phenyl -2 -chloro-4-(p-n-pentylbenzoyloxy)- benzoate; 80BE 4-n- octyloxyphenyl -4'-n- octyloxybenzoate.

Bergmann and Stegemeyer [463] showed the existence of two polymorphic forms BP I and BP II by DSC thermograph as well as by selective reflection and optical rotation measurements. The possibility of the existence of a third BP was first mentioned in 1980 [462]. A grey texture was detected between the isotropic liquid and the BP II platelet texture by polarizing microscopy. Such a texture was also observed by Marcus [464] and Meiboom and Sammond [465] and they called it a 'blue fog' or a 'fog phase'. Collings [466] provided convincing evidence for the stability of a BP III by optical rotatory dispersion measurements. Keiman et al. [467] resolved directly the BP II/BP III as well as the BP II/isotropic transition by high-precision specific heat measurements. From these results it became quite obvious that the fog phase is thermodynamically stable, and it has been called BP III while the CI–BP I, BPI–BP II and BP–III transitions are known to be first order, the BP III–IL transition is weakly first order.

In general, blue phases occur between the cholesteric and the isotropic liquid state. In polymorphic mesogens the phase sequence

$$S_A \rightarrow CI \rightarrow BP \rightarrow IL$$

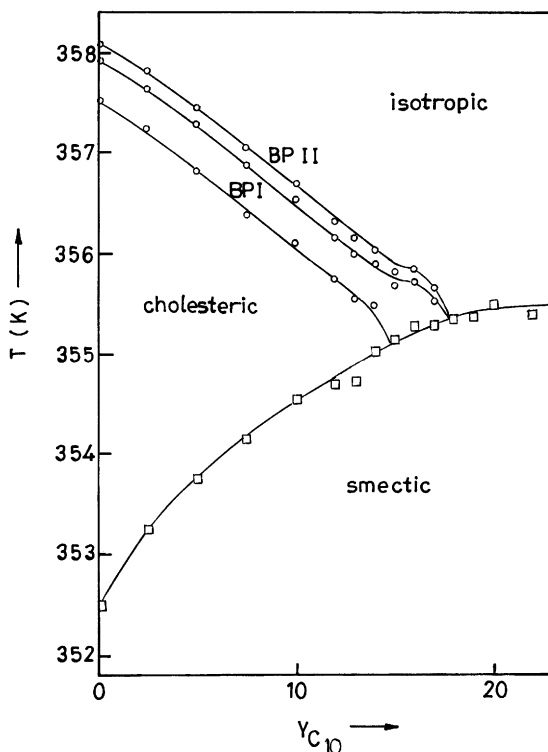


Fig. 31. Partial phase diagram of CM/C₁₀ system [468]. A direct transition from the S_A phase to BP I is observed.

has been observed with increasing temperature whenever the cholesteric pitch is small enough. The blue phase stability of cholesteryl myristate (CM) on admixing 4, 4'-di-*n*-decylazoxybenzene (C₁₀), which exhibits only S_A phase, is shown [468] in Fig. 31. It can be seen that on increasing the C₁₀ concentration the cholesteric range decreases finally to zero at 15 mol% whereas the BP ranges remain nearly constant. In mixture of 15–18 mol% C₁₀ a direct S_A-BP I transition occurs. These results show that the occurrence of a blue phase does not require the simultaneous existence of a cholesteric phase. Fig. 32 shows the variation of blue phase polymorphism with pitch. It is observed [466] that the BP III exists only in systems with very short pitches. The BP III span is extremely small (≤ 0.05 K). It decreases with increasing pitch and becomes zero at the so-called dimorphic pitch, P_x . The voltage temperature phase diagrams of mixture of the polar compound 4-hexyloxy-4'-cyanobiphenyl, M18, and its chiral 2-methylbutyl derivative, CB 115, have been investigated [43] in the range of 47–57 mol% CB 15. As can be seen, besides the well-known cholesteric nematic transition, a BP I \rightarrow Cl phase transition is indeed induced by the field. Also a field-induced BP II-Cl transition in all CB 15/M18 mixture has been found. In this case the magnitude of the cholesteric pitch does not play an important role during the field-induced phase transition. It is obvious from Fig. 33 that the coexistence line for the BP I \rightarrow Cl transition is inclined toward the ordinate whereas it runs parallel to the abscissa in case of the BP II \rightarrow Cl transition, i.e. the critical field strength for BP II \rightarrow Cl is independent of temperature.

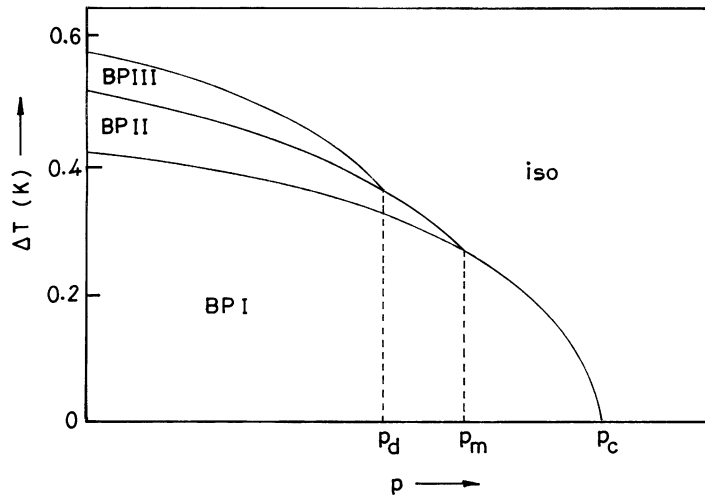


Fig. 32. Schematic phase diagram showing the variation of blue phase polymorphism.

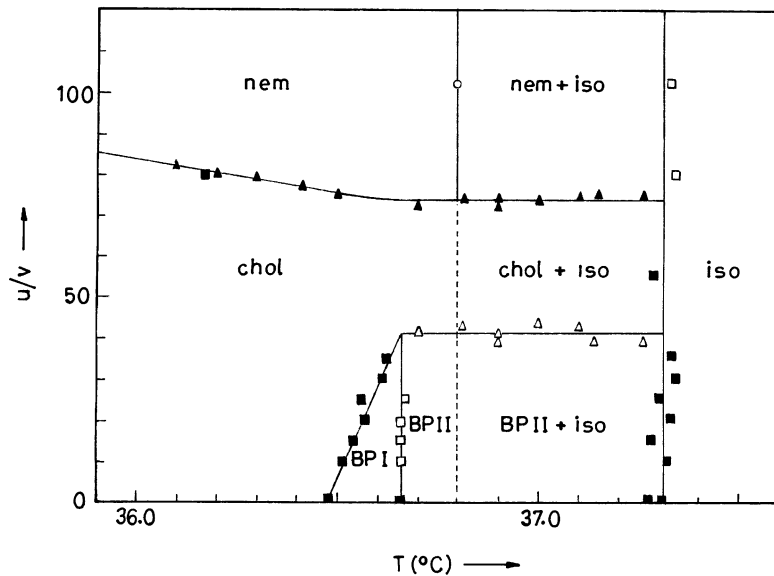


Fig. 33. Phase diagram showing voltage against temperature for a M18/CB 15 mixture (47 mol% CB 15).

Two different classes of theory have been applied to describe the blue phase structures [43,44,460,469], the Landau theory, and the defect theory. A detailed comparison of both the theories is given elsewhere [469]. Based on the common theme of a phenomenological free energy, two groups of workers have considered the application of Landau theory to blue phases from

different points of view. The first approach [470–478] uses a Landau free energy constructed from the most general tensorial order parameter for a nematic. The second approach due to Meiboom and co-workers [479–482] uses a Frank free energy for a chiral nematic and constructs blue phases from regular arrays of line defects (disclinations). The first approach works well when the gradient terms in Landau energy dominate, which is true when the molecular chirality is strong. The second approach is appropriate when the chirality is low. In this limit, the non-gradient (bulk) terms in the Landau energy are dominant.

The Landau free energy density expansion in powers of \mathbf{Q} and its gradients can be expressed as [44,460]

$$f = f_{\text{bulk}} + f_{\text{grad}} \quad (11.11a)$$

$$= A \text{Tr}(\mathbf{Q}^2) - \sqrt{6}B \text{Tr}(\mathbf{Q}^3) + C[\text{Tr}(\mathbf{Q}^2)]^2 + \frac{1}{4}K_1[(\nabla \times \mathbf{Q})_{ij} + 2q Q_{ij}]^2 + \frac{1}{4}K_0[(\nabla \cdot \mathbf{Q})_i]^2. \quad (11.11b)$$

Here the notation of Wright and Mermin [44] has been used in labelling the phenomenological coupling constants. Since the bulk and gradient free energies favour different structures, the minimization problem has not been solved. It is convenient to rescale the variables appearing in Eq. (11.11) to treat the system in terms of small numbers of important dimensionless parameters. The dimensionless free-energy density f^* , effective temperature T , order parameter Q^* , and length scale r' are defined as [478]

$$f^* = \left(\frac{C^3}{B^4}\right)f, \quad \tau = \left(\frac{C}{B^2}\right)A, \quad Q^* = \left(\frac{C}{B}\right)Q, \quad r' = 2qr. \quad (11.12)$$

This scaling is singular in the limits $B \rightarrow 0$ and $q \rightarrow 0$. It is, therefore, not suitable for describing the cases in which the exact free-energy minima are known. Except for these limits, however, the dimensionless variables do provide the natural scales of energy density, temperature, and length for a discussion of the blue phases. The dimensionless free-energy density now reads

$$f^* = f_{\text{bulk}}^* + f_{\text{grad}}^* \quad (11.13a)$$

$$= \tau \text{Tr}(\mathbf{Q}^{*2}) - \sqrt{6} \text{Tr}(\mathbf{Q}^{*3}) + [\text{Tr}(\mathbf{Q}^{*2})]^2 + \kappa^2\{[(\nabla \times \mathbf{Q}^*)_{ij} + Q_{ij}^*]^2 + \eta[(\nabla \cdot \mathbf{Q}^*)_i]^2\}. \quad (11.13b)$$

Here κ is the positive dimensionless chirality parameter

$$\kappa = q\left(\frac{CK_1}{B^2}\right)^{1/2} = q\xi = 2\pi\xi/P \quad (11.14a)$$

and

$$\eta = K_0/K_1. \quad (11.14b)$$

The rescaling shows that the strength of the chirality parameter κ determines whether the bulk (small κ) or the gradient (large κ) terms will dominate the free energy. The high-chirality behaviour can be described by Hornreich and Shtrikman [470–478] model in which the blue phase structures

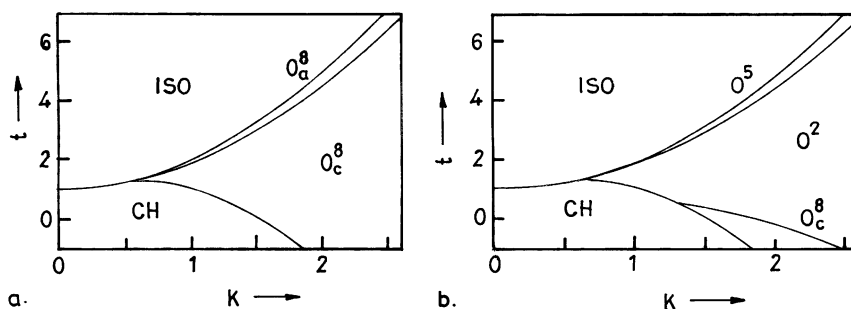


Fig. 34. Theoretical phase diagrams [478] with (a) two blue phases and (b) three blue phases. κ ($= 2\pi\xi/p$) is the chirality parameter and the reduced temperature is given as $t = (T - T^*)/(T_C - T^*)$ with T_C the clearing temperature and T^* the Landau temperature which occurs $\xi \rightarrow \infty$.

are viewed as expansions about the relatively simple blue phase order parameters derived in the limit of infinite chirality. The low chirality behaviour is given by the model proposed by Meiboom et al. [479] and subsequently developed by Meiboom and co-workers [480–482]. This model is characterized as a low-chirality theory, with the proviso that “low” means low enough for the helical phase to be only weakly biaxial. A detailed description and the findings of these models are summarized well by Wright and Mermin [44]. Typical theoretical BP phase diagrams as predicted by the works of Grebel et al. [478](b) are given in Fig. 34. The thermodynamic boundaries between the isotropic and cholesteric phases and the BPs are given as a function of chirality parameter. As found experimentally, all boundaries correspond to the first-order phase transition. None of the two phase diagrams include a phase with BP III properties of lacking long-range periodic order. These phase diagrams show a change of blue phase monomorphism to dimorphism and an increase of the BP temperature ranges on increasing the chirality. Fig. 34(b) predicts the occurrence of a third blue phase at very high chirality $\kappa > 1.3$. The topology of the theoretical phase diagrams is very sensitive to parameter variation and depends on the number of higher harmonic taken into account in the theoretical treatment [478]. Since the free-energy differences between the three blue phases are extremely small, a universal phase diagram is not expected from a theoretical point of view. Further, the use of only two characteristic parameters ξ and T^* also does not seem to allow for a universality of the temperature versus P^{-1} plot because the wide variety of systems with different molecular structure cannot be taken into account in this way.

It was observed that in low to moderate chirality systems, there occurs a first-order phase transition between the isotropic phase and BP III in chiral liquid crystals. However, recent experiments [483] have shown that high chirality systems exhibit no transition. Lubensky and Stark [483] introduced a scalar order parameter $\langle\psi_2\rangle = \langle(\nabla \times \mathbf{Q}) \cdot \mathbf{Q}\rangle$ to describe both the phases and developed a Landau–Ginzburg–Wilson Hamiltonian in ψ_2 and \mathbf{Q} . It has been predicted that the IL–BP III transition belongs to the same universality class (Ising) as the liquid–gas transition.

11.2. Transitions involving ferroelectric liquid crystals

The ferroelectricity in smectic phases requires that the molecules are chiral. The questions related to the concept of chirality, and its influences on the tilted smectic phases are being investigated

[29,484] actively at present. However, little is known about the basic thermodynamic functions of the S_C^* phase and $S_C^*-S_A^*$ phase transition, respectively. A chiral smectic phase is composed of optically active molecules and the optical activity arises as a result of molecular asymmetry. When the S_C phase is composed of optically active molecules, a macroscopic helical arrangement of the molecules is formed. The helix occurs as a result of a precession of the molecular tilt about an axis perpendicular to the layer planes as shown in Fig. 7b. When the S_C^* phase is cooled from the S_A^* or cholesteric or isotropic phase, the spontaneous polarization initially rises very rapidly but thereafter more slowly. In case of second-order phase transition, the spontaneous polarization is coupled to the change in tilt angle which occurs on cooling the mesophase. The tilt angle varies as

$$\theta_T = \theta_0(T_{AC} - T)^\alpha \quad (11.15)$$

where θ_T is the tilt angle at the temperature T , θ_0 is a constant, and the exponent α theoretically is equal to 0.5. The spontaneous polarization varies in a similar way as

$$P_s = P_0(T_{AC} - T)^\beta. \quad (11.16)$$

Here again theoretically the exponent $\beta \simeq 0.5$.

When some of the mesogenic molecules are made to be chiral, the centre of symmetry and mirror planes are lost and only the C_2 -axis remains (see Fig. 35). As a result, an imbalance arises with respect to the molecular dipoles along the C_2 -axis [484]. The time-dependent alignment of the dipoles along the C_2 -axis causes the spontaneous polarization (P_s) to develop along this direction and parallel to the layer planes. Since each layer essentially has a spontaneous polarization and the layers are stacked on top of each other in a helical arrangement, the layer polarizations consequently are averaged out to zero and the phase is described as helical [485]. However, if the helix is unwound, then the layer polarizations point in the same direction and the phase becomes ferroelectric. From symmetry arguments it has been shown that the spontaneous polarization can point in one of the two directions along the polar C_2 -axis leading to two possible polarization directions, $P_s(+)$ and $P_s(-)$ associated with it (see Fig. 36) [486,487]. The magnitude of P_s is mainly dependent on the tilt angle (θ) of the phase [487], the size of the dipole at the chiral centre and the degree of freedom that the chiral centre has to rotate about the long molecular axis.

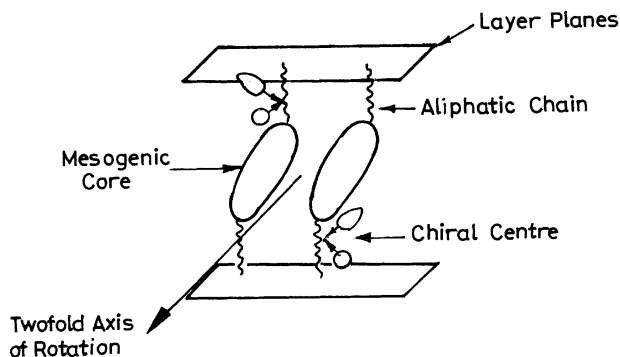


Fig. 35. The symmetry in the chiral smectic C^* phase.

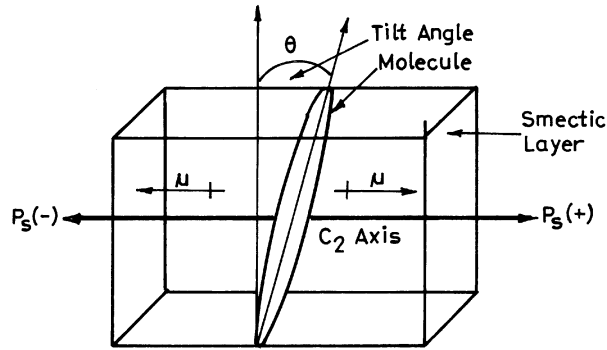


Fig. 36. Polarization direction in the smectic C* phase.

The molecular theory of chiral smectic phases can be constructed by extending those of achiral counterpart by incorporating the additional interaction term arising from the chiral nature of the molecules [484–492]. For the S_C^* phase, van der Meer and Vertogen [489] used a chiral interaction term of the type

$$u_{\text{chiral}} = -u_1(\hat{e}_i \cdot \hat{e}_j)(\hat{e}_i \times \hat{e}_j \cdot \hat{r}_{ij}) - u_3(\hat{e}_i \cdot \hat{r}_{ij})(\hat{e}_j \cdot \hat{r}_{ij})(\hat{e}_i \times \hat{e}_j \cdot \hat{r}_{ij}). \quad (11.17)$$

Using the dipole-induced dipole model of the S_C phase, these authors [489] calculated the equilibrium pitch of the structure from the minimization of the total free energy. In the S_C^* phase the pitch increases as the temperature is increased, attaining a maximum value within a few degrees of T_{C^*A} and then rapidly decreases to a small value at the transition temperature. Thus, the direct influence of the temperature variation of the tilt angle θ on the pitch can be observed only at temperatures slightly away from the T_{C^*A} . Assuming that the chiral dipolar molecules have a banana shape, Osipov and Pikin [490] have developed a model to study the temperature variation of pitch near T_{C^*A} . They considered that the ferroelectricity in S_C^* phase is induced due to chirality and molecular shape asymmetry and calculated the flexoelectric part of the polarization arising from the bend deformation which is present in a helical arrangement of the tilted molecules. It is supposed that the steric interactions of the banana-shaped molecules produce a strong temperature variation of the pitch near T_{C^*A} through the flexoelectric coefficient. Based on the idea that the biaxility of the layers which resist twisting goes to zero near T_{C^*A} , Goossens [491] made an attempt to explain the decrease of pitch close to T_{C^*A} .

Within the framework of phenomenological Landau theory considerable efforts have been made [29,69,493–500] to describe the transitions involving S_C^* phase and the temperature variation of pitch, polarization, tilt angle and dielectric susceptibility. Nakagawa [492] has related the Landau coefficient with the molecular parameters. Based on the generalized Landau model, the expression for the excess free-energy density in the S_C^* phase can be written as [29,493–500]

$$f_c^* = \frac{1}{2}A\theta^2 + \frac{1}{4}C\theta^4 + \frac{1}{6}D\theta^6 + \frac{1}{2\chi_0}P^2 + \frac{1}{4}\eta P^4 - \zeta P\theta - \frac{1}{2}dP^2\theta^2 - A_2q\theta^2 - A_4q\theta^4 + \frac{1}{2}K_{33}q^2\theta^2 - \mu qP\theta. \quad (11.18)$$

Eq. (11.18) has 11 phenomenological coefficients. The tilt angle θ plays the role of the primary order parameter for the $S_C^* - S_A$ transition. The first three terms correspond to the usual Landau coefficients for the $S_A - S_C$ transition. The polarization P can be considered as another order parameter. The contribution of the polarization terms to the total free energy is much smaller as compared to the θ dependent terms. The remaining terms arise due to the chirality of the system. A_2 is the Lifshitz term giving the helical structure. The higher order Lifshitz term A_4 has been included to account for the increase in pitch with temperature deep in the S_C^* phase. K_{33} is the bend elastic constant [37], χ_0 the dielectric susceptibility, μ the flexoelectric and ζ the piezoelectric coupling constant. The coupling between the transverse quadrupole moment and the tilt angle has been accounted by the biquadratic term with coefficient d whereas the η dependent term has been added for stability. The thermodynamic properties of the system can be derived by minimizing Eq. (11.18) with respect to θ , P and q . Close to T_{C^*A} , the ζ term is very important whereas θ is very small. At lower temperatures where θ assumes appreciable values, the biquadratic d term becomes very important. Thus, a cross-over between the two regimes in the variation of pitch with temperature is obtained and this leads to a maximum value at some temperature.

A phenomenological theory of static and dynamic behaviour in S_C^* phase based on the Landau-type free-energy expansion at the $S_C^* - S_A^*$ phase transition was reported initially by Indenbom et al. [69] and Zeks [493]. Based on the symmetry of the group representation for the S_C^* , Indenbom et al. proposed a Landau free-energy expansion including leading chiral bilinear coupling terms between polarization and the tilt angle. This expansion serves as a starting point for the description of $S_C^* - S_A^*$ transition but fails to explain most of the experimental results, characteristics of S_C^* phase. The biquadratic coupling term between tilt and polarization in addition to the bilinear coupling term was added to the free-energy expansion by Zeks [493]. He showed that the biquadratic terms are large compared to the chiral bilinear terms. The quadrupolar ordering, which is much larger than the polar ordering, exists in both the achiral and chiral smectic-C phases. The Zeks model [493] assumes that the three transverse axes, such as transverse dipole moment, axes of polar and quadrupolar ordering, are coincident. In general, these axes must point in different directions. Meister et al. [497] extended the Zeks model by considering the three axes in different directions and calculated the quadrupolar ordering. The experimental data on the temperature and electric field dependence of the tilt angle and the electroclinic effect of the S_C^* and S_A^* phases were analysed by Gießelmann and Zugenmaier [498,521] according to the generalized Landau expansion and the results of a microscopic model [497] for the spontaneous polarization. The results obtained by these authors, [498] support the evidence of quadrupolar ordering and biquadratic coupling for the understanding of $S_C^* - S_A^*$ transition. They [498] developed a fast, powerful method to study the dependence of mean-field coefficients with respect to the electroclinic effect, the specific heat singularity and the chirality. The model was extended to temperatures below the phase transition. It is experimentally confirmed that the $S_C^* - S_A^*$ transition temperature $T_{C^*A^*}$ is higher in chiral compounds in comparison to their non-chiral analogue. It has been shown theoretically by Padmni et al. [499] that the increase of $T_{C^*A^*}$ is due to the bilinear coupling between the tilt and polarization. Roy et al. [500] have developed a theoretical relationship between $S_C - S_A$ phase transition temperature of chiral smectic compound and that of its non-chiral analogue. These authors have determined the bilinear and biquadratic coupling constants and the quadrupolar order parameter from the extended microscopic model [497] in the S_C^* phase. It has been found that both the bilinear and biquadratic couplings are responsible for the shift of the transition

temperature of a chiral compound in comparison to its non-chiral analogue and that the shifting of transition temperature due to the bilinear coupling is enhanced more by the inclusion of the biquadratic coupling term in the Landau free-energy expansion. The experimental results show that the bilinear coupling coefficient is directly proportional to the reduced polarization, whereas the biquadratic coupling constant depends on the reduced polarization as well as on the molecular structure. Mukherjee [500] has calculated the anomalous parts of the specific heat capacity of $S_C^* - S_A$ phase transition using the fluctuation theory of Landau.

Assuming that a transverse quadrupole order exists in the tilted phase, not necessarily due to the interaction between the dipoles, Zeks et al. [501] have developed a microscopic model which is consistent with the Landau expression. The single-particle potential for the rotation of a molecule around its long axis can be expressed as

$$u(\psi) = -a_1\theta \cos \psi - a_2\theta^2 \cos 2\psi, \quad (11.19)$$

where ψ describes the transverse orientation of a molecule. Here the first term is like the piezoelectric coupling of the Landau expansion and the second achiral term gives the quadrupolar ordering.

Considerable effort has been made by several workers [502–507] to understand the effect of chirality on the S_C^* phase. Renn and Lubensky [506] predicted that the chiral smectics could exhibit a dislocated S_A phase called the twist-grain-boundary (TGB) phase. This was experimentally confirmed [503–505] by X-ray studies. All these observations are consistent with a twisted stack of two-dimensional S_A slabs where the smectic order parameter of a slab is a Landau-orbit solution of the linearized Ginzburg–Landau–de Gennes equations. Further, in several of the compounds and mixtures exhibiting S_A^* phase the existence of a $S_A - S_A^* - S_C^*$ multicritical point was observed. In view of the existence of such a multicritical point it is important to investigate whether the TGB phase obtained by entering from the S_A^* side is the same phase obtained by entering the S_A side. Lubensky and Renn [507] addressed the question how the Abrikosov flux-dislocation lattice behaves when the ratio of the twist penetration depth to the smectic coherence length $\kappa (= \lambda / \xi)$ diverges. These authors examined the approach to the $S_A - S_C$ boundary within the framework of the chiral Chen–Lubensky model [379] of the $N - S_A - S_C$ point. Using the same model, Renn [502] derived the mean-field phase diagram of the N^* (or CI)– $S_A - S_C^*$ point.

It has been shown that the S_C^* phase can exhibit transitions to the TGB_A , TGB_C or TGB_C^* phases. In addition, it was found that both the $N^* - TGB_A$ and $N^* - TGB_C$ transitions are possible, but that the $N^* - TGB_C^*$ transition does not occur. He also showed that the transition $TGB_A - TGB_C$ is replaced by the $TGB_A - TGB_C^*$ when the cholesteric pitch length P increases beyond $\sim 2P_C/3$, where P_C is the S_C^* pitch length.

Although an extensive set of experimental studies have been performed [508–516] on the ferro- and ferrielectric smectic phases, no clearcut conclusion could be drawn about their phase structures. Only indirect experiments, such as dielectric [517] and electrooptical measurements or conosopic figure observations [509,518,519] could establish the ferro-, antiferro- or ferrielectric nature of the reported phases. However, these data fail to provide any insight into the molecular steps of reorganization from one structure into another. Recently, Lorman et al. [520] have proposed a model for the description of the observed sequences of ferro-, ferri- and antiferroelectric smectic phases. The model assumes a bilayer smectic ordering and a mechanism consisting of an

azimuthal reorientation of the molecules at the transitions. This mechanism assumes that the tilt angles remain largely unchanged across the phases and that the molecule can turn freely on cones possessing fixed vertex angles (conical approximation). It has been found that three helicoidal ferroelectric structures are possibly stable, in which the helical pitch vary monotonically as a function of temperature.

12. Overview and perspectives

Liquid crystals exhibit a rich variety of phase transitions which have been studied extensively by both experimental and theoretical workers. These studies have played an important role in advancing both our understanding of liquid crystals and our ability to use them in applications. In this article, an attempt has been made to present a comprehensive analysis of the current understanding of the phase transitions in liquid crystals. Instead of attempting to compile the latest results and the published works till date, I have preferred to concentrate on and discuss the questions related to the concept and ideas employed and the methods developed for its study. More importantly, the field of phase transitions in liquid crystals has grown so vast that it is beyond the scope of this article to cover all the developments made so far. In view of making the article self-contained, first a brief review on the general information about the liquid crystals has been given. It describes the molecular structure and types of liquid crystals with specific emphasis on the molecular arrangement and criteria for their classification. The phase sequence, re-entrant behaviour, blue phases and phases of chiral smectics and discotics are also described. An effort has been made to explain in a systematic way how the order existing in liquid crystals can be understood in terms of distribution functions and order parameters. This is followed by a brief discussion on the thermodynamic properties at and in the vicinity of the phase transitions, which are needed to generate understanding about the molecular structure phase stability relationship, and on the critical analysis of most widely used experimental methods for measuring the transition properties.

The remaining part of the article, concerns with the review of the current status of the theoretical understanding with a particular emphasis on the ideas and concepts involved in the formalism and the methods adopted for numerical calculations. The Landau–de Gennes (LDG) theory of phase transitions in liquid crystals has been proved to be very rich in making qualitative predictions. As these do not depend on the actual values of the phenomenological expansion coefficients, they test the general assumption of the theory. The basic ideas of Landau theory are discussed. The strengths of the Landau–de Gennes theory are its simplicity and ability to predict the most important features of the phase transitions. The application of the LDG theory to investigate the N–I, N–S_A, N_u–N_b, S_A–S_C transitions and N–S_A–S_C multicritical point has been reviewed. The predictions of Landau theory in case of transitions involving hexatic smectic phases and chiral liquid crystals are also summarized. Since the formation of liquid crystals depends on the anisotropy in the intermolecular interactions, the questions concerning its role have been the subject of investigation from the beginning. The use of the molecular models, i.e., hard-particle-, Maier–Saupe-, and van der Waals types of theories, to the transitions involving mesophases has been discussed. The density functional approach provides a convenient way for the theoretical study of a large variety of problems of ordered phases. The salient features of the density functional theory and its application within the framework of modified weighted-density approximation to the N–I and N–S_A

transitions have been reviewed. The occurrence of re-entrant phase transition in liquid crystals and of blue phases in a narrow temperature range in chiral liquid crystals are the examples of unusual phase sequences observed in mesophase systems. The available information about these unusual phenomenon is summarized.

Computer simulations play a crucial role in relating experimental observations to the theoretical results obtained for model systems. It has already made a significant contribution to advancing the understanding of the behaviour observed near transitions between different liquid crystal phases. The results obtained from the available simulation studies of phase transitions in liquid crystals are summarized for the hard-particle-, Lebwohl–Lasher lattice-, and Gay–Berne models. The current status of the physics of liquid crystalline polymers with particular emphasis to the theory of nematic order in polymer solutions and melts and interacting semiflexible polymers is reviewed. We have also summarized the work done on the phase transitions in chiral liquid crystals.

The future directions of work in this area are likely to be the computer simulations for realistic potential models and the experimental measurements on biaxial nematic and smectics, hexatic smectics, ferroelectric, polymer liquid crystalline, discotic nematic and columnar, and lyotropic phases. Reliable experimental data are essential for the understanding of these phases. From a theoretical point of view, more important is the extension of existing theories to cholesteric, smectics, chiral smectics, columnar and polymer liquid crystals. Among the classes of theories which can be used, for this purpose, although the weighted density functional methods rank near the top as far as the incorporation of the realistic details of the microscopic interactions is concerned, it is extremely hard to obtain precise information about the correlation functions. This limits the applicability of the density functional theory. Numerical simulations are the best hope to provide answers not only to the many interesting and important questions but also to resolve elementary issues regarding these phases. With the advancement in the area of superfast computers, efficient algorithms and methods of analysing numerical data, simulation studies are becoming possible and more important. In addition, issues related to the simulations of many-body systems, such as the maximum size of the system that can be tackled in a simulation, the longest time over which the numerical experiments can be performed and the accuracy of results, could be resolved satisfactorily in recent years. All these indicate that computer simulations can play a crucial role in the study of phase transitions and critical phenomena in liquid crystals.

Acknowledgements

I am grateful to Prof. Y. Singh for many stimulating discussions and to Prof. O.N. Srivastava for his encouragement and support. The financial assistance received from Centre of Advanced Studies, U.G.C., Government of India (New Delhi) is thankfully acknowledged.

References

- [1] F. Reinitzer, Zur Kenntnis des cholesterinus, *Monatsch Chem.* 9 (1888) 421.
- [2] O. Lehmann, *Z. Physik Chem.* 4 (1889) 462.

- [3] (a) P.G. de Gennes, *The Physics of Liquid Crystals*, Clarendon Press, Oxford, 1974; (b) P.G. de Gennes, J. Prost, *The Physics of Liquid Crystals*, Clarendon Press, Oxford, 1993.
- [4] S. Chandrasekhar, *Liquid Crystals*, Cambridge Univ. Press, Cambridge, 1977, 1992.
- [5] D. Demus, L. Richter, *Texture of Liquid Crystals*, Leipzig, 1978.
- [6] G.R. Luckhurst, G.W. Gray (Eds.), *The Molecular Physics of Liquid Crystals*, Academic Press, New York, 1979.
- [7] M. Kleman, *Points, Lines and Walls*, Wiley, New York, 1983.
- [8] G.W. Gray, J.W. Goodby, *Smectic Liquid Crystals: Textures and Structures*, London, Leonard Hill, 1984.
- [9] H. Sackmann, *Polymorphism and phase transitions in liquid crystals*, Martin-Luther-Universitat Halle Wittenberg, Wissenschaftl. Beitrage 1986/52 N 17.
- [10] J.C. Toledano, P. Toledano, *The Landau Theory of Phase Transitions*, World Scientific, Singapore, 1987.
- [11] G.W. Gray (Ed.), *Thermotropic Liquid Crystals*, Wiley, New York, 1987.
- [12] P.S. Pershan, *Structure of Liquid Crystal Phases*, World Scientific, 1988.
- [13] G. Vertogen, W.H. de Jeu, *Thermotropic Liquid Crystals: Fundamentals*, Springer, Berlin, 1988.
- [14] P.J. Collings, *Liquid Crystals: Nature's Delicate Phase of Matter*, Princeton Univ. Press, Princeton, 1990.
- [15] (a) B. Bahadur (Ed.), *Liquid Crystals: Applications and Uses*, World Scientific, Singapore Vol. 1 (1990); (b) Vol. 2. (1991); (c) Vol. 3 (1992).
- [16] A.L. Tsykalo, *Thermophysical Properties of Liquid Crystals*, Gordon and Breach, New York, 1991.
- [17] I.C. Khoo (Ed.), *Physics of Liquid Crystalline Materials*, Gordon and Breach, Amsterdam, 1991.
- [18] S. Martellucci, A.N. Chester (Eds.), *Phase Transitions in Liquid Crystals*, Plenum Press, New York, 1992.
- [19] S. Kumar (Ed.), *Liquid Crystals in Nineties and Beyond*, World Scientific, NJ, 1995.
- [20] P.J. Collings, M. Hird, *Introduction to Liquid Crystals: Physics and Chemistry*, Taylor and Francis, London, 1997.
- [21] P.J. Collings, J.S. Patel (Eds.), *Handbook of Liquid Crystal Research*, Oxford Univ. Press, Oxford, 1997.
- [22] S. Elston, R. Sambles (Eds.), *The Optics of Thermotropic Liquid Crystals*, Taylor and Francis, London, 1998.
- [23] C.B. McArdle, *Side Chain Liquid Crystal Polymers*, Blackie, Glasgow, 1989.
- [24] A.M. White, A.H. Windle, *Liquid Crystal Polymers*, Cambridge Univ. Press, Cambridge, 1992.
- [25] A.A. Collyer, *Liquid Crystal Polymers: From Structures to Applications*, Elsevier, Oxford, 1993.
- [26] A. Blumstein (Ed.), *Polymer Liquid Crystals*, Plenum, New York, 1985.
- [27] C. Carfagna (Ed.), *Liquid Crystals Polymers*, Pergamon, Oxford, 1994.
- [28] L.A. Beresnev, *Ferroelectric Liquid Crystals*, Gordon and Breach, New York, 1988.
- [29] J.W. Goodby, R. Blinc, N.A. Clark, S.T. Lagerwall, M.A. Osipov, S.A. Pikin, T. Sakurai, K. Yoshino, B. Zeks, *Ferroelectric Liquid Crystals: Principles, Properties and Applications*, Gordon and Breach, Philadelphia, 1991.
- [30] A. Buka (Ed.), *Modern Topics in Liquid Crystals: From Neutron Scattering to Ferroelectricity*, World Scientific, Singapore, 1993.
- [31] S. Chandrasekhar, B.K. Sadashiva, K.A. Suresh, *pramana* 9 (1977) 471.
- [32] S. Chandrasekhar, *Adv. Liq. Cryst.* 5 (1982) 47; *Philos. Trans. Roy. Soc. London A* 309 (1983) 93; *Contemp. Phys.* 29 (1988) 527.
- [33] C. Destrade, P. Foucher, H. Gasparoux, N.H. Tinh, A.M. Levelut, J. Malthete, *Mol. Cryst. Liq. Cryst.* 106 (1984) 121.
- [34] H.T. Nguyen, C. Destrade, H. Gasparoux, *Phys. Lett.* 77 A (1979) 3.
- [35] H. Finkelmann, W. Meier, H. Scheuermann, *Liquid crystal Polymers*, in: B. Bahadur (Ed.), *Liquid Crystals: Applications and Uses*, Vol. 3, World Scientific, Singapore, 1992.
- [36] G. Friedel, *Ann. Phys.* 18 (1922) 273.
- [37] S. Singh, *Phys. Rep.* 277 (1996) 283.
- [38] M.J. Freiser, *Phys. Rev. Lett.* 24 (1970) 1041; *Mol. Cryst. Liq. Cryst.* 14 (1971) 165.
- [39] R. Alben, *Phys. Rev. Lett.* 30 (1973) 778; *J. Chem. Phys.* 59 (1973) 4299.
- [40] L.J. Yu, A. Saupe, *Phys. Rev. Lett.* 45 (1980) 1000.
- [41] S. Chandrasekhar, B.K. Sadashiva, S. Ramesha, B.S. Srikanta, *pramana- J. Phys.* 27 (1986) L713.
- [42] J. Malthete, L. Liebert, A.M. Levelut, *C.R. Acad. Sci. (Paris)* 303 (1986) 1073.
- [43] H. Stegemeyer, Th. Blumel, K. Hiltrop, H. Onusseit, F. Porsch, *Liq. Cryst.* 1 (1986) 3.
- [44] D.C. Wright, N.D. Mermin, *Rev. Mod. Phys.* 61 (1989) 385.

- [45] A.D.L. Chandani, Y. Ouchi, H. Takezoe, A. Fukuda, K. Terashima, K. Furukawa, A. Kishi, *Jpn. J. Appl. Phys. Lett.* 28 (1989) 1261.
- [46] E. Gorecka, A.D.L. Chandani, Y. Ouchi, H. Takezoe, A. Fukuda, *Jpn. J. Appl. Phys.* 29 (1990) 131.
- [47] S. Inui, S. Kawano, M. Saito, H. Iwana, Y. Takanishi, K. Hiraoka, Y. Ouchi, H. Takezoe, A. Fukuda, *Jpn. J. Appl. Phys. Lett.* 29 (1990) 987.
- [48] C. Zannoni, in: G.R. Luckhurst, G.W. Gray (Eds.), *The Molecular Physics of Liquid Crystals*, Acad. Press, New York, 1979 (Chapter 3).
- [49] Y. Singh, *Phys. Rep.* 207 (1991) 351.
- [50] S. Goshen, D. Mukamel, S. Shtrikman, *Mol. Cryst. Liq. Cryst.* 31 (1975) 171.
- [51] J.P. Straley, *Phys. Rev. A* 10 (1974) 1881.
- [52] Y. Singh, K. Rajesh, V.J. Menon, S. Singh, *Phys. Rev. E* 49 (1994) 501.
- [53] T.W. Stinson, J.D. Litster, *Phys. Rev. Lett.* 25 (1970) 503; *ibid* 30 (1973) 688.
- [54] C. DasGupta, *Int. J. Mod. Phys. B* 9 (1995) 2219; *J. Phys.* 48 (1987).
- [55] J.R. Dorfman, T.R. Kirkpatrick, J.V. Sengers, *Ann. Phys. Chem.* 45 (1994) 213.
- [56] E.M. Barrall II, in: F.D. Saeva (Ed.), *Liquid Crystals*, Mercel Dekker, Inc. 1979, p. 193 (Chapter 9).
- [57] R. Alben, *Mol. Cryst. Liq. Cryst.* 13 (1971) 193.
- [58] J.R. McColl, C.S. Shih, *Phys. Rev. Lett.* 29 (1972) 85.
- [59] A. Beguin, J. Billard, F. Bonamy, J.M. Buisine, P. Cuvelier, J.C. Dubois, P.L. Barny, *Mol. Cryst. Liq. Cryst.* 115 (1984) 1.
- [60] H. Zink, W.H. de Jeu, *Mol. Cryst. Liq. Cryst.* 124 (1985) 287.
- [61] S. Singh, Y. Singh, *Mol. Cryst. Liq. Cryst.* 87 (1982) 211.
- [62] P.G. de Gennes, (a) *Solid State Comm.* 10 (1972) 753; (b) *Phys. Lett.* 30 A (1969) 454.
- [63] P. Sheng, E.B. Priestley, The Landau de Gennes theory of liquid crystal phase transition, in: E.B. Priestley, P.J. Wojtowicz (Eds.), *Introduction to Liquid Crystals*, Plenum, New York, 1974, p. 143.
- [64] E.F. Gramsbergen, L. Longa, W.H. de Jeu, *Phys. Rep.* 135 (1986) 195.
- [65] L.D. Landau, *Phys. Z Sowjetunion* 11 (1937) 26 (in: D. Ter Haar (Ed.), *Collected papers of L.D. Landau*, 2nd Edition, Gordon and Breach, Science Publisher, New York, 1967, pp. 193–216).
- [66] L.D. Landau, E.M. Lifshitz, *Statistical Physics*, Vol. 1, 3rd Edition, Pergamon, Oxford, 1980.
- [67] N. Boccara, *Symmetries Brisses*, Hermann, Paris, 1976.
- [68] M.J. Stephen, J.P. Straley, *Rev. Mod. Phys.* 46 (1974) 617.
- [69] V.L. Indenbom, S.A. Pikin, E.B. Liginov, *Sov. Phys. Crystallogr.* 21 (1976) 632.
- [70] S.A. Pikin, V.L. Indenbom, *Sov. Phys. Usp.* 21 (1978) 487.
- [71] V.L. Indenbom, E.B. Liginov, M.A. Osipov, *Sov. Phys. Crystallogr.* 26 (1981) 656.
- [72] V.L. Indenbom, E.B. Liginov, *Sov. Phys. Crystallogr.* 26 (1981) 526.
- [73] W. Helfrich, *Phys. Rev. Lett.* 24 (1970) 201.
- [74] C. Rosenblatt, *Phys. Rev. A* 24 (1981) 2236.
- [75] A.J. Nacastro, P.H. Keyes, *Phys. Rev. A* 30 (1984) 3156.
- [76] P.K. Mukherjee, T.B. Mukherjee, *Phys. Rev. B* 52 (1995) 9964.
- [77] A.D. Rzoska, S.J. Rzoska, J. Ziolo, *Phys. Rev. E* 54 (1996) 6452.
- [78] P.K. Mukherjee, Private commun.
- [79] M.A. Anisimov, *Mol. Cryst. Liq. Cryst.* 162 (1986) 1.
- [80] P.K. Mukherjee, J. Saha, B. Nandi, M. Saha, *Phys. Rev. B* 50 (1994) 9778.
- [81] P.K. Mukherjee, M. Saha, *Phys. Rev. E* 51 (1995) 5745.
- [82] R.G. Priest, T.C. Lubensky, *Phys. Rev. B* 13 (1976) 4159.
- [83] P.K. Mukherjee, M. Saha, *Mol. Cryst. Liq. Cryst.* 307 (1997) 103.
- [84] K.G. Wilson, *Phys. Rev. B* 4 (1971) 3174, 3184.
- [85] P.K. Mukherjee, T.R. Bose, D. Ghosh, M. Saha, *Phys. Rev. E* 51 (1995) 4570.
- [86] B. Nandi, P.K. Mukherjee, M. Saha, *Mod. Phys. Lett. B* 10 (1996) 777.
- [87] P.K. Mukherjee, *Mod. Phys. Lett. B* 11 (1997) 107.
- [88] R. Tao, P. Sheng, Z.F. Lin, *Phys. Rev. Lett.* 70 (1993) 1271.
- [89] D.E. Martire, G.A. Oweimreen, G.I. Agren, S.G. Ryam, H.T. Peterson, *J. Chem. Phys.* 64 (1976) 1456; 72 (1980) 2500.

- [90] P.H. Keyes, J.R. Shane, *Phys. Rev. Lett.* 22 (1979) 722.
- [91] D.R. Nelson, R.A. Pelcovits, *Phys. Rev. B* 16 (1977) 2191.
- [92] P.B. Vigman, A.I. Larkin, V.M. Filev, *Sov. Phys. JETP* 41 (1976) 944.
- [93] Z.H. Wang, P.H. Keyes, *Phys. Rev.* 54E (1996) 5249.
- [94] P.K. Mukherjee, Ph.D. Thesis, Calcutta University, 1996.
- [95] G. Vertogen, W.H. de Jeu, *Thermotropic Liquid Crystals: Fundamentals*, Springer, Berlin, 1988 (Chapter 12).
- [96] T.E. Faber, *Proc. Roy. Soc. London Ser. A* 375 (1982) 579.
- [97] L. Onsager, *Ann. N.Y. Acad. Sci* 51 (1949) 627.
- [98] R. Zwanzig, *J. Chem. Phys.* 39 (1963) 1714.
- [99] G. Lasher, *J. Chem. Phys.* 53 (1970) 4141.
- [100] L.K. Runnels, C. Colvin, *J. Chem. Phys.* 53 (1970) 4219.
- [101] P.J. Flory, *Proc. Roy. Soc. A* 234 (1956) 73.
- [102] P.J. Flory, R. Ronca, *Mol. Cryst. Liq. Cryst.* 54 (1979) 289.
- [103] (a) M.A. Cotter, D.E. Martire, *J. Chem. Phys.* 52 (1970) 1902, 1909, 4500; (b) M.A. Cotter, *Phys. Rev. A* 10 (1974) 625.
- [104] M.A. Cotter, Hard particle theories of nematics, in: G.R. Luckhurst, G.W. Gray (Eds.), *The Molecular Physics of Liquid Crystals*, Acad. Press, New York 1979, p. 169.
- [105] B. Barboy, W.M. Gelbart, *J. Chem. Phys.* 71 (1979) 3053.
- [106] B.M. Mulder, D. Frenkel, *Mol. Phys.* 55 (1985) 1193.
- [107] J.D. Parson, *Phys. Rev. A* 19 (1979) 1225.
- [108] M. Warner, *Mol. Cryst. Liq. Cryst.* 80 (1982) 79.
- [109] B.J. Berne, P. Pechukas, *J. Chem. Phys.* 56 (1972) 4213.
- [110] S.D. Lee, (a) *J. Chem. Phys.* 87 (1987) 4972; (b) 89 (1988) 7036.
- [111] A. Wulf, A.G. de Rocco, *J. Chem. Phys.* 55 (1971) 12.
- [112] (a) F. Dowell, D.E. Martire, *J. Chem. Phys.* 68 (1978) 1088; (b) F. Dowell, *Phys. Rev. A* 28 (1983) 3520.
- [113] S. Tang, G.T. Evans, *J. Chem. Phys.* 99 (1993) 5336.
- [114] W.M. Gelbart, A. Ben Shaul, *J. Chem. Phys.* 77 (1982) 916.
- [115] A. Saupe, *J. de Phys. Colloq.* 40 (1979) C3.
- [116] J.P. Straley, *Mol. Cryst. Liq. Cryst.* 24 (1973) 7.
- [117] W. Maier, A. Saupe, *Z. Naturforsch.* 14a (1959) 882; 15a (1960) 287.
- [118] B. Widom, *J. Chem. Phys.* 39 (1963) 2808.
- [119] M.A. Cotter, *Mol. Cryst. Liq. Cryst.* 39 (1977) 173.
- [120] T.J. Krieger, H.M. James, *J. Chem. Phys.* 22 (1954) 796.
- [121] S. Chandrasekhar, N.V. Madhusudana, *Acta Crystallogr. A* 27 (1971) 303.
- [122] (a) R.L. Humphries, P.G. James, G.R. Luckhurst, *J. Chem. Soc. Faraday Trans. II* 68 (1972) 1031; (b) G.R. Luckhurst, C. Zannoni, P.L. Nordio, U. Segre, *Mol. Phys.* 30 (1975) 1345.
- [123] S. Marcelja, *J. Chem. Phys.* 60 (1974) 3599.
- [124] N.V. Madhusudana, S. Chandrasekhara, *Solid State Comm.* 13 (1973) 377.
- [125] J.G.J. Ypma, G. Vertogen, H.T. Koster, *Mol. Cryst. Liq. Cryst.* 37 (1976) 57.
- [126] P. Sheng, P.J. Wojtowicz, *Phys. Rev. A* 14 (1976) 1883.
- [127] N.V. Madhusudana, K.L. Savithramma, S. Chandrasekhara, *Pramana* 8 (1977) 22.
- [128] (a) G.R. Luckhurst, Molecular field theories of nematics, in: G.R. Luckhurst, G.W. Gray (Eds.), *The Molecular Physics of Liquid Crystals*, Acad. Press, New York, 1979, p. 85; (b) G.R. Luckhurst, C. Zannoni, *Nature* 267 (1977) 412.
- [129] (a) A. Wulf, *J. Chem. Phys.* 64 (1976) 104; (b) J.L. Kaplan, E. Drauglis, *Chem. Phys. Lett.* 9 (1971) 645.
- [130] R. Van der Haegen, J. Debruyne, R. Luyckx, H.N.N. Lekkerkerker, *J. Chem. Phys.* 73 (1980) 2469.
- [131] N.V. Madhusudana, Theories of liquid crystals, in: B. Bahadur (Ed.), *Liquid Crystals: Applications and Uses*, Vol. 1, World Scientific, Singapore, 1990, p. 37 (Chapter 2).
- [132] (a) M.A. Cotter, The Van der Waals approach to nematic liquid crystals, in: G.R. Luckhurst, G.W. Gray (Eds.), *The Molecular Physics of Liquid Crystals*, Acad. Press, New York, 1979, p. 181 (Chapter 8); (b) M.A. Cotter, *J. Chem. Phys.* 66 (1977) 1098, 4710.

- [133] (a) W.M. Gelbart, B.A. Baron, *J. Chem. Phys.* 66 (1977) 207; (b) W.M. Gelbart, A. Gelbart, *Mol. Phys.* 33 (1977) 1387; (c) B.A. Baron, W.M. Gelbart, *J. Chem. Phys.* 67 (1977) 5795.
- [134] J.G.J. Ypma, G. Vertogen, *Phys. Rev. A* 17 (1978) 1490.
- [135] W. Warner, *J. Chem. Phys.* 73 (1980) 6327.
- [136] K.L. Savithramma, N.V. Madhusudana, (a) *Mol. Cryst. Liq. Cryst.* 62 (1980) 63; (b) *ibid* 97 (1983) 407.
- [137] (a) S. Singh, K. Singh, *Mol. Cryst. Liq. Cryst.* 101 (1983) 77; (b) K. Singh, S. Singh, *Mol. Cryst. Liq. Cryst.* 108 (1984) 133; (c) S. Singh, T.K. Lahiri, K. Singh, *Mol. Cryst. Liq. Cryst.* 225 (1993) 361.
- [138] (a) P.J. Flory, R. Ronca, *Mol. Cryst. Liq. Cryst.* 54 (1979) 311; (b) F. Dowell, *Phys. Rev. A* 28 (1983) 1003; (c) F. Dowell, *Phys. Rev. A* 31 (1985) 2464, 3214.
- [139] P. Palfy-Muhoray, B. Bergesen, *Phys. Rev. A* 6 (1987) 2704.
- [140] M.D. Lipkin, D.W. Oxtoby, *J. Chem. Phys.* 79 (1983) 1939.
- [141] T.J. Slucking, P. Shukla, *J. Phys. A* 16 (1983) 1539.
- [142] (a) Y. Singh, *Phys. Rev.* 30A (1984) 583; (b) U.P. Singh, Y. Singh, *Phys. Rev.* 33A (1986) 2725; (c) J. Ram, Y. Singh, *Phys. Rev.* 44A (1991) 3718; (d) J. Ram, R.C. Singh, Y. Singh, *Phys. Rev.* 49E (1994) 5117; (e) R.C. Singh, J. Ram, Y. Singh, *Phys. Rev.* 54E (1996) 977; (f) R.C. Singh, Ph.D. Thesis, Banaras Hindu University, 1998; (g) R.C. Singh, J. Ram, Y. Singh, in preparation.
- [143] A. Perera, G.N. Patey, J.J. Weis, *J. Chem. Phys.* 89 (1988) 6941.
- [144] A.M. Somoza, P. Tarazona, *J. Chem. Phys.* 91 (1989) 517.
- [145] U.P. Singh, U. Mohanty, Y. Singh, *Physica* 158A (1989) 817.
- [146] F.C. Andrews, *J. Chem. Phys.* 62 (1975) 272.
- [147] P.A. Lebowitz, G. Lasher, *Phys. Rev.* 6A (1972) 426.
- [148] J. Vieillard Baron, *Mol. Phys.* 28 (1974) 809.
- [149] D.W. Rebertus, K.M. Sando, *J. Chem. Phys.* 67 (1977) 2585.
- [150] T. Boublik, I. Nezbeda, O. Tynko, *Czech. J. Phys. B* 26 (1976) 1081.
- [151] P.A. Monson, M. Rigby, *Mol. Phys.* 35 (1978) 1337.
- [152] C. Zannoni, (a) Computer simulations, in: G.R. Luckhurst, G.W. Gray (Eds.), *The Molecular Physics of Liquid Crystals*, Acad. Press, New York, 1979, p. 191 (Chapter 6); (b) *J. Chem. Phys.* 84 (1986) 424.
- [153] I. Nezbeda, T. Boublik, *Czech. J. Phys. B* 28 (1978) 353.
- [154] H.J.F. Jensen, G. Vertogen, J.G.J. Ypma, *Mol. Cryst. Liq. Cryst.* 38 (1977) 87.
- [155] (a) G.R. Luckhurst, P. Simpson, *Mol. Phys.* 47 (1982) 251; (b) G.R. Luckhurst, S. Romano, *Proc. Roy. Soc. London A* 373 (1980) 111.
- [156] (a) D. Frenkel, B.M. Mulder, *Mol. Phys.* 55 (1985) 1171; (b) D. Frenkel, B.M. Mulder, J.P. Mc Tague, *Phys. Rev. Lett.* 52 (1984) 287; (c) D. Frenkel, H.N.W. Lekkerkerker, A. Stroobants, *Nature London* 322 (1988) 822.
- [157] (a) R. Eppenga, D. Frenkel, *Mol. Phys.* 52 (1984) 1303; (b) D. Frenkel, R. Eppenga, *Phys. Rev.* 31A (1985) 1776.
- [158] M.P. Allen, D. Frenkel, *Phys. Rev. Lett.* 58 (1987) 1748.
- [159] A. Stroobants, H.N.W. Lekkerkerker, D. Frenkel, (a) *Phys. Rev. A* 36 (1987) 2929; (b) *Phys. Rev. Lett.* 57 (1986) 1452.
- [160] D. Frenkel, (a) *Mol. Phys.* 60 (1987) 1, (b) *J. Phys. Chem.* 92 (1988) 3280; (c) *Liq. Cryst.* 5. (1989) 929.
- [161] A. Beguin, J.C. Dubois, P. Le Barny, J. Billard, F. Bonamy, J.M. Busisine, P. Cuvelier, Sources of thermodynamic data on mesogens, *Mol. Cryst. Liq. Cryst.* 115 (1984) 1–326.
- [162] G.R. Luckhurst, in: L.L. Chapoy (Ed.), *Recent Advances in Liquid Crystalline Polymers*, Elsevier, London 1986, p. 105.
- [163] B. Deloche, B. Cabane, D. Jerome, *Mol. Cryst. Liq. Cryst.* 15 (1971) 197.
- [164] R.G. Horn, J. de Physique 39 (1978) 199, R.G. Horn, T.E. Faber, *Proc. Roy. Soc. (London) A* 368 (1979) 199.
- [165] (a) J.D. Bunning, D.A. Crellin, T.E. Faber, *Liq. Cryst.* 1 (1986) 37, (b) B. Bergersen, P. Palfy-Muhoray, D.A. Dunmur, *Liq. Cryst.* 3 (1988) 347.
- [166] H.C. Andersen, D. Chandler, J.D. Weeks, *Adv. Chem. Phys.* 34 (1976) 105.
- [167] B. Tjpto-Margo, G.T. Evans, *Mol. Phys.* 74 (1991) 85.
- [168] M. Nakagawa, T. Akahane, *Mol. Cryst. Liq. Cryst.* 90 (1982) 53.
- [169] P.J. Flory, R. Ronca, *Mol. Cryst. Liq. Cryst.* 54 (1979) 311.
- [170] A. Bellemans, *Phys. Rev. Lett.* 21 (1968) 527.

- [171] V.T. Rajan, C.W. Woo, *Phys. Rev. A* 17 (1978) 382, L. Feijoo, V.T. Rajan, C.W. Woo, *Phys. Rev. A* 19 (1979) 1263.
- [172] (a) D.R. Evans, G.T. Evans, D.K. Hoffman, *J. Chem. Phys.* 94 (1991) 8816; (b) G.T. Evans, E.B. Smith, *Mol. Phys.* 74 (1991) 79.
- [173] B. Tjpto-Margo, G.T. Evans, *J. Chem. Phys.* 94 (1990) 4546.
- [174] (a) M. Baus, J.L. Colot, X.G. Wu, H. Xu, *Phys. Rev. Lett.* 59 (1987) 2184, (b) J.L. Colot, X.G. Wu, H. Xu, M. Baus, *Phys. Rev. A* 38 (1988) 2022.
- [175] G. Vertogen, W.H. de Jeu, *Thermotropic Liquid Crystals, Fundamentals*, Springer, Berlin, 1988, p. 245 (Chapter 13).
- [176] J.A. Barker, D. Henderson, *Rev. Mod. Phys.* 48 (1976) 587.
- [177] J.F. Marko, (a) *Phys. Rev. Lett.* 60 (1988) 325; (b) *Phys. Rev.* 39A (1989) 2050.
- [178] C.N. Likos, N.W. Ashcroft, *J. Chem. Phys.* 99 (1993) 9090.
- [179] P. Honenberg, W. Kohn, *Phys. Rev.* 136B (1964) 864.
- [180] W. Kohn, L.J. Sham, *Phys. Rev. A* 140 (1965) 1133.
- [181] D. Mermin, *Phys. Rev.* 137 (1964) 1441.
- [182] J.L. Lebowitz, J.K. Percus, *J. Math. Phys.* 4 (1963) 116.
- [183] W.F. Saam, C. Ebner, *Phys. Rev. A* 15 (1977) 2566.
- [184] A.J.M. Yang, P.D. Fleming, J.H. Gibbs, *J. Chem. Phys.* 64 (1976) 3732.
- [185] J.K. Percus, in: H.L. Frisch, J.L. Lebowitz (Eds.), *The Equilibrium Theory of Classical Fluids*, Benjamin, New York, 1964.
- [186] R. Evans, *Adv. Phys.* 28 (1979) 143.
- [187] F.F. Abraham, *Phys. Rep.* 53 (1979) 93.
- [188] J.S. Rowlinson, B. Widom, *Molecular Theory of Capillarity*, Clarendon Press, Oxford, 1982.
- [189] A.D.J. Haymet, *Ann. Rev. Phys. Chem.* 38 (1987) 89.
- [190] M. Baus, *J. Phys. Condens. Matter* 2 (1990) 2111.
- [191] R.G. Parr, W. Yang, *Density Functional Theory of Atoms and Molecules*, Oxford Univ. Press, New York, 1989.
- [192] R.O. Jones, O. Gunnarsson, *Rev. Mod. Phys.* 61 (1989) 689.
- [193] T. Ziegler, *Chem. Rev.* 91 (1991) 651.
- [194] J.K. Labanowski, J. Andzelm (Eds.), *Density Functional Methods in Chemistry*, Springer, New York, 1991.
- [195] B.G. Johnson, P.M.W. Gill, J.A. Pople, *J. Chem. Phys.* 98 (1993) 5612.
- [196] S. Nordholm, M. Johnson, B.C. Freasier, *Aust. J. Chem.* 33 (1980) 2139.
- [197] P. Tarazona, (a) *Mol. Phys.* 52 (1984) 81; (b) *Phys. Rev. A* 31 (1985) 2672; erratum 32 (1985) 3148.
- [198] W.A. Curtin, N.W. Ashcroft, *Phys. Rev. A* 32 (1985) 2909.
- [199] A.R. Denton, N.W. Ashcroft, *Phys. Rev. A* 39 (1989) 426, 4701.
- [200] T.V. Ramakrishnan, M. Yussouff, *Phys. Rev.* 19B (1979) 2775.
- [201] A.D.J. Haymet, *J. Chem. Phys.* 78 (1983) 4641.
- [202] G.L. Jones, U. Mohanty, *Mol. Phys.* 54 (1985) 1241.
- [203] M. Baus, J.L. Colot, *Mol. Phys.* 55 (1985) 653.
- [204] W.R. Smith, D. Henderson, *Mol. Phys.* 3 (1970) 411.
- [205] (a) A. Perera, P.G. Kusalik, G.N. Patey, *J. Chem. Phys.* 87 (1987) 1295; 89 (1988) 5969; (b) A. Perera, G.N. Patey, *J. Chem. Phys.* 89 (1988) 5961; (c) J. Talbot, A. Perera, G.N. Patey, *Mol. Phys.* 70 (1990) 285.
- [206] D. Frenkel, in: J.P. Hansen, D. Levesque, J. Zinn-Justin (Eds.), *Liquids, Freezing and Glass Transition II*, 1989, Les Houches Lectures, North-Holland, Amsterdam, 1991.
- [207] (a) E. DeMiguel, L.F. Rull, M.K. Chalam, K.E. Gubbins, F.V. Swol, *Mol. Phys.* 72 (1991) 593; (b) E. DeMiguel, L.F. Rull, M.K. Chalam, K.E. Gubbins, *Mol. Phys.* 74 (1991) 405.
- [208] G.R. Luckhurst, R.A. Stephens, R.W. Phippen, *Liq. Cryst.* 8 (1990) 451.
- [209] F.J. Rogers, D.A. Young, *Phys. Rev.* 30A (1984) 999.
- [210] R. Holyst, A. Poniewierski, *Mol. Phys.* 68 (1989) 381.
- [211] W.L. McMillan, *Phys. Rev. A* 7 (1973) 1419.
- [212] J. Als-Nielsen, R.J. Birgeneau, M. Kaplan, J.D. Litster, C.R. Safinya, *Phys. Rev. Lett.* 39 (1977) 352.
- [213] P. Brisbin, R. De Hoff, T.E. Lockhart, D.L. Johnson, *Phys. Rev. Lett.* 43 (1979) 1171.
- [214] R.J. Birgeneau, C.W. Garland, G.B. Kasting, B.M. Octo, *Phys. Rev.* 24A (1981) 2624.

- [215] H. Morynissen, J. Thoen, W. Van Dael, *Mol. Cryst. Liq. Cryst.* 97 (1983).
- [216] J.M. Viner, C.C. Huang, *Solid State Comm.* 39 (1981) 789.
- [217] B.M. Ocko, R.J. Birgeneau, J.D. Litster, M.E. Neubert, *Phys. Rev. Lett.* 52 (1984) 208.
- [218] K.K. Chan, P.S. Pershan, L.B. Sorensen, F. Hardouin, *Phys. Rev. Lett.* 54 (1985) 1694, *Phys. Rev.* 34A (1986) 1420.
- [219] K.K. Chan, M. Deutsch, B.M. Ocko, P.S. Pershan, L.B. Sorensen, *Phys. Rev. Lett.* 54 (1985) 920.
- [220] M. Miranda, L.J. Kortan, R.J. Birgeneau, *Phys. Rev. Lett.* 56 (1986) 2264.
- [221] S.B. Ranavavare, V.G.K.M. Pisipati, J.H. Freed, *Chem. Phys. Lett.* 140 (1987) 255.
- [222] (a) C.W. Garland, G. Nounneiss, K.J. Stine, G. Heppke, *J. Phys. (Paris)* 50 (1989) 2291; (b) C.W. Garland, G. Nounneiss, *Phys. Rev. E* 49 (1994) 2964.
- [223] L. Chen, J.D. Brock, J. Huang, S. Kumar, *Phys. Rev. Lett.* 67 (1991) 2037.
- [224] G. Nounneiss, K.I. Blum, M.J. Young, C.W. Garland, R.J. Birgeneau, *Phys. Rev. E* 47 (1993) 1910.
- [225] L. Wu, M.J. Young, Y. Shao, C.W. Garland, R.J. Birgeneau, *Phys. Rev. Lett.* 72 (1994) 376.
- [226] W.L. McMillan, *Phys. Rev.* 6A (1972) 936.
- [227] B.I. Halperin, T.C. Lubensky, *Solid State Comm.* 14 (1974) 997.
- [228] J.H. Chen, T.C. Lubensky, *Phys. Rev. A* 14 (1976) 1202.
- [229] P.E. Cladis, W.A. Sarloos, D.A. Huse, J.S. Patel, J.W. Goodby, P.L. Finn, *Phys. Rev. Lett.* 62 (1989) 1764.
- [230] J. Prost, *Adv. Phys.* 33 (1984) 1.
- [231] R.F. Bruinsma, *Phys. Rev. A* 43 (1991) 5377.
- [232] (a) P.K. Mukherjee, *Mol. Cryst. Liq. Cryst.* 307 (1997) 1; (b) P.K. Mukherjee, K. Mukhopadhyay, *Phys. Rev. E*, in press.
- [233] K.K. Kobayashi, *J. Phys. Soc. Jpn.* 29 (1970) 101; *Mol. Cryst. Liq. Cryst.* 13 (1971) 137.
- [234] W.L. McMillan, *Phys. Rev.* 4A (1971) 1238, *Phys. Rev.* 23B (1971) 363.
- [235] R.B. Meyer, T.C. Lubensky, *Phys. Rev. A* 14 (1976) 2307.
- [236] J. Katriel, G.F. Kventsel, *Phys. Rev. A* 28 (1983) 3037.
- [237] A. Kloczkowski, J. Stecki, *Mol. Phys.* 55 (1985) 689.
- [238] D.A. Badalyan, *Sov. Phys. Crystallogr.* 27 (1982) 10.
- [239] C.D. Mukherjee, B. Bagchi, T.R. Bose, D. Gosh, M.K. Roy, M. Saha, *Phys. Lett.* 92A (1982) 403.
- [240] W. Wagner, *Mol. Cryst. Liq. Cryst.* 98 (1983) 247.
- [241] M. Nakagawa, T. Akahane, *J. Phys. Soc. Jpn.* 54 (1985) 69.
- [242] G.F. Kventsel, G.R. Luckhurst, H.B. Zewdie, *Mol. Phys.* 56 (1985) 589.
- [243] M. Hosino, H. Nakano, H. Kimura, *J. Phys. Soc. Jpn.* 46 (1979) 740, 1709.
- [244] X. Wen, R.B. Meyer, *Phys. Rev. Lett.* 59 (1987) 1325.
- [245] N.V. Madhusudana, B.S. Srikanta, M. Subramanya, Raj Urs, *Mol. Cryst. Liq. Cryst.* 108 (1984) 19.
- [246] R. Holyst, A. Poniewierski, *Mol. Phys.* 71 (1990) 561.
- [247] I.I. Ptichkin, *Sov. Phys. Crystallogr.* 36 (1991) 134.
- [248] M.P. Taylor, R. Hentschke, J. Herzfeld, *Phys. Rev. Lett.* 62 (1989) 800.
- [249] (a) F. Dowell, *Phys. Rev.* 28A (1983) 3520, 3526; (b) C. Rosenblatt, D. Ronis, *Phys. Rev. A* 23 (1981) 305; D. Ronis, C. Rosenblatt, *Phys. Rev. A* 21 (1980) 1687.
- [250] (a) F.T. Lee, H.T. Tan, Y.M. Shih, C.W. Woo, *Phys. Rev. Lett.* 31 (1973) 1117; (b) L. Senbetu, C.W. Woo, *Phys. Rev. A* 17 (1978) 1529.
- [251] K. Sokalski, *Physica* 113A (1982) 133.
- [252] C.D. Mukherjee, T.R. Bose, D. Ghosh, M.K. Roy, M. Saha, *Mol. Cryst. Liq. Cryst.* 124 (1985) 139.
- [253] E.M. Everyanov, A.N. Primak, (a) *Liq. Cryst.* 10 (1991) 555; (b) *ibid* 13 (1993) 139.
- [254] H. Wang, M.Y. Jin, R.C. Jarnagin, T.J. Bunning, W. Adams, B. Cull, Y. Shi, S. Kumar, E.T. Samulski, *Nature* 238 (1996) 244.
- [255] B. Mulder, *Phys. Rev. A* 35 (1987) 3095.
- [256] R. Holyst, A. Poniewierski, *Phys. Rev. A* 39 (1989) 2742.
- [257] A.M. Somoza, P. Tarazona, *Phys. Rev. Lett.* 61 (1988) 2566.
- [258] A. Poniewierski, R. Holyst, *Phys. Rev. Lett.* 61 (1988) 2461.
- [259] M.C. Mahato, M. Roy Lakshmi, R. Pandit, H.R. Krishnamurthy, *Phys. Rev. A* 38 (1988) 1049.
- [260] R.G. Priest, *Mol. Cryst. Liq. Cryst.* 37 (1976) 101.

- [261] F. Rondelez, *Solid State Comm.* 12 (1972) 1675.
- [262] R. Alben, *Solid State Comm.* 13 (1973) 1783.
- [263] B.I. Halperin, T.C. Lubensky, S.K. Ma, *Phys. Rev. Lett.* 32 (1974) 292.
- [264] (a) C.W. Garland, G. Nounesis, *Phys. Rev.* 49E (1994) 2964; (b) L. Longa, *J. Chem. Phys.* 85 (1986) 2974.
- [265] I. Lelidis, G. Durand, *J. Phys. II (Paris)* 6 (1996) 1359.
- [266] M.A. Anisimov, V.P. Voronov, A.O. Kulkov, F. Kholmurodov, *J. Phys. (Paris)* 46 (1985) 2137.
- [267] M.A. Anisimov, *Critical Phenomena in Liquids and Liquid Crystals*, Gordon and Breach, New York, 1991, p. 10.
- [268] W.H. de Jeu, *NATO School on Phase Transitions in Liquid Crystals*, Erice, Italy, May 1991.
- [269] C. Das Gupta, B.I. Halperin, *Phys. Rev. Lett.* 47 (1981) 1556.
- [270] T.C. Lubensky, *J. Chem. Phys.* 80 (1983) 31.
- [271] D.R. Nelson, J. Toner, *Phys. Rev. B* 24 (1981) 363.
- [272] J. Toner, *Phys. Rev. B* 26 (1982) 462.
- [273] B.R. Patton, B.S. Andereck, *Phys. Rev. Lett.* 69 (1992) 1556.
- [274] B.S. Andereck, B.R. Patton, *Phys. Rev.* 49E (1994) 1393.
- [275] J.G. Kirkwood, E. Monroe, *J. Chem. Phys.* 9 (1941) 514.
- [276] M. Nakagawa, T. Akahane, *J. Phys. Soc. Japan* 53 (1984) 1951.
- [277] J.W. Emsley, R. Hashim, G.R. Luckhurst, G.N. Rumbles, F.R. Vioria, *Mol. Phys.* 49 (1983) 1321.
- [278] J.W. Emsley, R. Hashim, G.R. Luckhurst, G.N. Shilstone, *Liq. Cryst.* 1 (1986) 437.
- [279] J.W. Emsley, G.R. Luckhurst, G.N. Shilstone, I. Sage, *J. Chem. Soc. Faraday Soc. Trans. II* 83 (1987) 371.
- [280] D. Catalano, C. Forte, C.A. Veracini, J.W. Emsley, G.N. Shilstone, *Liq. Cryst.* 2 (1987) 357.
- [281] E.M. Everyanov, V.A. Gunyakov, *Opt. Spectrosc.* 66 (1989) 72.
- [282] J.W. Emsley, G.R. Luckhurst, H.S. Sachdev, *Liq. Cryst.* 5 (1989) 953.
- [283] M.P. Fontana, B. Rosi, N. Kirov, I. Dozov, *Phys. Rev. A* 33 (1986) 4132.
- [284] P.E. Cladis, (a) *Phys. Rev. Lett.* 35 (1975) 48; (b) *Philos. Mag.* 29 (1975) 641; (c) in: S. Chandrasekhar (Ed.), *Proceedings of International Conference on Liquid Crystals*, Bangalore, Heyden, London, 1980, p. 105.
- [285] P.E. Cladis, R.K. Begardus, W.B. Daniels, G.N. Taylor, *Phys. Rev. Lett.* 39 (1977) 720.
- [286] D. Guillon, P.E. Cladis, J. Stamatoff, *Phys. Rev. Lett.* 41 (1978) 1598.
- [287] N.S. Chen, S.K. Hark, J.T. Ho, *Phys. Rev. A* 24 (1981) 2843.
- [288] T. Narayanan, A. Kumar, *Phys. Rep.* 249 (1994) 135.
- [289] A. Deerenberg, J.A. Schouten, N.J. Trappeniers, *Physica* 103A (1980) 183.
- [290] J.A. Schouten, *Phys. Rep.* 172 (1989) 33.
- [291] R.J. Tufeu, P.H. Keyes, W.B. Daniels, *Phys. Rev. Lett.* 35 (1975) 1004.
- [292] J.D. Cox, *J. Chem. Soc.* 4 (1952) 606.
- [293] T. Narayanan, A. Kumar, E.S.R. Gopal, *Phys. Lett. A* 155 (1991) 276.
- [294] R.G. Johnston, N.A. Clark, P. Wiltzins, D.S. Cannel, *Phys. Rev. Lett.* 54 (1985) 49.
- [295] V.P. Zaitsev, S.V. Krivokhizha, I.L. Fabelinskii, A. Tsitrovskii, L.L. Chaikov, E.V. Shvelts, P. Yani, *Sov. Phys. JETP Lett.* 43 (1986) 112.
- [296] S.V. Krivokhizha, O.A. Dugovaya, I.L. Fabelinskii, L.L. Chaikov, A. Tsitrovskii, P. Yani, *Sov. Phys. JETP* 76 (1993) 62.
- [297] G.B. Kozlov, E.B. Kryukova, S.P. Lobedev, A.A. Sobyenin, *Sov. Phys. JETP* 67 (1988) 1689.
- [298] M.J. Naughton, R.V. Chamberlin, X. Yan, S.Y. Ysu, L.Y. Chiang, M.Y. Azbel, P.M. Chaikin, *Phys. Rev. Lett.* 61 (1988) 621.
- [299] T.H. Lin, X.Y. Shao, M.K. Wu, P.H. Hoy, X.C. Jin, C.W. Chu, N. Evans, R. Bayuzick, *Phys. Rev. B* 29 (1984) 1493.
- [300] S. Katayama, Y. Hirokawa, T. Kanaka, *Macromolecules* 17 (1984) 2649.
- [301] H. Glusbrenner, H. Weingartner, *J. Phys. Chem.* 93 (1989) 3378.
- [302] R.B. Griffiths, in: R.E. Mills, E. Ascher, R.I. Jaffee (Eds.), *Critical Phenomenon in Alloys, Magnets and Superconductors*, McGraw-Hill, New York, 1971, p. 377.
- [303] P.E. Cladis, *Mol. Cryst. Liq. Cryst.* 165 (1988) 85.
- [304] L. Longa, W.H. de Jeu, *Phys. Rev. A* 26 (1982) 1632.
- [305] F.R. Bouchet, P.E. Cladis, *Mol. Cryst. Liq. Cryst. (Lett.)* 64 (1980) 97.

- [306] K.J. Lushington, G.B. Kasting, C.W. Garland, *Phys. Rev. B* 22 (1980) 2569.
- [307] R.Y. Dong, *Mol. Cryst. Liq. Cryst. (Lett.)* 64 (1981) 205.
- [308] R. Shashidhar, H.D. Kleinhan, G.M. Schneider, *Mol. Cryst. Liq. Cryst. (Lett.)* 72 (1981) 119.
- [309] P.E. Cladis, *Phys. Rev. A* 23 (1981) 2594.
- [310] A.R. Kortan, H.V. Kanel, R.J. Birgeneau, J.D. Lister, *Phys. Rev. Lett.* 47 (1981) 1206.
- [311] N. Hafiz, N.A.P. Vaz, Z. Yaniv, D. Affender, J.W. Doane, *Phys. Lett. A* 91 (1982) 411.
- [312] J.W. Emsley, G.R. Luckhurst, P.J. Parson, B.A. Timimi, *Mol. Phys.* 56 (1985) 767.
- [313] C.S. Hudson, *Z. Phys. Chem.* 47 (1904) 113.
- [314] G. Illian, H. Knepe, F. Schneider, *Ber. Bunsenges, Phys. Chem.* 92 (1988) 776.
- [315] F. Dowell, *Phys. Rev.* 36A (1987) 5046, (b) 38A (1988) 382.
- [316] G. Pelzl, S. Diele, I. Latif, W. Weissflog, D. Demus, *Cryst. Res. Technol.* 17 (1982) K 78.
- [317] S. Diele, G. Pelzl, I. Latif, D. Demus, *Mol. Cryst. Liq. Cryst. (Lett.)* 92 (1983) 27.
- [318] G. Sigaud, F. Hardouin, M. Mauzac, N.H. Tinh, *Phys. Rev. A* 33 (1986) 789.
- [319] F. Hardouin, A.M. Levelut, M.F. Achard, G. Sigaud, *J. Chim. Phys.* 80 (1983) 53.
- [320] C. Destrade, J. Malthete, N.H. Tinh, H. Gasparoux, *Phys. Lett.* 78A (1980) 82.
- [321] N.H. Tinh, J. Malthete, C. Destrade, *J. de Physique Lett.* 42 (1981) L-417.
- [322] K.W. Evans-Lutterodt, J.W. Chung, B.M. Ocko, R.J. Birgeneau, C. Chiang, C.W. Garland, E. Chin, J. Goodby, N.H. Tinh, *Phys. Rev. A* 36 (1987) 1387.
- [323] F. Hardouin, G. Sigaud, M.F. Achard, H. Gasparoux, *Phys. Lett.* 71 (1979) 347.
- [324] N.H. Tinh, *J. Chim. Phys.* 80 (1983) 83.
- [325] R. Shashidhar, B.R. Ratna, V. Surendranath, V.N. Raja, K.S. Prasad, C. Nagabhushana, *J. Phys. Lett. (Paris)* 46 (1985) L445.
- [326] N.H. Tinh, F. Hardouin, C. Destrade, A.M. Levelut, *J. Phys. Lett. (Paris)* 43 (1982) L33.
- [327] S. Chandrasekhar, *Proceedings of 10th International Liquid Crystal Conference, York, 1984*; *Mol. Cryst. Liq. Cryst.* 124 (1985) 1.
- [328] A. Nayeem, J.H. Freed, *J. Phys. Chem.* 93 (1989) 65.
- [329] G.R. Luckhurst, B.A. Timimi, *Mol. Cryst. Liq. Cryst. (Lett.)* 64 (1981) 253.
- [330] W.H. de Jeu, *Solid State Comm.* 41 (1982) 529.
- [331] T.R. Bose, D. Ghosh, C.D. Mukherjee, J. Saha, M.K. Roy, M. Saha, *Phys. Rev. A* 43 (1991) 4372.
- [332] L.V. Miramtsar, *Mol. Cryst. Liq. Cryst.* 133 (1986) 151.
- [333] J.O. Indekeu, A.N. Berker, *Phys. Rev. A* 33 (1986) 1158; *J. de Physique* 49 (1988) 353.
- [334] A.N. Berker, J.S. Walker, *Phys. Rev. Lett.* 47 (1981) 1469.
- [335] J.O. Indekeu, A.N. Berker, C. Chiang, C.W. Garland, *Phys. Rev. A* 35 (1987) 1371.
- [336] N.V. Madhusudana, J. Rajan, *Liq. Cryst.* 7 (1990) 31.
- [337] J. Prost, P. Barois, *J. Chim. Phys.* 80 (1983) 65.
- [338] P.S. Person, J. Prost, *J. Phys. Lett. (Paris)* 40 (1979) L-27.
- [339] J. Katriel, G.F. Kventsel, *Mol. Cryst. Liq. Cryst.* 124 (1985) 179.
- [340] R.F.M. Houtappel, *Physica* 16 (1950) 425.
- [341] D.W. Allender, M.A. Lee, N. Hafiz, *Mol. Cryst. Liq. Cryst.* 124 (1985) 45.
- [342] P.K. Kukherjee, *Liq. Cryst.* 22 (1997).
- [343] A. Saupe, P. Boonbrahm, L.J. Yu, *J. Chem. Phys.* 80 (1983) 7.
- [344] P. Boonbraham, A. Saupe, *J. Chem. Phys.* 81 (1984) 2076.
- [345] F. Biscarini, C. Chiccoli, P. Pasini, F. Semeria, C. Zannoni, *Phys. Rev. Lett.* 75 (1995) 1803.
- [346] P.O. Quist, *Liq. Cryst.* 18 (1995) 623.
- [347] S. Chandrasekhar, *Mol. Cryst. Liq. Cryst.* 124 (1985) 1.
- [348] C.A. Cajas, J.B. Swift, H.R. Brand, *Phys. Rev. A* 30 (1984) 1579.
- [349] C.H. Shih, R. Alben, *J. Chem. Phys.* 57 (1972) 3055.
- [350] C. Vause, J. Sak, *Phys. Rev.* 18B (1979) 1455; *Phys. Lett.* 65A (1978) 183.
- [351] Y. Rabin, W.E. McMullen, W.M. Gelbart, *Mol. Cryst. Liq. Cryst.* 89 (1982) 67.
- [352] D.L. Johnson, D. Allender, R. De Hoff, C. Maze, E. Oppenheim, R. Reynolds, *Phys. Rev.* 16B (1977) 470.
- [353] R.G. Calfish, Z.Y. Chen, A. Berker, J.M. Deutch, *Phys. Rev. A* 30 (1984) 2562.

- [354] Z.Y. Chen, J.M. Deutch, *J. Chem. Phys.* 80 (1984) 2151.
- [355] E.A. Jacobsen, J. Swift, *Mol. Cryst. Liq. Cryst.* 87 (1982) 29.
- [356] S.R. Sharma, P. palfy Muhoray, B. Bergerson, D.A. Dunmur, *Phys. Rev. A* 23 (1985) 3752.
- [357] T.C. Lubensky, *Mol. Cryst. Liq. Cryst.* 146 (1987) 55.
- [358] B.M. Mulder, Th. W. Ruijgrok, *Physica A* 113 (1982) 145.
- [359] I. Dozov, N. Kirov, B. Petroff, *Phys. Rev. A* 36 (1987) 2870.
- [360] R. Holyst, A. Poniewierski, *Mol. Phys.* 69 (1990) 193.
- [361] C. Tanford, *The Hydrophobic Effect*, Wiley, New York, 1973.
- [362] T.R. Taylor, J.L. Fergason, S.L. Arora, *Phys. Rev. Lett.* 24 (1970) 359; 25 (1970) 722.
- [363] E.I. Kats, V.V. Lebedev, *Physica A* 135 (1986) 601.
- [364] P.G. de Gennes, (a) *C.R. Acad. Sci* 274B (1972) 758; (b) *Mol. Cryst. Liq. Cryst.* 21 (1973) 49.
- [365] C.C. Huang, S.C. Lien, *Phys. Rev. Lett.* 47 (1981) 1917.
- [366] A. Wulf, *Phys. Rev.* 11A (1975) 365.
- [367] W.L. McMillan, *Phys. Rev.* 8A (1973) 1921.
- [368] D. Cabib, L. Benguigui, *J. Phys. (Paris)* 38 (1977) 419.
- [369] B.W. van der Meer, G. Vertogen, *J. Phys. (Paris)* 40 (1979) C3-222.
- [370] R.G. Priest, *J. Phys. (Paris)* 36 (1975) 437; *J. Chem. Phys.* 65 (1976) 408.
- [371] M. Matsushita, *J. Phys. Soc. Jpn.* 50 (1981) 1351.
- [372] W.J.A. Goossens, (a) *J. Phys. (Paris)* 46 (1985) 1411; (b) *Euro. Phys. Lett.* 3 (1987) 341; *Mol. Cryst. Liq. Cryst.* 150 (1987) 419.
- [373] G. Sigaud, F. Hardouin, M.F. Achard, *Solid State Comm.* 23 (1977) 35.
- [374] D. Johnson, D. Allender, D. Dehoff, C. Maze, E. Oppenheim, R. Reynolds, *Phys. Rev. B* 16 (1977) 470.
- [375] D.L. Johnson, *J. Chim. Physique* 80 (1983) 45.
- [376] R. Shashidhar, B.R. Ratna, S. Krishna Prasad, *Phys. Rev. Lett.* 53 (1984) 2141.
- [377] M.A. Anisimov, *Mol. Cryst. Liq. Cryst.* 162A (1988) 1.
- [378] K.C. Chu, W.L. McMillan, *Phys. Rev.* 15A (1977) 1181.
- [379] J. Chen, T.C. Lubensky, *Phys. Rev.* 14A (1976) 1202.
- [380] J. Prost, J.P. Marceron, *J. Phys. (Paris)* 38 (1977) 315.
- [381] L. Benguigui, *J. Phys. (Paris) Colloq.* 40 (1979) C3.
- [382] C.C. Huang, J.M. Viner, *Phys. Rev. A* 25 (1982) 3385.
- [383] G. Grinstein, J. Toner, *Phys. Rev. Lett.* 51 (1983) 2386.
- [384] X. Wen, C.W. Garland, M.D. Wand, *Phys. Rev. A* 42 (1990) 6087.
- [385] R. Pindak, D.E. Moncton, S.C. Davey, J.W. Goodby, *Phys. Rev. Lett.* 46 (1981) 1135.
- [386] (a) C.C. Huang, J.M. Viner, R. Pindak, J.W. Goodby, *Phys. Rev. Lett.* 46 (1981) 1289; (b) T. Pitchford, G. Nounesis, S. Dumrograttana, J.M. Viner, C.C. Huang, J.W. Goodby, *Phys. Rev. A* 32 (1985) 1938.
- [387] (a) T. Pitchford, C.C. Huang, R. Pindak, J.W. Goodby, *Phys. Rev. Lett.* 57 (1986) 1239; (b) R. Geer, C.C. Huang, R. Pindak, J.W. Goodby, *Phys. Rev. Lett.* 63 (1989) 540.
- [388] (a) R. Geer, C.C. Huang, R. Pindak, J.W. Goodby, *Phys. Rev. Lett.* 63 (1989) 540; (b) R. Geer, T. Stoebe, C.C. Huang, R. Pindak, S.W. Goodby, M. Cheng, J.T. HO, S.W. Hui, *Lett. Nature* 355 (1992) 152.
- [389] H. Pleiner, H.R. Brand, *Phys. Rev. A* 39 (1989) 1563.
- [390] J. Wang, T.C. Lubensky, *Phys. Rev. A* 29 (1984) 2210.
- [391] M.P. Allen, (a) *Liq. Cryst.* 8 (1990) 499; (b) *Philos. Trans. Roy. Soc. London A* 344 (1993) 323.
- [392] R.R. Netz, A.N. Berker, (a) *Phys. Rev. Lett.* 68 (1992) 333; (b) in: S. Martellucci, A.N. Chester (Eds.), *Phase Transitions in Liquid Crystals*, Plenum Press, New York, 1992.
- [393] D. Frenkel, in: S. Martellucci, A.N. Chester (Eds.), *Phase Transitions in Liquid Crystals*, New York, Plenum, 1992, p. 67.
- [394] U. Fabbri, C. Zannoni, *Mol. Phys.* 58 (1986) 763.
- [395] F. Biscarini, C. Zannoni, C. Chiccoli, P. Pasini, *Mol. Phys.* 73 (1991) 439.
- [396] Z. Zhang, O.G. Mouritsen, M.J. Zuckermann, *Phys. Rev. Lett.* 69 (1992) 1803.
- [397] Z. Zhang, M.J. Zuckermann, O.G. Mouritsen, *Mol. Phys.* 80 (1993) 1195.
- [398] J.A.C. Veerman, D. Frenkel, (a) *Phys. Rev. A* 45 (1992) 5632; (b) *Phys. Rev. A* 41 (1990) 3237.

- [399] E. Demiguel, L.F. Rull, K.E. Gubbins, *Phys. Rev. A* 45 (1992) 3813.
- [400] G.R. Luckhurst, P.S.J. Simmonds, *Mol. Phys.* 80 (1993) 233.
- [401] R. Memmer, H.G. Kuball, A. Schonhofer, (a) *Liq. Cryst.* 15 (1993) 345; (b) *Ber. Bunsen Ges. Phys. Chem.* 97 (1993) 1193.
- [402] A.L. Tsykalo, *Mol. Cryst. Liq. Cryst.* 129 (1985) 409.
- [403] D.J. Cleaver, D. Kralj, T.J. Sluckin, M.P. Allen, in: G.P. Crawford, S. Zumer (Eds.), *Liquid Crystals in Complex Geometries Formed by Polymer and Porus Network*, (Taylor and Francis, London, 1995).
- [404] Y.Y. Goldschmidt, in: D.H. Ryan (Ed.), *Recent Progress in Random Magnets*, World Scientific, Singapore, 1992, p. 151.
- [405] G.J. Zarragoicocoechea, D. Levesque, J.J. Weis, *Mol. Phys.* 75 (1992) 989.
- [406] J.A. Cuesta, D. Frenkel, *Phys. Rev. A* 42 (1990) 2126.
- [407] J.Y. Dunham, G.R. Luckhurst, C. Zannoni, J.W. Lewis, *Mol. Cryst. Liq. Cryst.* 60 (1980) 185.
- [408] P.E. Lammert, D.S. Rokhsar, J. Toner, *Phys. Rev. Lett.* 70 (1993) 1650.
- [409] C. Dasgupta, *Phys. Rev. Lett.* 55 (1985) 1771; *J. Phys. (Paris)* 48 (1987) 957.
- [410] R.J. Birgeneau, J.D. Litster, *J. Phys. Lett.* 39 (1978) L399.
- [411] R. Pindak, D.E. Moncton, S.C. Davey, J.W. Goodby, *Phys. Rev. Lett.* 46 (1981) 1135.
- [412] I.M. Jiang, S.N. Huang, J.Y. KO, T. Stoebe, A.J. Jin, C.C. Huang, *Phys. Rev. E* 48 (1993) 3240.
- [413] A.P.J. Emerson, G.R. Luckhurst, S.G. Whatling, *Mol. Phys.* 82 (1994) 113.
- [414] T. Odijk, *Macromolecules* 19 (1986) 2313.
- [415] H.N.W. Lekkerkerker, P. Coulon, R. Van der Haegen, R. Deblieck, *J. Chem. Phys.* 80 (1984) 3427.
- [416] A.N. Semenov, A.R. Khokhlov, *Sov. Phys. Usp.* 31 (1988) 988.
- [417] G.J. Vroege, H.N.W. Lekkerkerker, *Rep. Prog. Phys.* 55 (1992) 1241.
- [418] R. Deblieck, H.N.W. Lekkerkerker, *J. Phys. Lett. (Paris)* 41 (1980) 351.
- [419] J.K. Moscicki, G. Williams, *Polymer* 24 (1983) 85.
- [420] T. Odijk, H.N.W. Lekkerkerker, *J. Phys. Chem.* 89 (1985) 2090.
- [421] W.E. McMullen, W.M. Gelbart, A. Ben Shaul, *J. Chem. Phys.* 82 (1985) 5616.
- [422] P.J. Flory, A. Abe, *Macromolecule* 11 (1978) 1119.
- [423] A. Abe, P.J. Flory, *Macromolecule* 11 (1978) 1122.
- [424] P.J. Flory, R.S. Frost, *Macromolecule* 11 (1978) 1126.
- [425] R.S. Frost, P.J. Flory, *Macromolecule* 11 (1978) 1134.
- [426] T.M. Birshtein, B.I. Kolegov, V.A. Pryamitsyn, *Polym. Sci.* 30 (1988) 316.
- [427] A.R. Khokhlov, *Phys. Lett. A* 68 (1978) 135.
- [428] A.R. Khokhlov, A.N. Semenov, *Physica* 108A (1981) 526; *Macromolecules* 17 (1984) 2678.
- [429] A.R. Khokhlov, A.N. Semenov, *Physica* 112A (1982) 605.
- [430] S.K. Nechaev, A.N. Semenov, A.R. Khokhlov, *Polymer Sci.* 25 (1983) 1063.
- [431] G.J. Vroege, T. Odijk, *Macromolecules* 21 (1988) 2848.
- [432] R.R. Matheson, P.J. Flory, *Macromolecule* 14 (1981) 954.
- [433] T.M. Birshetin, A.R. Merkureva, *Polym. Sci. USSR* 27 (1985) 1208.
- [434] A.R. Khokhlov, *Polym. Sci USSR* 21 (1979) 2185.
- [435] M. Warner, P.J. Flory, *J. Chem. Phys.* 73 (1980) 6327.
- [436] A.R. Khokhlov, A.N. Semenov, *J. Statist. Phys.* 38 (1985) 161.
- [437] A.R. Khokhlov, A.N. Semenov, *Macromolecules* 19 (1986) 373.
- [438] V.V. Rusakov, M.I. Shliomis, *J. Phys. Lett. (Paris)* 46 (1985) 935.
- [439] X.J. Wang, M. Warner, *J. Phys. A* 19 (1986) 2215.
- [440] S.V. Vasilenko, V.P. Shibaev, A.R. Khokhlov, *Makromol. Chem. Rapid Comm.* 3 (1982) 917.
- [441] S.V. Vasilenko, A.R. Khokhlov, V.P. Shibaev, (a) *Polym. Sci.* 26 (1984) 606; (b) *Macromolecules* 17 (1984) 2270.
- [442] P. Corradini, M. Vacatello, *Mol. Cryst. Liq. Cryst.* 97 (1983) 119.
- [443] V.V. Rusakov, M.I. Shliomis, *Polym. Sci. USSR* 29 (1987)
- [444] V.P. Shibaev, N.A. Plate, *Adv. Polym. Sci.* 60/61 (1984) 173.
- [445] H. Finkelmann, G. Rehage, *Adv. Polym. Sci.* 60/61 (1984) 99.
- [446] N.A. Plate, V.P. Shibaev, *Comblike Polymers and Liquid Crystals*, Khimiya, Moscow, 1980 (in Russian).

- [447] P.J. Collings, J.S. Patel (Eds.), *Handbook of Liquid Crystal Research*, Oxford Univ. Press, Oxford, 1997, p. 71 (Chapter 3); p. 259 (Chapter 8).
- [448] R.G. Petschek, *Phys. Rev. A* 34 (1986) 1338.
- [449] Y.H. Kim, P. Pincus, *Biopolymers* 18 (1979) 2315.
- [450] X.J. Wang, M. Warner, *Liq. Cryst.* 12 (1992) 385.
- [451] W.J.A. Goossens, (a) *Mol. Cryst. Liq. Cryst.* 12 (1971) 231; (b) *J. de Physique* 40 (1979) C3-158.
- [452] B.W. Van der Meer, G. Vertogen, A.J. Dekker, J.G.J. Ypma, *J. Chem. Phys.* 65 (1976) 3935.
- [453] B.W. Van der Meer, G. Vertogen, A molecular model for the cholesteric mesophase, in: G.R. Luckhurst, G.W. Gray (Eds.), *The Molecular Physics of Liquid Crystals*, Academic Press, New York, 1979, p. 149 (Chapter 6).
- [454] H. Schrodinger, A molecular field theory of the cholesteric liquid crystal state in: G.R. Luckhurst, G.W. Gray (Eds.), *The Molecular Physics of Liquid Crystals*, Academic Press, New York, 1979, p. 121 (Chapter 5).
- [455] J.P. Straley, *Phys. Rev. A* 14 (1976) 1835.
- [456] G. Vertogen, B.W. Van der Meer, *Physica* 99A (1979) 237.
- [457] S.A. Brazovskii, S.G. Dmitriev, *Sov. Phys. JETP* 42 (1976) 497.
- [458] P.M.L.O. Scholte, G. Vertogen, *Physica* 113A (1982) 587.
- [459] G.T. Evans, *Mol. Phys.* 77 (1992) 969.
- [460] R.A. Pelcovits, P.J. Collings, J.S. Patel (Eds.), *Handbook of Liquid Crystal Research*, Oxford Univ. Press, Oxford, 1997, p. 71 (Chapter 3).
- [461] O. Lehmann, *Z. Phys. Chem.* 56 (1906) 750.
- [462] H. Stegemeyer, K. Bergmann, *Springer Ser. Phys. Chem.*, Vol. 11, 1980, p. 161.
- [463] (a) K. Bergmann, H. Stegemeyer, *Z. Naturforsch.* (a) 34 (1979) 251; (b) 34 (1979) 1031; K. Bergmann, P. Pollmann, G. Scherer, H. Stegemeyer, *Z. Naturforsch.* (a) 34 (1979) 253.
- [464] M. Marcus, *J. Phys. (Paris)* 42 (1981) 61.
- [465] S. Meiboom, M. Sammon, *Phys. Rev. A* 24 (1981) 468.
- [466] P.J. Collings, *Phys. Rev. A* 30 (1990) 1984; *Mol. Cryst. Liq. Cryst.* 113 (1984) 277.
- [467] R.N. Kleiman, D.J. Bishop, R. Pindak, P. Taborek, *Phys. Rev. Lett.* 53 (1984) 2137.
- [468] H. Onusseit, H. Stegemeyer, *Z. Naturforsch.* (a) 39 (1984) 658.
- [469] P.P. Croopker, *Mol. Cryst. Liq. Cryst.* 98 (1983) 31.
- [470] S.A. Brazovskii, S.G. Dmitriev, *Sov. Phys. JETP* 42 (1975) 497.
- [471] S.A. Brazovskii, V.M. Filev, *Sov. Phys. JETP* 48 (1979) 573.
- [472] R.M. Hornreich, S. Shtrikman, (a) *Bull. ISR. Phys. Soc.* 25 (1979) 46, (b) in: W. Helfrich, G. Heppke (Eds.), *Liquid Crystals of One and Two dimensional Order*, Springer, Berlin, 1980, p. 185; (c) *J. Physique* 41 (1980) 335; (d) *Phys. Lett.* 82A (1981) 345; (e) *Phys. Lett.* 84A (1981), 20, (f) *J. Physique* 42 (1981) 367; (g) *Mol. Cryst. Liq. Cryst.* 165 (1988) 183.
- [473] R.M. Hornreich, M. Kugler, S. Shtrikman, *Phys. Rev. Lett.* 498 (1982) 1404.
- [474] S. Alexander, in: N. Boccara (Ed.), *Symmetry and broken Symmetry in Condensed Matter Physics*, IDSET, Paris, 1981, p. 141.
- [475] S. Alexander, R.M. Hornreich, S. Shtrikman, in: N. Boccara (Ed.), *Symmetry and Broken Symmetry in Condensed Matter Physics*, IDSET, Paris, 1981, p. 379.
- [476] H. Kleinert, K. Maki, *Fortschr. Phys.* 29 (1981) 219.
- [477] R.M. Hornreich, M. Kugler, S. Shtrikman, *Phys. Rev. Lett.* 498 (1982) 1404.
- [478] H. Grebel, R.M. Hornreich, S. Shtrikman, (a) *Phys. Rev. A* 28 (1983) 1114, 3669; (b) *Phys. Rev. A* 30 (1984) 3264.
- [479] S. Meiboom, J.P. Sethna, P.W. Anderson, W.F. Brinkman, *Phys. Rev. Lett.* 46 (1981) 1216.
- [480] S. Meiboom, M. Sammon, D.W. Berreman, *Phys. Rev. A* 28 (1983) 3553.
- [481] S. Meiboom, M. Sammon, B.F. Brinkman, *Phys. Rev. A* 27 (1983) 438.
- [482] J.P. Sethna, *Phys. Rev. B* 31 (1985) 6278.
- [483] (a) Z. Kutnjak, C.W. Garland, J.L. Passmore, P.J. Collings, *Phys. Rev. Lett.* 74 (1995) 4859; J.B. Becker, P.J. Collings, *Mol. Cryst. Liq. Cryst.* 265 (1995) 163. (b) T.C. Lubensky, H. Stark, *Phys. Rev. E* 53 (1996) 714.
- [484] A.W. Hall, J. Hollingshurst, J.W. Goodby, P.J. Collings, J.S. Patel (Eds.), *Handbook of Liquid Crystal Research*, Oxford Univ. Press, Oxford, 1997, p. 40 (Chapter 2).

- [485] H.R. Brand, P.E. Cladis, P.L. Finn, *Phys. Rev. A* 31 (1988) 361.
- [486] N.A. Clark, S.T. Langerwall, *Ferroelectrics* 59 (1984) 25.
- [487] (a) J.S. Patel, J.W. Goodby, *Philos. Mag. Lett.* 55 (1987) 283; (b) J.W. Goodby, *J. Mater. Chem.* 1 (1991) 307.
- [488] L.M. Blinov, L.A. Beresnev, *Sov. Phys. Usp.* 27 (1985) 492.
- [489] B.W. Van der Meer, G. Vertogen, *Phys. Lett.* 74A (1979) 239.
- [490] M.A. Osipov, S.A. Pikin, (a) *Sov. Phys. Crystallogr.* 26 (1981) 147; (b) *Sov. Phys. Tech. Phys.* 27 (1982) 109; (c) *Mol. Cryst. Liq. Cryst.* 103 (1983) 57.
- [491] W.J.A. Goossens, *Liq. Cryst.* 1 (1986) 521.
- [492] M. Nakagawa, *Liq. Cryst.* 3 (1988) 63.
- [493] B. Zeks, *Mol. Cryst. Liq. Cryst.* 114 (1984) 259.
- [494] C.C. Huang, S. Dumrongrattana, *Phys. Rev. A* 34 (1986) 5020.
- [495] T. Carlsson, B. Zeks, A. Levstik, C. Filipik, I. Levstik, R. Blinc, *Phys. Rev. A* 36 (1987) 1484.
- [496] T. Carlsson, B. Zeks, C. Filipic, A. Levstik, R. Blinc, *Mol. Cryst. Liq. Cryst.* 163 (1988) 11.
- [497] R. Meister, H. Stegemeyer, *Ber. Bunsenges, Phys. Chem.* 97 (1993) 1242.
- [498] F. Gießelmann, P. Zugenmaier, *Phys. Rev. E* 52 (1995) 1762.
- [499] H.P. Padmani, N.V. Madhusudana, B. Shivkumar, *Bull. Mater. Sci.* 17 (1994) 1119.
- [500] (a) S.S. Roy, S.K. Roy, P.K. Mukherjee, *Int. J. Mod. Phys. B* 11 (1997) 3491; (b) P.K. Mukherjee, *Private commun.*
- [501] B. Zeks, T. Carlsson, C. Filipic, B. Urbane, *Ferroelectrics* 84 (1988) 3; B. Urbane, B. Zeks, *Liq. Cryst.* 5 (1989) 1075.
- [502] S.R. Renn, *Phys. Rev. A* 45 (1992) 953.
- [503] J.W. Goodby, M.A. Waugh, S.M. Stein, E. Chin, R. Pindak, J.S. Patel, *Nature* 337 (1988) 449; *J. Am. Chem. Soc.* 111 (1989) 8119.
- [504] G. Srajer, R. Pindak, M.A. Waugh, J.W. Goodby, J.S. Patel, *Phys. Rev. Lett.* 64 (1990) 1545.
- [505] O.D. Lavrentovich, Y.A. Nishtishin, V.I. Kulishov, Y.S. Narkevich, A.S. Tolochko, S.Y. Shiyanovskii, *Europhys. Lett.* 13 (1990) 313.
- [506] S.R. Renn, T.C. Lubensky, *Phys. Rev. A* 38 (1988) 2132.
- [507] T.C. Lubensky, S.R. Renn, *Phys. Rev. A* 41 (1990) 4392.
- [508] M. Fukui, H. Orihara, Y. Yamada, N. Yamamoto, Y. Ishibashi, *Jpn. J. Appl. Phys.* 28 (1989) L849.
- [509] E. Gorecka, A.D.L. Chandani, Y. Ouchi, H. Takezoe, A. Fukuda, *Jpn. J. Appl. Phys.* 29 (1990) 131.
- [510] A. Suzuki, H. Orihara, Y. Ishibashi, Y. Yamada, N. Yamamoto, K. Mori, K. Nakamura, Y. Suzuki, T. Hagiwara, Y. Kawamura, M. Fukui, *Jpn. J. Appl. Phys.* 29 (1990) L336.
- [511] M. Johno, Y. Ouchi, H. Takezoe, A. Fukuda, *Jpn. J. Appl. Phys.* 29 (1990) L111.
- [512] S. Inui, S. Kawano, M. Saito, H. Iwane, Y. Takanishi, K. Hiraoka, Y. Ouchi, H. Takezoe, A. Fukuda, *Jpn. J. Appl. Phys.* 29 (1990) L987.
- [513] H. Orihara, T. Fujikawa, Y. Ishibashi, Y. Yamada, N. Yamamoto, K. Mori, K. Nakamura, Y. Suzuki, T. Hagiwara, I. Kawamura, *Jpn. J. Appl. Phys.* 29 (1990) L333.
- [514] Y. Takanishi, K. Hiraoka, V.K. Agrawal, H. Takezoe, A. Fukuda, M. Matsushita, *Jpn. J. Appl. Phys.* 30 (1991) 2023.
- [515] J. Lee, Y. Ouchi, H. Takezoe, A. Fukuda, J. Watanabe, *J. Phys. Cond. Matter* 2 (1990) L103.
- [516] M. Hara, T. Umemoto, H. Takezie, A.F. Garito, H. Sasabe, *Jpn. J. Appl. Phys.* 30 (1991) L2052.
- [517] K. Hiraoka, A.D.L. Chandani, E. Gorecka, Y. Ouchi, H. Takezoe, A. Fukuda, *Jpn. J. Appl. Phys.* 29 (1990) L1473.
- [518] N. Okabe, Y. Suzuki, I. Kawamura, I. Isozaki, H. Takezoe, A. Fukada, *Jpn. J. Appl. Phys.* 31 (1992) L793.
- [519] T. Isozaki, H. Hiraoka, Y. Takanishi, A. Fukuda, Y. Suzuki, I. Kawamura, *Liq. Cryst.* 12 (1992) 59.
- [520] V.L. Lorman, A.A. Bulbitch, P. Toledano, *Phys. Rev. E* 49 (1994) 1367.
- [521] F. Gießelmann, P. Zugenmaier, *Phys. Rev. E* 55 (1997) 5613.